

# **Durable Reliability of Jack-up Platforms**

***The impact of Fatigue, Fracture and Effect of Extreme  
Environmental Loads on the Structural Reliability***

## **Proefschrift**

ter verkrijging van de graad van doctor  
aan de Technische Universiteit Delft,  
op gezag van de Rector Magnificus, prof. dr. ir. J.T.Fokkema,  
voorzitter van het College voor Promoties,  
in het openbaar te verdedigen

op woensdag 22 december 2004 om 13:00 uur

door

**Naser SHABAKHTY**

Master of Science in Structural Engineering,  
Isfahan University of Technology,  
Geboren te Karbala, Iraq

Dit proefschrift is goedgekeurd door de promotoren:

Prof. ir. S. Hengst

Prof. ir. A.C.W.M. Vrouwenfelder

Toegevoegd promotor:

Ir. H. Boonstra

Samenstelling promotiecommissie:

Rector Magnificus,

Prof. ir. S. Hengst,

Prof. ir. A.C.W.M. Vrouwenfelder,

Ir. H. Boonstra,

Prof. dr. ir. U. Nienhuis,

Prof. dr. ir. J.A. Pinkster,

Prof. dr. ir. T. Moan,

Prof. dr. ir. J. Wardenier,

Prof. ir. J. Meek,

voorzitter

Technische Universiteit Delft, promotor

Technische Universiteit Delft, promotor

Technische Universiteit Delft, toegevoegd promotor

Technische Universiteit Delft

Technische Universiteit Delft

Norwegian University of Science and

Technology, Norway

Technische Universiteit Delft

Technische Universiteit Delft, reserve lid

Durable Reliability of Jack-up platforms, The impact of Fatigue, Fracture and Effect of Extreme Environmental loads on the Structural Reliability / Naser Shabakhty

Thesis Delft University of Technology-With ref.-With summary in Dutch

ISBN 90-3700217-X

Keywords: Fatigue, Fracture, Reliability, Extreme environmental loads

Printed by: Sieca Repro b.v., Delft, The Netherlands

Copyright©2004, by N. Shabakhty

No part of the material protected by this copyright notice may be reproduced or utilized in any form or by any means, electronic or mechanical, including photocopying, recording or by any information storage and retrieval system, without permission of the author.

# **Durable Reliability of Jack-up Platforms**

***The impact of Fatigue, Fracture and Effect of Extreme  
Environmental Loads on the Structural Reliability***

## **Thesis**

presented for the degree of doctor  
at Delft University of Technology  
under the authority of the Vice-Chancellor, Prof. dr. ir. J.T.Fokkema,  
to be defended in public in the presence of a committee  
appointed by the Board for Doctorates

on Wednesday December 22, 2004 at 13:00 o'clock

by

**Naser SHABAKHTY**

Master of Science in Structural Engineering,  
Isfahan University of Technology  
Born in Karbala, Iraq

This thesis is approved by supervisors:

Prof. ir. S. Hengst  
Prof. ir. A.C.W.M. Vrouwenvelder

Adjunct supervisor:  
Ir. H. Boonstra

Composition of Examination Committee:

Vice-Chancellor,  
Prof. ir. S. Hengst,  
Prof. ir. A.C.W.M. Vrouwenvelder,  
Ir. H. Boonstra,  
Prof. dr. ir. U. Nienhuis,  
Prof. dr. ir. J.A. Pinkster,  
Prof. dr. ir. T. Moan,

Prof. dr. ir. J. Wardenier,  
Prof. ir. J. Meek,

Chairman  
Delft University of Technology, supervisor  
Delft University of Technology, supervisor  
Delft University of Technology  
Delft University of Technology  
Delft University of Technology  
Norwegian University of Science and  
Technology, Norway  
Delft University of Technology  
Delft University of Technology

*This Dissertation is dedicated to:*

*my late mother and my father,*

*my wife and my son,*

*my mother-in-law and my father-in-law*

*my educators*



## **Acknowledgments**

I am grateful to God for creating a beautiful world, for keeping me in a good health and giving me the ability to successfully finish my PhD research.

My special gratitude must be expressed to my promoters, prof. ir. S. Hengst and prof. ir. A.C.W.M. Vrouwenvelder, for their scientific supervision and guidance during the course of my study. Their valuable comments and patience were a great help.

I also express my sincere thanks to my supervisors dr. Pieter Van Gelder from Civil Engineering and ir. H. Boonstra from Marine Technology for their help and guidance, and friendly relation.

I am grateful to the instructor emeritus of Civil Engineering, ir J. H. Rakers for his help during the first year of my study when I had problems to find my way and he was guiding me to establish my research work.

I would like to express my appreciation to prof. Der Kiureghian from the University of California, Berkeley and prof. Ditlevsen from the Technical University of Denmark for providing me with the section of their book and their lecture notes prior to publication.

I give my recognition to prof. T. Moan, prof. dr. U. Nienhuis, and prof. dr. J. Wardenier for their most valuable comments as members of the examination committee. Thank also goes to prof. J. A. Pinkster from Marine Technology section of Delft University of Technology for willing as a member of examination committee.

Thank goes to Mrs. Nieuwland from Marine Technology, for her help and support in the course of my work. I would like to thank all related colleagues in Marine Technology of Delft University of Technology for their helpful cooperation throughout the present research work. I also thank Mrs. Sopers from the personnel department of the faculty of Design, Construction and Production for her help to prepare the resident permit and other official documents required during my stay in The Netherlands.

I express my appreciation to the Ministry of Science, Research and Technology of the Islamic Republic of Iran for providing me such an excellent opportunity to follow my education in The Netherlands.

I wish to heartily thank my wife, Mrs. Azadeh Gholamali, for her patience during troubles and her generous collaboration with me when I went through difficult situations. This work is dedicated to her with all my gratitude, although I can never compensate her kindness and patience. Finally, I express my sincere gratitude to my late mother and my father, to whom I not only owe my existence, but also for their guidance to be a good person. Moreover, I need to express my great appreciation to my mother-in-law and father-in-law for having patience during our long absence and for supporting us in the course of my study. I am also indebted to my son, Ali Reza, since my research work always consumed the time when I should have been with him.

## **Summary**

A variety of factors is governing the operational conditions of jack-up platforms. The platforms are moved to different locations, which are causing changes in water depth, environmental and seabed conditions, drilling depths, payload etc. Insight should be gained in how the different factors affect the lifetime in order to be able to make a reliable prediction of the safety. The structure of the jack-up platform, usually consisting of three legs, which are supporting the platform containing living quarters, installations for power generation, machinery and equipment for drilling or production facilities, differs from a fixed platform. Aspects as the need for more flexibility and the development of marginal fields, initiate also a trend for jack-up platforms to operate in deeper water.

The subject of this research project is durable reliability of jack-up platforms with the aim to explore the possibilities for the extension of the life-time. Aspects as fatigue, fracture and failure due to extreme environmental loads are investigated. The uncertainties in loads, material characteristics and structural modelling are investigated. A deterministic approach cannot properly take these uncertainties into account.

For the reliability calculations, a method, based on refined stress states, is presented. The fracture mode is of importance when extreme environmental loads are combined with an existing crack in a structural element, which may be due to the fabrication process or fatigue. To estimate the statistical information about the crack a method based on the Monte Carlo simulation technique is presented. This method uses a fatigue crack growth formulation to specify the crack size.

For the ultimate failure mode under extreme environmental loads the axial and bending stresses are combined to establish the time history of the usage factor.

Due to the redundancy of the structure the system effect may be important. For this purpose a method is presented to specify the limit state function for sequences of failure leading to structural collapse and the failure probabilities of these sequences are calculated.

The branch and bound technique is used to establish the branch tree to identify the important failure sequences. Then the system failure probability is calculated by combining the most important sequences leading to structural collapse. For this purpose The First Order Multi Normal approach (FOMN) and bound techniques are used.

For a case study, the 'Neka' platforms which was chosen in this thesis, the failure probability of the structural system in the combination of fracture and fatigue failure modes proved to be the most important. The results show significant system effects. The conclusion may be drawn that this type of structural failure deserves significant attention during the ageing of jack-up platforms.

This research work does not claim to have solved all issues related to the structural reliability of a jack-up platform. However, a number of valuable stepping-stones have been developed as a basis for further research.



# Contents

<b>Acknowledgments .....</b>	<b>I</b>
<b>Summary.....</b>	<b>II</b>
<b>Contents .....</b>	<b>III</b>
<b>1. Introduction .....</b>	<b>1</b>
1.1. Background.....	1
1.2. Focus .....	2
1.3. Organization .....	5
<b>2. Limit State Models.....</b>	<b>9</b>
2.1. Introduction .....	9
2.2. Source of uncertainties in marine environment .....	10
2.3. Fatigue mechanics .....	11
2.3.1. Fatigue crack growth model.....	12
2.3.2. Semi-elliptical crack propagation .....	13
2.3.3. Fatigue strength function and fatigue loading function .....	16
2.3.4. Stress distribution in tubular joints and long-term stress range .....	18
2.4. Fatigue Limit State .....	20
2.4.1. Uncertainty in fatigue characteristics.....	21
2.5. Ultimate limit state .....	22
2.5.1. An approach to specify the ultimate limit state.....	23
2.6. Fracture mechanics .....	24
2.6.1. Fracture mechanics criteria .....	24
2.6.2. Failure assessment diagram.....	25
2.7. Fracture limit state .....	27
2.8. Concluding remarks.....	29
<b>3. Reliability Analysis .....</b>	<b>31</b>
3.1. Introduction .....	31
3.2. Analytical approximation methods.....	32
3.2.1. Transformation to the standard Normal space .....	32
3.2.2. First Order Reliability Method (FORM).....	33
3.2.3. Second Order Reliability Method (SORM) .....	34
3.3. Simulation methods .....	36

---

3.3.1. Monte Carlos Simulation (MCS) .....	36
3.3.2. Importance Sampling Method (IS).....	37
3.4. System Reliability.....	38
3.4.1. Series and parallel systems.....	38
3.4.2. Simulation technique.....	39
3.4.3. Using bounds technique .....	40
3.4.4. Branch and bound search algorithm.....	40
3.4.5. Response Surface Method (RSM).....	42
3.4.6. Conditional and unconditional failure probability .....	42
3.5. Example application .....	44
3.5.1. Example of fatigue limit state function .....	44
3.5.2. Example of ultimate limit state function .....	47
3.5.3. Example of fracture limit state function.....	49
3.6. Concluding remarks.....	51
<b>4. Component Reliability of Jack-up Platforms.....</b>	<b>53</b>
4.1. Introduction .....	53
4.2. Model of Neka Platform .....	55
4.3. Fatigue reliability.....	58
4.3.1. Stress calculation and distribution .....	58
4.3.2. The bending to membrane stress ratio and selecting of a geometry function .....	63
4.3.3. Effect of spectral models on fatigue reliability .....	66
4.3.4. Variation of fatigue reliability with overall damping of platform.....	67
4.3.5. Effect of nonlinear and wide-banded stress models on fatigue reliability .....	69
4.4. Updating of fatigue reliability through inspection results .....	71
4.4.1. Event updating through inspection results .....	71
4.4.2. Updating fatigue reliability through inspection with no-crack detection .....	73
4.4.3. Updating fatigue reliability through inspection with crack detection .....	74
4.5. Reliability of jack-up platform in extreme environmental loads.....	75
4.5.1. Extreme environmental loads.....	75
4.5.2. Reliability in extreme environmental loads function .....	78
4.6. Fracture reliability .....	81
4.7. Conclusions .....	86
<b>5. System Reliability of Jack-up Platforms .....</b>	<b>89</b>
5.1. Introduction .....	89
5.2. System reliability due to a sequence of fatigue failures .....	90
5.2.1. Formulation of the first fatigue failure.....	90
5.2.2. Sequence of joint failures in fatigue.....	91
5.2.3. Search technique to identify dominating failure sequences .....	94
5.2.4. System reliability of the Neka jack-up platform .....	95
5.3. System reliability in combination of fatigue failure with extreme environmental loads.....	105

---

5.4. System reliability for a combination of fatigue failure with fracture failure modes.....	109
5.4.1. Fatigue failure of the first joint followed by a fracture failure of the second joint .....	109
5.4.2. Fracture failure of the first joint followed by a fracture failure of the second joint .....	113
5.4.3. Fracture failure of the first joint followed by a fatigue failure of the second joint .....	114
5.4.4. System failure probability calculation for combinations of fracture and fatigue failure.....	117
5.5. Concluding remarks.....	118
<b>6. Conclusions.....</b>	<b>121</b>
6.1. General.....	121
6.2. Reliability computation approaches .....	122
6.3. Fatigue reliability.....	124
6.4. Extreme sea states.....	126
6.5. Fracture reliability methods.....	126
6.6. System reliability calculations .....	127
6.7. Main findings.....	129
6.8. Future developments in the reliability analysis of jack-up platforms.....	130
<b>Nomenclature .....</b>	<b>132</b>
<b>References.....</b>	<b>136</b>
<b>Appendices.....</b>	<b>141</b>
Appendix A: Geometry function.....	146
Appendix B: Description of jack-up platform .....	149
Appendix C: Sea scatter diagram.....	154
Appendix D: Influence Factors (Stress Concentration Factors).....	156
Appendix E: The computer programs .....	158
Appendix F: Calculation procedure of Correlation between limit state functions.....	168
Appendix G: Modelling of random variables .....	171
Appendix H: Long-term failure probability.....	174
Appendix I: Failure probability for combined fatigue and fracture failure modes .....	176
<b>Samenvatting.....</b>	<b>179</b>
<b>Curriculum Vitae.....</b>	<b>180</b>



# **1. INTRODUCTION**

---

## **1.1 BACKGROUND**

Jack-up structures are generally used for exploration and production of hydrocarbons. The combination of mobility, the possibility to elevate the platform above the sea level for a range of water depths, and to serve as a fixed platform made them attractive in the offshore industry over the last 40 years.

Various circumstances and conditions are influencing the ageing of jack-up platforms. The jack-up platform is a movable object, which is basically being designed to work at any location, worldwide for given maximum water depths and sea states, combined with different sea bed conditions. Moreover the platform is often transported with the legs in fully raised position, from one offshore location to another, resulting in completely different loads on the structure.

During the pre-loading, required on locations with a soft seabed, unexpected and asymmetrical loadings may be the result when a sudden soil failure takes place. During drilling operations the loads on the structure will vary with the well depth. Because of the differences in water depth at different locations, the leg length supporting the structure may differ considerably, as well as the loading resulting from the environmental conditions (sea-state, winds and currents, the position of the platform above the water level, depending on e.g. wave height and tidal differences.

Differences in temperatures have an effect on the aggressiveness of seawater influencing the corrosion, variations in water depth will cause that the area, which is attacked by both wind and water, cannot be properly protected by e.g. cathodic protection while the coating, being subject to mechanical damages is vulnerable.

These conditions are differing for fixed platforms designed for a specific location with predictability of the environmental conditions and hence the loading and other factors influence the ageing of the structure.

This is also a reason that in practice for the design of a jack-up a deterministic approach is used by analyzing the most severe environmental circumstances for the different conditions,

which may be expected during the lifetime, whereby for each new operational situation a thorough analysis will be made, based on known environmental parameters.

The introduction of high tensile steels in the leg of a jack-up structure, improved clamping systems and innovative solutions to transfer the forces from the legs into the platform have been leading to considerable reductions in weight and higher payloads which made it possible to improve the performance and increase the operational water depth.

Over the time the offshore industry moved into deeper waters with more severe conditions. The jack-up platforms followed this trend and are today also used as production platforms. The increasing investments launched the search for costs reductions and the extension of the lifetime is an important parameter influencing the efficiency. The deterministic approach may well be suitable for the basic design. On the other hand the number of factors influencing the lifetime is large, is difficult to predict and is originating from different sources. The analysis of the effect of ageing on the lifetime requires other approaches which make it possible to combine different factors. Methods such as reliability calculations can be helpful to gain insight in this complex matter.

## 1.2 FOCUS

The deterioration process is not only limited to a specific material or human life, it encompasses everything belonging to this world but the types of deterioration differ from one to another. For instance, in human life, disability might be a sign of aging or deterioration but for materials, change of geometry, loss of thickness or reduction of strength could be the first sign of a deterioration process. Nowadays, researchers are giving more attention to the deterioration processes of specific structures such as nuclear power plants. Also for offshore platforms deterioration may have a significant impact, not only from economical viewpoint, but also with regard to physical damage and potential environmental pollution. In fact, due to deterioration, the actual safety of a structural system, as estimated at the time of design, even when checked continuously during its lifetime, decreases. As a matter of fact, deterioration introduces the time factor into the design and it is not possible to deal with it without considering a design or service life. In order to assess the current and future performance of an existing structure with respect to extension of the projected lifetime or because of the appearance of significant signs of damage, consideration should be given to the deterioration of any element of a structure.

The question, “how is it possible to get a better insight into the factors influencing the lifetime of a jack-up structure” cannot be answered without bringing a priority in the different causes for failure. Although the interests of the offshore industry are primarily on the economical aspects, it is clear that the environmental aspects are of principal importance. It is therefore mandatory to be able to predict the operational lifetime of offshore platforms by including the impact on the deterioration processes e.g. fatigue.

The focus of the industry has been primarily on production facilities, which require huge investments compared to the facilities needed during the exploration phase. However the importance of exploration is increasing with the continuous increasing demand for oil and gas while the reserves are not increasing in the same pace.

From a preliminary literature study it became apparent that the research of the effect of ageing on the lifetime of jack-up platforms is rather limited and consequently not much is known about the ageing of jack-up platforms. Much research has been performed to investigate the fatigue reliability of jacket type platforms (Karadenize et al. 1983, Shetty, 1992 and Dalane, 1993) or Tension Leg Platforms (Hovde, 1995) but for jack-up structures this has been restricted to extreme environmental loads (Karunakaran, 1993, Daghigh, 1997 and Cassidy, 1999). So little attention has been paid to investigate the fatigue reliability of jack-up platforms. For jack-up platforms, as Onoufriou (1999) states, the structural configuration and modes of operation differ significantly from fixed platforms and therefore further work is needed to develop a reliability technique based on existing methods currently applied to jacket platforms.

One of the differences between jack-ups and fixed offshore structures is non-linearity in nature of response due to P- $\delta$  effect, the drag term in the hydrodynamic load calculation and the integration of wave loads to the actual water surface, even if the structure behaves linearly. This non-linearity has an influence on the response and cannot be modelled properly by a linear traditional approach as often used for fixed platforms, (Karunakaran, 1993). Furthermore, due to this non-linearity, the suitable procedure to predict the distribution function of non-linear responses for both reliability calculations under fatigue degradation and extreme environmental loads becomes essential. Often these distributions are obtained for axial and bending stresses separately, Daghigh (1997). This approach gives conservative results because maximum axial and bending stresses may not occur at the same time. Furthermore, sometimes the state of axial stresses changes from tension to compression, which shows the failure mode is altered from yielding to buckling, and using only one failure mode in yielding or buckling for the whole process would not sufficiently reflect the damage state. Hence, a proper procedure is required to improve this method.

The investigation of Sharp (1992) on damaged offshore structures installed in the North Sea for the period up to 1987 shows that the highest percentage of damage requiring repair arises from fatigue degradation. Figure 1.1 shows the type of damage requiring repair and it can be

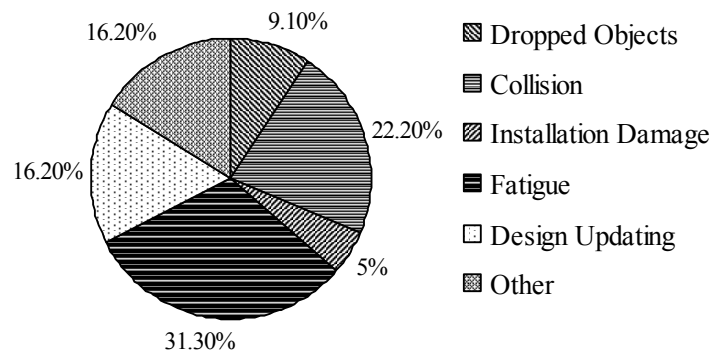


**Figure 1.1** Observation of damage on offshore platforms, (after Sharp, 1992)

observed that fatigue degradation represents a significant part (31.3%) of the damages of offshore platforms. This is one of the reasons to focus this study on a reliability method to be used in an engineering environment for movable, complex, dynamically sensitive jack-up structures for deep water, when fatigue and extreme environmental loads are the main causes of failure.

With the increasing water depths for jack-up operations, as described in DNV (1992), the fatigue degradation becomes even more important and the strength reduction due to this degradation should be taken into account not only in the design stage but also during the lifetime of the structure. The main reasons are:

- Increase of water depth leads to more flexible structures, which means that the dynamic amplification of the response will increase.
- To meet the economic requirements to operate in deep water the trend is to increase the strength of the legs of platforms and, at the same time limit, as much as possible the increase in size or weight. This leads to the application of high strength steel material, which might increase the possibility of fatigue failures.
- When operating in areas with more severe sea conditions, the wave loads that are important in connection with fatigue may become more dominant.

The jack-up structure consists of various components and behaves in a nonlinear and dynamic manner. Since many degradation phenomena may influence the fatigue of the structure and reduce the strength, the uncertainties in fatigue characteristics and environmental loads change the value of the deterministic approaches in comparison to a probabilistic method.

Because of the complexity and magnitude of the problem of ageing, this research is limited to a methodology for a reliability calculation of the structure of jack-up platforms due to fatigue, fracture and finally extreme environmental loads. When these types of platforms have been in operation for a great part of their original design-life, and the intention is to extend their utilization, the research into the effect of factors influencing the safety of the structures with regard to extreme environmental loads and fatigue (or a combination) is essential. Apart from the uncertainties in loads, material characteristics and structural modelling, a deterministic method cannot adequately deal with these uncertainties.

Most of the work on structural reliability refers to the reliability of single structural components where it is possible to use reliability methods such as FORM, SORM and Monte Carlo Simulation. The design practice of today is therefore mainly based on component level. However, the safety of the overall structure (the system) may be of greater interest since the system reliability takes into account the effects on the whole system, and the structural system consists of many individual elements of which the failure of one element may not lead to a system collapse.

Since the classification societies require regular inspections of jack-up platforms during regular intervals over the lifetime, this may provide useful information that can be used to monitor the condition of the structure. The probability of a structural failure may therefore be updated with the use of the outcome of these inspections and makes it possible to treat the uncertainty associated with fatigue and inspection processes.



This leads to the following main problem for this research work:

- The limited availability of investigations on the fatigue damage of jack-up platforms and the need to consider the structural damage, when an extension of the lifetime is being anticipated.
- The possibility of fatigue damage, also when a jack-up platform is used as a production facility i.e. a permanent facility.
- The uncertainty in the characteristics of fatigue, environmental loads or material properties, which makes the deterministic approach less suitable.
- The specific structural stress states of jack-up platforms, which differ from other bottom founded offshore platforms such as jacket or tension leg platforms.
- The possibility of combination of fatigue damage with the other failure modes such as extreme environmental loads or fracture.
- The failure of one element may not lead to structural collapse. The behaviour of a structure as a system should therefore be taken into account.

The intention is to take the following steps to analyse these problems:

- Extending a reliability approach, which can be used to monitor the safety of jack-up platforms till the end of their service life.
- Specify a degradation model in accordance with the fatigue damage.
- Investigate the possibility of the combination of fatigue damage with other failure modes such as extreme environmental loads and fracture.
- Explore the system effect on the reliability of the structure and compare it with the component reliability.
- Determine the failure probability due to fatigue damage and investigate the factors that can change this failure probability.

Summarizing, the main question is *“How is it possible to determine the reliability of complex and dynamically sensitive offshore structures such as jack-up platforms on component and system level due to extreme environmental loads and subjected to degradation by fatigue?”*

The key questions of this research work are:

- How can we determine the reliability of a structure on component and system level and improve this method so it may be used for complex, dynamic sensitive structures such as jack-up platforms?
- How can a reliability analysis be improved to consider degradation due to fatigue?
- Which factors have a significant effect on the reliability of structures?

### 1.3 ORGANIZATION

The structure of this research work is illustrated in figure 1.2. the work has been divided into four sections. The first and last sections are devoted to describe the research problem and the findings from this work. The second section shows the theoretical principles required for the reliability analysis and presents the basic concept of uncertainty in the offshore environment. In addition, the mechanical failure criteria, which define safe and failure states of

components, are discussed in this section. These failure criteria actually form our limit state functions required in the third chapter. In the third section, the application of reliability approaches described in the second section is shown for a jack-up structure and several parameters influencing the reliability calculation are investigated.

Chapter 2 focuses on fatigue and fracture mechanics and describes a method to determine the fatigue strength and the loading function. Several formulations for the geometry function, which play an important role in the fatigue strength function, are presented. Moreover, several models for the fatigue loading function are discussed. The fracture failure is one of the important failure modes of structures when extreme environmental loads are combined with a crack, which may exist in a structural element due to the fabrication process or due to fatigue. In the following sections of this chapter the fracture mechanics criterion is presented and the failure assessment diagram concept, which accounts for the interaction of elasto-plastic and fracture failures, is discussed.

In a reliability calculation it is needed to specify the limit state function. At first the limit state functions are presented for fatigue failure and sources of uncertainties in this formulation are discussed. The ultimate limit state function is then introduced based on the design code for offshore structures and at the end the fracture limit state is presented.

Chapter 3 gives a brief review of the structural reliability theory, and provides descriptions of the various methods for component and system reliability analysis required in this research. At first, analytical approximation methods such as First Order Reliability Method (FORM) and Second Order Reliability Method (SORM) are presented and then the Monte Carlo (MCS) simulation techniques and the Importance Sampling method (IS) are discussed. Furthermore, a brief description of the most common methods of system reliability by FORM and simulation techniques is presented. In addition, the branch and bound technique to

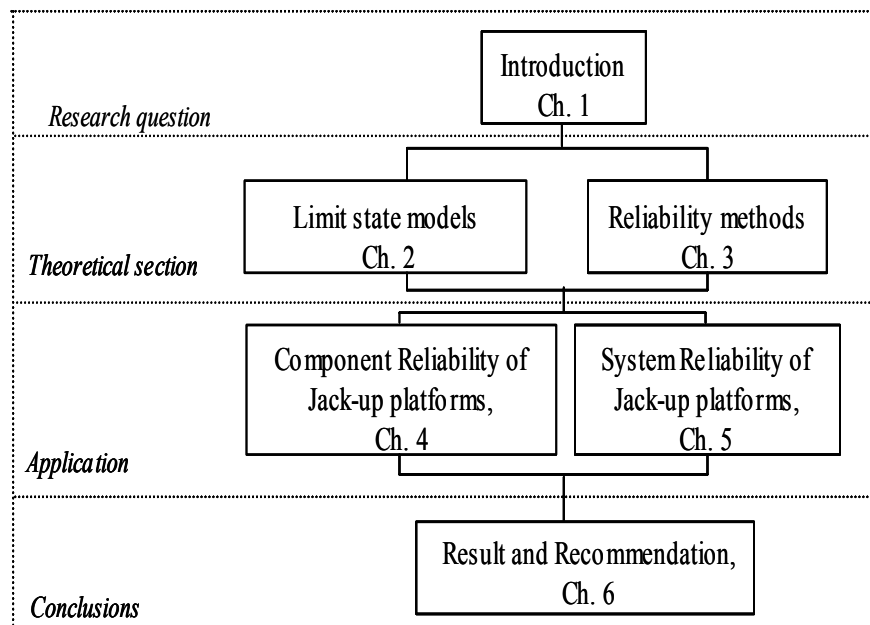


**Figure 1.2** Outline of thesis

identify the important failure sequences leading to system collapse are discussed and the response surface technique, which is an important method when random parameters cannot explicitly be specified in the limit state function, is presented. At the end, the results of several methods of FORM, SORM, MCS and IS are compared for three limit state functions of fatigue, fracture and extreme environmental loads.

Chapter 4 shows the application of the reliability method at component level for several failure modes. First the reliability of structures based on a fatigue failure mode is studied and the effect of several factors such as the geometry function, the structural damping, spectra and stress models are examined. Furthermore, the updating of fatigue reliability based on inspection results and the methods of inspections are investigated. Furthermore, the traditional formulation for the ultimate limit state function in extreme environmental loads is presented and an approach is recommended to determine the reliability of structural elements under extreme environmental loads using the time history of the usage factor.

The combination of fatigue and extreme environmental loads becomes often critical and may lead to fracture. This type of failure mode has been investigated in this chapter as well and a new method in accordance with the fatigue crack growth formulation is presented to specify the crack size needed in fracture limit state function. The reliability results of the fracture assessment diagram recommended by the British Standard Institute (BS7910, 1999) are compared with the reliability results of the Dijkstra method (Dijkstra et al., 1994).

A system reliability formulation for fatigue failure is given in Chapter 5. At first, a procedure for a system reliability calculation based on the sequence of fatigue failures is presented and then this method is applied for the jack-up platform. The weakened structure after the first fatigue failure, may fail in combination with extreme environmental loads. Therefore, the system reliability based on a combination of fatigue with extreme environmental loads and a fracture failure are investigated in detail in this chapter as well.

Chapter 6 summarizes the main conclusion from this work and suggests areas for future work.



## 2. LIMIT STATE MODELS

---

### 2.1 INTRODUCTION

The objective of a structural design is to build proper structures meeting functional, safety and economical requirements. These aspects are closely connected to each other and an iterative procedure is necessary to achieve an optimal design. The consequences of failure concern the safety of humans, pollution, and the cost of structures and equipment. Therefore, the assessment of the safety of offshore platforms including jack-up rigs is becoming increasingly important.

The current design practice is to use safety factors for a number of failure modes or limit states. Limit state means that the structure is at its limits to meet a set of defined requirements. When the structure fulfils this requirement, it is in the safe state. Vice versa, the structure is in the failure state when this requirement is not met. The boundary between the safe and failure state is called the limit state function or performance function.

For offshore structures four limit states are generally recognized in the regulations, e.g. DNV specification (notes no. 30.6,1992):

- Fatigue Limit State (FLS)
- Ultimate Limit State (ULS)
- Serviceability Limit State
- Progressive Collapse Limit State

The fatigue limit state is defined in relation to the danger of failure considering the effect of cyclic loading and material degradation. The ultimate limit state refers to a failure due to loss of capacity resulting from the maximum loading. The serviceability limit state is defined in accordance with the requirements for normal operations or the durability of a structure e.g. a limitation on excessive vibrations. The progressive collapse limit state refers to failures due to abnormal load effects e.g. impact or accidental loads.

In this chapter, the procedures to determine the fatigue and ultimate failure modes are presented and briefly discussed in relation to their importance to assess the safety over the lifetime. The uncertainties in these limit states will be dealt with as well. The other limit state discussed in this chapter is fracture failure mode. In fact, this type of failure mode is a

specific form of material toughness under extreme environmental loads when defects are present in joints due to fatigue or fabrication. The background and importance of these three limit states for the reliability analysis of jack-up platforms in relation to this research will be explained.

## 2.2 SOURCES OF UNCERTAINTIES IN MARINE ENVIRONMENT

Several sources of uncertainties exist in the marine environments. They can generally be divided into two main categories, i.e. physical and knowledge uncertainties (Ditlevsen and Madsen 1996, Melchers 1999). The knowledge uncertainty is further split up into measurement, statistical and model uncertainty.

The knowledge uncertainties can be reduced by collecting accurate information or using sophisticated models. Physical uncertainty, also named inherent or intrinsic uncertainty shows the natural randomness of quantity. This type of uncertainty can further be measured in the terms of relative frequencies of observation in specified intervals or other relevant sets. The wave height, wind speed and the fatigue parameters are the examples of this type of uncertainties for offshore structures.

The measurement uncertainty arises from inaccuracies in the methods and tools used to assess a quantity. Better instruments or measuring systems can reduce this type of uncertainty. The statistical uncertainty arises from the limit number of samples of observation. The uncertainty in this category may reduce if a larger number of sample sizes are used. A distribution function and its parameters are determined from a specific limited sampling size. The Bayesian approach can help to modify the original distribution function when more sample sizes are available.

The model uncertainty is the uncertainty due to imperfection and the idealization made in the formulation of models for loads and resistances. This type of uncertainty has two sources. The first source of model uncertainty comes from the restriction in the number of basic random variables to idealize the process and ignores other random variables, which are considered to be of secondary importance for the mathematical model. Another source is resulting from the idealization of the mathematical expression.

The most important sources of uncertainties in offshore structures are, Hovde (1995):

1. Material fatigue parameters.
2. Environmental conditions such as data for long-term variation of sea states.
3. Spectra and wave load modelling.
4. Structural modelling.

Some of these sources of uncertainty, such as the material fatigue parameters  $C$  and  $m$ , initial and critical crack sizes in the crack growth model or wave height variations of the sea states are fundamentally random in nature. Other sources of uncertainty such as wave load modelling or structural modelling are due to imperfect or incomplete knowledge of exact modelling. In reliability analysis, uncertainties are generally represented by random variables in which the statistical characteristics such as mean values, standard deviations, or in some

situation the correlation between variables are presented to specify the statistic nature of random variables.

In order to determine the reliability or the failure probability due to fatigue or fracture failure modes, it is required to investigate the mechanics of fatigue and fracture and become aware of the parameters that may have influence on them. In this chapter the fatigue and fracture mechanics are therefore presented in detail and the various parameters that may have influence are discussed.

## 2.3 FATIGUE MECHANICS

To specify a fatigue limit state, it is required to know the mechanical behaviour of fatigue. Fatigue is the process of damage accumulation in material initiated from yielding in the material by the sliding of atomic layers. This sliding is caused by a combination of dislocations and local stress concentrations and each slip, however small, is related to small deteriorations in the material structure, Sobczyk and Spencer (1992). The dislocations are increasing under cyclic stresses and combined to each other cause the plastic deformations. Microscopic cracks are thus created and joined to each other to produce final major cracks. The total time of two phases of crack initiation and growth constitute the complete lifetime of fatigue damage accumulation, as shown in figure 2.1.

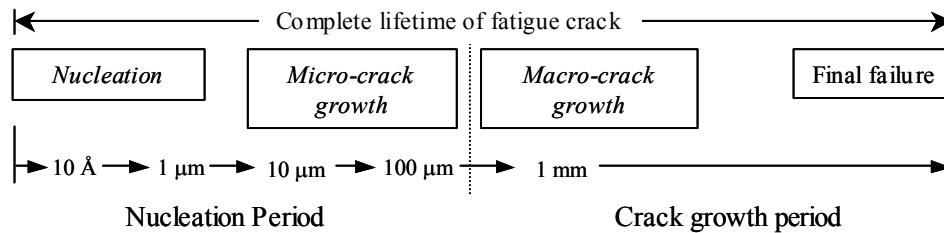


**Figure 2.1** Nucleation and propagation of crack (after Sobczyk and Spencer, 1992)

The fatigue crack typically occurs on the free surface of the body at places of high stress concentrations e.g. weld toes, surface imperfections, grinding boundaries, etc. Based on the material properties and the type of loading, the nucleation phase can be of a different importance in estimating the fatigue life. Experimental observations indicate that at high-cycle fatigue (low stress amplitudes) a significant proportion of the usable fatigue life might be consumed by the crack initiation period whereas at low-cycle fatigue (high stress amplitude), fatigue crack starts to develop in the early cycles, Collins (1993). In addition, in some structural details such as offshore platforms where defects are practically unavoidable due to the fabrication process, crack propagation may be considered to begin during the first load application, Baker et al. (1988).

Two methods can generally be used to evaluate fatigue damage. The first method, which is based on fatigue tests, is named the S-N curve approach. The S-N approach is normally suitable to evaluate actual details against a set of standard experiments but this method cannot provide a proper notification during the operating time, especially when a crack due to fatigue damage occurs. Another approach, known as the crack propagation, is based on the relation between propagation of the crack size and the stress range. As the dimension of the crack size is involved in this method, the inspection of the structure during operation and the

detection or no detection of any crack may provide a reasonable result for updating the safety of platform. Because of this benefit, this approach is utilized in this research work to specify the fatigue limit state function. As the formulation of the fatigue limit state function with this method involves several parameters, which should be clearly defined and examined, a detailed description of this approach is required and presented in the following section.

The fatigue crack growth model is presented in the following section in detail and the semi-elliptic model of crack propagation will be discussed next. The stress intensity factor models applied for tubular joints by different researchers are briefly reviewed. The fatigue strength and loading functions are introduced and the stress distribution, hot spot stress, long-term stress ranges in tubular joint are discussed afterwards. The fatigue safety margin or limit state function is presented in section 2.4. This section ends by describing the uncertainties in fatigue characteristics and types of probabilistic models used to specify the random variables.

### 2.3.1 Fatigue crack growth model

The fatigue crack growth model is based on fracture mechanics and assumes the existence of a flaw or crack e.g. at the weld toe due to a welding process. The starting point for a description of crack propagation in fracture mechanics is the relation between the crack growth rate,  $da/dN$ , and the stress intensity factor range,  $\Delta K = K_{max} - K_{min}$ .

A typical representation of crack growth behaviour in steel material obtained from experimental data is illustrated in figure 2.2, Naess (1985). As shown in this figure, the crack growth actions in metals can generally be categorized into three phases i.e. crack initiation, crack propagation and final fracture.

The first region, the crack initiation phase is related to microscopic material behaviour and a rational theory describing this stage is limited. A description given by Sobczyk and Spencer (1992) relates the time consumed by crack nucleation and the time that the micro-crack grows

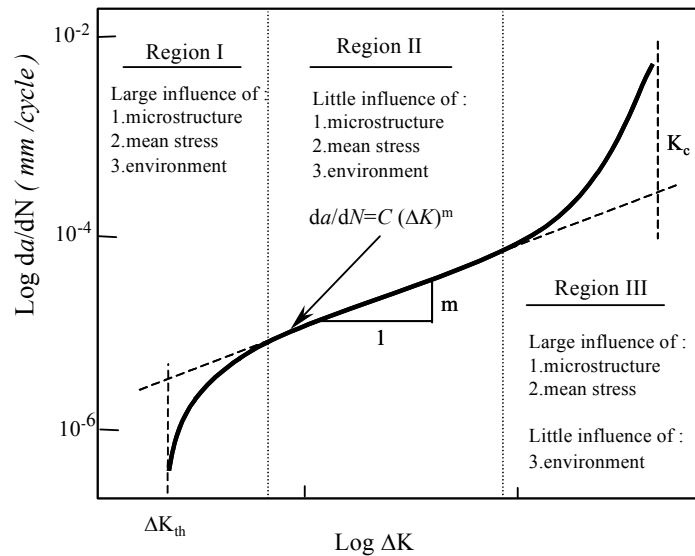


**Figure 2.2** Representation of fatigue crack growth in steel structure, Naess (1985)



to make a macro-crack of a measurable size, see figure 2.1. Since defects are always supposed to be present in welded structures due to the fabrication process, the initiation stage is usually considered less important and crack initiation is consequently neglected.

The second part of crack propagation is usually assumed to be the period with the largest contribution to the fatigue lifetime. During this phase, the crack propagation is stable, follows a power law relation, and is relatively insensitive to microstructure and tensile properties. During the last phase, when the maximum stress range intensity factor  $\Delta K$  in the applied stress cycle reaches a value of about 70 percent of the material fracture toughness  $K_C$ , the crack growth rate,  $da/dN$  increases rapidly due to the interaction between fatigue and the fracture mechanism, leading to an unstable fracture at  $\Delta K = K_C$ .

Since the most important contribution of a crack propagation comes from the second phase, the crack growth is often idealized as the dotted line in figure 2.2. The general description of this line, originally presented by Paris and Erdogan (1963), is now accepted as the formulation for fatigue crack growth in metal. Based on this formulation the increment in the crack size  $dr(\phi)$  during a load cycle  $dN$  at a specific point along the crack front is related to the range of the stress intensity factor  $\Delta K_r(\phi)$  for that specific load cycle with

$$\frac{dr(\phi)}{dN} = C_r(\phi)(\Delta K_r(\phi))^m, \quad \Delta K_r(\phi) > 0 \quad (2.1)$$

where  $C_r(\phi)$  and  $m$  are fatigue parameters for that specific point along the crack front, and  $\phi$  is the location angle. By extending this expression in the directions of depth and length, the expressions for the propagation of the crack in the depth and the surface of flaw can therefore be specified. More details on this approach are presented in the following sections.

### 2.3.2 Semi-elliptical crack propagation

To derive an expression for the propagation of a crack in the depth and the surface of flaw, the problem is simplified by considering that the fatigue crack growth has initially a semi-elliptical shape and remains semi-elliptic during the propagation of a crack, see figure 2.3. The crack depth ( $a$ ) and the crack length ( $2c$ ) are regarded as two parameters sufficient to describe the crack front during propagation. As a consequence of this assumption, the following pair of differential equations is used instead of the general equation (2.1) for the deepest point and the end-point of the crack at the surface, Raju and Newman (1981).

$$\frac{da}{dN} = C_A(\Delta K_A)^m, \quad a(N_0) = a_0 \quad (2.2)$$

$$\frac{dc}{dN} = C_C(\Delta K_C)^m, \quad c(N_0) = c_0 \quad (2.3)$$

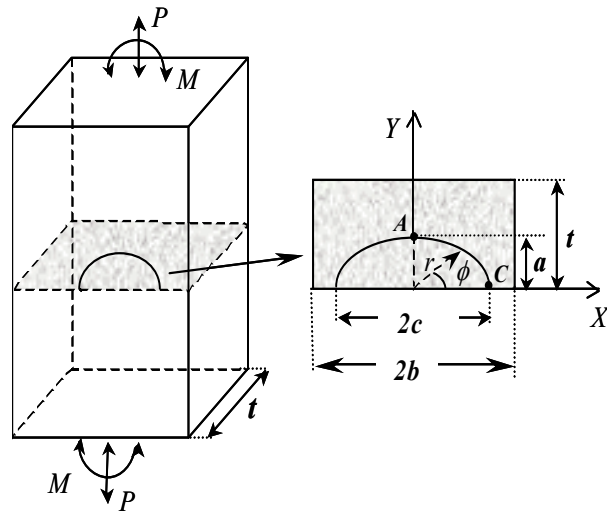


**Figure 2.3** Semi-elliptical surface crack, Raju and Newman (1981)

Two subscripts  $C$  and  $A$  refer to the end point and the deepest point of the crack, respectively. Shang-Xian (1985) revealed that the material parameters  $C_A$  and  $C_C$  are independent of the crack growth model and could only be related to each other by the following expression.

$$C_A = 1.1^m C_C \quad (2.4)$$

Moreover, Shang-Xian showed that the material property  $m$  depends on the fatigue crack propagation and is independent of the crack size in both directions of depth and surface. The failure criterion normally refers to a critical value of the crack depth  $a$  or the crack length  $c$ , thus it is convenient to rewrite the last equations as follows,

$$\frac{dc}{da} = \frac{C_C}{C_A} \left( \frac{\Delta K_C}{\Delta K_A} \right)^m, \quad c(a_0) = c_0 \quad (2.5)$$

$$\frac{da}{dN} = C_A (\Delta K_A)^m, \quad N(a_0) = N_0 \quad (2.6)$$

The general expression for the stress intensity factor is  $K = Y\sigma\sqrt{\pi a}$ , where the geometry function  $Y$  accounts for the effect of all boundaries, i.e. width, thickness, crack front, etc. If substitute this expression in equation (2.5), it will be clear that this equation is independent of the stress history and solely depends on the propagation of the crack.

The calculation of stress intensity factors for tubular joints is a difficult task due to the complex geometry and the three dimensional nature of the stress distribution. The fatigue crack observed in the member joint is highly irregular and an exact analytical solution does not exist. However, in the last decay several attempts have been made to develop approximations for tubular joints. These can be grouped into two main categories: experimental stress intensity factors and analytical stress intensity factors. Several stress intensity factors can be found in the handbooks such as Sih (1973), Tada et al. (1973, 2000), Rooke and Cartwright (1976) for idealized components, specific crack geometries and a simple stress distribution while the most applied geometry functions in offshore structure are originating from modifications of expressions presented by Raju and Newman (1981) for plates, later modified for pipes and rods, subjected to remote membrane and bending stresses, Raju and Newman (1986).

Based on the results of a three-dimensional finite elements analysis, Raju and Newman (1981) developed an empirical expression for the stress intensity factor  $K(\phi)$  for a surface crack in a finite plate subjected to tension and bending loads. The equation has been fitted on the finite element results for two types of remote tension and bending loads applied to a surface cracked-plate. The inferred stress intensity equation from this research is given by

$$K(\phi) = (\sigma_t + \sigma_b) \sqrt{\pi a} (1/Q)^{1/2} \frac{1 + H\sigma_b/\sigma_t}{1 + \sigma_b/\sigma_t} F\left(\frac{a}{t}, \frac{a}{c}, \frac{c}{b}, \phi\right) \quad (2.7)$$

where  $\sigma_t$  is the remote uniform tension stress,  $\sigma_b$  is the remote outer-fibre bending stress. Also,  $a$  is the crack depth,  $c$  is the half of crack length,  $t$  is the thickness of plate,  $b$  is the half width of panel. Moreover,  $\phi$  is the angle that defines the position of considered point,  $Q$  is the shape factor,  $F$  and  $H$  define the boundary-correction factor. In the investigation of Raju and Newman (1986) to determine the stress intensity factors of rods and pipes, they demonstrated that the difference in stress intensity factors between semi-elliptical cracks in a plate and a pipe with a low thickness to diameter ratio is small. Later Karlsen (1986) observed good

agreement between the results of finite element analyses of K and T joints and the Raju-Newman's expression with correction factors to assume the local stress concentration introduced at the weld toe.

The stress intensity factors based on the Raju and Newman approach for the deepest point  $A$  ( $\phi = \pi/2$ ) and the end surface point  $C$  ( $\phi = 0$ ) of tubular elements are specified with

$$\begin{aligned}\Delta K_A &= \Delta \sigma_{total} \sqrt{\pi a} Y_A \\ \Delta K_C &= \Delta \sigma_{total} \sqrt{\pi c} Y_C\end{aligned}\quad (2.8)$$

$Y_A$  and  $Y_C$  are geometry functions for the deepest and end surface points of the crack and are specified in accordance with the following expressions.

$$Y_A = (1/Q)^{1/2} \frac{1+H_A\alpha}{1+\alpha} F\left(\frac{a}{t}, \frac{a}{c}, 0, \frac{\pi}{2}\right) \quad (2.9)$$

$$Y_C = (1/Q)^{1/2} \frac{1+H_C\alpha}{1+\alpha} F\left(\frac{a}{t}, \frac{a}{c}, 0, 0\right) \quad (2.10)$$

$\sigma_{total}$  and  $\alpha$  are the summation and the ratio between remote bending and membrane stresses, respectively.  $H_A$  and  $H_C$  are the  $H$ -values taken at  $\phi = \pi/2$  and  $\phi = 0$ , respectively. Details about  $F$ ,  $Q$  and  $H$  functions are presented in Appendix A.

Now, if the stress intensity factors are substituted in expression (2.5), it is clear that this expression is independent of the stress ranges and only depends on the crack growth shape and stress ratio ( $\alpha$ ). By either fixing the ratio of  $a/c$  or expressing the crack length ( $2c$ ) as a function of the crack depth ( $a$ ) with the method presented by Shang-Xian (1985), equation (2.5) can be reduced to a constant and solved independently of equation (2.6). This model is referred to as a one-dimensional crack growth model.

For offshore tubular elements, Kirkemo (1988) recommends using Raju-Newman's expression with a weld toe correction factor given by Smith and Hurtworth (1984) to consider the effect of a discontinuity in the weld toe due to the welding. The geometry function derived in this work is the multiplication of  $Y_{unwelded}$  and  $M_k$ , where  $Y_{unwelded}$  is the geometry function of a semi-elliptical crack using a linear stress field (Raju and Newman equation) with a fixed aspect ratio. According to this approach, the geometry function expression for a constant  $a/c$  and  $\alpha$  equal to 0.15 and 5 respectively is given by,

$$\begin{aligned}Y_{welded} &= M_k(a)Y_{unwelded} \\ Y_{unwelded} &= 1.08 - 0.7(a/t) \\ M_k(a) &= 1.0 + 1.24 \exp(-22.1(a/t)) - 3.17 \exp(-357(a/t))\end{aligned}\quad (2.11)$$

where  $t$  is the thickness of an element and  $a$  is the crack depth. In another investigation, Aghakouchak and Stierner (2001) recommend the following expression for the geometry function of a tubular element,

$$Y_A = 1.4557 - 6.352(a/t) + 20.833(a/t)^2 - 30.506(a/t)^3 + 15.744(a/t)^4 \quad (2.12)$$

which was established based on the polynomial fitting of the mean value of experimental data. However, the applied stress ratio and crack aspect ( $a/c$ ) for deriving this expression are not clear.

Moan et al. (1993) modified the approach of Kirkmo considering the variations of the aspect ratio,  $a/c$  with a propagation of a crack. They explained that the two-dimensional crack growth model proposed by Raju and Newman might give a wrong aspect ratio evolution due to coalescence of the crack. From fatigue tests it is observed that, when the joint is subjected to a fatigue load, multiple micro-cracks are initiated in the region of the maximum hot spot. These micro-cracks grow independently for some time and coalescence occurs from a single long dominant crack. Therefore, the aspect ratio presented in this research is divided into two stages, one before coalescence, the other one during and after coalescence of the crack.

The geometry functions derived, based on these methods, are a simplification of the complexity of the problem. Hence, usually in the reliability analysis a random geometry correction factor  $\delta_Y$  is used to consider uncertainties arising from this simplification, crack coalescences and weld geometry effects, Shetty (1992).

Since the selection of the geometry function may influence the reliability index, and no preference is given for tubular joints especially for jack-up platforms, these geometry functions will be compared in chapter 4 to select a proper geometry function.

### 2.3.3 Fatigue strength function and fatigue loading function

Jack-up structures are subjected to (oscillatory) stresses due to environmental loading. To specify an expression to relate the propagation of the crack through the thickness of a specific element with the number of stress ranges, the geometry function derived in the preceding section is substituted in equation (2.6). Under a variable amplitude loading, the integration of this equation through the thickness from an initial defect size  $a_0$  to a crack size  $a(t)$  after time  $t$  gives the following expression.

$$\int_{a_0}^{a(t)} \frac{da}{C_A (Y_A \sqrt{\pi a})^m} = \sum_{i=1}^{N(t)} S_i^m \quad (2.13)$$

where  $S_i$  is substituted for  $\Delta\sigma_{i,total}$  in the stress intensity equation and shows the stress-range magnitude for the  $i^{\text{th}}$  stress cycle. Moreover,  $N(t)$  is the number of stress cycles likely to occur during the service time. Since the right hand side of this equation is only depending on the loading and the left hand side to the crack growth, we name them as the fatigue loading function,  $\psi_L(t)$  and the fatigue strength function,  $\psi_R(t)$  respectively. For offshore structures, it is assumed that the stress cycle interaction effects are usually of minor importance, (Shetty 1992). In such case, the distribution of the fatigue loading function in accordance with the long-term wave condition may be specified independent of a fatigue strength function and the interaction of cycles can be ignored.

A direct procedure of calculating the distribution of the loading function is based on simulating the stress time-history, and counting all the stress cycles in accordance with a specific cycling counting method. When the stress process is narrow-banded, the stress cycle can easily be identified and the stress range distribution can simply be specified with the standard deviation of the stress process and using a Rayleigh distribution. But this is not a case for a wide-banded stress range, as usually occurs in offshore structures and more sophisticated cyclic counting methods have to be used. Several counting methods have been presented in Downing and Socie (1982). The rainflow counting method is a widely used

approach because it gives good results on a fatigue damage prediction. Since the rainflow counting method is computationally very expensive, a much simpler approach such as peak counting methods have been recommended for marine structures.

The peak counting method is an accepted alternative method to the rainflow counting. In this method, the local maximums of the stress process are of more concern and each of these local maxima are paired with the local minima of the same size. This assumption is conceptually validated, as in a large stress process it is possible to find for each local maximum a local minimum of the same magnitude. The distribution function of these local maximums can therefore be derived using Gaussian or non-Gaussian assumptions on the original stress process, Madsen et al. (1986).

Since the stress cycle in equation (2.13) is random, for a large number of stress cycles  $N(t)$  the summation term can approximately be estimated with its expected values as

$$\psi_L(t) \approx E \left[ \sum_{i=1}^{N(t)} S_i^m \right] = E[N(t)]E[S^m] \quad (2.14)$$

The expected number of stress ranges  $E[N(t)]$  and  $m^{\text{th}}$  value of stress range  $E[S^m]$  can be specified if the probability density function of the stress range is known. In the case of the peak counting method, the expected number of stress ranges may be taken as the expected number of peaks in the stress time history, hence,  $E[N(t)] = \nu_p t$  and the  $m^{\text{th}}$  expected stress range can be determined with,

$$E[S^m] = \int_0^{\infty} S^m f_S(s) ds \quad (2.15)$$

in which  $f_S(s)$  is the probability distribution of stress range ( $S$ ) and  $\nu_p$  is the expected frequency of the peaks. Where the stress process is stationary, Gaussian and narrow-banded it can be shown that the stress peaks and stress ranges follow a Rayleigh distribution. For this case, the fatigue loading function can simply be assessed from

$$\psi_{L, nb}(t) = \nu_0 t (2\sigma\sqrt{2})^m \Gamma\left(\frac{m}{2} + 1\right) \quad (2.16)$$

where  $\nu_0$  is the expected frequency of zero-crossings of the stress process. Moreover,  $\sigma$  is the root mean square value of the stress process and  $\Gamma(\cdot)$  is the Gamma function. Due to its simplicity, the Rayleigh distribution is widely used in design practices for modelling stress ranges in tubular joints but as already stated, the exact stress process in offshore structures is wide-banded and non-linear. Sarkani et al. (1996) showed the narrow-banded assumption can reduce the time to fatigue failure. Hence, the wide-banded model should be used in the fatigue damage calculation. It is interesting to note that if the stress process is wide-banded and Gaussian, the distribution of a stress peak in accordance with the bandwidth parameter varies between Rayleigh and Gaussian distribution, Wirsching et al. (1995).

Wirsching and Light (1980) presented an empirical correction factor for wide-banded fatigue damages. The correction term is based on simulating the time history of a specific wide-banded stress process and using the rainflow counting method to estimate the stress range. The correction factor of this specific wide-banded process is therefore estimated by

comparing it with a narrow-banded result. This approach is repeated for several spectra bandwidth parameter  $\varepsilon$  and the final expression for the loading function is derived as follows,

$$\psi_L(t) = \lambda \psi_{L,nb}(t) = [a + (1-a)(1-\varepsilon)^b] \psi_{L,nb}(t) \quad (2.17)$$

$$a = 0.926 - 0.03m, \quad b = 1.587m - 2.323$$

where in this expression  $\lambda$  is the Wirsching correction factor and  $m$  is the fatigue material characteristic as explained in section 2.3.2. It is notable that the correction factor generally approaches the narrow-banded results when the spectra bandwidth approaches to one.

In another procedure, based on results derived from extensive time history simulations of wide-banded stress spectra, Zhao and Baker (1990) recommended to use the combination of two distribution functions to specify the whole stress range distribution. According to the technique described in this research the characteristics of the theoretical distribution function, e.g. mode and moments, are specified in a way to be as close as possible to the characteristics of the distribution function obtained from simulation. This model is finally validated by comparing with the rainflow counting method. The probability distribution presented in this research is a combination of Weibull and Rayleigh distributions using a weighting parameter  $\omega$ , which is depending on the spectra irregularity factor ( $\alpha$ ). The loading function specified in this research is as follows,

$$\psi_L(t) = v_p t (2\sigma)^m [(1-\omega)(\sqrt{2})^m \Gamma(1 + \frac{m}{2}) + \omega(8-7\alpha)^{-m/b} \Gamma(1 + \frac{m}{b})] \quad (2.18)$$

where,

$$\omega = (1-\alpha) / [1 - \sqrt{\frac{2}{\pi}} \Gamma(1 + \frac{1}{b}) (8-7\alpha)^{-1/b}] \quad (2.19)$$

$$b = \begin{cases} 1.1 & \text{for } \alpha \leq 0.9 \\ 1.1 + 9(\alpha - 0.9) & \text{for } \alpha > 0.9 \end{cases}$$

where  $v_p$  is the expected frequency of peak and the spectra irregularity factor ( $\alpha$ ) is related to the spectral bandwidth ( $\varepsilon$ ) with  $\alpha^2 = 1 - \varepsilon^2$ .

The assumption of Gaussianity in a stress process can be violated due to the non-linearity in a structure, the drag term of hydrodynamic loads and the variability in the submerged sections when the waves are passing a structure. Hence, Gaussian models may significantly misrepresent the stress process. For a non-Gaussian process, Winterstein (1988) and Jensen (1990) have shown the Hermit model may provide better results than other distribution models because it is possible to take the higher moments (up to four) of the stress process into account.

### 2.3.4 Stress distribution in tubular joints and long-term stress range

In fatigue crack growth analysis, the determination of the critical stress for each component is an essential task. The stress analysis of tubular joints, although basically simple in geometry, is complicated, while even much more complicated details are being used in the offshore industry. In addition, the presence of the weld at the intersection causes major variations in the stress distribution. This complex stress distribution is generally controlled by the combination of three nominal, geometry and notch stresses, Etube (2001).

Stresses resulting from the finite element analysis of structures as beam and column elements are termed the nominal stresses. These nominal stresses are obtained from the finite element analysis using the external loads and finite element modelling of the structure. The nature of such stresses is entirely dependent on the shape configuration of the joints and the type of loading. The second stresses, geometrical stresses, arise from the differences in the stiffness of brace and chord wall, which varies along the intersection, causing the tube wall to bend in order to ensure compatibility in the deformation of the chord and brace walls at the intersection. This deformation, which depends on the mode of loading, therefore changes the stress distribution and produces the geometrical stresses. The notch stresses are the result of discontinuities introduced at the weld toe due to an abrupt change. These stresses are influenced by the weld size and the weld geometry, and are independent of the overall joint geometry.

The complexity in the calculation of geometrical and notch stresses and the need to better represent the stress distribution in tubular joint leads to the use of stress concentration factors in fatigue analysis.

In fatigue analysis, it is assumed that the hot spot stresses entirely control the fatigue life of tubular welded joints and occur at places, which are most highly stressed. This is a stress at the weld toe calculated by scaling the nominal stresses and using a Stress Concentration Factor (SCF). As the fatigue damage may occur anywhere around the intersection, the hot spot stresses should not only be evaluated for a specific point. Hence, several points around the circumference of the intersection with the most highly and likely damage potential should be selected as the places for fatigue damage occurrence.

Since fatigue is the damage accumulation of the long-term distribution of the stress ranges in a specific joint, the short-term loading function expressed in the last section can not directly be applied for the long-term calculation of fatigue damage, hence a modification is required. If the long-term wave climate is represented by several sea-states, the long-term cumulative fatigue loading over a service exposure time  $t$  can be related by a weighted summation of the load contribution from an individual short-term sea state,

$$\psi_L^l(t) = \sum_{i=1}^k E_i[S^m] \omega_i t P_i \quad (2.20)$$

where  $E_i[S^m]$  and  $\omega_i$  are the  $m^{\text{th}}$  expected of the stress range and the weighting function, respectively.  $P_i$  is the relative occurrence frequency of  $i^{\text{th}}$  sea-state and the superscript  $l$  in this formulation indicates the long-term summation. When the stress process is narrow-banded, the average peak of response will be almost the same as the average zero crossing. However, in a jack-up structure, as well as in other sensitive dynamic structures, this may not be a valid assumption and the original frequency derived from the stress process should be incorporated due to the wide-banded nature of the process. The weighting factor therefore is expressed for each sea state as  $\omega_i = v_{p_i} / v^l$ , where  $v_{p_i}$  is the average peak-frequency of the stress-cycles in the specific sea-state.  $v^l$  is the long-term average frequency of the stress range and can be estimated from the following expression.

$$v^l = \sum_{i=1}^k v_{p_i} P_i \quad (2.21)$$

As in a fatigue calculation the number of sea states is usually large, it is desirable to use a distribution, which makes it possible to model and analyze the stress ranges in the long-term. Due to its simplicity, the Weibull distribution is often used as a long-term distribution of stress ranges and its parameters can be found by fitting them on the combination of the outcome of several short-term descriptions of the stress range. By using the Weibull distribution function for the long-term stress range, the loading function can be obtained with the expression,

$$\psi_L^l(t) = v^l t^m A^m \Gamma(1 + \frac{m}{B}) \quad (2.22)$$

where  $A$  and  $B$  are scale and shape functions of the Weibull distribution, respectively. The final expression for the propagation of a fatigue crack in the specific hot spot point of the joint can be obtained by substituting the loading function into formulation (2.13). Hence, the final expression to relate the fatigue strength function to the fatigue loading function is as follows.

$$\int_{a_0}^{a(t)} \frac{da}{C_A (Y_A \sqrt{\pi a})^m} = v^l t^m A^m \Gamma(1 + \frac{m}{B}) \quad (2.23)$$

This expression is the original formulation to relate the fatigue crack growth  $a(t)$  with the fatigue loading function.

## 2.4 FATIGUE LIMIT STATE FUNCTION

In a reliability analysis, the fatigue limit state function or safety margin must be defined. The fatigue limit state function shows the limit between safe and failure state. The element is in a safe state if a specific requirement, here the fatigue resistance, is fulfilled and vice versa the element is in a failure state when this requirement is not met.

In the fatigue degradation process, usually the strength of a structural detail is described in terms of time to failure because the strength degrades over the time. The time of propagation of a crack from the initial size  $a_0$  to a specific size  $a(t)$  is given by equation (2.23). The time required to develop a critical crack size such as  $a_{Cr}$  can be determined with

$$\tau_{cr} = \frac{1}{v^l A^m \Gamma(1 + \frac{m}{B})} \int_{a_0}^{a_{Cr}} \frac{da}{C_A (Y_A \sqrt{\pi a})^m} \quad (2.24)$$

where the critical crack size may be specified based on the through-the-thickness crack of a tubular element. This critical propagation time of crack  $\tau_{cr}$  is subjected to several sources of uncertainties, which are coming from the modelling and the characteristics of the sea environment, the structure and fatigue. Some of these uncertainties are random in nature (inherent) while others are random due to lack of knowledge.

Development of through-the-thickness cracks may not cause a significant change in strength or stiffness of a member to provoke section failure. The crack should propagate significantly along the circumference of a tubular section before final failure occurs. The time to develop such a crack will be a combination of the time to develop a through-the-thickness crack and the time needed for the crack to propagate around the circumference. Hovde (1995) claimed that this extra time is most likely small when compared to the time required to develop a through-the-thickness crack and the conservative assumption would be to neglect this time.



Contrary to this opinion, Hanna and Karsan (1989) revealed that the time to develop a section failure ( $\tau_f$ ) could be related to the time of the first through-the-thickness crack with  $\tau_f = \delta_{tf} \tau_{Cr}$ , where  $\delta_{tf}$  being a random correction factor. Test data showed that  $\delta_{tf}$  is relatively independent of the stress parameters and can be represented by a random variable. However, in a probabilistic approach for the scheduling of the inspections time of the British Gas platforms provided by WS Atkins, a constant deterministic value of 1.11 is reported, which this value is based on reviewing the published information and in-house data carried out by Oakely et al. (1994).

To take into account the uncertainty in loads, stress calculation and stress concentration factors, Dalane (1993) recommended to modify the stress range described in the previous sections by multiplying them with the three random model corrections factors,  $\delta_F$ ,  $\delta_S$  and  $\delta_{SCF}$ , each one representing the uncertainty in the loads, stress calculation and stress concentration factors in the specific hot-spot point respectively. Fatigue failure is therefore defined when the random fatigue propagation time ( $\tau_f$ ) becomes less than the service time of the structure. The safety margin or limit state function required in fatigue reliability can therefore be expressed with

$$g(\tau) = \tau_f - \tau_{\text{Service time}} = \frac{\delta_{tf}}{v^l \delta_F^m \delta_S^m \delta_{SCF}^m A^m \Gamma(1 + \frac{m}{B})} \int_{a_0}^{a_c} \frac{da}{C_A (\delta_Y Y_A \sqrt{\pi a})^m} - \tau_{\text{Service time}} \quad (2.25)$$

where  $\tau_{\text{Service time}}$  is the service time of the structure. The structure is in a safe state when this limit state function is larger than zero and vice versa, is in failure state when it is smaller than zero. The probability of occurrence of such an event is called the probability of fatigue failure.

### 2.4.1 Uncertainty in fatigue characteristics

The characteristics of crack growth are usually generated in laboratories under constant amplitude and cyclic loading on simple specimens with known stresses. During controlled crack growth tests under constant amplitude loading, the propagation of a crack shows considerable scatter, Virkler et al. (1979). Among several probabilistic models proposed to describe the stochastic nature of crack propagation, it seems that a simple random modelling of the parameters  $C$  and  $m$  in the Paris and Erdogan equation yields a proper representation.

In the random crack growth approach, either both or just one of the material parameters  $C$  and  $m$  may be expressed as random variables. The test result showed negative correlation between these parameters with a typical magnitude of  $-0.95$ , (see e.g. Tanaka et al., 1981, Cortie and Garrett, 1988). However, this correlation is not based on the physical property of the crack growth parameters but follows from the mathematical form of the crack propagation law, Madsen (1997). In common practice, the value of  $m$  is fixed and all the uncertainty is expressed through the value  $C$ , Hovde (1995). A general approach is to assume a lognormal distribution for  $C$ . In accordance with the DNV specification (notes no. 30.2, 1984), the mean of  $\ln C$  is  $-29.84$  for an element in air or in the case of cathodic protection with the standard deviation of  $0.55$ , and  $m$  is supposed as a deterministic parameter, which is equal to  $3.1$ . For an element in seawater without cathodic protection, the mean and standard deviation of  $\ln C$  in accordance with this specification are recommended to be  $-31.01$  and  $0.77$  respectively, and  $m$  is  $3.5$ . However, these values are proposed for use when no other relevant data are available. Several other intermediate values of the standard deviations are

recommended by e.g. Faber et al. (1992), Shetty and Baker (1990), Snijder et al. (1987), respectively 0.29, 0.25, 0.30. In this research work, the values recommended in the DNV specification are applied.

In fatigue reliability analysis, it is necessary to specify the statistical characteristics of the initial crack size. The crack is assumed to initiate from very small defects, which originate from the welding process. The size and occurrence rates of defects vary considerably and are influenced by the fabrication yard, the welding procedure, the welding position, the type of joints, etc. (Baker et al., 1988), which as a matter of fact are all factors of uncertainty.

Data on probabilistic types of initial weld defects are rarely reported. Kountoris and Baker (1989) recommended using lognormal distribution with a mean of 0.73 and standard deviation 0.78 for initial weld defects. These values are obtained through statistical analysis of a large amount of weld defect data from the Conoco Hutton Tension Leg Platforms. However, these values may lead to incorrect results for tubular joints because the quality and quantity requirements for the detection of weld defects in a TLP differ significantly from those in tubular joints of jackets or jack-up platforms. The latest investigation on non-propagating crack detection during the period from 1972 till 1995 on North Sea jacket platforms by Moan et al. (2001) showed that the initial crack depth could be specified by an exponential distribution with a mean value of 0.38 mm. However, they explained that using this value for fatigue calculations without any modification of the fracture mechanics and response analysis model could lead to overly conservative results. Bokalrud and Karlsen (1982) found that the initial crack depth could be expressed by the exponential distribution with a mean value of 0.11 mm.

The threshold on the stress intensity range is imposed to consider the effect of a non-crack propagation section of crack growth, see figure 2.2. However, in reliability analysis this threshold limit is often ignored. This assumption may lead to a conservative result for the failure probability calculation of fatigue limit state, Hovde (1995).

## 2.5 ULTIMATE LIMIT STATE

The objective of structural design is to ensure that the stresses resulting from maximum loading on a structure are adequately below the specific limit. This condition requires the use of the ultimate limit state in a reliability analysis. The ultimate limit state refers to a failure due to the loss of capacity caused by the maximum environmental loading. Typically, two types of ultimate limit states may be utilized for a reliability calculation of jack-up platforms.

The first ultimate limit state is based on a global response of the platform and the global failure caused by the overturning moment or shear force. This type of ultimate limit state has been applied in the research projects of Karunakaran (1993), Jensen et al. (1991) and Van de Graaf et al. (1993). In this method, it is not possible to investigate the failure of an individual element or joint due to the extreme environmental load. However, failure of an individual element or joint may reduce the resistance of the structure significantly.

The second ultimate limit state function refers to the loss of capacity of a structural element or joint in accordance with the formulation specified in the codes such as API RP 2A-LRFD

(1993) or NORSOK (1998). This approach has already been applied for jacket platforms by Shetty (1992) and Dalane (1993), and for a jack-up platform by Daghigh (1997).

In the present research study the ultimate limit state function has been derived based on the second approach. Details are presented in the following sections. First, the concept of a usage factor or a utilization ratio is discussed. Furthermore, a new methodology is recommended to consider the correlation between random variables in the ultimate limit state function directly.

Several formulations are given in the design code to specify different types of losing capacity due to the interaction of several types of loading configurations. These formulations, which are also known as failure modes or criteria, are usually expressed as a normalized function of the stresses in the members. They should not exceed a specific value i.e. one. The value of this function is generally referred to as the “utilization ratio” or “usage factor”,  $U$ , and a code failure occurs if it exceeds this value. An example of a utilization ratio for buckling of a tubular member in combination of compression and bending stresses is presented in API RP 2A-LRFD (1993) as follows,

$$U_{Buckling} = \frac{f_C}{F_{cn}} + \frac{1}{F_{bn}} \sqrt{\frac{C_{my}^2 f_{by}^2}{(1 - \frac{f_C}{F_{ey}})^2} + \frac{C_{mz}^2 f_{bz}^2}{(1 - \frac{f_C}{F_{ez}})^2}} \quad (2.26)$$

where  $f_C$  is the axial compression stress,  $f_{by}$  and  $f_{bz}$  are the bending stresses in  $y$  and  $z$  direction respectively.  $F_{cn}$  and  $F_{bn}$  are the nominal capacity of the element in axial compression and bending stresses, which depend on the characteristics of the elements. Other parameters of this formulation are presented in API RP 2A-LRFD(1993). In the next chapters, other formulations of usage factors for combination of tension and bending stresses are presented. It should be kept in mind that all the strength reduction factors in the formulation are setting into one to represent the ultimate limit of failure. The structural element is in a safe state when the usage factor expression is less or equal than one and it is in the failure state when it exceeds one.

Based on a code specification, various failure modes for each member and a connection may be specified e.g. yielding, punching or buckling. Daghigh (1997) investigated these failure modes for a jack-up platforms and Dalane (1993) for a jacket platform. They concluded that the most important failure mode for jack-up and jacket structures is the stability failure mode. However, it has not been investigated whether this is the case for bracing elements when these components are under both axial tension and compression stresses. Therefore, in the following section a methodology to specify the ultimate limit state for a combination of different failure modes that may occur in structural elements is presented.

### 2.5.1 An approach to specify the ultimate limit state

The structural elements during the lifetime of a structure are under different combinations of loads, such as the combination of tension and bending stresses or compression and bending stresses. A single specific failure mode cannot sufficiently represent the potential of the failure of an element. Furthermore, the correlation of stress distributions such as axial and bending stresses should be taken into account in reliability analysis.

In the research of Daghigh (1997), the reliability analysis has been carried out based on determination of a probability distribution of maximum stresses (axial and bending stresses) using the time history of axial and bending stresses separately and the ultimate (buckling) limit state, however, without any assumption on the correlation between stresses or the possibility of the changes in the failure modes (yielding or buckling) over the stress process. To overcome this shortcoming and consider this effect simultaneously a method proposed by Videiro and Moan (1999) is considered here.

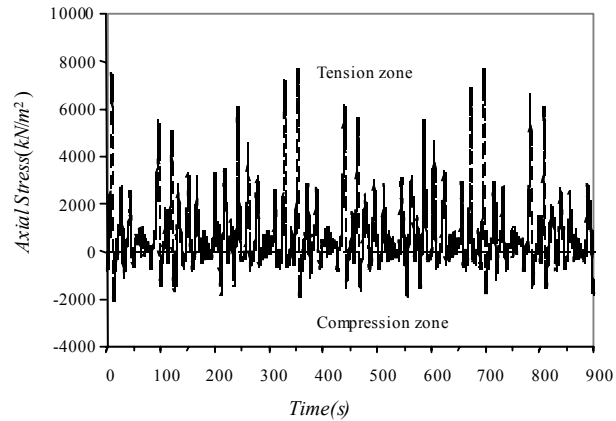


**Figure 2.4** Axial stress in bracing element of jack-up platform,  $H_S=16.1\text{m}$

The method is based on the application of the probability distribution determined with the time history of the utilization ratio and not on the probability distribution of axial and bending stresses individually. By using the time history of the usage factor, it becomes possible to model different failure modes when the stress-state of a structural element changes during the time. For example, the bracing element of a jack-up structure is occasionally under the combination of tension and bending stresses or compression and bending stresses, see figure 2.4. Therefore, it is possible to simulate the time history of the usage factor applying two failure modes, one when the element is under combination of axial tension and bending stresses and another one when under compressive and bending stresses.

## 2.6 FRACTURE MECHANICS

The fracture failure mode is an important failure mode of a structure when extreme environmental loads are combined with a crack, which may be present in a structural element as a built-in crack resulting from the fabrication process or from fatigue. As already illustrated in the crack growth diagram figure 2.2, the material fracture toughness is a limit to the stress intensity factor. In a simple way this is a limit for fracture criteria, which the stress intensity of the flawed element should not violate. However, the actual fracture behaviour is more complex. In the following sections the fracture mechanics criterion is presented and the concept of the failure assessment diagram, which accounts for the interaction of elasto-plastic and fracture failure, is discussed.

### 2.6.1 Fracture Mechanics criteria

The fracture failure involves the unstable propagation of a crack, which may be caused either from a brittle or a ductile behaviour of materials. The fracture mechanic models are therefore grouped into two categories, namely; the linear elastic fracture mechanics methods (LEFM), where brittle fracture governs; and the elasto-plastic fracture mechanics methods (EPFM), where ductile fracture failure is dominating. It is important to note that the most approaches available to model fracture mechanics are only suitable in restricted situations and should be

handled with care. For example, the linear elastic fracture mechanics methods i.e., the energy balance approach and the stress intensity approach, should not be used for structures exhibiting a significant plastic flow around the crack tip, while the crack tip opening displacement (CTOD) method and the J-integral method are the methods available for structures that show an elasto-plastic behaviour, Shetty (1992).

Among several elastic-plastic fracture mechanics methods, the method presented by the British standard Institute is most widely used in the offshore industry. The early version of this guidance is based on so called CTOD design curve derived from wide plate tests, PD6493 (BSI, 1980), but has nowadays been revised and updated in BS7910 (1999) based on the J-integral method.

The applicability of linear elastic fracture mechanics (LEFM) has been investigated by Turner (1984) who demonstrated that the method might be satisfactory when applied on a very small crack tip plastic zone such as in the case of high tensile material under plain strain. However, this approach may lead to incorrect results when the size of a plastic zone is large. It is more convenient for a practical application to adapt the procedure to cover the entire range from linear elastic to fully plastic behaviour, i.e. an analysis that accounts for both brittle fracture and plastic collapse. The failure assessment diagram (FAD) recommended by the British Standard Institute (BS7910, 1999) is an example of such an analysis. At low stresses, this analysis reduces to LEFM but predicts a collapse well, and at intermediate and high stresses the method applies the EPFM model if necessary.

## 2.6.2 Failure Assessment Diagram

The failure assessment diagram recommended in BS7910 (1999) has been developed to describe the interaction between fracture and collapse of flawed structures. This standard offers three levels of assessment methods based on complexity and accuracy appropriate for a specific situation. All these three levels are expressed in the failure assessment diagrams where the vertical axis is a ratio of the parameters causing failure in terms of fracture mechanics and the horizontal axis is the ratio of the parameters causing plastic collapse (see figure 2.5). Structural failure occurs when the checking point is located outside the failure assessment diagram and no-failure takes place when it is located inside this diagram. However, the acceptability can still be demonstrated even if an initial assessment shows that the existing flawed element is unacceptable. This validation can be done by improving the quality of the input data in fracture mechanics or applying a higher assessment level of the fracture assessment diagram.

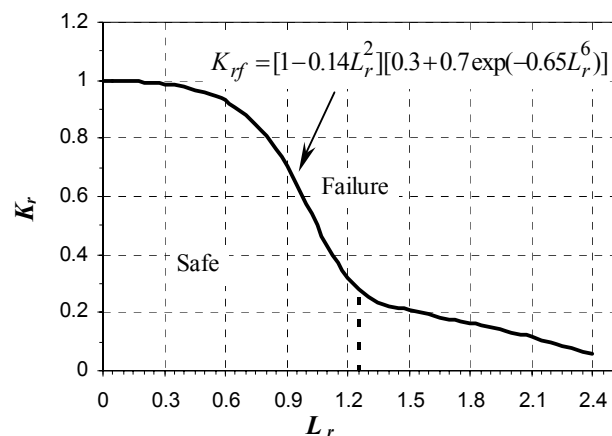


**Figure 2.5** Failure Assessment Diagram, BS 7910 (1999)

The first level of the failure assessment diagram presented in BS7910 is a conservative preliminary procedure,

which is easy to apply. For this level, the fracture assessment diagram is specified in accordance with the material data on fracture toughness and the applied stress. The second level, which is more complicated than the first one, provides the normal procedure for a general analysis. This level is an elastic-plastic based approach and uses detailed material stress-strain behaviour. The failure assessment diagram is proposed on the basis of a fracture analysis of power law hardening materials relating fracture toughness to stress flow. This method gives good results for materials with high strain hardening behaviour. The third level is the most advanced method and mainly used for ductile materials, which exhibit some stable amount of crack growth before fracture, O'Dowd (2001).

The failure assessment diagram of level 2 is suitable for most materials, which do not exhibit a yield discontinuity in the stress-strain curve. This diagram is described by the following expression,

$$K_{rf} = [1 - 0.14L_r^2][0.3 + 0.7\exp(-0.65L_r^6)] \quad \text{for } L_r \leq L_{r,max} \quad (2.27)$$

where  $L_r$  is the plastic collapse parameter and  $K_{rf}$  is the non-dimensional fracture parameter at failure. The failure assessment diagram of this level is shown in figure 2.5. The failure assessment diagram is a curve varying from  $K_{rf}=1$  at  $L_r=0$  to  $K_{rf}=0$  while  $L_r$  is changing from 0 to a very large value. At high values of  $L_r$  the cracked component will be in a situation of general yielding and may fail due to plastic collapse instead of fracture.

For this situation of general yielding the EPFM analysis is not satisfactory and hence a cut-off is imposed on the failure assessment curve at  $L_r = L_{r,max}$  where beyond this limit  $K_{rf}$  is taken to be zero. It should be noted that the failure assessment diagram was derived as a lower bound on a number of test results and is therefore expected to be conservative. The cut-off limit,  $L_{r,max}$ , is defined as the ratio of the average of the ultimate strength and the yield strength to the yield strength of material,  $(\sigma_Y + \sigma_U)/2\sigma_Y$ .  $L_{r,max}$  varies from 1.15 for low alloy steels and welds to about 1.8 for austenitic steels. Marley (1991) and Hovde (1995) recommended using the value of 1.25 for typical welded details of marine structures, because it is a typical cut-off limit for mild steel welds. However, care should be given for the high strength steel material used in the jack-up platforms. For the typical high strength material, the cut-off limit of 1.04 is obtained from the test results, Etube (2001).

The fracture parameter  $K_r$  in the failure assessment diagram is formulated as, (BS7910, 1999)

$$K_r = K_r^p + K_r^s + \rho_c = \frac{K_I^p + K_I^s}{K_{IC}} + \rho_c = \frac{Y(a)\sqrt{\pi a}(\sigma^p + \sigma^s)}{K_{IC}} + \rho_c \quad (2.28)$$

in which  $K_I$  is the linear elastic stress intensity factor and  $K_{IC}$  is the material fracture toughness,  $\sigma^p$  and  $\sigma^s$  are primary and secondary stresses, respectively. Furthermore,  $\rho_c$  is a correction factor to account for the plasticity interaction and is defined by the following expression, BS7910 (1999),

$$\rho_c = \begin{cases} \rho & L_r \leq 0.8 \\ 4\rho(1.05 - L_r) & 0.8 < L_r \leq 1.05 \\ 0 & 1.05 < L_r \end{cases} \quad (2.29)$$

where

$$\rho = 0.1\left(\frac{\sigma^S L_r}{\sigma^P}\right)^{0.714} - 0.007\left(\frac{\sigma^S L_r}{\sigma^P}\right)^2 + 0.00003\left(\frac{\sigma^S L_r}{\sigma^P}\right)^5 \leq 0.25 \quad (2.30)$$

$L_r$  is the plastic collapse parameter and defined as the ratio between the reference section stress ( $\sigma_{ref}$ ) and the yield strength ( $\sigma_y$ ),

$$L_r = \frac{\sigma_{ref}}{\sigma_y} \quad (2.31)$$

As is clear from equation (2.28), the total stresses can be separated into primary ( $\sigma^P$ ) and secondary stresses ( $\sigma^S$ ). The primary stresses are resulting from all external loads caused by waves and winds, currents and sustained loads. Secondary stresses are the result from residual stresses in the structure due to welding and fabrication and are generally considered as self-balancing over the brace-chord assembly at the joint. The estimation of the magnitude and distribution of residual stresses in welded components is very complicated and depend on the type of weld, the overall geometry of the joint, the heat input during welding process, the speed of welding process, and the yield strength of the material, etc. These stresses may also be removed using post weld heat treatment of the weld and surrounding parent material. However, it is not possible in practice to relieve stresses in all joints in a structure or to control the stress relieving process properly. Therefore, the design codes often recommend a conservative value of tensile yield strength to account for the effect of the residual stresses which are considered to be uniformly distributed through the thickness of plate close to the weld, Shetty (1992).

To calculate the plastic collapse parameter ( $L_r$ ), two methods are presented in BS7910 (1999), one in line with the local collapse analysis and another one based on global collapse. In the local collapse analysis, the reference section stress ( $\sigma_{ref}$ ) is computed from an appropriate formulation based on crack shape, joint geometry and applied loads. However, it is stated that this method may lead to conservative results whilst the use of the global approach tends to give a more realistic prediction of plastic collapse in tubular joints. In the global collapse analysis, the joint capacity is therefore taken into account and the plastic collapse parameter is presented with the following expression,

$$L_r = \left(\frac{\sigma_f}{\sigma_y}\right) \left\{ \frac{\sigma_a}{\sigma_{ac}} + \left( \frac{\sigma_{ab,i}}{\sigma_{bc,i}} \right)^2 + \frac{\sigma_{ab,o}}{\sigma_{bc,o}} \right\} \quad (2.32)$$

where  $\sigma_f$  is the flow strength which is specified to be the average of the yield and the ultimate tensile strength ( $\sigma_f = (\sigma_y + \sigma_u)/2$ ).  $\sigma_a$ ,  $\sigma_{ab,i}$  and  $\sigma_{ab,o}$  are the applied axial, in-plane and out-of-plane bending stresses; and  $\sigma_{ac}$ ,  $\sigma_{bc,i}$  and  $\sigma_{bc,o}$  are the plastic collapse strength in the cracked condition for the axial, in-plane and out-of-plane bending capacity of the joint respectively.

## 2.7 FRACTURE LIMIT STATE

In the sections (2.4) and (2.5), it is shown how the limit state of fatigue and ultimate environmental loading can be specified. Sometimes, the jack-up platform is under extremely high magnitude loading and due to fatigue or as a result of fabrication processes, small defects may occur in tubular joints. The combination of a very high single load with a small crack may cause an unstable crack extension. Moreover, the use of high tensile steels, which

is the trend in the offshore industry with the aim to reduce weight and cost in deep water operations, increases the risk of fracture failure. This shows that it would be valuable to present a method to take into account this type of failure in the reliability analysis. Furthermore, this type of failure criterion has not yet been applied in the reliability analysis of jack-up platforms.

To establish a fracture limit state for a reliability analysis, the fracture assessment diagram can be used to extend the probabilistic model by treating the major source of uncertainty through a set of random variables. The safety margin is therefore formulated as,

$$g_{f1} = K_{rf} - K_r = [1 - 0.14L_r^2][0.3 + 0.7 \exp(-0.65L_r^6)] - K_r \quad (2.33)$$

where  $K_r$  is a fracture parameter, which is defined by equation (2.28) and  $K_{rf}$  is the fracture failure parameter described with expression (2.27). In this expression, it is required to specify the crack dimension at extreme loads. The crack dimension  $a(t)$  may be taken as the random initial weld defect dimension  $a_0$  used in the crack growth or more appropriately using the crack dimensions after a service exposure of duration  $t$  when fatigue is considered.

The fracture failure occurs due to extreme primary loading. The maximum stresses can be calculated from the maximum wave loads in a marine structure and can be related to random environmental parameters, Marley (1991) and Hovde (1995).

Dijkstra et al. (1994) presents a method to describe the fracture limit state function in accordance with the fracture results of 38 fracture experiments for tubular and wide plate elements as shown in figure 2.6. He recommends using the circular limit state to represent the fracture failure appropriately, where the angle of spreading is given to be independent and only the radius of a circle would be a relevant parameter to represent the failure mode. The fracture limit state is therefore described through this method with,

$$g_{f2} = R_f - R_{act} \quad (2.34)$$

where  $R_f$  is the radius of the fracture failure while it is recommended to suppose a lognormal distribution in such as way that its mean and standard deviation is setting into 1.7 and 0.4 respectively (Dijkstra et al., 1994).  $R_{act}$  is the acting fracture radius and is specified through the following expression depending on the plastic collapse parameter  $L_r$  and the fracture parameter  $K_r$ ,

$$R_{act} = \sqrt{K_r^2 + L_r^2} \quad (2.35)$$

This method is also recommended in the draft of JCSS (2004) for fracture probabilistic analysis of metallic structures, however a lower standard deviation of 0.306 is proposed.

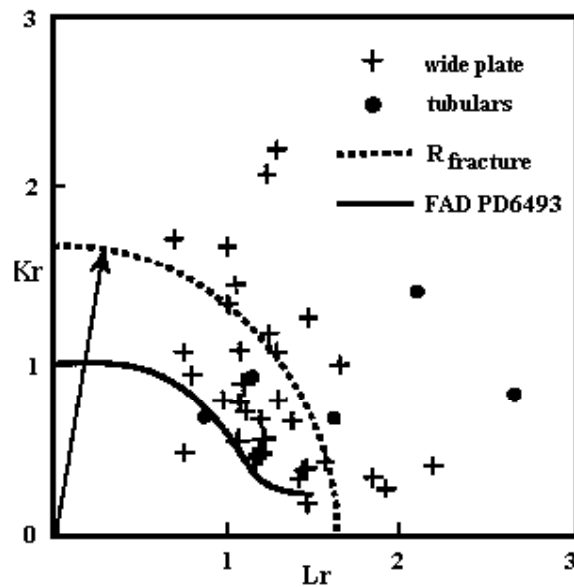


Figure 2.6 Dijkstra method to specify fracture limit state



## 2.8 CONCLUDING REMARKS

In this chapter, three limit state functions of fatigue; ultimate and fracture have been presented in detail. At first, the fatigue crack mechanism has been described using the semi-elliptical crack growth propagation model. An important factor in the crack growth formulation is the geometry function. One factor influencing the geometry function is the bending to membrane stress ratio. Several geometry functions have been presented in the literature. Since, these functions have been derived for the special case of tubular elements in a jacket platform, the direct application of these formulations may lead to incorrect estimations of fatigue and fracture reliability for jack-up platforms. Some modifications should therefore be applied before any application. This aspect will be investigated in chapter 4 in detail, and a new formulation based on the jack-up stress state (bending to membrane stress ratio) and the correction due to weld toe profile will be presented.

The fatigue crack may propagate during the service time of the platform and reduces the strength of structural elements. The combination of fatigue damage (crack) and the extreme environmental loads may increase the failure probability of the structure. Due to this problem, the ultimate and fracture failure modes are also considered in this investigation and the failure probability for these failure scenarios shall be calculated. The limit state functions for these two failures modes have been presented in detail.

For the ultimate limit state, an approach proposed by Videiro and Moan (1999) is described in detail. The benefit of this method is the direct application of the interaction formulation when the stress state of the element changes from tension to compressions. Moreover, the correlation between the stresses (axial and bending) is also implicitly incorporated in the formulation.

The fracture failure of the jack-up may differ from the jacket platform due to structural configuration and dimensions, the effect of the jacking mechanism and the use of high strength materials in the legs. The further investigation on this type of failure mode will be essential, if extreme environmental loads occur after the development of a serious (fatigue) crack. For the fracture failure, at first a brief review of the fracture mechanic has been presented. Then, two approaches of failure assessment diagram recommended by BS 7910 (1999) and Dijkstra et al. (1994) have been described.

To some extent the three failure mechanisms seem to overlap. Fatigue will probably always lead to some kind of fracture or yielding. Collapse due to yielding is present in both the fracture and the ultimate limit states. On the other hand, given the present formulations as taken from the literature, it is not possible to leave one out, without an unaccounted for reduction of the failure domain. Note also that in all three limit state models different material parameters may play a role. They also seem to refer to different levels of structural detail: member, cross section or local hot spot point. Maybe that in the future these formulations can be better streamlined.



### 3. RELIABILITY ANALYSIS

---

#### 3.1 INTRODUCTION

In the previous chapter, formulations of limit states according to three failure criteria of fatigue, ultimate and fracture mechanics have been presented and the uncertainties in the parameters of the limit states functions have been described. In this chapter, the focus is on the description of different reliability approaches to estimate the failure probability. The aim is to investigate the accuracy of reliability approaches for calculation of the failure probability for each limit state function and compare the calculation time required for each method.

The reliability methods are generally categorized into four levels of increasing complexity of approach (see for instance; Melchers, 1999, and Nowak and Collins, 2000). The first level is the deterministic reliability method and uses only one “characteristic” value to describe each uncertain variable. Examples of this method are the load and resistance factor formats or the allowable stresses method applied in the code specifications. Nowadays these specifications are upgraded to a higher level by using the partial safety coefficient derived with higher levels. The next level is the second moment method. In this level, mean and variance of variables are used to describe uncertainty in the random variables. Sometimes to supplement this method, the correlation between random variables may further be taken into account. The third level, which adopted in this research, utilizes the joint probability distribution of all uncertain variables to describe their randomness. Finally, the level four method incorporates the engineering economic aspects into level three and optimizes with respect to cost and utility. This level is often used to assess the target reliability required in the reliability calculation.

In the third level, if the joint distribution functions of all basic random variables are known,  $f_X(x)$ , and a failure mode specified by  $g(x)$  describes the limit state function the failure probability can then be evaluated with the following integral,

$$P_f = \int \int \cdots \int_{g(x) \leq 0} f_X(x) dx \quad (3.1)$$

The analytical solution of this integral cannot be generally carried out except for very simple models and alternative techniques are needed for complex problems in reliability analysis. The alternative methods are analytical approximations, Monte Carlo Simulations (MCS) and

numerical integration methods. More details about these methods can be found in Ditlevsen and Madsen (1996), Melchers (1999), Nowak and Collins (2000).

The numerical integration method is only suitable for a case with the limited number of random variables and the simple limit state function, Der Kiureghian (2004). Therefore, this approach would not be appropriate for the case of fatigue or fracture limit state due to incorporating several random variables with a complex limit state function. The analytical approximations such as first and second order reliability method (FORM and SORM) or simulation methods such as Monte Carlo and important sampling would be more appropriate for the general complex case of limit state such as fatigue and fracture. However, the simulation-based method is more time consuming and sometimes in the case of MCS may not lead to the appropriate results (according to the coefficient of variation of estimated failure probability) when the number of simulations is beyond of computer limitations.

In the following sections, the approximation and simulation methods applicable for the evaluation of the component and system reliability are briefly reviewed. By using several examples, their efficiency and accuracy are investigated for the fatigue, ultimate and fracture limit state functions, presented in the previous chapter.

### 3.2 ANALYTICAL APPROXIMATION METHODS

The analytical approximation methods are generally categorized into the First Order Reliability Method (FORM) and the Second Order Reliability Method (SORM). In these approximation methods, the original problem is first transformed into a standard normal probability space and the failure probability is then calculated by converting the original hyperplane failure surface into the tangential and quadratic approximation. Transformation to the standard normal space is of importance in a reliability analysis because the reliability index in this space has a geometry interpretation as the shortest distance to origin, Hasofer and Lind (1974).

#### 3.2.1 Transformation to the standard Normal space

In the approximation methods, the reliability calculation should be carried out in the standard independent normal space. Since the original basic random variables are in general not mutually independent and normally distributed, a procedure is required to transform the vector of basic variables,  $X$ , into a vector of independent standard normal variables,  $U$ . In most cases the Rosenblatt transformation procedure can be performed, Hohenbichler and Rackwitz (1981), i.e.;

$$\Phi(U_i) = F(X_i | X_1, X_2, \dots, X_{i-1}) \quad i=1, 2, \dots, n \quad (3.2)$$

where  $\Phi(\cdot)$  is the standard normal distribution and  $F(X_i | X_1, X_2, \dots, X_{i-1})$  is the cumulative distribution of  $X_i$  conditional on  $X_1, X_2, \dots, X_{i-1}$ .

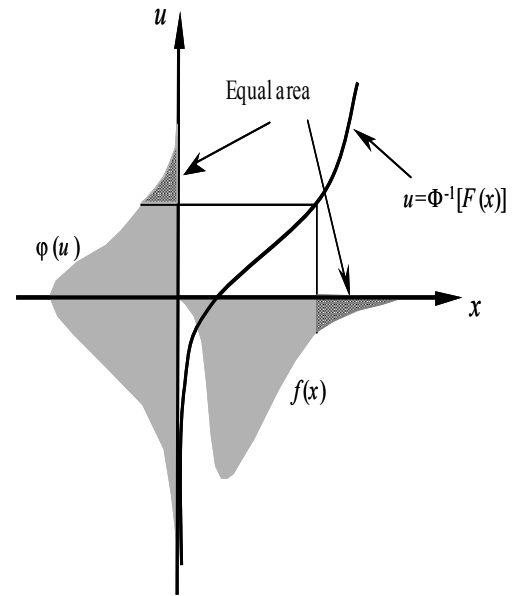


**Figure 3.1:** Transformation of single random variable into Normal standard space

The vector of mutually independent standard normal variables,  $U=[U_1, U_2, \dots, U_n]$ , can separately be transformed by

$$T: U_i = \Phi^{-1}(F(X_i | X_1, X_2, \dots, X_{i-1})) \quad i=1, 2, \dots, n \quad (3.3)$$

This transformation is usually carried out numerically step by step, i.e. the first step  $X_1$  is transformed into a standard normal variable and followed in the second step by a transformation of  $X_2 | X_1$  into standard normal variables and this procedure is continuing to the end, see figure 3.1. In the Rosenblatt transformation, the joint distributions of variables are important to be available but in some situations only the marginal probability distribution with a correlation coefficient between the random variables are available. In this case, the Nataf transformation (Der Kiureghian and Liu, 1986) can be applied. In the Nataf transformation, the equivalent Normal random variables can be obtained by the following expression,

$$T: \quad u = L_0^{-1} \begin{Bmatrix} \Phi^{-1}(F(X_1)) \\ \vdots \\ \Phi^{-1}(F(X_n)) \end{Bmatrix} \quad (3.4)$$

where  $L_0$  is the Choleski decomposition of the correlation matrix  $R_0$ , i.e.  $R_0 = L_0 L_0^T$ . The  $R_0$  is the correlation matrix between random variables in the Normal space,  $R_0 = [\rho_{0,ij}]$ , and can be related to the correlation of random variables in the original space,  $R = [\rho_{ij}]$ , for each two random variables with the following expression, (Der Kiureghian and Liu, 1986).

$$\rho_{ij} = \int_{-\infty}^{\infty} \int_{-\infty}^{\infty} \left( \frac{x_i - \mu_i}{\sigma_i} \right) \left( \frac{x_j - \mu_j}{\sigma_j} \right) \varphi_2(z_i, z_j, \rho_{0,ij}) dz_i dz_j \quad (3.5)$$

The close form approximate expression to relate  $\rho_{0,ij}$  with  $\rho_{ij}$  is provided in Der Kiureghian and Liu (1986) for several probability distributions. This approach has been used in the reliability program in this research work to calculate the correlation in the Normal space. Moreover, the Nataf transformation is applied to determine the equivalent normal random variables.

### 3.2.2 First Order Reliability Method (FORM)

In the first order reliability method, the random variables are firstly transformed into the standard normal space by one of the methods explained in the previous section and the failure surface is then replaced by its tangent hyperplane. The reliability index in this space is defined as the shortest distance between this tangent hyperplane and origin and an iteration procedure must be carried out to search for the shortest distance. According to this procedure, the transformed tangent hyperplane on the failure surface is given by,

$$g(x) = g_u(T^{-1}(u)) \Rightarrow g_u(u) = \beta - \sum_{i=1}^n \alpha_i u_i \quad (3.6)$$

where  $\beta$  is the first order reliability index and defined as the shortest distance from the origin to the failure surface and its sign is determined as the sign of  $g_u(0)$ , see figure 3.2.  $\alpha_i$  is the component of the unit normal to the failure surface with direction towards the failure space (direction cosine) and  $T^{-1}$  is inverse transformation specified in equation (3.3). The closest

point to the origin on the failure surface is defined as the design point,  $u^*$ , and can be determined by a search algorithm with the purpose to minimize  $\sum(u_i^2)$ . An iteration algorithm presented by Liu and Der Kiureghian (1991) or Nowak and Collins (2000) can be used to determine this minimum distance to the origin, which gives the reliability index. More details about these two methods are given in appendix E.1.

By minimizing this function, the design point can be determined with  $u_i^* = \beta \alpha_i^*$  in such a way that the component of the unit vector is given by

$$\alpha_i^* = -\frac{\partial g_u(u_i^*) / \partial u_i^*}{\left[ \sum_{j=1}^n \left( \partial g_u(u_j^*) / \partial u_j^* \right)^2 \right]^{1/2}} \quad (3.7)$$

The direction cosine  $\alpha_i^*$  is a measure of the sensitivity of the reliability index to change in the corresponding random variable,  $u_i^*$ . Furthermore, a positive  $\alpha$ -value indicates a load variable and a negative  $\alpha$ -value indicates a resistance variable. The quantity  $(\alpha_i^*)^2$  is commonly attributed to the importance factor of the variable and the value is an indication of the uncertainty fraction that can be associated with the corresponding random variable.

The failure probability according to this method can be determined with,

$$P_{f, \text{FORM}} = P[g_u(u) \leq 0] = \Phi(-\beta) \quad (3.8)$$

In the iteration procedure of the FORM approach for finding the shortest distance from the origin, care should be given to the search algorithm because sometimes the iteration process leads to the global maximum instead of minimum. Furthermore, for failure surfaces with several minimum points, the iteration procedure may only focus on one of the local minima instead of a global one (local minimum). It thus becomes necessary to try several starting points for the iteration routine or generally apply another procedure such as MCS to determine the failure probability.

In the case of a highly nonlinear failure surface, the FORM algorithm sometimes may not represent the exact failure probability content and other procedures such as SORM or Monte Carlo Simulation techniques will be more essential and proper than using the FORM method.

### 3.2.3 Second Order Reliability Method (SORM)

The FORM method presented in the previous section, generally gives accurate results for practical engineering problems. However, when the failure surface is highly nonlinear, the approximation used in this method may not satisfactorily represent the failure probability content of the original failure surface and a modification to increase the accuracy of this

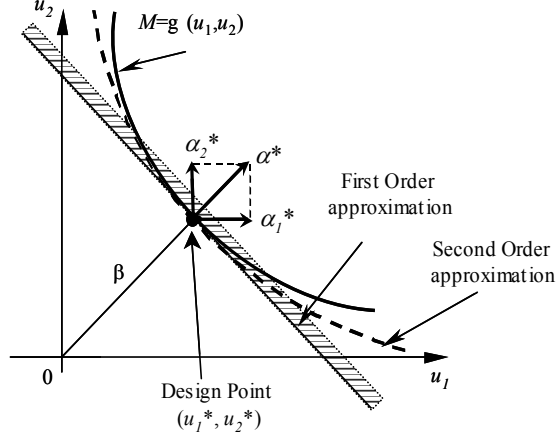


**Figure 3.2:** First and second order approximation of limit state in standard Normal space

method is essential. For this situation, the quadratic approximation to the failure surface at the design point is suggested to give a better estimation than tangent hyperplane, see figure 3.2, (Tvedt, 1983, Breitung, 1984; Der Kiureghian et al., 1986).

The quadratic approximation is therefore carried out by using the second order Taylor expansion of the limit state function in standard normal space, hence,

$$g_u(u) = \beta \sum_{i=1}^n \alpha_i u_i + \frac{1}{2} \sum_{j=1}^n \sum_{i=1}^n (u_i - u_i^*) D_{ij} (u_j - u_j^*) \quad (3.9)$$

where  $\beta$  is the first order reliability index and  $D_{ij} = H_{ij} / |\nabla g(u^*)|$ .  $H_{ij}$  is the second order partial derivation of the limit state function and  $\nabla g(u^*)$  is the gradient vector of the limit state at the design point. Due to the application of the second order of Taylor series expansion, this approach is nominated the second order reliability method (SORM). Based on this formulation Breitung (1984) gave an asymptotic expression for the failure probability when the reliability index is approaching infinity,  $\beta \rightarrow \infty$  in term of main curvatures of the limit state function at the design point. The failure probability can therefore be calculated with,

$$P_{f,SORM} = \Phi(-\beta) \prod_{j=1}^{n-1} (1 - \beta \kappa_j)^{-1/2} \quad (3.10)$$

where  $\kappa_i$  for  $j=1,2,\dots,n-1$  are the main curvatures of the limit state at the design point. This method may not give a good probability content for the small reliability index,  $\beta$ ; therefore Tvedt (1983) provided a three-term approximation to the exact failure probability as

$$P_{f,SORM} = A_1 + A_2 + A_3 \quad (3.11)$$

where  $A_1$ ,  $A_2$  and  $A_3$  can be calculated with the following expressions;

$$\begin{aligned} A_1 &= \Phi(-\beta) \prod_{j=1}^{n-1} (1 - \beta \kappa_j)^{-1/2} \\ A_2 &= [\beta \Phi(-\beta) - \phi(\beta)] \left\{ \prod_{j=1}^{n-1} (1 - \beta \kappa_j)^{-1/2} - \prod_{j=1}^{n-1} (1 - (1 + \beta) \kappa_j)^{-1/2} \right\} \\ A_3 &= (\beta + 1) [\beta \Phi(-\beta) - \phi(\beta)] \left\{ \prod_{j=1}^{n-1} (1 - \beta \kappa_j)^{-1/2} - \operatorname{Re} \left[ \prod_{j=1}^{n-1} (1 - (i + \beta) \kappa_j)^{-1/2} \right] \right\} \end{aligned} \quad (3.12)$$

$\phi(\cdot)$  is the standard normal density function and  $i$  in the third term is an imaginary unit. As is clear, the first term of the Tvedt approach is the same as the Breitung approximation and the other terms are the higher order modification expressions applied in this method. The SORM reliability index can therefore be estimated with,

$$\beta_{SORM} = -\Phi^{-1}(P_{f,SORM}) \quad (3.13)$$

In addition to these two methods, several improvements on the second order approximations are also presented in literature, for instance the asymptotic improvement presented by Hohenbichler and Rackwitz (1988) or a modified close form approximation provided by Koyluoglu and Nielsen (1994).

In the FORM and SORM methods, the focus has been on the approximation of the original limit state with the first and second terms (order) of the Taylor series and searching the design point. In these methods, no attention has been given to the type of the final probability distribution of the performance function. If the final distribution is known or specified, it

would be an easy task to calculate the failure probability. This idea is followed by Tichy (1994) and Zhao and Ono (2001), who employ the higher moment of the performance function to specify the characteristics of the probability distribution.

Tichy (1994) recommended using the three-parameter lognormal distribution in which up to the third moment of the performance function is applied to specify the characteristics of the lognormal distribution. Later Zhao and Ono (2001) use a more refined distribution function such as Pearson, Johanson and Edgeworth's series with up to the fourth moment of the performance function to specify the characteristics of the distributions. To determine the higher moments of performance function, the point estimation method has been utilized in this research. Actually, these approaches can be suggested as a modified level two which could be used for level three. Since the accuracy of the point estimation method depends on the nonlinearity of the limit state function and may lead to an inaccurate failure probability, Daghigh and Shabakhty (2003) applied the Monte Carlo Simulation technique to improve the calculation of the higher moment of the limit state function. Furthermore, they extended this method to be used in a system reliability calculation, however the results showed more dependency on nonlinearity of the limit state function and may not provide accurate results if the limit state is nonlinear.

### 3.3 SIMULATION METHOD

The analytical approximation methods presented in the previous sections usually give a good approximation on the general limit state function with a small probability of failure. Nevertheless, when the limit state function is not continuous or the probability distributions of the random variables are not continuous either, the accuracy or feasibility of these methods become doubtful and an alternative method should be applied. An alternative to the analytical approximation method is the Monte Carlo Simulation (MCS) technique. The simulation method may occasionally be the only applicable approach for a reliability calculation. The base of this method is on the simulation of random variables according to their probability distributions. In the following sections a brief description of this method and an improved method based on Importance Sampling (IS) are presented.

#### 3.3.1 Monte Carlo Simulation (MCS)

The basis of Monte Carlo simulation is simply on the mathematical interpretation of the integral in equation (3.1). This means that instead of solving this equation with numerical or analytical methods, the integral is calculated by counting the number of the acquired specific outcomes (here failures) in the total simulation.

To calculate the failure probability according to this method, equation (3.1) should be modified with the multiplication of an indicator function,  $I(\cdot)$ , which takes the value 'one' for outcomes in the failure states and the value 'zero' in safe state, therefore,

$$P_f = \int \int \dots \int_{g(x) \leq 0} f_X(x) dx = \int \int \dots \int_x I(g(x) \leq 0) f_X(x) dx \quad (3.14)$$

It means that the indicator function identifies the integration domain and as is clear from this equation, the failure probability is easily calculated as the expectation of indicator function. An estimate to the failure probability can therefore be given with



$$\hat{P}_f = E_x[I(g(x) \leq 0)] = \frac{1}{N} \sum_{i=1}^N (I(g(x_i) \leq 0)) \quad (3.15)$$

where  $x_i$  is the  $i^{\text{th}}$  random vector simulated from the joint distribution function  $f_x(x)$  and  $N$  is the total number of simulations. The accuracy of this estimation is therefore dependent on the number of total simulations and increases by increasing the number of simulations. However, the number of simulations required to achieve a certain level of accuracy depends on an unknown failure probability. This method, which gives an unbiased estimate of the failure probability, is usually referred to as the Crude Monte Carlo simulation, Melchers (1999). An estimate for the variance of a failure probability estimator is given by Nowak and Collins (2000) as,

$$\text{Var}[\hat{P}_f] = \frac{\hat{P}_f(1 - \hat{P}_f)}{N - 1} \approx \frac{\hat{P}_f}{N - 1} \quad (3.16)$$

The failure probability in the structural reliability problems is generally small; therefore, a considerable amount of simulations has to be generated to get a sufficient number of outcomes in the failure state. For instance, if the target failure probability is somewhere around 0.0001 (according to a reliability index 3.71) and the coefficient of variation of the estimated failure probability is restricted to ten percent, one million simulations are required to reach such accuracy. Therefore, the Crude Monte Carlo simulation is in most cases of structural reliability extremely time consuming and impractical for a very low failure probability and a further improvement of the simulation technique is required. The importance sampling technique is one of such techniques and is reviewed in the following section.

### 3.3.2 Importance Sampling Method (IS)

The purpose of importance sampling is to improve the simulation technique by focusing on the important section of a failure space and not on the entire possible space. This procedure therefore reduces the number of simulations and is shown to give sufficient accuracy in practice, (Melchers, 1989; Ibrahim, 1991; Engelund and Rackwitz, 1993).

According to this procedure, the sampling is carried out in the vicinity of the design point by using a new distribution function  $h_x(x)$  instead of the original joint distribution function of random variables,  $f_x(x)$ , therefore the failure probability can be estimated with,

$$P_f = \int \int \dots \int_x I(g(x) \leq 0) \frac{f_x(x)}{h_x(x)} h_x(x) dx = E_x \left[ I(g(x) \leq 0) \frac{f_x(x)}{h_x(x)} \right] \quad (3.17)$$

where  $h_x(x)$  is the importance-sampling density function and an unbiased estimate of the failure probability can be obtained by,

$$\hat{P}_f = \frac{1}{N} \sum_{i=1}^N I(g(x_i) \leq 0) \frac{f_x(x_i)}{h_x(x_i)} \quad (3.18)$$

in such a way that  $x_i$  is simulated from the importance sampling,  $h_x(x)$  instead of the original probability distribution,  $f_x(x)$ . The appropriate selection of this distribution in reliability analysis becomes very important because it affects the required number of simulations and the accuracy of estimation. A criterion for selecting the importance sampling distribution is to minimize the variance of the failure probability estimator and therefore this method is known

as the variance reduction technique. For the failure probability estimator defined by equation (3.15), the variance of estimator can be specified with, Melchers (1999),

$$Var[\hat{P}_f] = \frac{\frac{1}{N} \sum_{i=1}^N \left( I(g(x_i) \leq 0) \frac{f_X(x_i)}{h_X(x_i)} \right)^2}{N} - \frac{\hat{P}_f^2}{N} \quad (3.19)$$

It is obvious that the most optimal importance sampling function is a function, which its value is one in the failure state and zero in the safe state. However, it is extremely difficult to specify such a function for the general case. Some feasible importance sampling techniques are proposed in the literature, e.g. conditional expectation, (Mebarki and Sellier, 1995), directional sampling, (Nie and Ellingwood, 2000), Markov simulation algorithm (Au and Beck, 1999) and Latin hypercube sampling, (Olsson et al., 2003).

A reasonable strategy to specify an importance sampling density function would be to simulate around the first order reliability (FORM) design point. The sampling density may therefore be selected as the independent multi-normal probability density function with mean values equal to the design point and the variance one.

### 3.4 SYSTEM RELIABILITY

In the previous sections, it is described how to estimate the failure probability of a single limit state but in practical situations, more than one limit state function should be considered whether or not failure of one element leads to structural collapse. This situation is therefore concerned with the computing of the reliability of a structural system.

For the safety assessment, even for simple structures composed of just one element, various failure modes such as fatigue, fracture or ultimate failure under combination of stresses should be supposed. Moreover, the structural system is originally composed of many members and joints and using only one failure mode may not sufficiently represent the safety of the complete system. In system reliability, the concern is on the combination of these failure modes and the calculation of the system failure probability based on the significant failure sequences leading to a structural collapse.

In the following sections, a brief description of the most common methods of system reliability by FORM and simulation techniques is presented. In addition, the branch and bound technique to identify the important failure sequences leading to system collapse is discussed. Also, the response surface technique, which is an important method when the random parameters cannot explicitly be incorporated in the limit state function, is presented. In the end, the conditional and unconditional failure probability is discussed to mix all time-dependent and time-independent random variables in the failure probability calculation.

#### 3.4.1 Series and parallel systems

The system failure (collapse) event can be considered as the combination of basic failure events (elements) in series and parallel arrangement in which each of the elements in the parallel system constitutes by failure events and each series system comprises of a member of parallel systems. Hence, the final system failure probability can be estimated based on the

probability of occurrence of such a system failure event. According to this model, the whole system can be split up into series systems where its component is a parallel sub system.

In the parallel system, the system failure occurs when all of the components in the system fail. Therefore, if the first order approximation is used to describe the hyperplane, the failure probability of this parallel system with  $n$  components described by the limit state functions,  $g_i(u)$ , can be calculated with, (Thoft-Christensen and Murotsu ,1986):

$$\begin{aligned} P_f &= P\left(\bigcap_{i=1}^n g_i(u) \leq 0\right) = P\left(\bigcap_{i=1}^n (\beta_i - \alpha_i^T u \leq 0)\right) \\ &= P\left(\bigcap_{i=1}^n (-\alpha_i^T u \leq -\beta_i)\right) = \Phi_n(-\boldsymbol{\beta}, \mathbf{R}) \end{aligned} \quad (3.20)$$

where  $\mathbf{R}$  is the correlation matrix between the limit state function and defined with elements  $\mathbf{R}_{ij} = \alpha_i^T \alpha_j$ . The  $\boldsymbol{\beta} = [\beta_1, \beta_2, \dots, \beta_n]^T$  is the vector of the first order reliability indices of each limit state and  $\Phi_n(\cdot)$  is the standard multi-normal distribution function.

In contrast to the parallel system, the series system fails if any of its components fails. Using the same first order approximation, the failure probability of series system can therefore be calculated with

$$\begin{aligned} P_f &= P\left(\bigcup_{i=1}^n g_i(u) \leq 0\right) = P\left(\bigcup_{i=1}^n (\beta_i - \alpha_i^T u \leq 0)\right) \\ &= 1 - P\left(\bigcap_{i=1}^n (\alpha_i^T u \leq \beta_i)\right) = 1 - \Phi_n(\boldsymbol{\beta}, \mathbf{R}) \end{aligned} \quad (3.21)$$

The calculation of the probability of failure of series and parallel systems are therefore reduced to the evaluation of the standard multi-normal integral  $\Phi_n(\boldsymbol{\beta}, \mathbf{R})$ . However, the calculation of this integral is difficult for problems of large dimensions, but several approximation methods have been given in the literature such as the efficient methods proposed by, Hohenbichler and Rackwitz (1983), Tang and Melchers (1987), a product of conditional marginal distribution presented by Pandey (1998), Pandey and Sarkar (2002) and finally an elegant and efficient simulation algorithm developed by Ambartzumian et al. (1998).

### 3.4.2 Simulation Technique

The simulation methods explained in the section 3.3 can be extended to apply for system reliability. The indicator function should be changed in such a way that it reflects the characteristic of the system, i.e.

$$I\left[\bigcup_{i=1}^n g_i(x) \leq 0\right] = \begin{cases} 1 & \text{if } [\cdot] \text{ is true} \\ 0 & \text{if } [\cdot] \text{ is false} \end{cases} \quad (3.22)$$

for series systems and

$$I\left[\bigcap_{i=1}^n g_i(x) \leq 0\right] = \begin{cases} 1 & \text{if } [\cdot] \text{ is true} \\ 0 & \text{if } [\cdot] \text{ is false} \end{cases} \quad (3.23)$$

for parallel systems.

To use the advantage of the importance sampling technique, a direct application of a uni-modal sampling density function as shown in the section 3.3.2 is not sufficient in system reliability and some care should be given because it may lead to very large errors, Melchers (1991). Instead, the multi-modal sampling function presented in Melchers (1990) or a sequential conditioned importance sampling method described by Ambartzumian et al. (1998) might be useful to apply in system reliability calculations.

### 3.4.3 Using bounds technique

Rather than using FORM approximation or simulation methods, an alternative approach is to develop an upper and lower bound on the probability of failure of a structural system. The crude bound on the failure probability of any series system when the failure modes are somewhere between completely independent and fully dependent, is given by, (Boole, 1854 and Cornell, 1967);

$$\max_{i=1}^n [P(F_i)] \leq P_f \leq 1 - \prod_{i=1}^n [1 - P(F_i)] \quad (3.24)$$

Since this bound is too wide for some practical systems, a narrower bound is recommended by Ditlevsen (1979). The Ditlevsen upper bound for a series system is given by

$$P_f \leq \sum_{i=1}^n P(F_i) - \sum_{i=2}^n \max_{j < i} [P(F_i \cap F_j)] \quad (3.25)$$

and the lower bound by

$$P_f \geq P(F_1) + \sum_{i=2}^n \max \left\{ \left[ P(F_i) - \sum_{j=1}^{i-1} P(F_i \cap F_j) \right], 0 \right\} \quad (3.26)$$

It is notable that the sequence of numbering can have an affect on the Ditlevsen bounds. Therefore, to obtain the best narrowest bound many different numbering sequences should be tested.

### 3.4.4 Branch and Bound search algorithm

In offshore structures such as jack-up platforms, failure of one element may not lead to a system failure and several elements may fail before the system collapses. Identification of these failure sequences is therefore essential in system reliability.

For typical structures, a large number of failure sequences leading to a system collapse can be expected but only a few of them contribute significantly to the system failure probability. To identify the important failure sequences, which have large probabilities of occurrence, a specific search technique should be used.

A robust search technique is the branch and bound search technique (Guenard 1984, Thoft-Christensen and Murotsu, 1986), which identifies the collapse sequences in decreasing order of importance. The first sequence identified based on this technique has the largest probability of occurrence and the second one has the second largest probability of occurrence and so on. Following this procedure, it is possible to generate a failure tree and to evaluate the upper and the lower bound on the system reliability.

The first step in the branch and bound technique is to start from an intact structure and to compute the failure probability for each member or joint (based on type of limit state) in the structure. This shows the first branches in the failure tree. Suppose the failure probability of element  $m_1$  has the maximum probability in the failure tree. The focus now shifts to this element and the damaged state of this member ( $m_1$ ), hence the failure sequence leading to the second failure element (supposed here to be  $m_2$ ) is specified. This is the most likely to occur damage state. The subsequent failure represents the next branch in the failure tree and shows the second damage state e.g. failure of member  $m_2$  followed by  $m_1$  and the probabilities of such damage states should be computed. The sequence of failures leading to this damage state is therefore the most likely to occur system collapse. The focus then shifts to the next most likely damage state and the probability leading to this damage state is computed as well. This process continues until the next collapse state is identified and its probability is calculated. By combining all probabilities of these failure sequences, the final system failure probability can be specified.

The sequence of events corresponding to the system collapse for the failure of  $n$  members in a given sequence with the highest probability of occurrence can be expressed with,

$$E_1 = E_{m_1}^0 \cap E_{m_2}^{m_1} \cap \dots \cap E_{m_n}^{m_1, m_2, \dots, m_{n-1}} \quad (3.27)$$

where  $E_{m_j}^{m_1, m_2, \dots, m_{j-1}}$  is the event that member  $m_n$  in the failure sequence will fail next, given that  $m_1, m_2, \dots, m_{j-1}$  members already failed in that sequence. Since the focus was on the globally most likely to occurring damage state, the system collapse reached in this way is the most important one and has the highest probability of occurrence.

The system collapse might happen in another scenario than the most likely one; therefore, other important failure sequences should be taken into account in the system reliability. The second most important failure sequence can be identified by continuing the branch and bound technique and focusing on the second most likely damage state that leads to the second system collapse. To identify all important system collapses, this process should be pursued until all the important failure sequences are identified, i.e. all failure sequences with a relatively high probability of occurrence. The system failure probability is then the probability that any of these important sequences will occur. If  $k$  possible failure sequences are identified in the brand and bound technique, the system event  $E_{sys}$  can easily be formulated as the event that any one of the  $k$  failure sequences occur, i.e.

$$E_{sys} = E_1 \cup E_2 \cup \dots \cup E_k \quad (3.28)$$

where  $E_j$  is the event corresponding to  $j$ th failure sequences leading to system collapse and specified in the same way of equation (3.27). The final system failure probability can therefore be computed with the following expression.

$$P_{sys} = P \left( \bigcup_{i=1}^k \left( \bigcap_{j=1}^n \left\{ g_{m_{i,j}}^{1,2,\dots,j-1}(x) \leq 0 \right\} \right) \right) \quad (3.29)$$

It is important to note that the sequence of failure given in equation (3.27) should be formulated as the intersection of two other events  $E_{m_j}^{m_1, m_2, \dots, m_{j-1}} = F_{m_j}^{m_1, m_2, \dots, m_{j-1}} \cap S_{m_j}^{m_1, m_2, \dots, m_{j-1}}$  where  $F_{m_j}^{m_1, m_2, \dots, m_{j-1}}$  corresponds to the failure of member  $m_j$  and  $S_{m_j}^{m_1, m_2, \dots, m_{j-1}}$  corresponds to survival of

the remaining members. Since the survival events are related to the intersection of several events according to the remaining elements, the exact calculation of the sequence of failure involves a large number of intersections. To simplify the computation, the second event is neglected in the structural system reliability analysis, i.e. it is assumed that  $E_{m_j}^{m_1, m_2, \dots, m_{j-1}} \approx F_{m_j}^{m_1, m_2, \dots, m_{j-1}}$ .

This approximation may usually cause a small error in the final estimation of the system failure probability because the neglected events may have a large probability of occurrence, and the approximation of events  $E_i$  are overlapping each other resulting in a small error in the probability calculation of the union of the events, (Guenard, 1984).

### 3.4.5 Response Surface Method (RSM)

In the reliability analysis of an offshore structure, the uncertainty in random variables such as yielding stress, which is related to the mechanical characteristic of structure, may have a significant effect on the response of platform and therefore on the calculated failure probability. Since these random variables cannot explicitly be incorporated in the limit state function, a specific technique such as the response surface method can be applied.

The basic concept of a response surface is generally to approximate the implicit limit state function  $g(x)$  by using an explicit polynomial function,  $\hat{g}(x)$ . The method follows a simple algorithm using the Monte Carlo Simulation method to generate random variables and the response surface function is fitted on the results of simulation, (Lee et al., 1993, Das and Zheng, 2000) i.e.,

$$\hat{g}(x) = a_0 + \sum_{i=1}^r a_i x_i + \sum_{i=1}^r b_i x_i^2 \quad m=2r+1 \quad (3.30)$$

where  $r$  is the number of random variables and  $m$  is the number of points for which the limit state function should be evaluated. The suitability of the response surface obtained in this way relies mainly on the proper selection of sampling points. Bucher and Bourgund (1990) utilized the elementary statistical information of basic random variables i.e. mean values and standard deviations, to increase the efficiency and accuracy of simulations applied to specify the response surface. This procedure has been later modified by Kim and Na (1997) using the vector projection approach to shift the sampling point close to the response surface.

### 3.4.6 Conditional and unconditional failure probability

In the reliability analysis, it is essential to distinguish types of random variables originating from time variation of a random process. Based on time variation, the random variables are generally categorized into three types. The first one ( $Z$ ) represents uncertainty in variables, which are independent of time and named time-independent random variables, see figure (3.3). The initial crack size, material fatigue characteristics, drag and inertia coefficients of hydrodynamic loads or physical and mechanical characteristics of structures such as diameter, thickness or modulus of elasticity are all examples of this type of random variables, Loseth and Bjerager (1989).

Another type of variables is related to the time and is called time dependent random variables. Some of the time dependent random variables vary little or may remain nearly constant during a short period of time,  $Y(t)$  but over a longer period of time these will vary too. The significant wave height ( $H_s$ ) and the zero crossing period ( $T_z$ ) in a scatter diagram

are examples of this type of random variables. Other time dependent variables have a fast variation with time and represent deviations from the slow process,  $X(t)$ . Wave surface elevation, wave velocity and acceleration, the stresses in the structural elements such as axial and bending stresses are all the examples of this type of random variables.

The fast process may be conditionally related to the slow process,  $X(t)=X(Y(t),Z,t)$  such as wave surface elevation which is considered for a given value of the significant wave height. Furthermore, the slow process such as a wave surface variation is often assumed stationary for the average period of a sea state duration. Hence, the stochastic process,  $Y(t)$  can be approximated by  $N$  rectangular pulses with duration  $D=T/N$ . The problem of combining  $N$  sea states can therefore be approximated with the combination of a conditionally independent short-term response, Loseth and Bjerager (1989).

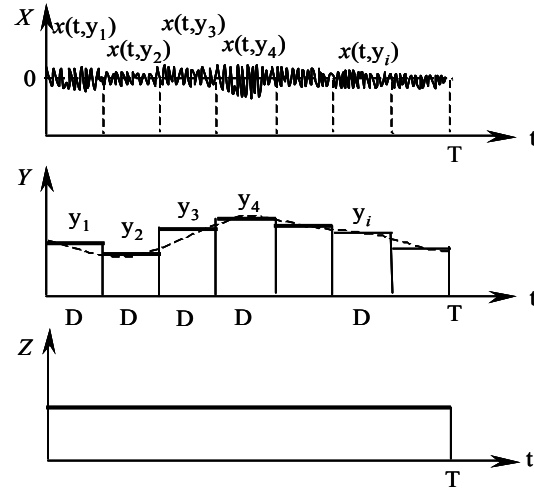


**Figure 3.3** Representation of time-independent,  $Z$ , slow time-variation,  $Y$ , and fast time-variation,  $X$ , random variables, Loseth and Bjerager (1989)

In both the fatigue and ultimate limit state, the stresses are fast time variations and the interest is on the determination of failure probability of the structure in the long-term. Therefore, the appropriate method to determine the long-term failure probability based on the fast stress process is a main concern. Two approaches can generally be applied to determine the long-term failure probability.

In the first method, which is usually applied in fatigue reliability, the long-term stress distribution is calculated through the combination of short-term stress range distributions and the failure probability is then calculated using the fatigue limit state function with parameters of the long-term stress range distribution.

In the second method, which is often used for failure probability calculations of the ultimate limit state function, the short-term failure probability is calculated for each sea-state in the scatter diagram and the long-term failure probability is obtained by combining the short-term failure probabilities. To simplify this method, a kind of response surface method may be utilized to relate the parameters of the short-term stress distributions in the scatter diagram and use this response surface to determine the long-term failure probability. This method has been applied in the research work of Karunakaran (1993) to determine the long-term failure probability of a jack-up platform.

In case of the second method, the failure probability for a particular slow process (short term sea-state) can be evaluated with

$$P(F_S | y_i, z) = P\{g(X(y_i), Z, t) \leq 0 | Y = y_i, Z = z\}; t \in [0, T] \quad (3.31)$$

$P(F_S/y_i,z)$  is the conditional failure probability for a given set of random time-dependent,  $y_i$ , for example individual sea-state and time-independent random variables,  $z$ .  $T$  is the reference period for the reliability analysis. Usually,  $T$  is referenced to one year or to the required service time of a structure called design lifetime. The long-term probability of failure can be obtained from the combination of conditional failure probability for each individual short-term sea-state. This long-term failure probability is calculated by combining for each individual sea-state,  $Y_i$  from all sea states  $i=1,2,\dots,N$  with the following expression,

$$P(F_L | z) = \int_Y P(F_S | y_i, z) f_Y(y) dy \quad (3.32)$$

$P(F_L | z)$  is the conditional failure probability for a given set of time independent random variables,  $z$ , and  $f_Y(y)$  is the probability density distribution of a slow time-dependent process. In practice, such an analysis requires a considerable amount of computation time and effort, since large numbers of short-term simulation are required. By integrating equation (3.32) for time-independent random variables, the unconditional failure probability can finally be evaluated. Mathematically, the final failure probability can be determined with the following expression,

$$P(F_L) = \int_Z P(F_L | z) f_Z(z) dz \quad (3.33)$$

where  $P(F_L)$  is the unconditional failure probability and  $f_Z(z)$  is the joint density function of time independent random variables.

The long-term approach described in this section may be a complex and time-consuming task but leads to an improved failure probability calculation. To simplify the calculation time the randomness of the slow time-variation process may be modelled by a specific probability distribution using the concept of the return period to specify the extreme event of this process. The return period is defined as the average time between two successive statistically independent events. Hence, the extreme event of the slow process is estimated through the probability distribution fitted on the slow process,  $f(y)$  according to observed data and using the return period (say 50 or 100 years) to specify the extreme events. This model is often applied in the offshore industry to specify the design storm or the highest significant wave height that may occur during the lifetime of a structure.

### 3.5 EXAMPLE APPLICATION

In this section, some examples are given to show the accuracy and sensitivity of the reliability approach as presented in this chapter for several limit state functions. Furthermore, these examples provide a comparison of the different strategies used for reliability calculations.

#### 3.5.1 Example of the fatigue limit state function

To investigate the efficiency and to compare the accuracy of the reliability methods, the fatigue limit state function presented in the second chapter is considered here. To take into account the uncertainties in the hydrodynamic loads, the stress calculations and the stress concentration factors, the final stress range distribution model has been modified by multiplying three random variables,  $\delta_F$ ,  $\delta_S$  and  $\delta_{SCF}$ , of which each one represents the uncertainty in the loads calculation, the stress calculation and the stress concentration factor in the specific hot-spots, respectively. They have a lognormal distribution with the mean value equal to one and coefficients of variation of 0.1, 0.15 and 0.1 respectively. Due to the



one leg detailed model of the jack-up platform, a higher value of 0.15 is assumed for the coefficient of variation of the stress model uncertainty. Furthermore, to simplify the calculation the geometry function is assumed constant in this example. The statistical parameters of the basic random variables are given in table 3.1 with the following fatigue limit state function,

$$g(X) = \delta_{tf} \int_{a_0}^{a_c} \frac{da}{C_A (\delta_Y Y_A \sqrt{\pi a})^m} - v^l \tau \delta_F^m \delta_S^m \delta_{SCF}^m A^m \Gamma(1 + \frac{m}{B}) \quad (3.34)$$

To determine the reliability index through this limit state function, two computer programs have been provided in line with the first (FORM) and second order (SORM) procedures described in this chapter. The reliability indices are calculated and shown in table 3.2 for the service time of structures varying from 10 to 30 years.

Two other computer programs based on Monte Carlo (MCS) and Importance Sampling (IS) simulation techniques have been prepared to check the accuracy of the first and second order approximation solutions. A rule of thumb for a sufficient number of simulations is that the crude Monte Carlo simulation should be carried out with at least  $100/P_f$  samples (see e.g. DNV, notes no. 30.6, 1992), where  $P_f$  is the prospected failure probability. However, it is also recommended that the simulation should be carried out in such a way that the estimated  $P_f$  has a coefficient of variation less than 10%. According to this rule of thumb and taking the lowest failure probability determined in the SORM method is 0.0003357 ( $\beta = 3.401$ ), therefore at least 298000 simulations are required. We tried  $3.0E5$  simulations to calculate the failure probability in the Monte Carlo Simulation.

The calculated coefficients of variation for each simulation technique is shown between the parenthesis in front of the reliability results for the service time varying from 10 to 30 years in table 3.2. The largest coefficient of variation calculated according to the number of simulations was 9.53%, which is less than 10%.

**Table 3.1:** Characteristics of variables in the fatigue limit state function

Variable	Distribution	Mean value $\mu$	Coeff. of Var. COV	Imp. factor $\alpha^2$ (%)
$a_0$ (mm)	Exponential	0.11	1.00	11.80
$a_c$ (mm)	Normal	28.0	0.04	2E-4
$\ln C_A$ (N, mm)	Normal	-29.84	St. Dev.=0.55	23.96
$\delta_{tf}$	Lognormal	1.50	0.50	20.23
$\delta_Y$	Normal	1.00	0.10	7.28
$\delta_F$	Lognormal	1.00	0.10	8.67
$\delta_S$	Lognormal	1.00	0.15	19.38
$\delta_{SCF}$	Lognormal	1.00	0.10	8.67
$A$ (N/mm <sup>2</sup> )	Fixed	11.47	----	----
$B$	Fixed	1.22	----	----
$v$ (Cycle/year)	Fixed	6.277E+6	----	----
$m$	Fixed	3.10	----	----



To compare the calculation time of each method, the time spent for the calculation 10- years service time is shown in the second section of table 3.2 for each method. It is clear that the FORM and SORM approaches require less computation time than the simulation methods. The FORM approach generally takes less calculation time than other approaches and the difference of this method is not so significant compared to the others and it may be concluded that this approach is appropriate for fatigue reliability calculations.

To compare the accuracy of the results determined by the program developed for this specific purpose called FRP (Fatigue Reliability Program) and a standard reliability program such as STRUREL, the same limit state function has been entered into the STRUREL and the results are shown in the last two columns of table 3.2. Comparison of the results shows small difference and good accuracy between both programs. The difference may be related to the calculation algorithm for derivation of the limit state. In STRUREL, the derivation of the limit state function is calculated using the finite difference method but in the FRP programs, this derivation is obtained analytically since the expression of the limit state function was available analytically.

Based on the comparison of the results of the reliability approaches derived in this example, it may generally be concluded that the FORM approach gives appropriate results for the fatigue limit state function and can be used in the following chapters for the fatigue reliability calculation of jack-up platforms.

### 3.5.2 Example of ultimate limit state function

In this section, the ultimate limit state function is used to investigate the efficiency of the reliability methods. The ultimate limit state is specified based on API RP2A-LRFD (1993) and is simplified for tubular cross section as follows,

$$g(X) = 1 - \left( \frac{f_a}{F_{cn}} + \frac{C_m f_{bm}}{F_{bn} \left(1 - \frac{f_a}{F_e}\right)} \right) \leq 0 \quad (3.35)$$

where  $f_a$  and  $f_{bm}$  are the axial compressive and maximum bending stresses in the elements and  $F_{cn}$ ,  $F_b$  and  $F_e$  are the nominal axial compressive, bending and Euler buckling strengths respectively and are given by API (1993). These parameters are dependent on diameters, lengths, thicknesses, elastic section modules, module of elasticity, etc and can finally be related to a yielding stress. Therefore, three random variables are assumed, two for compressive and bending strength and one for yielding stress. The Weibull distributions are used to fit on the maximum results of time history simulation of compressive and bending stresses and the Gumbell distributions are used to extend for the extreme results of storm duration (3 hours). The random variables and their characteristics are given in table 3.3.

Four computer programs are provided for the reliability calculations based on the ultimate limit state function according to the FORM, SORM, important sampling (IS) and Monte Carlo simulation techniques described in the previous sections and the results are shown in table 3.3.

The MCS result is calculated for 3.0E5 simulations as already done for the first example and also shown in table 3.3. As is clear from this table, although the calculation time of the MCS

approach took longer than any of the other methods, this technique does not lead to good results for this number of simulations. Based on the rule of thumb recommended by DNV (notes no. 30.6, 1992) for the number of simulations, at least  $1.28E8$  simulations should be carried out. This number of simulations exceeded the memory restriction of the available computer and could therefore not be carried out. Therefore, we restrict to use  $1.28E7$  simulations and the result of MCS is shown in the last row of the table 3.3. The coefficient of variation of this number of simulations is better than before but is not sufficient, not being less than 10 percent.

The importance sampling method is carried out according to the 5000 simulations with the multi-normal distribution function for the importance sampling density function. The mean value of this distribution is set equal to the design point derived in the FORM solution and the unit variance. This corresponds to the coefficient of variation of 3.96 % in calculation. The reliability index derived with this method is compared with FORM and two SORM approaches in table 3.3.

The FORM method requires the minimum calculation time compared to the other methods. The MCS method spends a lot of time to calculate the failure probability and may generally not be an appropriate method when the calculation time is limited.

The FORM result shows good agreement with the important sampling but the SORM approach gives a somewhat less conservative outcome than FORM. The non-linearity imposed in the SORM technique may be suggested as a reason for this difference.

The sensitivity analysis based on the importance factors of the random variables shows a high influence of axial and yielding stresses with 62.39% and 21.65% respectively. The bending stress has the lowest influence with a total uncertainty of 15.96%.

**Table 3.3:** Probabilistic data for the ultimate limit state function and calculated reliability index

Variable	Distribution	Mean value $\mu$	Coeff. of Var. COV	Imp. factor $\alpha^2$ (%)
$f_a (kN/m^2)$	Gumbel	177352.23	0.132	62.39
$f_b (kN/m^2)$	Gumbel	243123.90	0.133	15.96
$\sigma_Y (kN/m^2)$	Lognormal	689000.0	0.080	21.65
FORM*			$\beta=4.746$	$P_f=1.037E-6$
SORM*			$\beta=4.616$	$P_f=1.956E-6$
FORM	4.070 CPU-Second		$\beta=4.746$	$P_f=1.036E-6$
SORM (Breitung)	4.080 CPU-Second		$\beta=4.626$	$P_f=1.866E-6$
SORM (Tvedt)	4.130 CPU-Second		$\beta=4.627$	$P_f=1.855E-6$
Important Sampling	11.64 CPU-Second		$\beta=4.639$	$P_f=1.748E-6$ (COV=3.96%)
MCS (3.0E5)	414.69 CPU-Second		$\beta=4.504$	$P_f=3.333E-6$ (COV=100%)
MCS (1.28E7)	1879.0 CPU-Second		$\beta=4.617$	$P_f=1.9466E-6$ (COV=20%)

\* Reliability index determined with STRUREL program

To compare the results of the provided computer programs and a standard reliability program such as STRUREL (1997), the same limit state function has been employed in STRUREL and the results are given in the first two rows of the second section of table 3.3. A comparison of the results shows good accuracy between the FORM results but a somewhat larger difference between the SORM approaches. These differences can be related to the different formula used in STRUREL and the developed program. In STRUREL the SORM result is estimated in accordance with the method presented by Hohenbichler and Rackwitz (1988) but in the developed program the method presented by Breitung and Tvedt has been applied.

As the final consequence of comparison of these results, the FORM approach can be supposed to prepare a good outcome for this limit state and may be the appropriate method to be applied for further calculation in the next chapters.

### 3.5.3 Example of fracture limit state function

In this example, we use the fracture mechanics limit state and investigate the efficiency and accuracy of several reliability methods presented in this chapter through this limit state. The fracture limit state function is presented in the second chapter based on the mechanics of fracture and it is shown that structural elements are in the failure state if the following expression becomes less than zero,

$$g(X) = K_{rf} - K_r = [1 - 0.14L_r^2][0.3 + 0.7 \exp(-0.65L_r^6)] - \frac{\delta_Y Y(a) \sqrt{\pi a} (\delta_F \delta_{SCF} \sigma^P + \sigma^S)}{K_{IC}} - \rho_c \quad (3.36)$$

The parameters of this expression have been presented in detail in section 2.7. Here the three random modification variables  $\delta_Y$ ,  $\delta_F$  and  $\delta_{SCF}$  are added. As for the fatigue limit state function, these three random variables are used to consider the uncertainties in the geometry function, the load calculation and the stress concentration factor. The global plastic analysis has been employed to specify the collapse plastic parameter ( $L_r$ ). The statistical characteristics of the random variables for the fracture limit state function are presented in table 3.4. As is clear from this table, a relatively brittle steel type has been chosen to specify the fracture toughness. More details about the random variables are given in appendix G.

**Table 3.4:** Statistic characteristics of random variables in fracture limit state function

Variable	Distribution	Mean value $\mu$	Coeff. of Var. COV	Imp. factor $\alpha^2$ (%)
$\sigma^P$ (kN/m <sup>2</sup> )	Gumbel	169700	0.035	0.04
$K_{IC}$ (kN/m <sup>2</sup> √mm) *	Lognormal	6500000	0.25	55.66
$\sigma_Y$ (kN/m <sup>2</sup> )	Lognormal	689000	0.08	3.83
$a_0$ (mm)	Exponential	0.11	1.00	37.70
$\delta_Y$	Normal	1.00	0.10	2.09
$\delta_F$	Lognormal	1.00	0.10	0.34
$\delta_{SCF}$	Lognormal	1.00	0.10	0.34

\* This fracture toughness corresponds to the CTOD equal 0.3

To specify the characteristics of the Gumbel distribution of the primary stress, the Weibull distribution is fitted on the maximum of the time history simulation of the primary stresses and the Gumbel distribution is utilized for the extension of the storm duration (3 hours). This type of extreme response calculation is the same approach as the extreme stress calculation in the ultimate limit state function, the differences are that the axial and bending stresses are firstly modified with the stress concentration factor and subsequently combined with each other to give the final primary stress.

Three computer programs are provided for reliability calculations according to the FORM, SORM and important sampling (IS) procedures described in the previous sections and the results are calculated for the secondary to yield stress ratio ( $\sigma^S / \sigma_Y$ ) varying from 0.4 to 1.0.

The failure probabilities calculated by FORM, SORM and importance sampling technique are compared in table 3.5. The Monte Carlo Simulation has not been done here because of the problem of memory restriction described in the previous example; instead, the importance sampling is carried out for 5000 simulations with the multi-normal distribution function for the importance sampling density function. The mean value of this distribution is set into the design point derived in the FORM solution and using the variance equal to one. This corresponds to the maximum coefficient of variation of 4.75 % in our estimation and this approach may generally be supposed to lead to an accurate result and constitutes the basis for a comparison. The obtained reliability index derived with this method is compared with FORM and two SORM approaches in table 3.5.

By comparing the results, it can clearly be observed that the FORM method gives good approximate results compared to IS, while SORM provides a slightly closer estimation on the failure probability to the IS solution.

**Table 3.5** Reliability results for fracture limit state function

$\sigma^S / \sigma_Y$	FORM	SORM (Breitung)	SORM (Tvedt)	Import Samp. (Cov %)	FORM*	SORM*
0.4	8.599	8.607	8.607	8.606 (4.75)	8.600	8.608
0.6	7.772	7.786	7.786	7.787 (4.52)	7.773	7.787
0.8	7.116	7.134	6.134	7.133 (4.20)	7.117	7.135
1.0	6.579	6.600	6.600	6.595 (4.01)	6.580	6.601
<hr/>						
FORM			0.120 CPU-Second		$\beta=6.579$	
SORM (Breitung)			0.140 CPU-Second		$\beta=6.600$	
SORM (Tvedt)			0.150 CPU-Second		$\beta=6.600$	
Important Sampling			8.192 CPU-Second		$\beta=6.595$	

\* Reliability index determined with STRUREL program

To compare the results of the provided computer programs and a standard reliability program such as STRUREL, the same limit state function is applied in the STRUREL and the results

are given in the two last columns of table 3.5. A comparison of the results shows good accuracy between the FORM results of both programs. The same trend is observed for the SORM results as well.

The sensitivity analysis based on the importance factor shows a great influence of the fracture toughness and crack size with a combination of 93.36%, while the primary stress has the lowest influence on the total uncertainty.

By comparing the reliability results, the general conclusion can be drawn that the FORM approach provides an appropriate approximation result to calculate the reliability index for the fracture limit state. Furthermore, the calculation time for this method is less than for the other methods.

### 3.6 CONCLUDING REMARKS

In this chapter, the reliability methods for the calculation of the failure probability or reliability index have been presented. Furthermore, by using several examples the accuracy of these methods for the calculation of the failure probability based on three fatigue, fracture and ultimate limit state functions were investigated.

At the first step, the non-Normal variables should be transformed into the Normal space with one of the transformation methods presented in this chapter. The Nataf transformation technique is used to determine the equivalent random variable in the Normal space. The first order approximation (FORM) method is used to calculate the reliability index. This method is based on the first order Taylor series expansion of the limit state in the normal space, using a tangent hyperplane to approximate the original space. Moreover, an iteration algorithm presented by Liu and Der Kiureghian (1991) or Nowak and Collins (2000) can be used to determine the minimum distance to the origin, which gives the reliability index. When the limit state is nonlinear, the first order may not be appropriate and therefore the second order (SORM) of Taylor series is applied to approximate the limit state function. Furthermore, the Monte Carlo simulation and the important sampling (IS) techniques may be used to evaluate the failure probability.

According to the presented method, several computer programs are provided for the fatigue, fracture and ultimate limit state functions and the results and computation time are compared. To test the accuracy of the provided programs, the same limit state functions have been entered into STRUREL and the results are checked with the acquired solution of the provided programs. The results show good agreement between the FORM results of STRUREL and the provided programs. Furthermore, the FORM approach takes less calculation time but give an acceptable approximation of the failure probability.





## **4. COMPONENT RELIABILITY OF JACK-UP PLATFORMS**

---

### **4.1 INTRODUCTION**

In the second chapter, a procedure to derive fatigue, fracture and ultimate limit state functions under extreme environmental loads has been described. Due to the stress state of a jack-up platform, a direct application of the fatigue limit state function using a traditional geometry function may lead to an incorrect estimation of the reliability index and a modification is therefore required before considering any application. This modification is presented in this chapter using the correct membrane to bending stress ratio calculated from the time history of the hot spot stress at the specific point. The differences in the fatigue reliability results between the traditional geometry function and this method are discussed.

Furthermore, the impact of wave spectra, the total damping in the structure and the stress range distributions on the calculation of the fatigue reliability has to be investigated. Based on these investigations a proper selection of the models for wave spectra, total damping and non-linear and wide-banded models of stress range distributions and related parameters has to be made. These aspects are investigated in this chapter, the results are compared and conclusions drawn. The inspection of a platform may provide valuable information to update the failure probability of the structure. The formulation and the procedure to update the fatigue reliability according to the inspection information are explored in this chapter and it is shown that the detection or non-detection of cracks may affect and change the fatigue reliability.

The stress state of a jack-up platform changes due to the cyclic behaviour of hydrodynamic loads in such a way that it varies from tension to compression or vice versa. The traditional approach is to use a limit state for compression or tension separately to check the possibility of failure but in this section an attempt is made for a new approach, by combining these two limit state functions and applying the concept of the time history of the usage factor. Finally, the results are compared with the traditional approach.

Since the fatigue damage discloses its effect as a crack occurs in structural joints, the combination of this crack with the extreme environmental loads may cause a significant fracture failure. This type of failure is subject of the last section of this chapter and a

**Flowchart for Structural Reliability Analysis of Jack-ups under Fatigue, Extreme Environmental loads and Fracture**

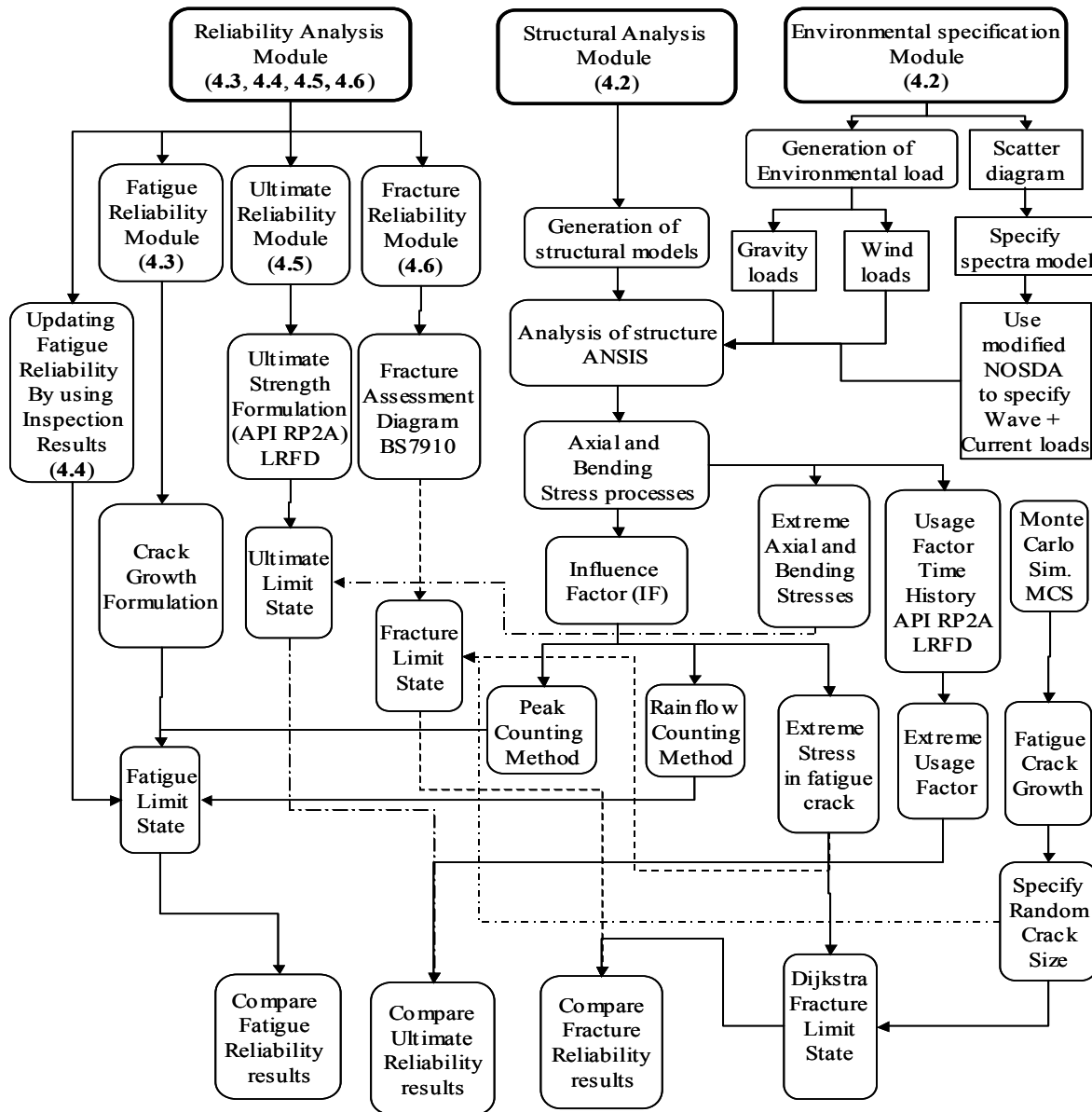


**Figure 4.1:** Schematic presentation of the reliability analysis procedure followed in this section

procedure to calculate the failure probability due to the fracture failure is discussed and presented.

Figure 4.1 shows the schematic flowchart of the calculation procedures and the basic steps that will follow in the rest of this chapter. The number shown in each box of the flowchart refers to the number of the section describing the details.

## 4.2 MODEL OF NEKA PLATFORM

In order to be able to obtain, examine and investigate the reliability of a jack-up platform, the Neka jack-up model is considered here. The overall configuration and dimensions of this platform are shown in figure 4.2 and the finite element model used in this research is given in figure 4.3. Since the fatigue damage originates in the intersections or joints of the elements, the stress distribution around the joints should be specified. Due to memory restriction of the computer, all structural details of the platform cannot be modelled and only a detail of one

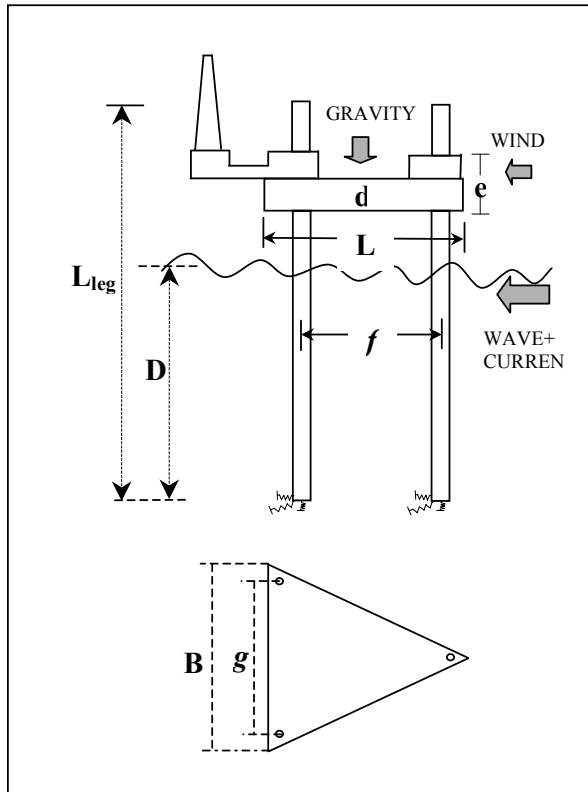


**Figure 4.2** Overview of Neka jack-up platform

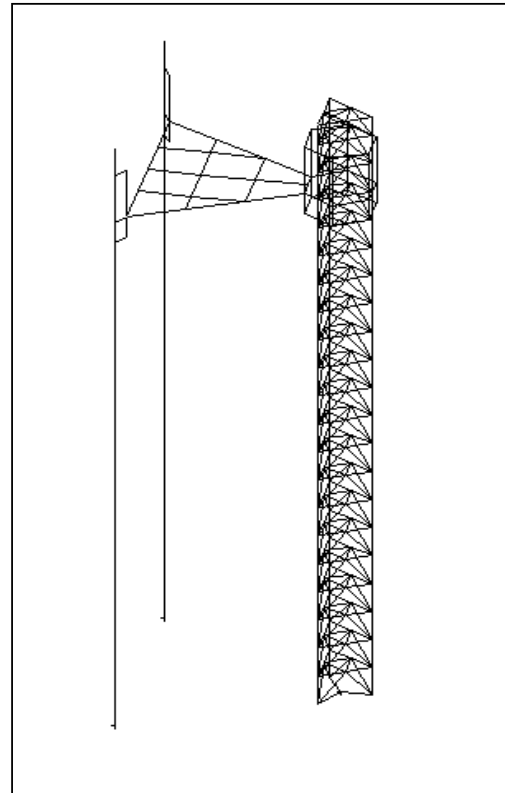


**Figure 4.3** Finite elements model of Neka jack-up

leg is considered here. However, the validation of the main concept of this research may not be violated by this simplification. For the other two legs, the truss legs are idealized as string beam elements with the equivalent stiffness and hydrodynamics properties described in the Site Specific Assessment of Mobile Jack-up Units, Bulletin 5-5A (Bennett, 994). The adapted computer model is a three-dimensional space frame with totally 524 elements and 229 nodes.

The platform rests on spudcans at the base of each leg. The soil-structure interaction may be an important aspect in the dynamic response of a jack-up, depending on the soil condition. This subject has been investigated by Cassidy (1999), Shabakhty and Daghigh (2003). Generally, two methods can be applied to model the soil-structure interaction. The finite element method is sophisticated and expensive but makes it possible to consider the variation of the soil properties with depth. In the second model, the foundation is modelled as a rigid body and the spring representing the soil is used as an uncoupled element. This method is a

more simple and popular approach, which can be applied in the modelling of soil-structure interaction, Etube (2001). The second approach is employed here because the focus of this research work has been on the structural aspects of the jack-up platform.

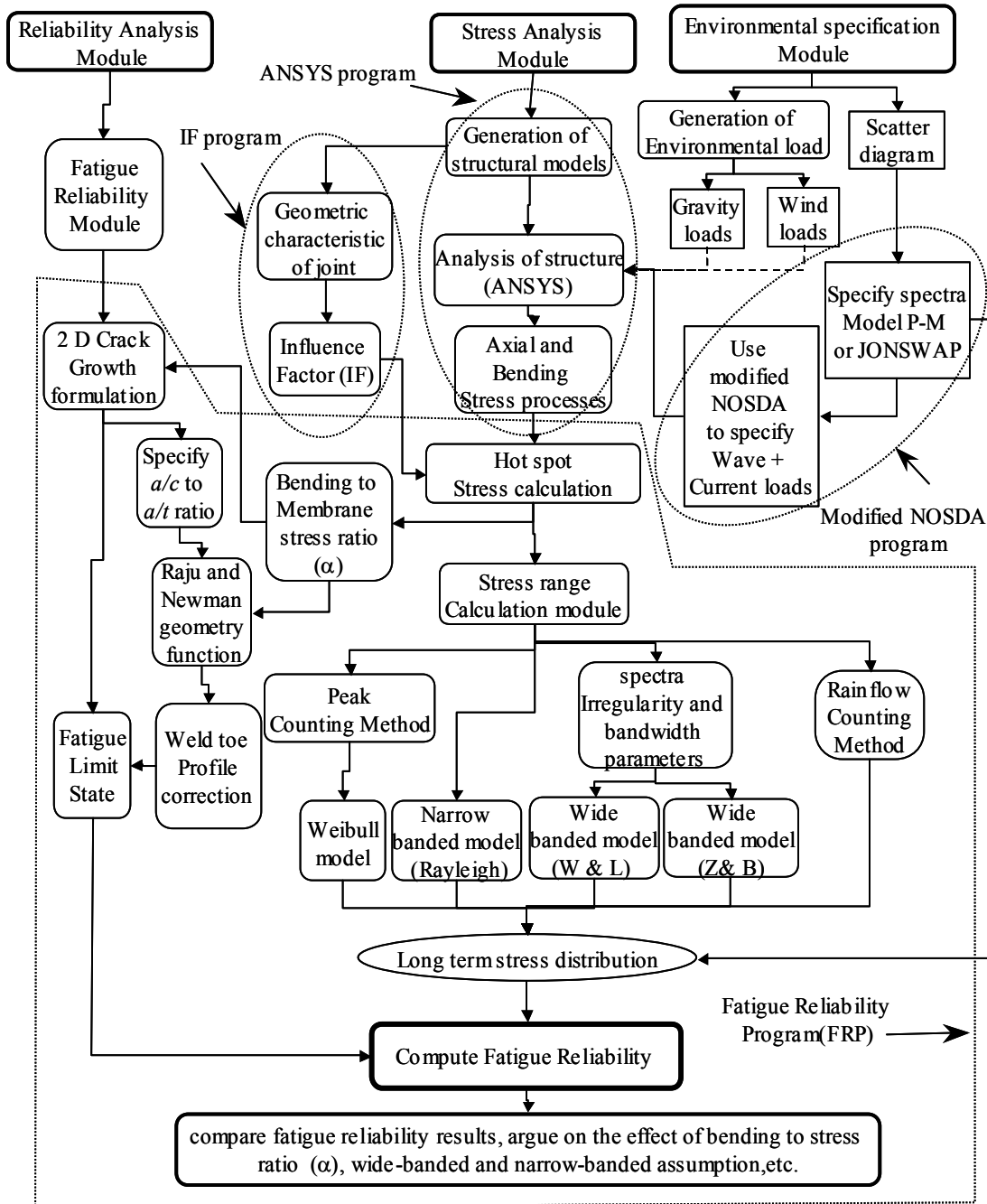
The leg hull connections are a permanent structural factor of the platform behaviour and should be given proper attention. For the purpose of this study these connections are represented by linear springs located at the position of the lower and upper guide levels. The leg-hull interface is a three-dimensional structure and the realistic behaviour is complicated due to the effect of the clearance in leg-guides, backlash in the jacking system and the resulting interaction. The jack-up model under investigation is provided with a fixation system consisting of a clamping mechanism and in this case the linear spring model is generally considered to properly represent the leg-hull connection. The direction of the dominant wave loading is longitudinal from the fore leg to the aft legs, perpendicular to the line connecting the two aft legs. This assumption is on the bases of the critical direction leading to structural failure, Daghigh (1997). The reference sea states ( $H_S$ ,  $T_Z$ ) are selected from the scatter diagram of the Hutton area (Marex 1979) and the hydrodynamic loads corresponding to each sea state are calculated with the NOSDA program, (Liu and Massie, 1988).

To obtain the hydrodynamic loads on the jack-up platform an improved version of the NOSDA program is developed. The original NOSDA program uses the Deterministic Spectrum Amplitude (DSA) for the simulation of the wave surface. In this method, the wave surface in each time step is computed by using the Airy wave theory with the uniform random phase. But, as Grigoriu (1993), Morooka and Yokoo (1997) demonstrated, this approach does not lead to the Gaussian nature of the wave surface except for a high number of random phase combinations. Hence, for a limited number of phase combinations, they recommend to apply the random Rayleigh amplitude in addition to the random phase because this model better represents the Gaussian nature of the wave surface. This model is known as the Non-Deterministic Spectrum Amplitude (NDSA) and is applied in the modified version of the NOSDA program, see appendix E.

**Table 4.1** Characteristic of jack-up platform

Characteristics	Quantity
Platform length	$L=54.86\text{ m}$
Platform width	$B=53.34\text{ m}$
Hull depth	$d=7.62\text{ m}$
Spacing between fore and aft legs	$f=35.45\text{ m}$
Spacing between aft legs	$g=40.95\text{ m}$
Guides distance	$e=14.3\text{ m}$
Total leg length	$L_{\text{leg}}=125\text{ m}$
Water depth	$D=95.0\text{ m}$

The wave particle velocity and acceleration according to this method can be calculated with the first and second derivation of the wave surface through the Airy wave theory. The wave kinematics up to the instantaneous water surface is taken into account using the Wheeler stretching profile (1970). The water particle kinematics are therefore simulated at the nodal points along the submerged and surface-piercing elements in order to obtain accurate nodal point forces through the numerical integration of the distributed hydrodynamic force intensities.



The hydrodynamic loads arising from currents are calculated by simply adding the current velocity given by a current profile to the simulated water particle velocity. In this research work, only the tidal current velocity is taken into account with the power exponent type model recommended by DNV (2000) to model the variation of current velocity with the water depth. The maximum tidal current velocity 1.2 m/s at the still water level corresponds to a 50-year return period recommended by Marex report (1979) is adopted in the same

direction of the wave propagation. For fatigue analysis, the current loads can normally be neglected as recommended in the Site Specific Assessment of Mobile Jack-up Units, Bulletin 5-5A (Bennett, 994).

The static wind load for the elements outside of the water is calculated and added to the wave and current loads. The wind velocity variation is described through the DNV (2000) specification and the reference wind velocity of 36.5 m/s for a 50-year return period as recommended by Marex (1979) is applied in the dominating wave direction. Since in the fatigue reliability calculation the stress range is of more interest, this static load is only applied for the ultimate and fracture reliability analysis and ignored in the fatigue reliability calculation. Moreover, in the following section the overall damping of 5 percent is used for the low and medium sea states in the fatigue reliability sections and 11 percent for the structural response for high sea states in the extreme environmental loads and fracture failure sections to consider the effect of relative velocity according to the recommendation of Daghigh (1997). However, in the section 4.3.4 the variation of fatigue reliability with the damping ratio will be investigated.

### 4.3 FATIGUE RELIABILITY

The component reliability of a jack-up structure based on a fatigue limit state function depends on several parameters such as stress distribution models, bending to membrane stress ratio, wave spectra models and structural damping, which each one can change the estimated failure probability. In this section, these effects will be investigated in detail and it will be shown how they may affect and change the estimated failure probabilities or reliability indices.

The detail and steps followed in this section are shown in figure 4.4. Furthermore, several computer programs are written or developed to calculate the fatigue reliability index in this section. As it is observed from figure 4.3, they generally consist of four original programs. ANSYS is used for the Finite Element analysis and for obtaining axial and bending stresses in each joint of element. In this research work, only the dynamic analysis has been carried out to compute the stresses. The modified version of NOSDA is also developed to calculate the hydrodynamic loads. The IF and FRP programs are written to calculate the Influence Factor (IF) and the Fatigue Reliability (FRP) in each hot spot point of the joint of the structure. More details about the original concept of these programs are discussed in appendix D and E, respectively.

#### 4.3.1 Stress calculation and distribution

As described in the second chapter, the computation of the stress parameter is essential for a fatigue reliability calculation. Since fatigue is the structural degradation arising from the combination of stress ranges in several sea states, the long-term distribution of the stress ranges must be obtained. This may conveniently be carried out by combining the possible environmental conditions as a finite set of stationary sea states, characterized by the significant wave height ( $H_s$ ) and the zero-crossing period ( $T_z$ ). A short-term stress range distribution can therefore be established by using the time history of the stress response, and the fitting of a specific distribution on the stress ranges. The final long-term distribution is then specified by combining the short-term results in such a way that the various occurrences

of each sea state are taken into account through the wave scatter diagram. The wave scatter diagram of the Hutton area (Marex 1979) is used in this research work, see appendix C. Firstly the scatter diagram is divided into five blocks, in which each sea state in the centre point of the block represents that block. The stress process of each sea state is then calculated using the ANSYS finite element program. The hot-spot stress is calculated by multiplying the nominal stress derived in the finite element analysis with the Stress Concentration Factor (SCF). Several SCF's have been presented in the literature, e.g. Kuang et al. (1975), Wordsworth and Smedly (1978), Efthymiou (1988), Hellier et al. (1990) with different formulations for the SCF. The discrepancy between these formulations is mainly due to the type of method used for the analysis, the location of the SCF calculation, the chord end fixation conditions and the range of joint geometries studied to develop the equation. The formulations of Efthymiou cover most of the geometry of the joints in the supposed jack-up model and also consider different types of loading conditions from in planar and non-planar bracing elements. This formulation has therefore been used in this work. Since some differences may be observed between the predicted SCF and the test results, in the reliability method this discrepancy is expressed in the term of the random correction model,  $\delta_{SCF}$ , Shetty (1992).

Several points around the brace-chord intersection can be considered as the highest potential points for the fatigue damage. According to the DNV RP-C203 (2002) recommendation, the hot-spot stresses should be calculated for 8 points around the intersection as illustrated in figure 4.5 in such a way that its angular distribution covers the whole section for each 45 degrees around the intersection of joint.

The hot-spot stresses are calculated through the method presented in Efthymiou (1988) using the Influence Factor ( $IF$ ), which considers the effect of the SCF arising in planar and non-planar braces, with the following expression,

$$\sigma_{hs,i}(t) = \sum_{j=1}^n IF_{ij} \frac{F_{nom,j}(t)}{A_j} = \sum_{j=1}^n IF_{ij} \sigma_{n,j} \quad (4.1)$$

where  $F_{nom,j}$  are the nominal sectional forces and moments determined from the finite element analysis,  $A_j$  are the corresponding sectional constants (e.g. area or sectional modulus), and  $n$  is the total number of degrees of freedom in all bracing member ends and in the two chord ends. In general, there are six load cases for each free end, but a common approach for the fatigue analysis of offshore platforms is to neglect the effect of the torsional moment and shear forces in the fatigue damage calculation, Kirkemo (1988). The axial tension loads, the

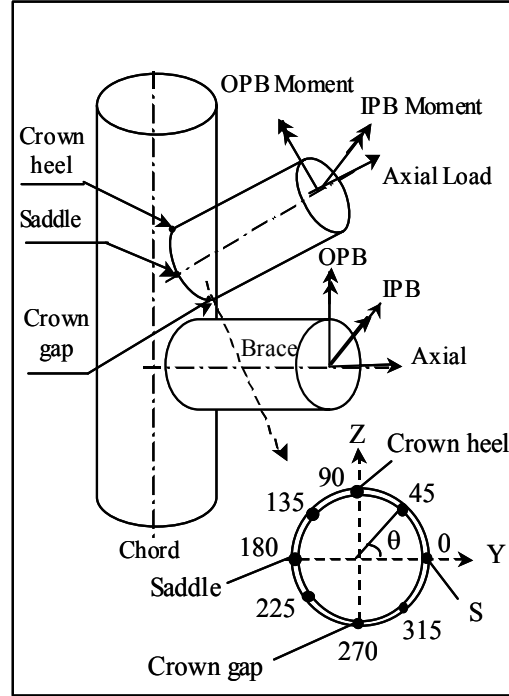


**Figure 4.5** Hot-spot points around intersection of brace/chord

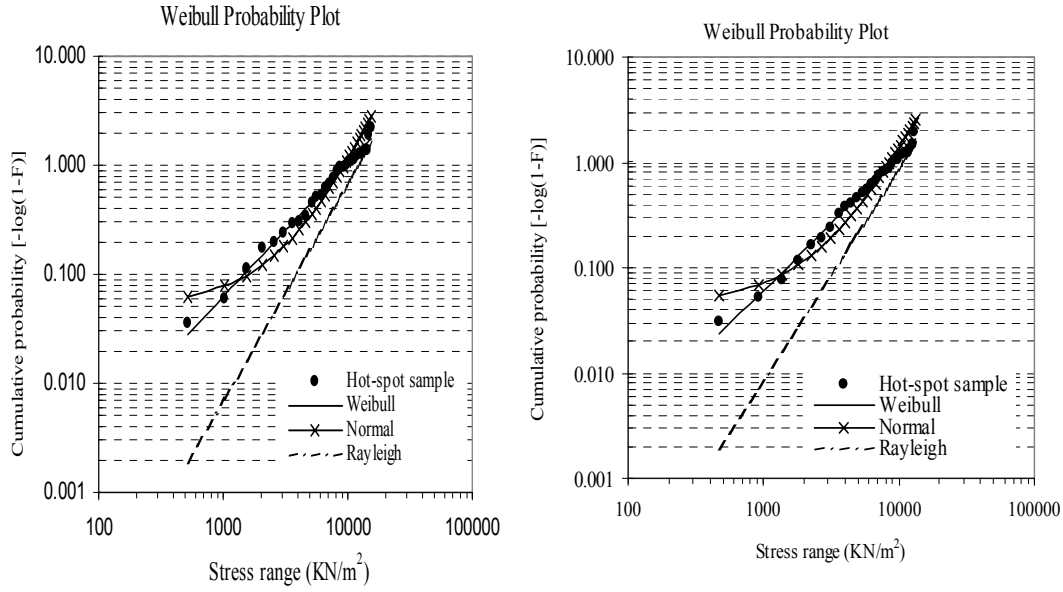


**Figure 4.6:** Stress range distribution for significant wave height 5.0 m at saddle point ( $\theta=0$ ) (Right) and crown point ( $\theta=90$ ) (Left)

in plane and out of plane bending moments are consequently used for each free end and the hot-spot stresses are calculated for 8 points around the intersection of brace and chord. In the reliability calculation, the distribution function of the stress range should be specified. This distribution can be determined using the peak counting method presented by Madsen et al. (1986). According to the peak counting method, the stress range is defined as twice the value of the local maxima of the stress time history. It means that all local maxima above zero are counted and paired with a local minimum of the same size independent of their locations in the time history. Several distribution functions may be supposed to fit on the stress range but the goodness of fit can be applied to ranking according to its significance.

The statistical analysis of the hot-spot stress ranges for the diagonal bracing element below the guiding system (element number 295 in figure 5.2) in the connection with the chord element is carried out for 8 points around the intersection, see figure 4.6. The results show that the Weibull distributions gives the highest ranking among several distribution functions e.g. Normal, Rayleigh, Lognormal, Pareto, Gamma and Erlang based on the goodness of fit using the Chi-square test. The same rank is observed through the Kolmogorov-Smirnov (K-S) and Anderson-Darling test (A-D). The K-S test uses the absolute deviation of the fitted distribution from the sample distribution and the A-D test measures the quadratic deviation of the fitted distribution to the sample distribution, with a higher weighting factor in the tails.

It should be noted that if the stress process was stationary, Gaussian and narrow-banded, it could be expected that the stress range follows the Rayleigh distribution. However, this is not the case for the jack-up platform under investigation because of the nonlinearity in the stress process. This nonlinearity is actually arising from the drag terms in the hydrodynamic load calculation, the P- $\delta$  effect and the integration of water particle kinematics up to the instantaneous water surface individually or in combination of them. Furthermore, it is shown



by Karunakaran (1993) that the statistical nature of the response for the excitation near to the resonance of the platform may approach the Gaussian or Normal distribution (Normalization). Therefore, we suppose three (Weibull, Rayleigh and Normal) distribution functions to fit on the stress range by the using Maximum Likelihood (ML) method and these distributions are compared with the samples of the hot spot stress ranges for two saddle and crown points (zero and 90 degrees) around the intersection of the joint in figure 4.6. As can be seen from this figure, the Rayleigh distribution has a poor fitting on the data, while the Weibull distribution gives a better approximation. Furthermore, the Normal distribution shows significant differences for the lower tail and intermediate values of data. This trend is observed for other hot-spot points around the intersection as well and it is generally supposed that the Weibull distribution could appropriately be applied to model the hot-spot stress distribution around the intersection.

**Table 4.2:** The Weibull distribution parameters of stress ranges for several sea states in a diagonal bracing around an intersection (A is the scale and B the shape parameter of a Weibull distribution).

Position ( $\theta$ )	0	45	90	135	180	225	270	315
Hs=1.75(A)	8.232	7.603	4.450	5.104	6.220	5.282	4.594	7.674
(B)	1.6563	1.6471	1.6631	1.6493	1.6420	1.6422	1.6453	1.6142
Hs=3.25(A)	14.468	13.572	7.894	9.098	11.055	9.409	8.246	13.624
(B)	1.4090	1.4495	1.4337	1.4458	1.4308	1.4376	1.4605	1.4151
Hs=5.00(A)	19.532	17.601	10.510	12.009	14.659	12.493	10.797	18.296
(B)	1.2877	1.2230	1.2896	1.2705	1.2673	1.2804	1.2642	1.2840
Hs=7.75(A)	24.795	23.150	13.570	15.431	18.789	15.928	13.852	22.889
(B)	1.1562	1.1737	1.1892	1.1638	1.1562	1.1550	1.1560	1.1173
Long (A)	12.543	11.587	6.814	7.805	9.503	8.084	7.035	11.736
Term (B)	1.4713	1.4606	1.4848	1.4760	1.4673	1.4741	1.4768	1.4571

The Weibull distribution has been already used for other response quantities e.g. base shear, overturning moment and deck displacement by Kjoey et al. (1989) and Karunakaran (1993). Daghigh (1997) used this for two cases of quasi-static and dynamic response of jack-up platforms. It is interesting to note that in case the Weibull shape parameter (B) approaches to one, this distribution function represents the exponential distribution and when it comes near to two, it gives the shape of Rayleigh distribution. From table 4.2, it can be observed that, when the significant wave height decreases the shape parameter of the Weibull distribution increases, causing the stress range to approach the Rayleigh distribution.

In fact for lower significant wave heights, the behaviour of the structure can be considered as being quasi-static and therefore the stress range should approach the Rayleigh distribution but the drag term in the Morison equation changes the distribution tail from Rayleigh to exponential. The deviation of the stress distribution from Rayleigh to exponential can be reduced by the presence of the dynamic amplification for the higher significant wave heights as observed from table 4.2. These results have already been reported in the research work of Farnes and Moan (1994).

As can be seen from the comparison of the Weibull scaling parameters (A) in table 4.2, this parameter increases by an increasing significant wave height. Since in the fatigue limit state function the loading function is proportional to the scaling parameter of the material fatigue characteristic (parameter  $m$ ), an increase in the scaling parameter enhances the failure probability for the constant fatigue strength. However, a decline of the shape parameter intensifies this enhancement but it should be kept in mind that the occurrence of this sea state is rarely observed. The long-term distribution of the stress range is calculated and illustrated in table 4.2. It can easily be observed that the high contribution in the long-term stress range is coming from the lower sea states because of the high occurrences of these sea states in the scatter diagram.

**Table 4.3:** Reliability index and failure probability around the intersection of a diagonal bracing element (element no. 295) using the Kirkemo model for the geometry function, the service time ( $\tau$ ) is set to 20 years.

Position ( $\theta$ )	0	45	90	135	180	225	270	315
$H_S = 1.75$ ( $P_f$ )	3.71E-5	1.23E-5	7.81E-10	1.42E-8	5.31E-7	2.84E-8	1.79E-9	1.69E-5
( $\beta$ )	3.962	4.218	6.038	5.552	4.880	5.429	5.903	4.146
$H_S = 3.25$ ( $P_f$ )	3.92E-2	2.04E-2	6.24E-5	3.75E-4	3.53E-3	5.86E-4	9.48E-5	2.44E-2
( $\beta$ )	1.760	2.047	3.836	3.371	2.694	3.246	3.732	1.970
$H_S = 5.0$ ( $P_f$ )	2.59E-1	2.04E-1	3.49E-3	1.37E-2	6.20E-2	1.79E-2	5.35E-3	1.98E-1
( $\beta$ )	0.645	0.827	2.697	2.208	1.538	2.098	2.552	0.849
$H_S = 7.75$ ( $P_f$ )	6.68E-1	5.63E-1	5.05E-2	1.26E-1	3.19E-1	1.56E-1	6.89E-2	6.16E-1
( $\beta$ )	-0.436	-0.159	1.639	1.144	0.470	1.011	1.484	-0.294
Long term ( $P_f$ )	9.22E-3	4.59E-3	4.95E-6	4.00E-5	5.34E-4	6.58E-5	8.67E-6	5.32E-3
( $\beta$ )	2.356	2.605	4.420	3.944	3.272	3.824	4.297	2.554

To calculate the fatigue reliability, the same expression as equation (3.34) is applied here with the three random model corrections,  $\delta_F$ ,  $\delta_S$  and  $\delta_{SCF}$ , to take into account the uncertainties in the hydrodynamic load, the stress calculation and the stress concentration factor, respectively, i.e.

$$g(X) = \delta_{tf} \int_{a_0}^{a_{cr}} \frac{da}{C_A (\delta_Y Y_A \sqrt{\pi a})^m} - v^l \tau \delta_F^m \delta_S^m \delta_{SCF}^m A^m \Gamma(1 + \frac{m}{B}) \quad (4.2)$$

The random variables have the same statistical uncertainty as shown in table 3.1 and the Weibull distribution parameters are used according to the table 4.2. The reliability calculation has been carried out using the Kirkemo model for the geometry function and the stress range distributions are calculated and given in table 4.3.

The results show that the zero and 315-degree hot-spot positions are more critical than the other points and give the highest failure probability, see table 4.3. However, this cannot be generalized for other members of the structure and each one should be investigated separately to find the critical hot spot. Since the Kirkemo model of the geometry function is used in these calculations and this model is based on a bending to membrane stress ratio 5, these

results cannot directly be applied for jack-up platforms and a correction is required before any application. Section 4.3.2 discusses this correction, by using the exact bending to membrane stress ratio derived from time history of the hot spot stress process.

### 4.3.2 The bending to membrane stress ratio and selecting of a geometry function

In the calculation of the fatigue damage of tubular joints, the geometry function plays an important role because it takes into account the correction arising from boundary effects due to the loading and crack geometry, Etube (2001).

In the second chapter, several approaches to determine the geometry function are discussed and presented, e.g. Kirkemo, Moan and Aghakouchak. It should be noted that all these geometry function formulations may not directly be applied for the fatigue reliability analysis of jack-up platforms because they have been specified from the individual bending to membrane stress ratio ( $\alpha$ ) (four in the case of the Moan and five in the Kirkemo formulation), which is originally derived from the stress distribution of fixed jacket platforms. Therefore, this ratio would not be a reliable case for the stress distribution of the jack-up platforms. Consequently, it is necessary to modify the geometry function through the specific bending to membrane stress ratio calculated from the stress analysis of the jack-up platforms and hence obtain a new geometry function through this new  $\alpha$  ratio. Moreover, a correction in the geometry function should be applied to consider the discontinuity of the welding toe profile ( $M_k(a)$  in formulation 2.11), Smith and Hurworth (1984). This type of stress ratio modification and weld toe correction is applied in the computer program developed for this purpose and its flowchart is shown in the figure 4.4. By using this stress ratio in the crack growth formulation, it is also possible to derive an expression to constitute the relation between the crack aspect ( $a/c$ ) and the propagation of the crack through the thickness ( $a/t$ ). This relationship must be specified in the two-dimensional Raju and Newman geometry function because it describes the shape of crack propagation.

The variation of the reliability index with the bending to membrane stress ratio ( $\alpha$ ), is calculated and shown in figure 4.6 for an example of a diagonal bracing element of the platform below the jacking system in the forward leg (element no. 295) and at the zero hot-spot. In this calculation, the Raju and Newman formulation is applied to calculate the geometry function because with this approach it is possible to take the variation of the stress ratio  $\alpha$  and  $a/c$  into account. As can be seen from figure 4.7, the reliability index of the zero  $\alpha$  gives the lowest value but this value increases with an increasing value of  $\alpha$ . The stress process is pure membrane when  $\alpha$  approaches to zero and using this ratio in the fatigue reliability calculation may lead to a conservative result. On the contrary, the stress process is pure

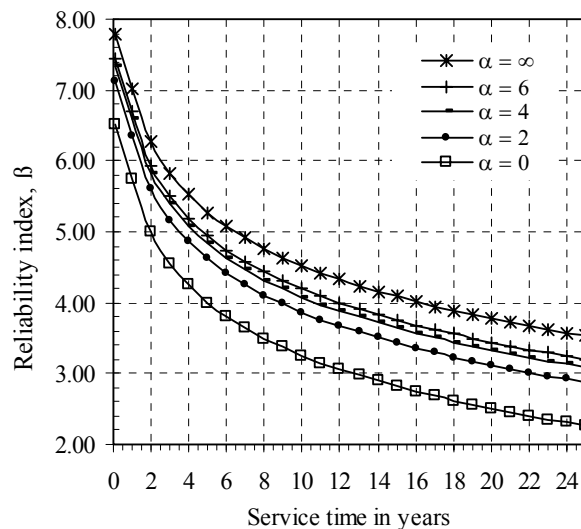


**Figure 4.7** Reliability index  $\beta$  as function of time for different  $\alpha$  ratios at zero hot spot

bending when  $\alpha$  is approaching to infinity and applying this stress ratio in a reliability calculation may lead to a higher reliability index. Therefore, the calculation of the appropriate  $\alpha$  ratio is essential and should be based on the actual stress process.

**Table 4.4:** The expected bending to membrane stress ratio in the stress-peak for several sea states in a diagonal bracing of a jack-up structure (element no.295) below the lower guide.

Position ( $\theta$ )	0	45	90	135	180	225	270	315
$H_S = 1.75$	1.0438	0.6816	0.1680	0.8283	1.0246	0.7029	0.1694	0.8315
$H_S = 3.25$	0.9922	0.6593	0.0837	0.7627	0.9876	0.6810	0.0886	0.7584
$H_S = 5.00$	0.9770	0.6525	0.0682	0.7328	0.9643	0.6650	0.0700	0.7364
$H_S = 7.75$	0.9618	0.6490	0.0538	0.7220	0.9568	0.6499	0.0553	0.7137
Long term	1.0135	0.6685	0.1208	0.7833	1.0002	0.6835	0.1235	0.7884

The calculated  $\alpha$  ratios for several hot spots of element no. 295 are shown in table 4.4. The value of  $\alpha$  changes for each hot-spot point and sea state but in the most cases the sea state variation is not significant. However, the maximum range is restricted to one and it shows that the behaviour of the peak stress in this element is predominated by equal bending to membrane stress ratio. This can be related to the configuration of the leg structure, in which the axial stress of the element is higher than the bending stress. The long-term  $\alpha$  ratio can be calculated by combining the  $\alpha$  ratio of each sea state according to its occurrence probability. This long-term  $\alpha$  is calculated and shown in the last row of table 4.4 as well.

The Raju and Newman geometry function formulation is derived for tube shape elements without any discontinuity in the shape but the exact tubular joints in offshore structures have discontinuity in shape due to the weld profile. The Moan and Kirkemo's formulation considers this discontinuity by using a correction term presented by Smith and Hurworth (1984). Consequently, it is required to apply this correction term in the Raju and Newman formulation to consider the discontinuity of weld toe profile. By using this  $\alpha$  and applying the correction term given by Smith and Hurworth (1984) for the discontinuity in shape due to the weld toe profile, the final reliability indices for several hot spots of brace element number 295 are calculated for a number of service times and illustrated in figure 4.8. As becomes clear from this figure, the zero hot spot intersection gives the lowest

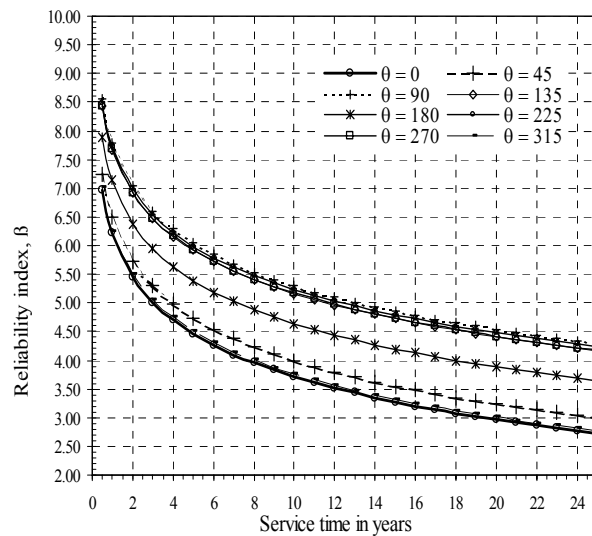


**Figure 4.8** Reliability index  $\beta$  as function of service time for different hot-spots ( $\theta$ )

reliability index (the maximum failure probability) and in contrary  $\theta=180$  gives the highest reliability index during the service time of the structure. The intersection of this element can generally be divided into four hot-spot zones in which the most critical zones to fatigue failure are located between angles of 315 and 45 degrees.

To show the differences between the reliability results of the formulation presented by the three approaches of Kirkemo, Moan and Aghakouchak in comparison with the proposed method, the reliability indices are calculated for these methods and compared in table 4.5. Furthermore, the results of the Raju and Newman formulation without correction proposed by Smith and Hurworth are also calculated and illustrated in table 4.5. As can be seen from the reliability results, the reliability index through the Raju and Newman formulation without the weld toe profile correction gives a higher value than the others and should not be used directly in a reliability calculation. The reason for this difference can be related to the correction term for the consideration of the discontinuity in the shape due to the weld toe profile. The reliability indices derived according to the Kirkemo's geometry function give conservative values. However, compared to Moan's formulation, no significant difference can be observed. Actually, this difference can be related to the coalescence of micro cracks in the initial phase of the crack propagation assumed in the Moan's approach and ignored in the Kirkemo's proposal. The Aghakouchak formulation gives a lower reliability index than Raju and Newman but a higher one than Moan and Kirkemo and is close to the proposed method in this research. It is not clear which correction Aghakouchak applied to incorporate the discontinuity in the welding profile or the bending to membrane stress ratio.

**Table 4.5:** The calculated reliability index or failure probability for different geometry function formulations, service time is 20 years.

Method		Kirkemo	Aghakouchak	Moan	Two dimensional Raju and Newman	Proposed method
Position ( $\theta$ )						
0	$\beta$	2.3565	3.0102	2.5532	3.7114	2.9629
	$P_f$	9.225E-3	1.305E-3	5.336E-3	1.0307E-4	1.524E-3
45	$\beta$	2.6046	3.2465	2.7944	3.9608	3.2398
	$P_f$	4.599E-3	5.842E-4	2.599E-3	3.7357E-5	5.980E-4
90	$\beta$	4.4195	4.9947	4.5455	5.3938	4.5418
	$P_f$	4.947E-6	2.947E-7	2.739E-6	3.4492E-8	2.788E-6
135	$\beta$	3.9441	4.5390	4.081	5.1551	4.4113
	$P_f$	4.006E-5	2.825E-6	2.2439E-5	1.268E-7	5.138E-6
180	$\beta$	3.2719	3.8909	3.420	4.5954	3.8838
	$P_f$	5.341E-4	4.995E-5	3.137E-4	2.160E-6	5.142E-5
225	$\beta$	3.8235	4.4225	3.967	5.1522	4.4814
	$P_f$	6.577E-5	4.8772E-6	3.643E-5	1.288E-7	3.708E-6
270	$\beta$	4.2967	4.8755	4.4276	5.277	4.4205
	$P_f$	8.669E-6	5.426E-7	4.763E-6	6.5649E-8	4.924E-6
315	$\beta$	2.5540	3.1982	2.7452	3.8118	3.0089
	$P_f$	5.325E-3	6.915E-4	3.024E-3	6.898E-5	1.311E-3

The proposed method gives higher reliability indices than the Kirkemo and Moan approaches but lower ones than the Aghakouchak and the two-dimensional Raju and Newman methods without a correction term of the weld toe profile. The differences can be related to the bending to membrane stress ratio assumption used in each method. In the proposed method the actual bending to membrane stress ratio is first calculated from the time history of the stress process and then substituted in the two-dimensional Raju and Newman formulation with a correction term for the weld toe profile to determine the final geometry function.

### 4.3.3 Effect of spectral models on fatigue reliability

The fatigue reliability calculation requires that the stress distribution of the stress range according to the wave characteristics, and the corresponding wave spectral densities are known. Both models are subject to uncertainties. For dynamically sensitive structures such as jack-up platforms, the choice of the spectral model may have a significant effect on the prediction of the stress range distribution and changes the fatigue reliability. In this section, the emphasis is therefore on the investigation of the effect of spectral model choice on the estimated fatigue reliability indices.

There are several wave spectra to represent the wave energy but the appropriate choice of spectra varies with the location and condition, depending on some variables such as wind duration and fetch length. The P-M, (Pearson-Moskowitz, 1964) and the JONSWAP (Hasselmann et al., 1973) spectra are two widely implemented spectra in the design of offshore structures. The P-M model is used to represent severe storm wave conditions in offshore structural design where the fetch length and the duration of the wind are infinite; this model is named a full-developed sea spectrum. The JONSWAP spectrum has been mainly developed for the fetch limited sea condition of the North Sea, which looks peakier than the P-M spectrum. In the preceding sections, the P-M spectrum is used to represent the wave energy but in this section, the result of this model will be compared with the JONSWAP spectrum.

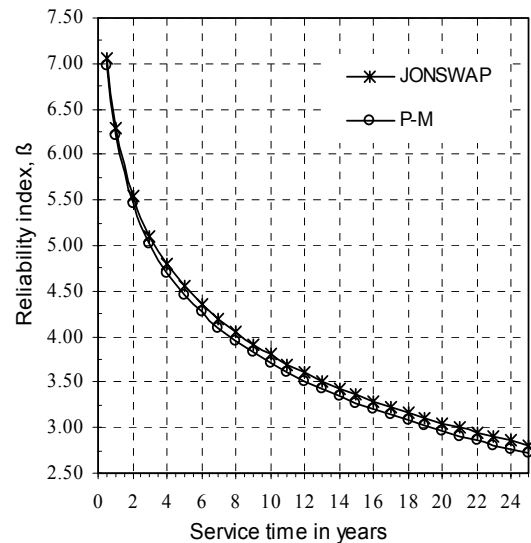


**Figure 4.9** Comparison of reliability index ( $\beta$ ) between P-M and JONSWAP spectra in the zero hot spot of the element no. 295

The fatigue reliability computation is carried out for element number 295 at the zero hot spot. The results are illustrated in figure 4.9 and show that the use of the P-M spectrum gives a lower reliability index than the JONSWAP spectrum but the differences are not so high, especially during the first five years of service time. However, these differences increase with the service time of the platform.

#### 4.3.4 Variation of fatigue reliability with overall damping of platform

The response of a jack-up platform is estimated according to the solution of the dynamic equation of motion of a structural model, which typically is carried out with a Finite Element Method (FEM). Part of the energy in the dynamic equation dissipates within the damping term of the equation and some uncertainty is included in the choice of this term.

The total damping consists of three elements: structural, soil and hydrodynamic damping. The structural damping is described by a linear viscous damping and can be modelled with a proportional Rayleigh model. The proportional Rayleigh model damping means that the damping is proportional to either one or both of stiffness and mass, in which the proportionality factors can be estimated according to the important natural frequencies of a structure.

The soil-structure interaction is an important aspect in the jack-up dynamic response and this area is getting research interest, Cassidy (1999), Shabakhty et al (2003). The soil-structure interaction model is indeed in a nonlinear manner and soil damping in this model is automatically accounted for by the hysteretic behaviour of the nonlinear model but usually the linearized model is applied. When the linearized soil-structure interaction modelling is employed, the soil damping can be introduced by specifying linear dampers at the foundation nodes. However, it is often difficult to calculate the required characteristics of damping coefficients corresponding to the linearized soil-structure interaction analysis. Therefore, the soil damping is often accounted for by increasing the damping level specified in a proportional Rayleigh model for the structure, Karunakaran (1993).

The hydrodynamic damping is implicitly modelled as part of the hydrodynamic load term when the generalized Morison equation is used to calculate the hydrodynamic load. The hydrodynamic damping becomes important only in case where the structural movements are large compared to the diameter of the loaded member and it is recommended to discard this effect when the movements are less than the diameter of the loaded member, DNV (2000). This situation mainly occurs for low and medium sea states. Moreover, experimental studies on jack-up platforms have shown that the hydrodynamic damping can sufficiently be expressed as fixed damping added to the structural damping, Grundlehner (1995).

There are several approaches to measure the structural damping. The structural damping can be measured from the free vibration of a structural model in a laboratory test. In this method, the transit response of the structure in still water is registered from the specific initial displacement and the damping of the structure is calculated according to the logarithmic decay of response.

The estimated and recommended overall damping of jack-up platforms in literature gives different values. For example, in an analytical investigation of Torhaug (1996) 3% damping ratio is

**Table 4.6:** The loading function, zero and peak frequency for several damping ratios at zero hot-spot of element 295

Damping Ratio	Fatigue loading function			$v_0$	$v_P$
	Service time				
	2	10	25		
↓					
2.0%	3720	18603	46506	0.199	0.224
5.0%	2108	10542	26355	0.158	0.195
7.0%	1876	9383	23457	0.149	0.184
10.0%	1734	8671	21678	0.141	0.169

assumed to be an adequate value to reflect the overall damping of the model under investigation. In the other work, Etube (2001) recommends to use a 4% damping ratio. Moreover, the model test of a jack-up carried out by Marine Structures Consultant (MSC) in the offshore wave basin of the Danish Hydraulic institute in Denmark gives a total value of 5% damping, Karunakaran and Spidsoe (1995). Batista et al. (1986) report higher values ranges from 10.5% to 11.5% and lower values between 2% to 4% are also given in Hambly et al. (1990). The overall damping ratio of jack-up platforms appears to vary significantly from 2 up to 10 percent and there is consequently some uncertainty in the proper selection of this value. Direct incorporation of the damping uncertainty in the fatigue reliability calculation is a difficult task, in particular when the time history simulation of the stress process is used to determine the stress range distribution. In the following section an attempt is made to investigate the variation of the damping ratio with fatigue reliability by changing this ratio.

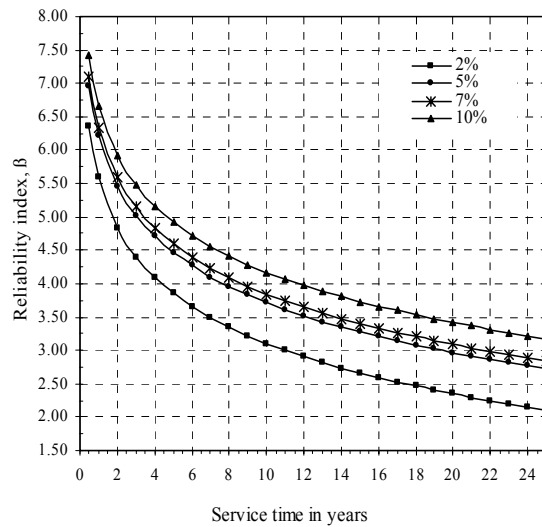


**Figure 4.10** Comparison of reliability index  $\beta$  for several damping ratios

The ranges between 2% and 10% are assumed here for the overall damping ratio of the proposed jack-up platform. The short-term stress range distributions are calculated for the zero hot-spot position of element 295 and the long-term distributions are determined through the occurrence of each sea state for each damping ratio. The fatigue reliability indices are calculated for several service times using the method described in section 4.3.2 taking into account the bending to stress ratio, the correction of the geometry function for discontinuity in the weld toe profile and finally using the 2-D method of Raju and Newman to specify the crack aspect ratio ( $a/c$ ).

The reliability indices are calculated and shown in figure 4.10. As becomes clear from this figure, the reliability indices increase for a higher damping ratio and decrease by increasing the service time. The increase in reliability indices for the damping ratio between 5% and 7% is not high but is significant between the 2% and 10% ratio. These differences can be related to the response of the platform in each damping ratio according to the value of the fatigue loading function and the number of stress ranges. For the 10% damping ratio, the fatigue loading function has the smallest value compared to other ratios. Furthermore, the number of stress ranges, which is related to the number of the zero or peak frequency (according to narrow or broad-banded assumption), has for the 10% damping ratio the lowest values, see table 4.6, therefore the reliability indices will normally increase in this case. However, as can be observed from this table, the difference between 5 and 7 percent damping ratio is not so much. According to these results, it becomes clear that the uncertainty in damping can considerably change the fatigue reliability and more investigation should be carried out to specify the damping ratio. The damping ratio may be incorporate in the reliability calculation as a random variable and the reliability calculation is carried out by using a method described in section 3.4.6 as a time independent variable or applying the response surface technique as



given in section 3.4.5. However, this aspect is not pursued further in this research work and a deterministic value of 5 % damping ratio is applied for the structural analysis in the case of the significant wave height being less than 10 m as recommended by Daghigh (1997).

#### 4.3.5 Effect of nonlinear and wide-banded stress models on fatigue reliability

As described in section 2.3.3, in case the stress process is Gaussian and narrow-banded, the stress cycle follows the Rayleigh distribution. But the validity of this model is doubtful for a drag-dominated offshore structure like this jack-up platform due to the nonlinearity in the stress process. This nonlinearity can be observed when the skewness and kurtosis of the hot spot stress processes are compared for several sea states in table 4.7. This nonlinearity, as may be observed from this table, increases by increasing the significant wave height. The

comparison of the irregularity factor for the lower sea state with other sea states, of which the lower one is likely to be more Gaussian than the other ones, shows that the narrow-banded assumption cannot be validated. The band correction is therefore recommended in several publications. For example Wirsching and Light (1980) give only a correction term in accordance with the bandwidth parameter. Zhao and Baker (1990) propose a combination of two Weibull and Rayleigh probabilistic models according to the bandwidth parameters. Winterstein (1988) demonstrates that the Hermite model may provide a better probabilistic model for the stress range than the other probabilistic models, because in this model it is possible to take the higher statistic moments of the non-linear response into account.

**Table 4.7:** The Statistical characteristics of stress processes in zero hot spot for element no.295

Sea State ( $H_s$ )	Skewness	Kurtosis	Irregularity Factor ( $\alpha$ )	Spectra Bandwidth ( $\epsilon$ )
1.75	0.0663	3.3041	0.9051	0.4251
3.25	-0.0738	3.5947	0.8577	0.5141
5.00	-0.3792	3.8476	0.7563	0.6542
7.75	-1.0226	4.8925	0.6333	0.7739
10.45	-1.7780	7.9906	0.4619	0.8870

**Table 4.8:** The calculated loading function for different wide-banded and nonlinear models at zero degree hot-spot point when the service time is 20 years.

Model	Peak Counting	Narrow-banded (Rayleigh)	Wide-banded (W. & L.)	Wide-banded (Z. & B.)	Hermite (W.)	Rainflow Counting
$H_s = 1.75$	5237.9	5507.9	4484.4	5041.8	6003.8	7828.9
$H_s = 3.25$	38113	32502	26638	29213	38149	54811
$H_s = 5.00$	110890	80279	65398	73387	106980	121500
$H_s = 7.75$	337890	244320	195650	231060	432380	298809
$H_s = 10.45$	537460	363590	296480	331540	801020	514281

In this section an attempt is made to examine the nonlinear Hermite (Winterstein, 1988) model and other wide-banded correction models presented by Wirsching and Light (1980), Zhao and Baker (1990), and compare the fatigue reliability indices estimated in accordance

with these method and rainflow counting method. Also, the fatigue reliability results of the traditional narrow-banded Rayleigh and the proposed Weibull model (peak counting) are compared.

Firstly, the loading functions necessary in reliability estimation are calculated according to each method and the fatigue reliability indices are then calculated for several sea states. The results of the fatigue loading function are given in table 4.8. By using these loading functions in fatigue limit state, the fatigue reliability indices are calculated and presented in table 4.9 respectively.

The rainflow counting method gives the highest loading function for the three lower sea states but for the two higher sea states lower than the peak counting and the non-linear Hermite model. For the lower sea states, the differences between the loading functions for all methods are not significant but grow with an increasing significant wave height.

The two wide-banded correction approaches presented by Wirsching and Light (W&L), and Zhao and Baker (Z&B) generally give lower loading functions than the Narrow-banded assumption (Rayleigh model) but the nonlinear Hermite approach proposed by Winterstein (W.) provides the highest loading function. The stress range in the Hermite model depends only on the kurtosis of the hot spot stress process, which for lower sea state tends to approach the Gaussian distribution but deviates significantly for higher sea state, see table 4.7.

**Table 4.9:** The calculated reliability index ( $\beta$ ) for different models of loading function when the service time is 20 years.

Model	Peak Counting	Narrow-banded (Rayleigh)	Wide-banded (W. & L.)	Wide-banded (Z. & B.)	Hermite (W.)	Rainflow Counting
$H_S = 1.75(m)$	4.049	3.995	4.217	4.090	3.901	3.614
$H_S = 3.25$	1.905	2.077	2.291	2.191	1.904	1.514
$H_S = 5.00$	0.756	1.104	1.324	1.200	0.795	0.658
$H_S = 7.75$	-0.436	-0.089	0.148	-0.030	-0.700	-0.305
$H_S = 10.45$	-0.932	-0.515	-0.296	-0.416	-1.357	-0.885

The reliability indices are calculated for each sea state and illustrated in table 4.9. Generally, the results of the rainflow counting method are conservative compared to other methods. The W&L correction model gives higher reliability indices than others. For the lowest sea states the results of most methods, except the rainflow counting, are close to each other but for higher sea states good agreement can be observed between the rainflow and the peak counting method. The narrow-banded assumption and the band corrections models (W&L and Z&B) generally give a higher reliability index and using these methods may lead to unconservative results.

Generally, it can be concluded that the proposed Weibull model gives a good approximation for the higher sea state and almost the same trend as other methods for the lower sea states comparing to the rainflow counting method.

#### 4.4 UPDATING OF FATIGUE RELIABILITY THROUGH INSPECTION RESULTS

The inspection of jack-up platforms may provide good information for risk management related to the hazard of loss of structural integrity. The Classification societies therefore prescribe regular annual, intermediate and full inspection programs, which could be undertaken at intervals of 1, 2 and 4 years respectively, Onoufriou and Dixon (1996). Moreover, a jack-up platform can be dry-docked, making it possible to clean and inspect the entire structure in detail, which is raising the quality of the inspection and repairs. Uncertainties incorporated in the inspection procedures and the results of inspections such as detecting or not detecting any crack could be used for fatigue reliability updating.

Methods to update the reliability or failure probability are generally divided into three main categories for which a selection depends on the available information and additional details of the structure. They are categorized into event updating, variable updating and statistical updating, Moan and Song (2000).

The number of random variables considered in the reliability calculation can be changed according to the uncertainties in variables but the inspection information may be used to update the basic variables. This type of updating is known as variable updating and the failure probability can therefore be calculated by replacing the updated random variables in the new safety margin. In this type of updating, a sensitivity analysis could also be carried out to limit the number of basic random variables without impairing the accuracy of the results.

Updating of the statistic characteristics of random variables like the mean value, the standard deviation or the type of probability distribution is called statistical updating. Sometimes the inspection of joints provides information about the distribution of the basic random variables such as the distribution of initial crack size. Also, more tests on fatigue characteristics and a regression analysis may reveal statistic characteristics other than supposed already, all these new information could be applied for statistical updating.

##### 4.4.1 Event updating through inspection results

The inspection of jack-up platforms provides information about the existence or non-existence of fatigue cracks. The detection or no detection of cracks, which are depending on the inspection quality, incorporates uncertainty and they could be specified through the events represented by the equations 4.4 and 4.5 for detection and no detection of crack respectively. These events can be used to update the failure probability and this type of updating is known as event updating. The updated failure probability can be estimated with calculating the following conditional probability,

$$P_f^U = P [g(X) \leq 0 | E_I] = \frac{P [(g(X) \leq 0) \cap E_I]}{P [E_I]} \quad (4.3)$$

where  $E_I$  is the possible result from inspection event and  $g(X)$  is the safety margin (limit state function) described by equation 4.2.

Basically two results can be imagined from inspection. Firstly, crack detected, measured and eventually repaired and secondly, no crack detected. If during an inspection process a crack is

detected and measured at time  $t_I$ , the event or event margin corresponding to the detection of the crack is expressed with,

$$E \equiv \left[ \int_{a_0}^{a_I} \frac{da}{C_A (\delta_Y Y_A \sqrt{\pi a})^m} - v^I t_I \delta_F^m \delta_S^m \delta_{SCF}^m A^m \Gamma(1 + \frac{m}{B}) \approx 0 \right] \quad (4.4)$$

where  $a_I$  is the measured crack size at time  $t_I$  and is a random variable due to uncertainty in the interpretation of a measurement instrument. Other terms in equation 4.4 are the same expression as in equation 4.2. The failure probability may then be calculated using the condition probability presented in equation 4.3.

An inspection does not increase the reliability of the structure, but makes it possible to take the corrective action such as repair if a crack is detected. The safety margin after repair follows the same expression as equation 4.2 with the exception that a revised initial crack size and fatigue characteristic after the repair should be utilized in this expression.

If no crack is detected during the inspection process, this means that no crack exists or that the existing crack size is too small to be detected by the inspection instrument or applied inspection method. The event margin for this case for the inspection time at  $t_I$  can be specified with,

$$E_{\text{no crack}} \equiv \left[ \int_{a_0}^{a_D} \frac{da}{C_A (\delta_Y Y_A \sqrt{\pi a})^m} - v^I t_I \delta_F^m \delta_S^m \delta_{SCF}^m A^m \Gamma(1 + \frac{m}{B}) > 0 \right] \quad (4.5)$$

where  $a_D$  is the detectable crack size. Since the detectable crack size depends on the inspection method and the detection instrument, it should also be regarded as a random variable and specified by a specific Probability Of Detection (POD) curve. Several formulations of POD are available but a commonly exponential distribution is used, Moan et al. (2001),

$$P_D(a_D) = 1 - \exp\left(-\frac{a_D}{\lambda_D}\right) \quad (4.6)$$

In which  $\lambda_D$  is the mean detectable crack size. If the same joint with the same POD is inspected several times, it is expected that a repeated inspection should improve the chances of finding the defects. For  $n$  inspection times and the same POD as in formulation 4.5 for each inspection, the likelihood of a successful POD can be improved and be calculated through the following term,

$$P_{D,n}(a_D) = 1 - \exp\left(-\frac{na_D}{\lambda_D}\right) \quad (4.7)$$

where  $P_{D,n}(a_D)$  is the POD after  $n$  independent inspections of the same joint. It seems from equation 4.7 that after applying several inspections with an unfavourable technique, a reasonable success can be expected if the inspection is repeated several times. This expression can only be used when each inspection result is independent from the results of other inspections. Since this is difficult in practice to achieve by the same inspection team i.e. repeating the same inspection without being influenced by the results of earlier inspections, it might be better to carry the inspection out at different times or by different teams. However,

usually it might be easier to do several inspections at one time, in particular during a dry-docking period. Usually the specialized and experienced teams carry out the inspections. When cracks are found, the location and size are registered, and depending on the finding the decision for repair will be taken. The repair will be inspected again to check it has been executed properly. However, in case that a crack or imperfection is considered not to be significant, a repair may be postponed to the following inspection. During fabrication the initial inspection of the structure is a part of the production process and a similar procedure will be followed. This is the usual practice of the classification societies.

The inspection procedures of offshore structures are usually carried out through field inspection by visual checks of joints or more sophisticated non-destructive tests (NDT) such as Magnetic Particle Inspection (MPI), Eddy Current Inspection (ECI), alternating current field measurement (ACFM) or flooded member detection (FMD) to detect the surface defects. Also, the Ultrasonic Testing (UT) and Alternating Current Potential Drop (ACPD) are used to measure the depth of surface defects, Baker and Descamps (1999). The success of an inspection technique to detect or measure the crack size varies from one NDT method to other one. For any given NDT, there is always a critical size below which a crack may not be detected. Moreover, where a crack size is measured, it must be treated with a certain uncertainty depending on the accuracy of the utilized equipment and the skills of the operators.

#### 4.4.2 Updating fatigue reliability through inspection with no-crack detection

To illustrate the process of updating the fatigue reliability through the inspection information, the same joint of the brace element (element number 295) in the previous section is considered and the inspection method is specified through the exponential distribution with the mean detectable size equal to 1.3 mm. This type of inspection is related to the MPI method with a 90 % probability of detection of a 40 mm long crack, Kirkemo (1988). In this model, the surface length of crack ( $2c$ ) is measured by MPI and the fatigue crack aspect ratio ( $a/c$ ) is assumed to be equal to 0.15 for tubular elements.

Supposing the inspection is carried out at a 4-year service time with no crack detection, figure 4.11 shows the results of a reliability updating. As is clear from this figure, the inspection of the joint increases the fatigue reliability, which decreases with the service time and become higher than the no-inspection results at the end of the service time. A joint may be inspected repeatedly and independently, involving an improved POD. In figure 4.11, the influence of

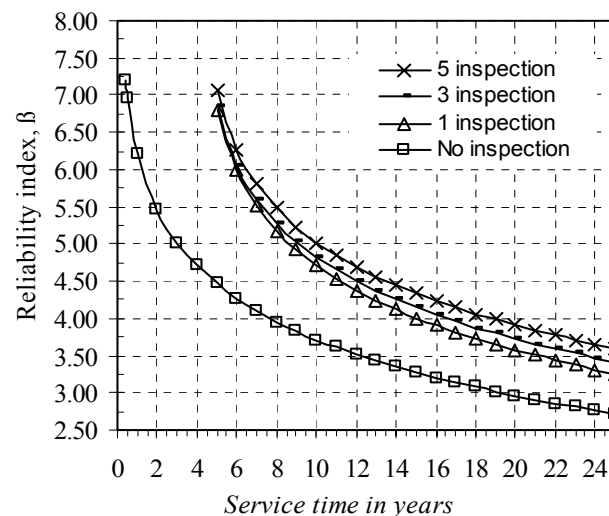


**Figure 4.11** Effect of inspections on updating of fatigue reliability without crack detection, inspections at 4 years

repeated inspections on reliability updating is shown for three and five periodical inspections of the same joint. It is observed that this effect has some positive influence on the fatigue reliability, however this is very low up to 8 year but increases with the service time after that period.

This approach gives an idea to establish a criterion for the inspection of a platform. The inspection time can e.g. be scheduled in such a way that a minimum level of reliability, which can be called the target reliability, is maintained. When the reliability index reaches this level, an inspection is recommended. For the second inspection time, the same process could be followed and continued for the next inspection time by retaining the fatigue reliability up to the end of service time higher than the target reliability. More details about this method and scheduling method are given in Onoufriou (1999) and Shabakhty et al. (2002).

#### 4.4.3 Updating the fatigue reliability through inspection with crack detection

If the inspection information leads to the detection and measurement of a specific crack size, and finally the crack is repaired, the event margin for this inspection information can be specified through the expression 4.5 and the safety margin is modified according to the new material fatigue characteristics. To investigate this type of updating on fatigue reliability, the same joint as in the previous section is considered here again and the assumption is that the crack is detected and measured during the inspection process after the 4th year of service time with a mean detection size of 4 mm. Furthermore, due to the uncertainty in the measurement the crack size is assumed to follow the normal distribution with a coefficient of variation of 0.10, Moan and Song (2000).

After the repair, the uncertainty in the initial crack size, material fatigue characteristics and geometry function may change due to variation of material characteristics but it is supposed that the same material will be used after repair. Hence, the statistic characteristics of the initial crack size ( $a_0$ ), fatigue characteristics ( $m$  and  $C$ ) and geometry function will follow the same probabilistic models as the previous one and are also assumed to be statistically independent. The updated reliability through this type of inspection is shown in figure 4.12. The reliability index increases immediately after repair but drops below the level obtained by the no- inspection after 12 years service time. This may be related to entering a larger uncertainty than anticipated in the fatigue reliability calculation, which is acting after repair.

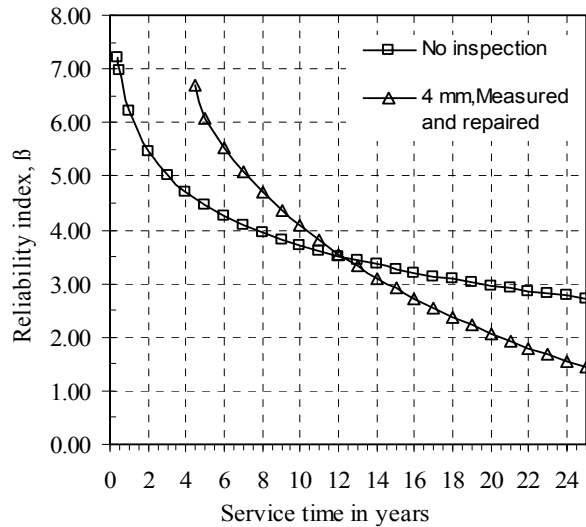


**Figure 4.12** Fatigue updating through crack detection, measuring and finally

Comparing figure 4.11 and 4.12, it can be noted that the increase in the reliability index is higher in case of no-detection of a crack than in the case of the finding and repairing of any

crack. This can be related to the fact that in the scenario of detection of a crack it may be expected to find a new crack in the future. The finding of a crack is for instance an indication that the stresses are higher than expected.

#### **4.5 RELIABILITY OF JACK-UP PLATFORM IN EXTREME ENVIRONMENTAL LOADS**

One of objectives of a design code is to ensure that the stresses in the structural elements resulting from extreme environmental loads are adequately below the specific limit. There are several failure modes for each member and connection in a design code. Each of these failure modes e.g. buckling, punching or yielding is usually expressed as a function of the stresses in the members and normalized in such a way the combination is retained below a value of 1.0. The value of this function is generally known as the “utilization ratio”,  $U$ , and code failure occurs if it exceeds 1.0.

The time history of stress response in structural elements of offshore structures such as jack-up platforms is not always in a specific state due to cyclic behaviour of wave loads and often varies from tension into compression and vice versa from compression into tension. One single failure mode may not sufficiently represent the potential of the failure of an element and some modification should be applied when the stress state changes. In this section, the reliability calculation according to the traditional method of using one failure mode for yielding or buckling is compared with the new method which combines these two failure modes by using the time history of usage factors and the results are finally compared with each other.

##### **4.5.1 Extreme environmental loads**

To calculate the structural response under extreme environmental load commonly three approaches may be used concerning the complexity and time consuming of each one, Farnes and Moan (1994). These methods are categorized into design wave, design storm and finally long-term approach.

In the design wave approach, the extreme environmental wave loads can be specified for a specific wave height and associated wave period according to a typical return period, say 50 years, and the hydrodynamic loads are estimated using a proper wave theory depending on the water depth and wave steepness. By applying the calculated hydrodynamic loads in this way, the maximum response can easily be determined through the analysis process.

In the design storm method, the extreme environmental load is specified for a significant wave height and zero crossing period according to specific return period, as carried out for the design wave method. Wave energy spectra such as P-M or JONSWAP are used to express the distribution of the wave energy upon the wave frequency range in this sea state. The hydrodynamic loads can finally be calculated using this wave spectra with the uniform random phase lag as explained in section 4.2 for DSA or in combination with a random Rayleigh distribution of amplitude for NDSA. The maximum response is finally predicted using the specific distribution function to fit on the peak of time history of response.

The long-term approach is more complex and time consuming than other methods but yields an improved estimate of extreme response. In this method the sea states are specified through the scatter diagram and the hydrodynamic load and response for each sea state in a scatter diagram is calculated using the method described for the design storm. A specific distribution function, such as the Weibull or Hermite distribution is fitted on the peak response for each sea state and the long-term distribution function of response is calculated using the combination of these short-term responses through the occurrence probability of sea states described in the scatter diagram. To simplify this approach without reducing the accuracy, Farnes and Moan (1994) recommended to divide the scatter diagram into several blocks and assumed that each short term response function changes slowly from each block to an other one for slightly and moderate non-Gaussian response process and is kept constant within each blocks. The final expression for response distribution is smoothed in a way that the contribution of all blocks is accounted for.

To reach a certain level of accuracy to predict the short-term response distribution of a platform, we require a long time history simulation of the hydrodynamic loading and the application of these loads in a finite element program to determine the time history of the stress response. In the last decade, a specific approach has been developed to prevent this long time history simulation using the constrained wave simulation approach in such a way that the most probable extreme wave crest occurs in a shorter time of simulation, Tromans et al. (1991). Therefore, the extreme structural response can directly be related to the extreme wave crest. The validation of this assumption has been investigated for quasi-statically responding structures by Tromans et al. (1992) and later for dynamic sensitive structures such as jack-up platforms by Harland et al. (1996) and Taylor et al. (1997). They compared the results of the constrained simulation technique with the long time history simulation and concluded that the constrained technique gives adequate approximation.

To specify the extreme environmental loads for a jack-up structure, the design storm method has been used. Therefore, it is required to establish a probabilistic approach to predict the extreme environmental load for a specific return period, assumed to be 50 years here. The inverse FORM method recommended by Winterstein et al. (1993) is applied because in this method it is possible to take the joint distribution of random environmental parameters into account.

In this approach, the contour of environmental parameters such as the significant wave height and zero crossing period is related to a specific return period,  $T_r$ , according to the following expression,

$$\sqrt{U_1^2 + U_2^2} = \Phi^{-1}\left(1 - \frac{T_{SS}}{T_r}\right) \quad (4.8)$$

where  $T_{SS}$  is the sea state duration (here 3 hours) and two auxiliary normal random variables  $U_1$  and  $U_2$ , which can be specified through the distribution function of the significant wave height,  $F_{H_S}(h_s)$  and the conditional zero crossing period,  $F_{T_Z|H_S}(t|h)$  respectively with the following formulations,

$$\begin{aligned} U_1 &= \Phi^{-1}(F_{H_S}(h_s)) \\ U_2 &= \Phi^{-1}(F_{T_Z|H_S}(t|h)) \end{aligned} \quad (4.9)$$



Figure 4.13 shows the  $H_s$ - $T_z$  contour for 10, 20, and 50 years return periods derived for the Hutton area according to the scatter diagram of the Stevenson station, Marex (1979). The three parameter Weibull distribution is fitted on the significant wave height and the conditional lognormal distribution is applied to specify the zero crossing period conditioning the significant wave height, see appendix C.

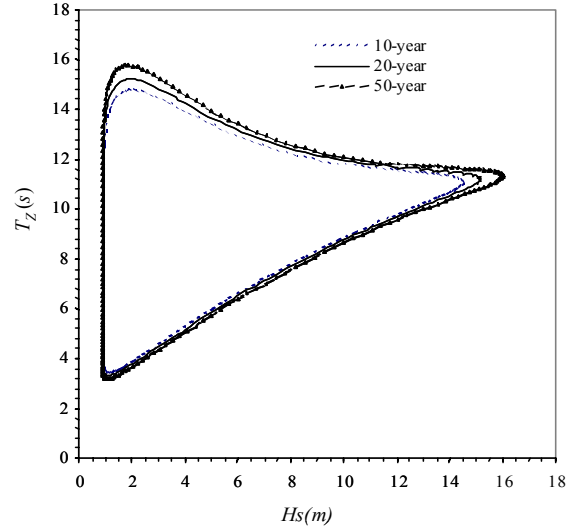


**Figure 4.13**  $H_s$ - $T_z$  contours according to the Winterstein method for several return periods

The extreme hydrodynamic loads on the structure can be supposed to occur with the highest wave height during a specific return period, say 50 years and the maximum stresses in the structural elements will consequently result from this wave height. As can be observed from figure 4.13, according to the Winterstein method for 50 years return period, the highest wave height is 16.1 meter, with an associated zero crossing period of 11.30 second. This observation is in good agreement with the recommendation of the Marex report for extreme wave heights but gives a discrepancy in the zero crossing period. In the Marex report, the zero crossing period is derived by limiting the steepness of wave height into  $1/18$ , which results in a zero crossing period of 13.6 seconds. However, it should be kept in mind that the advantage of the Winterstein method for predicting the extreme environmental load is that the joint distribution function of the significant wave height and zero crossing period has been appropriately taken into account.

To compare the discrepancy of the results of these two methods, the time history of axial and bending stresses are calculated through the finite element analysis (ANSYS program) and a specific distributions function such as Weibull is fitted on the maximum response according to the method described by Farnes and Moan (1994). The Weibull probability distribution function is found to be a proper distribution to be used for response calculations due to its flexibility, its simplicity to fit on the sample distribution and finally its possibility to define the extreme value properly, Karunakaran (1993). This distribution function has already been utilized for the response calculation of jack-up platforms by Farnes (1990), Kjeoy et al. (1989) and Daghigh (1997). The Hermite model has also been employed to model the probability distribution function of response by Torhaug (1996) due to its possibility to take the higher statistical moments of the stress processes into account to specify the Hermite distribution.

If the response maxima follow the Weibull distribution, the extreme response will follow a Gumbel type I extreme value distribution, Gumbel (1958). The expected value of the extreme response may then be calculated in terms of the Weibull parameters of the maxima with the following expression, Bury (1975),

$$X_{mpme} = \mu + \alpha \left[ (\ln(N))^{\frac{1}{\lambda}} + \frac{0.57722}{\lambda} (\ln(N))^{\frac{1-\lambda}{\lambda}} \right] \quad (4.10)$$

where  $\mu$ ,  $\alpha$ ,  $\lambda$  are the shift, scaling and shape parameters of the Weibull distribution and  $N$  is the number of maximums within the storm duration. The results of the expected values of the extreme responses for axial and bending stresses in several elements below the lower guide in the forward leg are calculated and given in table 4.10 for two design storms methods, one as proposed by Winterstein and the other one with the wave steepness limitation method recommended in Marex.

**Table 4.10:** The estimated expected value of extreme stress responses in several elements of the structure below the lower guide according to the design storm derived from the Winterstein approach and the recommendation of Marex for a 50-year return period (unit *MPa*).

Element	Winterstein method $H_s=16.1, T_z=11.3$		Marex Recommendation $H_s=16.1, T_z=13.6$	
	Axial stress	Bending stress	Axial stress	Bending stress
D. Brace (Ele. no.295)	79.4	108.0	67.0	93.4
D. Brace (Ele. no.296)	-77.1	107.1	-67.8	92.4
H. Brace (Ele. no.169)	-37.0	89.1	-31.9	79.0
H. Brace (Ele. no.170)	51.4	105.9	45.9	98.8

As can be seen from this table, the design storm through the Winterstein method gives higher stress responses than the Marex recommendation. The design sea storm recommended by Winterstein is applied in the following section because not only in this method the joint distribution of the significant wave height and the zero crossing period can be taken appropriately into account but also this method gives the higher extreme stress values for structural elements.

#### 4.5.2 Reliability in extreme environmental loads

By using the wave characteristics specified in the preceding section, the axial and bending stress responses of jack-up structures can be calculated and the Weibull distributions are used to fit on the maximum axial and bending stress responses. The reliability calculation can therefore be carried out by using the ultimate limit state functions described in API RP 2A-LRFD(1993) for several elements below the lower guide by checking the combination of tension or compression with the bending stresses. In this specification, two limit state functions or usage factors are presented for the combination of tension and bending stresses as follows,

$$U_{t1} = 1 - \cos\left(\frac{\pi}{2} \frac{f_t}{\sigma_y}\right) + \frac{\sqrt{f_{by}^2 + f_{bz}^2}}{F_{bn}} > 1 \quad (4.11)$$

$$U_{t2} = \frac{f_t}{\sigma_y} > 1 \quad (4.12)$$

and three expressions for the combination of compression and bending stresses,

$$U_{C1} = \frac{f_C}{F_{cn}} + \frac{1}{F_{bn}} \sqrt{\frac{C_{my}^2 f_{by}^2}{(1 - \frac{f_C}{F_{ey}})^2} + \frac{C_{mz}^2 f_{bz}^2}{(1 - \frac{f_C}{F_{ez}})^2}} > 1 \quad (4.13)$$

$$U_{C2} = 1 - \cos\left(\frac{\pi}{2} \frac{f_C}{F_{xc}}\right) + \frac{\sqrt{f_{by}^2 + f_{bz}^2}}{F_{bn}} > 1 \quad (4.14)$$

$$U_{C3} = \frac{f_C}{F_{xc}} > 1 \quad (4.15)$$

The structural elements should be checked for all these limit state functions. It should be noted that all the resistance reduction factors in these expressions are set to the value one to represent the ultimate capacity of an element.

The axial stress in the structural elements are not always in the same stress state due to the cyclic action of wave loads and may change from compression into tension as shown for the brace element below the lower guide (element 296) in figure 4.14. Therefore an approach is required to take into account this variation of axial stress. This approach is originally based on the time history of the usage factor recommended by Videiro and Moan (1999). To derive the reliability of the elements using this approach, the time history of the usage factor should firstly be derived according to the stress state of an element, i.e. if the element is in tension, using the combination of tension and bending, equations 4.11 and 4.12, and if the element is in compression using the combination of compression and bending, equations 4.13 until 4.15, see figure 4.14. Therefore, the usage factor is specified applying the maximum values derived from these limit state functions in each step of the time history and the Weibull distribution is used to fit on the maximums of the time history simulation of the usage factor.

To extend the maximum result for the extreme prediction of storm duration, there are generally three approaches to be used to predict the extreme distribution. These are the *Poisson* type model, the extreme value distribution of independent maxima (or minima) based on the multiplication law and finally the asymptotic *Gumbel* distribution. Daghigh

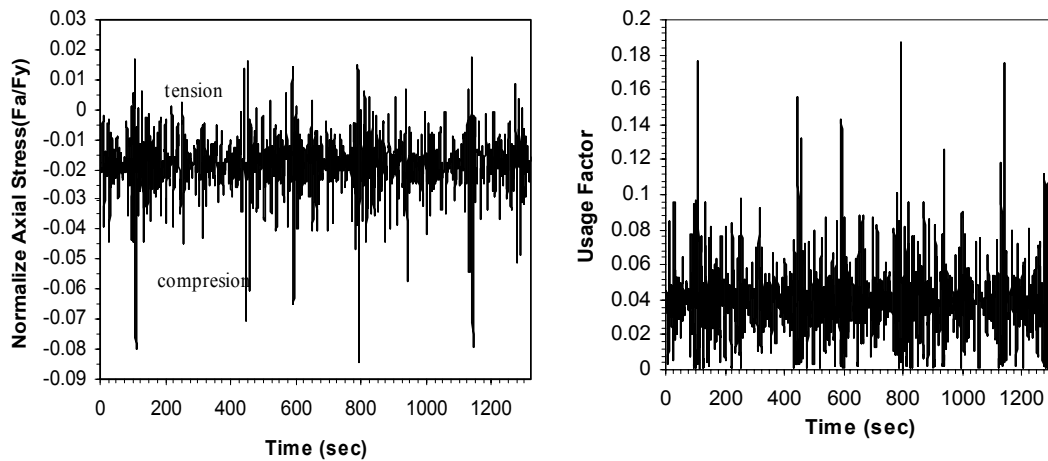


**Figure 4.14** Time history of axial stress (left) and usage factor (right) in brace element no. 296

(1997) investigated these three methods for a jack-up platform and concludes that the Gumbel distribution gives the highest failure probability. Therefore, the asymptotic Gumbel model is used as the basis to extend the extreme response of the usage factor for the storm duration (three hours) in the following sections. The failure probability is therefore calculated where the probability of the Gumbel distribution is less than one.

Since the reliability result of the proposed method has not been compared with the traditional method in the research work of Videiro and Moan (1999), the results of the proposed method are compared with the traditional methods in table 4.11. Two cases are considered for the traditional methods, one without correlation between axial and bending stress and other one with correlation. For the traditional method, firstly the distribution functions of axial and bending stresses are calculated from the time history of the stress process individually. The Weibull distributions are then fitted on the maximums of the stress process. The Gumbel distributions are used to extend the extremes of the stress distribution for storm duration (3 hours) and the reliability calculations are carried out for each limit state function described by equations 4.11 through 4.15 individually regarding the axial tension or compression of an element. The smallest reliability (highest failure probability) is therefore assumed to be the critical one.

**Table 4.11:** Comparing the calculated reliability indices according to the traditional approach without and with correlation between axial and bending stresses and using the proposed approach.

Element	Traditional approach		Proposed approach using time history of usage factor
	without correlation	with correlation	
D. Brace (Ele. no.296)	8.075	6.041	6.689
D. Brace (Ele. no.295)	11.236	8.290	8.762
Chord (Ele. no.52)	5.358	3.855	3.948
Chord (Ele. no.53)	5.269	3.754	3.861

The results of the proposed method are compared in table 4.11 for some elements below the lower guide comparing with the traditional method for two cases, considering the correlation between axial and bending stresses and without this correlation. This correlation is calculated based on time history of axial and bending stresses. As can be seen from the calculated reliability indices in table 4.11, the results of the proposed method are generally lower than the traditional method without correlation but are in good agreement when the correlation effect is taken into account. The difference between these two methods (the proposed and the traditional method with correlation) can be related to the variation of axial stresses from tension to compression. It means that in the traditional method only the maximum of the time history of the tension section in the case of the yielding, or the compression section of the time history in the case of the buckling, has been taken to specify the distribution function of the axial stress, which ignoring other section of the time history in this model. But in the proposed method, the distribution function is established through the maximum time history of the usage factor, and the variation of the stress state from tension to compression is directly incorporated in the time history of the usage factor.

It could be stated that the general benefit of the proposed approach in comparison with the traditional method is that not only the correlation between axial and bending stresses but also the axial stress variation (from compression to tension or vice versa) can directly be taken into account in the reliability calculation.

The design storm approach is based on the wave height with the specific return period. However, during the lifetime of platform, in reality, the structure may experience the bigger wave height than is expected with return period more than 50-years; say 100. Hence, the exact reliability index (or the failure probability) should be obtained based on the long-term approach to incorporate possible wave heights that may occur during the lifetime of the platform. To determine the long-term reliability index, an approximate method is presented in appendix H. The design storm approach turns out to give relatively high reliability indices. This means that if this approach is being maintained in the future, a higher value for the return period of the sea state should be selected; say 100 or 200 years instead of 50 years. To avoid possible misunderstanding, it should be noted that this statement only deals with the mathematical equivalence of the two methods. It is not a plea for a heavier design. The optimum design should follow from a proper risk analysis, involving all kinds of safety measures and failure consequences.

#### 4.6 FRACTURE RELIABILITY

The combination of extreme environmental loads with a small crack in structural joints due to fabrication process or fatigue degradation may cause unstable crack extension and fracture failure. The mechanism of this type of failure mode has already been presented in section 2.5 and a new method to calculate the failure probability through this failure mode is given in the following section.

By using the failure assessment diagram of level 2 recommended by the British Standard Institute (BS7910, 1999), the following expression has been derived in section 2.7 for fracture limit state function.

$$g_{f1} = K_{rf} - K_r = [1 - 0.14L_r^2][0.3 + 0.7 \exp(-0.65L_r^6)] - \frac{\delta_Y Y(a) \sqrt{\pi a} (\delta_F \delta_{SCF} \sigma^p + \sigma^s)}{K_{IC}} - \rho_c \quad (4.16)$$

where, the three random modification variables  $\delta_Y$ ,  $\delta_F$  and  $\delta_{SCF}$  are added to consider the uncertainties in the geometry function, the load model calculation and stress concentration factor respectively.

The fracture assessment formulation recommended in BS7910 is a lower bound on the test results and it may be expected that most failures occur far from this limit and this formulation may contain a relatively significant level of safety, Muhammad et al. (2000).

As described in chapter 2, Dijkstra et al. (1994) presents a method to describe the fracture limit state function according to fracture results of 38 experiments. He recommends using the circular limit state to represent the fracture failure where the angle of spreading is given to be independent and only the radius of the circle would be a relevant parameter to represent the failure mode. The fracture limit state is therefore defined through this method given by,

$$g_{f2} = R_f - R_{act} \quad (4.17)$$

where  $R_f$  is the radius of the fracture failure. It is recommended to approximate  $R_f$  with a lognormal distribution in such as way that its mean and standard deviation is set to 1.7 and 0.4 respectively (Dijkstra et al, 1994.).  $R_{act}$  is the acting fracture radius and is specified through the following expression depending on the plastic collapse parameter  $L_r$  and the fracture parameter  $K_r$ ,

$$R_{act} = \sqrt{K_r^2 + L_r^2} \quad (4.18)$$

In both expressions of the fracture limit state functions, it is required to specify the crack size. In this research we supposed that a crack in a structural joint arises from fatigue degradation and propagates with an increasing service time of the structure. The crack size is a random parameter because it depends on several other random variables such as fatigue characteristics, hydrodynamic load, stress and stress concentration factors, geometry function and finally initial crack size. This random fatigue crack size  $a_i$  can be determined using the crack growth formulation in fatigue with the following expression.

$$\int_{a_0}^{a_i} \frac{da}{\left(\delta_Y Y_A \sqrt{\pi a}\right)^m} = C_A N^l \tau \delta_F^m \delta_S^m \delta_{SCF}^m A^m \Gamma\left(1 + \frac{m}{B}\right) \quad (4.19)$$

As some of the parameters of this expression are random variables, the Monte Carlo Simulation (MCS) technique has been applied to simulate the random variables. The simulated variables are therefore placed in this expression and the formulation is solved to determine the crack size. By repeating this simulation several times the statistics of the random crack size can be calculated. The results of the simulation method for a random crack size according to the characteristic of the stress response of element 295 below the lower guide of the forward leg as well as its histogram are shown in figure 4.15 for 4 to 20 years service time.

The statistical analysis of the crack size shows that the lognormal distribution gives the best fit among several distribution functions e.g. Normal, Rayleigh, Weibull, Gamma and Beta based on tests of goodness of fit using the Chi-square test. The same trend is also observed using the Kolmogorove-Smirnov (K-S) and Anderson-Darling (A-D) tests. The fitted lognormal distributions with the simulated histograms are shown in figure 4.15. As is clear from this figure, an appropriate approximation between the fitted distribution and the simulated histogram of random fatigue crack size can be observed.

To compare the fracture reliability results for two limit state functions described in this section, equations 4.16 and 4.17 have been applied and the calculated crack size through the fatigue propagation expression are substituted in these equations. The reliability analysis has been carried out by the FORM method. The statistical characteristics of random variables in these expressions have the same characteristic as given in table 3.4 except the lognormal distribution is used to specify the crack size. The mean and standard deviation of the crack size is calculated for the service time range from ½ to 25 years and given in table 4.12. The Weibull distribution is fitted on the maximum of the time history simulation of the primary stress and the Gumbel distribution is utilized to extend for the storm duration (3 hours). The original interaction of fatigue and fracture is complex. In this thesis this time-variant problem is approximated by a time-invariant method. Furthermore, the stress calculation is carried out with the design storm method. The encountered sea state during the critical part of the

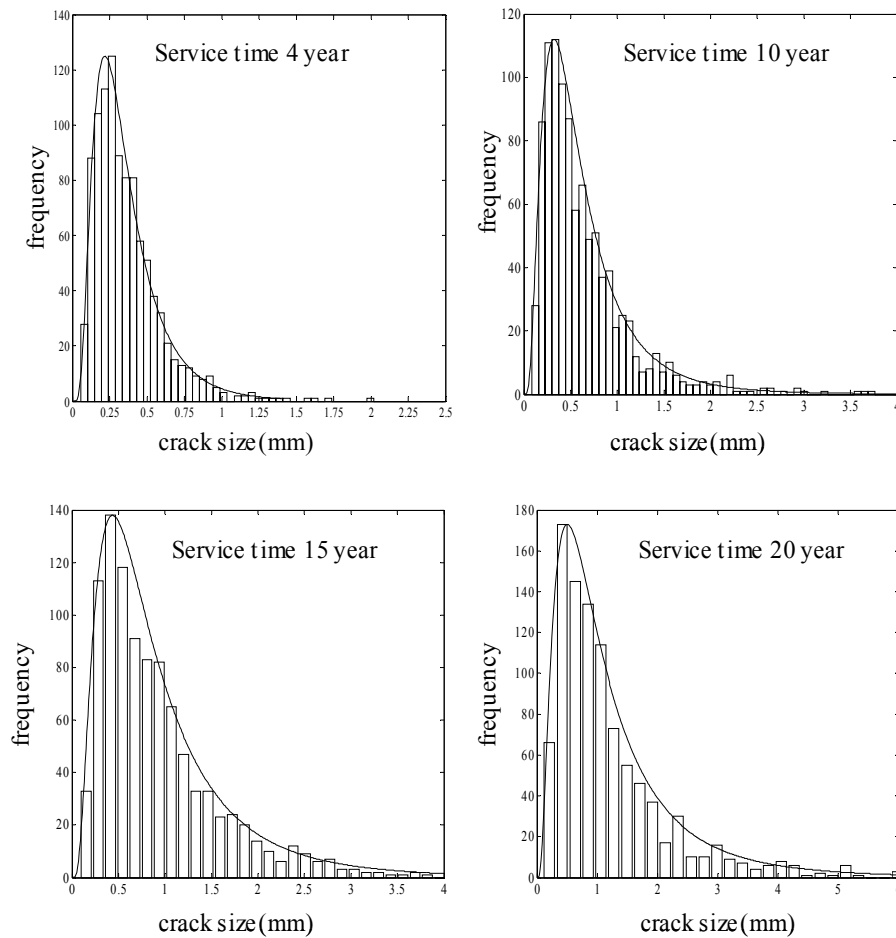


**Figure 4.15** Comparing the histogram and fitted lognormal density function of the crack size for several service times through fatigue crack propagation using the Monte Carlo Simulation

lifetime of structure may be higher or lower than the wave height with a 50 years return period. These issues will be discussed in section 5.4 in details.

**Table 4.12:** The mean and standard deviation of crack size calculated according to fatigue crack growth formulation for varying service time

Service time (years)	$\frac{1}{2}$	1	4	8	10	15	20	25
Mean (mm)	0.174	0.200	0.368	0.555	0.651	0.987	1.309	1.575
St. dev. (mm)	0.109	0.122	0.238	0.399	0.505	0.842	1.238	1.520

This type of extreme response calculation is the same approach as the extreme stress calculation in the ultimate limit state function but the differences are that the influence factors

are applied in axial and bending stresses to consider the hot spot stress. The calculated Gumbell distribution of primary stress has the mean value 169700 (MPa) and a coefficient of variation 0.035.

According to the BS 7910 (1999), generally two approaches can be applied to specify the plastic collapse parameter ( $L_r$ ) in the fracture limit states, one based on the global collapse analysis and the other one in accordance with the local collapse analysis. However, in this specification the global collapse method is preferred for tubular joint in offshore structure because the local approach usually gives conservative result while the use of the global approach tends to give more realistic predictions of plastic collapse. In case of a global approach, the plastic collapse parameter can be calculated from,

$$L_r = \left( \frac{\sigma_f}{\sigma_y} \right) \left\{ \frac{\sigma_a}{\sigma_{ac}} + \left( \frac{\sigma_{ab,i}}{\sigma_{bc,i}} \right)^2 + \frac{\sigma_{ab,o}}{\sigma_{bc,o}} \right\} \quad (4.20)$$

where  $\sigma_f$  is the flow strength which is specified to be the average of the yield ( $\sigma_y$ ) and the tensile strength ( $\sigma_u$ ).  $\sigma_a$ ,  $\sigma_{ab,i}$  and  $\sigma_{ab,o}$  are the applied axial, in-plane and out-of-plane bending stresses.  $\sigma_{ac}$ ,  $\sigma_{bc,i}$  and  $\sigma_{bc,o}$  are the plastic collapse strength in the cracked condition for the axial, in-plane and out-of-plane bending capacity of joint respectively.

**Table 4.13** The characteristic of the Weibull distribution and the expected value of the extreme applied stress in the intersection of element 295 with the chord

Variable (unit)	$\mu$ (kN/m <sup>2</sup> )	$\alpha$ (kN/m <sup>2</sup> )	$\lambda$	N	Extreme Stress response(kN/m <sup>2</sup> )
$\sigma_a$	14785	6476.5	0.89365	1800.3	81798
$\sigma_{ab,i}$	4055.9	1920.3	0.92955	1615.9	21951
$\sigma_{ab,o}$	76.03	25.454	0.84965	1879.3	375.1

The applied axial, in-plane and out-of-plane bending stresses are calculated from the stress analysis of the structure using the Weibull distribution to fit on the maximum of stress process.

The expected values of the extreme responses can therefore be calculated in terms of the Weibull parameters such as expression 4.10. The results of the expected value of extreme applied axial, in-plane and out-of-plane bending stresses are respectively illustrated in table 4.13 for element 295.

The plastic collapse strength in the cracked condition for the axial, in-plane and out-of-plane bending capacity of an element can be calculated in accordance with the formulation presented in the Norwegian specification (NORSOK standard, Revision 1, 1998). We utilized this specification because in this code the plastic strength of the cracked joint can directly be estimated with the following expression,

$$\sigma_{ac} = F_{AR} \sigma_{a,un} \quad , \quad \sigma_{bc,i} = F_{AR} \sigma_{b,i} \quad , \quad \sigma_{bc,o} = F_{AR} \sigma_{b,o} \quad (4.21)$$



Where  $\sigma_{a,un}$ ,  $\sigma_{b,i}$  and  $\sigma_{b,o}$  are the axial, in-plane and out-of-plane bending capacity of un-cracked joint and the modification term  $F_{AR}$  is given by the following expression,

$$F_{AR} = \left(1 - \frac{A_c}{A}\right) \left(\frac{1}{Q_\beta}\right)^{m_q} \quad (4.22)$$

$A_c$  is the cracked area of the brace/chord intersection and  $A$  is the full area of the brace/chord intersection. For part-thickness cracks,  $m_q=0.0$  and the cracked area can be calculated from the crack size dimension,  $A_c=0.5*\pi ac$  (where  $a$  is the crack depth and  $c$  is half of the crack length).

The un-cracked resistance of the joint is calculated in accordance with the NORSOK specification using the geometry characteristic of the intersection of element 295 with the chord (such as ratio between brace and chord thickness, diameter, etc) for the K bracing configuration, and the results are  $\sigma_{a,un}=2.116\sigma_y$ ,  $\sigma_{b,i}=3.598\sigma_y$  and  $\sigma_{b,o}=2.481\sigma_y$  for the axial, in-plane and out-of-plane bending strength respectively. By substituting these values in expression 4.20, a formulation can be provided to relate the plastic collapse with the crack size and the yield stress. Therefore, the plastic collapse parameter ( $L_r$ ) in each iteration of the reliability program is determined in accordance with the statistics of the crack size and other random variables in the searching algorithm of the FORM method.

**Table 4.14:** Comparison the reliability index results through two proposed fracture limit state functions for random crack propagation during the service time and the secondary stress to yield stress ratio ( $\sigma^S/\sigma_Y$ ).

$\sigma^S/\sigma_Y$	$g_{f1}$				$g_{f2}$			
	0.4	0.60	0.80	1.0	0.4	0.60	0.80	1.0
Service time								
1/2 year	5.981	5.346	4.755	4.238	6.115	5.568	5.091	4.679
1 year	5.934	5.293	4.699	4.179	6.071	5.522	5.044	4.631
4 year	5.831	5.181	4.578	4.052	5.979	5.425	4.943	4.528
8 year	5.623	4.954	4.335	3.795	5.794	5.229	4.739	4.318
10 year	5.587	4.913	4.290	3.746	5.760	5.193	4.700	4.276
15 year	5.469	4.782	4.147	3.591	5.654	5.079	4.579	4.150
20 year	5.397	4.701	4.057	3.494	5.588	5.008	4.504	4.070
25 year	5.342	4.639	3.988	3.417	5.537	4.953	4.444	4.007

The reliability calculation is carried out for several secondary stresses to yield stresses ratios ( $\sigma^S/\sigma_Y$ ) varying from 0.4 to 1.0 and a service time varying from 1/2 to 25 years.

Table 4.14 shows the reliability results calculated through the failure assessment diagram  $g_{f1}$ , expression (4.16), and the method recommended by Dijkstra  $g_{f2}$ , equation (4.17). As can be seen from this table, the Dijkstra method gives overall higher reliability indices than the failure assessment diagram and the discrepancy between these two methods increases with increase of the service time of platforms. Furthermore, the results show that the reliability indices decline with enhancing the secondary stress to yield stress ratio. The size of the

fatigue crack will enlarge by increasing the service time of the platform and it could be generally concluded that the possibility of fracture failure increases.

## 4.7 CONCLUSIONS

The reliability of jack-up platform in component level is calculated for three failure modes of fatigue, extreme environmental loads and fracture and several factors, which can affect this calculation are discussed and the results are compared with each other.

Among several distribution functions fitted on the short-term stress range, through the test of goodness of fit, it is concluded that the Weibull distribution gives the highest rank between the fitted distributions and is therefore appropriated for application in fatigue reliability calculations.

In fatigue reliability calculations the geometry function plays an important role because it takes into account several corrections arising from the effects of loading and crack geometries. Since the structural characteristic of a jack-up platform differs significantly from a fixed jacket platform, the behaviour of the structure is different and the traditional expression for the geometry function used in tubular elements of jacket platforms should not directly be applied for jack-up platforms and some modification is required before any application. It is shown that the bending to membrane stress ratio ( $\alpha$ ) may change the fatigue reliability considerably if a proper ratio is not selected in the fatigue reliability analysis of jack-up platforms. Moreover, the calculation of this ratio shows that it varies between zero and one for several hot spot pints around the intersection of a brace element and differs significantly from the recommended value of 4 or 5 for jacket platforms by Moan and Kirkemo respectively. By using the calculated bending to membrane stress ratio ( $\alpha$ ) and the two-dimensional geometry function presented by Raju and Newman, a new geometry function is specified for jack-up elements in accordance with the actual bending to membrane stress ratio. However, the fatigue reliability indices calculated in this way might give excessive values if the correction of the weld toe profile is not employed. In this comparison, the same model uncertainty has been considered for the reliability calculation. However, in the actual situation, the model uncertainty may differ. But this issue does not change the final conclusion because the bending to membrane stress ratio will vary for a jack-up compared to jacket platforms and this difference should be incorporated in the fatigue crack growth calculation.

Two widely used wave spectra in offshore engineering are P-M and JONSWAP. The first spectrum is used for the fully developed sea states and the second one for the fetch limit condition. The proper selection of the type of spectra may often be doubtful and in question. To investigate the effect of the choice of a spectrum on the fatigue reliability, the fatigue reliability calculation has been carried out for these two spectra models and the fatigue reliability indices are compared with each other in figure 4.9. The results show that the JONSWAP spectrum generally gives a higher reliability index for the selected element in the jack-up under investigation but the differences are not significant for the first five years of the service time.

The estimated and reported overall damping of jack-up platforms in the references vary significantly from 2 to 10% and hence there is some uncertainty about the proper selection of this value. The effect of the variation of the overall structural damping on the fatigue reliability has also been investigated. The results show that the fatigue reliability indices grow with an increase of the damping ratio, as can be seen from figure 4.10. However, this growth is not so significant for damping ratios between 5 and 7% but is important for values between 2 and 10%. Hence, a proper selection of the overall damping ratio for jack-up structure will be an essential task before any fatigue reliability calculation and it may significantly change the estimated reliability index.

The stress process in a jack-up structure is nonlinear and broad-banded. The distribution of the nonlinear and broad-banded stress process can be determined using the rainflow counting method. Since this method is complex and time consuming, less complex and easier analytical formulations are recommended in the literature to take into account the broad-banded effect by correction of the narrow-banded assumption. Two such models presented by Wirsching and Light (W&L), Zhao and Baker (Z&B) as well as the nonlinear Hermite model described by Winterstein are examined and the fatigue reliability results are compared with the rainflow counting method. Furthermore, the results of the narrow-banded (Rayleigh) and the proposed Weibull distribution model of the stress range are also compared with the rainflow counting method. As can be seen from table 4.9, the rainflow counting method gives the lowest fatigue reliability indices compared to the other methods for several sea states. The correction model of W&L gives the highest reliability indices and would be unconservative if used in a reliability analysis. The Narrow-banded and Z&B correction models generally give also higher reliability indices than the rainflow counting method but they are close to each other and lower than W&L. The nonlinear Hermite model shows some discrepancy for the higher sea state. The proposed Weibull model gives a better approximation for the higher sea states than other methods and a little higher for the lower sea states compared to the rainflow counting method. However, the results of the lower sea states of the proposed method are close to other methods, indicating that this method is an acceptable alternative method to the rainflow counting.

The inspection of a platform during operation provides valuable information to update the fatigue reliability. The application of this information in the reliability updating of a jack-up platform is shown for two cases in section 4.4. The fatigue reliability increases with applying the inspection information for no-crack detection or other situations such as detecting a crack, measuring and finally repairing.

The maximum stresses in the structural elements occur when the platform is confronted with extreme sea states that may occur in a specific return period. The inverse FORM method presented by Winterstein is used to specify the extreme sea state or design storm for a 50-year return period. An approach is presented to determine the reliability of structural elements under extreme environmental loads using the time history of the usage factor. The results of traditional methods for two cases with and without correlation between axial and bending stresses are compared with the proposed method in table 4.11. It is shown that the proposed method gives a good approximation for the reliability calculation of the ultimate limit state when the correlation between axial and bending stresses is taken into account. Furthermore, the benefit of the proposed method is that the axial stress state variation can directly be accounted in the reliability calculations.

---

The combination of fatigue and extreme environmental loads may become critical leading to fracture failure. This type of failure mode has also been investigated in this research and the results of the fracture assessment diagram recommended by the British Standard Institute (BS7910, 1999) are compared with the Dijkstra (Dijkstra et al., 1994) method in table 4.14. The results show that this method gives lower reliability indices than Dijkstra for several secondary to yield stress ratios and service times but the maximum difference between them is restricted to 17% in the case of secondary stress to yield stress ratio equal one.

The crack size is an important factor in the fracture limit state function. This crack is assumed to occur through fatigue degradation and is therefore specified with the fatigue crack growth expression. Since some of the parameters in the fatigue formulation are random variables, the MCS technique has been applied to simulate variables. The statistical characteristics of the random crack size for several service time periods of platforms are estimated and it is shown that the lognormal distribution gives the best distribution according to the test of the goodness of fit using the Chi-square as shown in figure 4.15.

## 5. SYSTEM RELIABILITY OF JACK-UP PLATFORMS

---

### 5.1 INTRODUCTION

In the previous chapters, a procedure to calculate the reliability for fatigue, fracture and ultimate failure modes has been described. As the jack-up structure is an assembly of several elements, failure of one element may not lead to structural collapse. This reserve strength relates to the redundancy of the structure and can be taken into account by using system reliability approaches.

Most research works on system reliability of jack-up platforms focus on overload failure, e.g. Daghigh (1997) and Karunakaran (1993), and little attention has been given to fatigue failures. The primary reason for this may be associated to past and present assumptions made for the design and construction of a jack-up platform. This platform is designed for a combination of maximum water depth and environmental conditions, which allows to operate on all locations where the conditions are within these limits. Nowadays the jack-up platforms are designed to operate in deeper water or for operations for longer periods of its lifetime on a specific site. Hence, the fatigue damage should be highlighted as an important aspect, Onoufriou (1996). This is in particular the case for various types of offshore platforms. For jacket platforms research has been carried out by e.g. Karadeniz et al. (1983), Shetty (1992), Karamchandani et al. (1992), and tension leg platforms by Hovde (1995), Siddiqui and Ahmad (2001). Since the structural model and stress distribution in jack-up structures differ from these types of offshore platforms, further research on the system reliability of jack-up platforms in sequences leading to structural collapse is required.

In system reliability, the interest is the occurrence of a sequence of element failures leading to structural collapse and its probability of occurrence. There are very large numbers of sequences leading to structural collapse and it is not possible in practice to include all of them in the calculation. However, only few of the failure sequences contribute significantly to the total failure probability. Hence, a search technique can be used to identify the important failure sequences and the system failure event may be approximated as the union of the identified sequence events leading to the structural collapse.

In this chapter a methodology is presented for the system reliability calculation of jack-up platforms as a consequence of sequences of fatigue failures. The base of this method is on the

procedure described by Dalane (1993). The benefit of this method is the possibility of using the FORM method to determine the failure probability in the sequence of fatigue failures. Furthermore, the correlation among the elements as well as the correlation between the failure modes can be taken into account explicitly. The branch and bound technique can be used to identify the important sequences in the branch tree leading to a system collapse. This approach is applied to calculate the system reliability for the jack-up (Neka) platform under investigation and the system effect is shown through the calculated system reliability index.

After fatigue failure of the first element, the weakened structure may fail due to overload in the next storm. This overload may cause elements to fail in yielding or buckling, or in a combination of these, with a propagation of the fatigue crack leading to the fracture failure. These types of failures are discussed in this chapter and the system failure probabilities are obtained for combination of a fatigue failure with extreme environmental load failures and fracture failures.

## 5.2 SYSTEM RELIABILITY DUE TO A SEQUENCE OF FATIGUE FAILURES

Due to the redundancy of structures, failure of the first element in fatigue may not lead to system collapse. After a member has failed, the applied loading continues to be supported by the remaining members, and a redistribution of the forces in the structure takes place. It may be expected that each remaining element in the damaged structure has already some fatigue damage accumulated and due to the increase or decrease of the stresses, the rate of damage accumulation may change.

In the proposed system formulation, the two-dimensional crack growth method is used to estimate the time for developing a through-thickness crack at a critical hot spot in a section, (Shabakhty et al., 2003). A correction factor is included to account for the fact that section failure usually occurs some time after the development of a through-thickness crack. A crack or a fatigue failure may develop at both ends of a member. Hence, it is convenient to assume two end joints, instead of a member, in order to define where the fatigue failure occurs. Moreover, to obtain the critical hot spot, each joint is divided into 8 points regularly distributed around an intersection and the calculation should be repeated for all points to identify the critical hot spot. The bending to membrane stress ratio from the stress history is correctly taken into account for each point and the geometry function needed in crack growth formulations is modified and extended through this ratio, as described in section 4.3. The proposed formulation properly models the total damage at a joint in the critical hot spot, i.e. it accounts for the changes in stresses due to failures of other members.

In the following sections, an expression for the first fatigue failure is reformulated using the fatigue limit state function described in section 2.4. This expression has been extended in such a way that it will be possible to consider several sequences of fatigue joint failure, when the first joint failure occurs and is followed by other joint failures respectively.

### 5.2.1 Formulation of the first fatigue failure

The growth of a fatigue crack at a given hot spot is modelled with the Paris-Erdogan law, as described in the second chapter. The propagation of the crack is a function of several fatigue

and load parameters, of which some have random characteristics. The crack growth parameters can therefore be divided into two sections, the parameters that are related to the fatigue loading function, and the others that are related to the fatigue strength function. By applying some modification factors mentioned in the previous chapters to take into account the model uncertainties in the hydrodynamic load, the stress calculation and finally the stress concentration factor, the fatigue loading function can be specified as,

$$\psi_L(T) = \underbrace{v^l \delta_F^m \delta_S^m \delta_{SCF}^m A^m \Gamma(1 + \frac{m}{B})}_{\eta} T = \eta T \quad (5.1)$$

and the fatigue strength function as,

$$\psi_R(a_{th}) = \delta_{tf} \int_{a_0}^{a_{th}} \frac{da}{C \delta_Y^m [Y(a)(\sqrt{\pi a})]^m} \quad (5.2)$$

The time-to-failure can therefore be linked to the propagation of the crack through the thickness and a random correction model to consider a section failure. The time-to-failure for a specified joint based upon this model has random characteristics due to the fact that it depends on many random variables. The static characteristics of these variables are shown in table 5.1. By using this expression, the random time-to-failure of the joint e.g.  $J_1$  can be specified by the following expression.

$$T_{J1} = \frac{\psi_R(a_{th})}{\eta} = \frac{\delta_{tf,J1}}{v_{J1}^l \delta_{F,J1}^m \delta_{S,J1}^m \delta_{SCF,J1}^m C_{J1} A_{J1}^m \Gamma(1 + \frac{m}{B_{J1}})} \int_{a_{0,J1}}^{a_{th,J1}} \frac{da}{\delta_{Y,J1}^m [Y(a)(\sqrt{\pi a})]^m} \quad (5.3)$$

If this random time-to-failure becomes less than the lifetime of the structure ( $T_{life}$ ), fatigue failure is expected to occur in this joint and vice versa. If it is greater than the expected lifetime it means that the joint is functioning well. Therefore, the limit state function required in the reliability analysis based on fatigue failure of the first joint can be expressed by

$$g_{J1} = T_{J1} - T_{life} \quad (5.4)$$

and its probability of failure determined with the following expression.

$$P_{fJ1} = P[g_{J1} \leq 0] = P[T_{J1} - T_{life} \leq 0] = P[T_{J1} \leq T_{life}] \quad (5.5)$$

This expression will be used for each joint in the structure and its failure probability can be calculated. The joint with the highest failure probability is likely to be the first joint to fail. However, this may not be generally true and other possibilities should be considered. The branch and bound technique can be applied to determine the most important failure sequences of the joints under fatigue and concentrate the attention on these failure sequences.

### 5.2.2 Sequence of joint failures in fatigue

The next step is to establish a formulation for the next joint to fail when the first failure occurs. In this case, when the first joint, which fails due to fatigue degradation is  $J_1$  and the relevant element is disconnected from the structure, the next joint that fails subsequently might be a joint  $J_2$ . The total random time to reach the sequence failure of joint  $J_2$  can

therefore be divided into the time when the first joint is in an intact state and reaches to failure,  $T_{J1}$ , and the time of failure of joint  $J_2$ , i.e.  $T_{J2fJ1} - T_{J1}$ , see figure 5.1.

In terms of the linear damage accumulation model for fatigue damage, the joint  $J_2$  has a fatigue strength function like expression 5.2, but the fatigue loading function is the combination of two terms. The first one is the fatigue loading function in joint  $J_2$  when joint  $J_1$  is in an intact state and reaches to failure and the next one from the failure of joint  $J_1$  to  $J_2$ . The total fatigue loading function can therefore be estimated from the following expression,

$$\psi_{LJ2}(T_{J2}) = \psi_{LJ2}(T_{J1}) + \psi_{LJ2fJ1}(T_{J2fJ1} - T_{J1}) \quad (5.6)$$

where  $\psi_{LJ2}(T_{J2})$  is the total fatigue loading function of joint  $J_2$ ;  $\psi_{LJ2}(T_{J1})$  and  $\psi_{LJ2fJ1}(T_{J2fJ1} - T_{J1})$  are the fatigue loading functions of joint  $J_2$  before and after failure of joint  $J_1$  respectively.

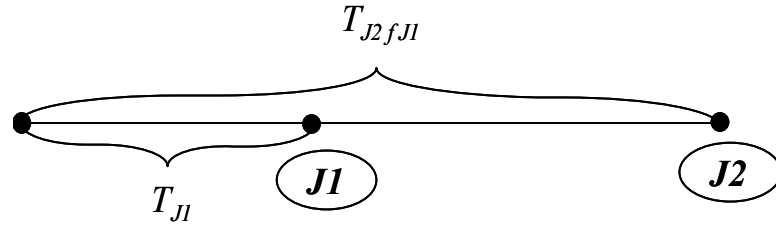


**Figure 5.1** Sequence of fatigue failure of joint  $J_2$  followed by  $J_1$

By using equation 5.6 as a loading function and applying the same modification factors to consider the uncertainties in the hydrodynamic load, the stress concentration factor and the time to section failure, the following expression can be generated to relate the fatigue strength function and loading function of joint  $J_2$ .

$$\begin{aligned} \delta_{fJ2} \int_{a_{0J2}}^{a_{thJ2}} \frac{da}{\delta_{YJ2}^m [Y(a)(\sqrt{\pi a})]^m} &= v_{J2}^l \delta_{FJ2}^m \delta_{SJ2}^m \delta_{SCFJ2}^m C_{J2} A_{J2}^m \Gamma(1 + \frac{m}{B_{J2}}) T_{J1} \\ &+ v_{J2fJ1}^l \delta_{FJ2}^m \delta_{SJ2fJ1}^m \delta_{SCFJ2}^m C_{J2} A_{J2fJ1}^m \Gamma(1 + \frac{m}{B_{J2fJ1}}) (T_{J2fJ1} - T_{J1}) \end{aligned} \quad (5.7)$$

As may be noted from this expression, the left hand side is the fatigue strength function and the right hand side shows the total fatigue loading at the time of failure. The modification  $\delta_{fJ2}$  is applied to consider the correction of section failure. This modification is then modelled independent of the loading function i.e. does not change when the fatigue loading function changes. The time to failure of  $J_2$  followed by  $J_1$  can therefore be expressed by reformulating expression 5.7 as,

$$T_{J2fJ1} = \frac{\delta_{fJ2} \int_{a_{0J2}}^{a_{thJ2}} \frac{da}{\delta_{YJ2}^m [Y(a)(\sqrt{\pi a})]^m} - v_{J2}^l \delta_{FJ2}^m \delta_{SJ2}^m \delta_{SCFJ2}^m C_{J2} A_{J2}^m \Gamma(1 + \frac{m}{B_{J2}}) T_{J1}}{v_{J2fJ1}^l \delta_{FJ2}^m \delta_{SJ2fJ1}^m \delta_{SCFJ2}^m C_{J2} A_{J2fJ1}^m \Gamma(1 + \frac{m}{B_{J2fJ1}})} + T_{J1} \quad (5.8)$$



and the failure probability can be calculated for the sequence failure of joint  $J_2$  followed by  $J_1$  with,

$$P_{f J_2 f J_1} = P[(T_{J_2 f J_1} \leq T_{life}) \cap (T_{J_1} \leq T_{life}) \cap (T_{J_1} \leq T_{J_2})] \quad (5.9)$$

The last term in the right hand side of the expression 5.9 is added to confirm the sequence of  $J_2$  followed by  $J_1$ . This condition, however, can easily be released without introducing an important error. The only consequence is that the failure domain is enlarged with a part of another failure scenario, but this will automatically be accounted for in the system analysis. So, for reason of simplicity, 5.9 is replaced by the following expression.

$$P_{f J_2 f J_1} \approx P[(T_{J_2 f J_1} \leq T_{life}) \cap (T_{J_1} \leq T_{life})] \quad (5.10)$$

To find a formulation for the higher sequences of a joint failure, the same approach as for two-sequence failures can be utilized. Assume that the failure of joint  $J_n$  is followed by the failure of joints  $J_1, J_2, \dots, J_{n-1}$  respectively, the loading function can then be specified by the combination of all relevant loading functions in the sequence of the failures respectively, i.e.,

$$\psi_{L(J_n)} = \psi_{L J_n}(T_{J_1}) + \psi_{L J_n f J_1}(T_{J_2 f J_1} - T_{J_1}) + \dots + \psi_{L J_n f J_1 f J_2 \dots f J_{n-1}}(T_{J_n f J_1 f J_2 \dots f J_{n-1}} - T_{J_{n-1} f J_1 f J_2 \dots f J_{n-2}}) \quad (5.11)$$

By using this loading function and applying the same modification factors to represent the uncertainty in the load, stress and concentration factor, the following general equation can be derived for the time to failure of joint  $J_n$  when a failure of joints  $J_1, J_2, \dots, J_{n-1}$  have already occurred respectively,

$$T_{J_n f J_1 \dots f J_{n-1}} = \frac{\delta_{f J_n} \int_{a_{0,J_n}}^{a_{th,J_n}} \frac{da}{\delta_{Y_{J_n}}^m [Y(a)(\sqrt{\pi a})]^m} - \sum_{i=1}^{n-1} \psi_{L J_n f J_1 f J_2 \dots f J_i}(T_{J_i f J_1 f J_2 \dots f J_{i-1}} - T_{J_{i-1} f J_1 f J_2 \dots f J_{i-2}})}{v_{J_n f J_1 \dots f J_{n-1}}^l \delta_{F_{J_n}}^m \delta_{S_{J_n f J_1 \dots f J_{n-1}}}^m \delta_{SCF_{J_n}}^m C_{J_n} A_{J_n f J_1 \dots f J_{n-1}}^m \Gamma(1 + \frac{m}{B_{J_n f J_1 \dots f J_{n-1}}})} + T_{J_{n-1} f J_1 \dots f J_{n-2}} \quad (5.12)$$

The fatigue loading function for this sequence failure of joints can be obtained from,

$$\psi_{L J_n f J_1 f J_2 \dots f J_{n-1}} = v_{J_n f J_1 f J_2 \dots f J_{n-1}}^l \delta_{F_{J_n}}^m \delta_{S_{J_n f J_1 f J_2 \dots f J_{n-1}}}^m \delta_{SCF_{J_n}}^m C_{J_n} A_{J_n f J_1 f J_2 \dots f J_{n-1}}^m \Gamma(1 + \frac{m}{B_{J_n f J_1 f J_2 \dots f J_{n-1}}}) \quad (5.13)$$

Hence, the final failure probability of the sequences of  $k$  joints failure i.e.  $J_1, J_2, J_3, \dots, J_k$  can be calculated with the intersection of all these component failures i.e.,

$$P_{f J_k f J_1 f J_2 \dots f J_{k-1}} = P[\bigcap_{i=1}^k (g_{J_i f J_1 f J_2 \dots f J_{i-1}} \leq 0)] = P[\bigcap_{i=1}^k (T_{J_i f J_1 f J_2 \dots f J_{i-1}} \leq T_{life})] \quad (5.14)$$

The same assumption of expression 5.9 can be applied here to confirm the occurrence of the sequences of  $k$  joint failure i.e.  $J_1, J_2, J_3, \dots, J_k$ , respectively.

The number of joint failures that should be taken into account in the sequences depends on the redundancy of the structure and the importance of the joint failures with respect to system collapse. In a redundant structure, numerous sequences can be supposed to cause the system to collapse and make the system reliability calculation a hard computational work. However, it is observed that all these sequences do not participate significantly in the final failure probability and only some of them contribute considerably, hence the search technique is established to identify the important sequences.

### 5.2.3 Search technique to identify dominating failure sequences

In redundant offshore structures, innumerable failure sequences can be expected to occur but only some of them contribute significantly to the collapse or system failure and others have a very low probability of occurring. In system reliability, identification of these important sequences is essential and several methods have been developed to distinguish dominant failure sequences. These methods can be generally classified into two categories, deterministic and probabilistic approaches.

Incremental loading and plastic collapse analysis are two examples of deterministic methods. In the incremental loading, the random variables are fixed at their mean values and a deterministic analysis is performed to identify the sequence of section failures leading to structural collapse. By assuming a proportional loading condition, the load factor is gradually increased to cause a sequence of element failures, Daghigh (1997). To determine additional failure sequences, the value of some variables can be modified and a deterministic analysis is repeated to specify a new failure sequence. This method basically uses a deterministic search strategy and obtains important failure paths without many repetitions of structural analysis, but can not ensure that all the probabilistically dominant failure paths are identified, Moses (1982).

In plastic collapse analysis, an ideal plastic behaviour of a material is considered and based on this model the analytical formulation for the plastic limit state function is developed. Hence, the final plastic mechanism leading to structural collapse is identified using the  $\beta$ -unzipping method in connection with basic plastic mechanisms. It is not possible to guarantee that the  $\beta$ -unzipping method identifies all significant mechanisms but reasonably good results may be expected. Since some of the plastic mechanisms are excluded in this method, the reliability index determined with this approach is therefore an upper bound of the correct generalized system reliability index, Thoft-Christensen and Murotsu (1986).

The simulation-based and branch and bound techniques are two main methods of probabilistic approaches. The simulation-based method is constructed on the bases of the Monte Carlo simulation technique and is a computationally expensive tool for reliability assessment of large structures. The structural analysis needs to be repeated several times for each sampling point, taking into account the numbers leading to failure of the structure. Furthermore, to increase the efficiency and reduce the simulation time, an importance sampling technique in combination with the directional simulation technique can be employed, Waarts and Vrouwenvelder (1998).

The branch and bound technique, which is used in this research work, is the most robust method to specify system failure, Thoft-Christensen and Murotsu (1986). In this approach the failure sequences are identified based on the sequences in decreasing order of importance. This means that the first failure sequence belongs to the largest probability of failure which has the maximum probability of occurrence corresponding to the damaged state and the second one is the second largest one and so on. Therefore, the first step will be to compute the failure probability of each joint by using expression 5.5 for most of the joints in the structure with a high failure probability. As a result, the calculated failure probability shows the first branches in the failure tree. Let joint  $J_1$  has the largest computed failure probability i.e. the most likely damaged state. The focus should now shift from this joint to the next joint

failure, assumed here to be joint  $J_2$ . This failure sequence in fact represents a new damage state in the failure tree and the failure probability can be calculated with an expression such as equation 5.10. Note that the probability of occurrence of this damage state is the probability that joint  $J_1$  fails and joint  $J_2$  fails subsequently. However, this can be extended for other joints in the structure to determine their failure probability. Hence, the sequence with a maximum probability of failure in the second branch leads to the next damage state with a maximum probability of occurrence. This process continues to reach the damage state, which constitutes a collapse of the system. The sequence of failures leading to this damage state is the most-likely sequence. Since the focus until now was on the most-likely damage state with maximum probability of occurrence, the collapse state reached in this way is the most important one and is named the collapse state with the highest probability of occurrence.

The system collapse may happen in another sequence than expected and considered already. Hence, the contribution of other collapse sequences should be taken into account. To establish a different system collapse, it is necessary to consider other scenarios that may occur and lead to a system collapse. The system collapse based on the maximum probability of occurrence is the sequence with the highest failure probability but it is possible to shift the focus in a branch tree to the next failure sequence, which has the second highest probability, i.e. the next most-likely to occur damage state. If this is not the collapse state, the search technique is continued until the damage states under study constitute the system collapse. The sequence leading to this system collapse is the second most important failure sequence. If this process is continued for other failure sequences i.e. third, fourth most-likely damage states, it will be possible to identify several collapse states and their probability of occurrence. Since some of these collapse states are not disjoint, the total system probability is computed based on the union of these collapse sequences.

In this research, the branch and bound technique has been established to identify the sequences leading to a system collapse and the system probability of failure is determined through the combination of the most-likely failure sequences leading to a system collapse.

#### **5.2.4 System reliability of the Neka jack-up platform due to a sequence of fatigue failures**

To illustrate the procedure of determining the system reliability based on a sequence of fatigue failures, the Neka jack-up platform (see figure 5.2) is considered here again. Due to computer memory restriction, it is not possible to use the full details of the three legs. In addition, the simulation results shows that the critical stresses usually occur in the first leg for several sea states for the considered wave direction. Thus, we shift the focus to the detailed models of the forward leg and suppose that failure of this leg causes the structural collapse. However, the present approach can be exercised for a fully detailed model of the three legs. The configuration of the Neka jack-up platform and the element number is illustrated in figure 5.2. This figure shows the finite element model utilized in the structural analysis and the details of the elements below the lower guide in the first leg.

Fatigue failure usually occurs in the intersection of an element at a welding joint. Hence, for each member in the structure two potential fatigue failures can be expected at the ends of each member. An element fails and is separated from the structure if a joint failure in any of

the ends of an element occurs. From the finite element analysis of the structure, it is observed that structural collapse often occurs when any two brace members of the structure in one bay fail or if a chord member fails.

The hot spot stresses around the intersection (8 points) are computed using the time history of the stress process described in section 4.3 and the long-term distribution functions of all the hot spot points are calculated for each joint through the peak counting method and by applying the influence function described in section 4.3. The bending to membrane stress ratios are calculated for all hot spot points according to the stress time history and the geometry function is modified by using this ratio and a correction term to consider discontinuities arising from the welding toe profile, as recommended by Smith and Hurworth (1984).

The characteristics of uncertain parameters of the fatigue limit state function in equation 5.4 have been discussed in section 2.4.1 and appendix G, summarized in table 5.1. The random fatigue characteristic,  $C$ , is modelled as a lognormal distribution in which the mean value and standard deviation of its natural logarithm are  $-29.84$  and  $0.55$  for joints in air and  $-31.01$  and  $0.77$  for joints in seawater, respectively (units  $N$  and  $mm$ ). These values are selected in accordance with the DNV (1984) specification. The other fatigue characteristic ( $m$ ) in line with this specification is taken as a deterministic parameter, which is equal to  $3.1$  for joints in air and  $3.5$  for joints in seawater.

For each member in the structure, the two-end joints denoted as S for the start and E for the end of an element are considered and the fatigue reliability calculations are carried out for eight hot spot points regularly distributed in the intersection (varying from zero to 315

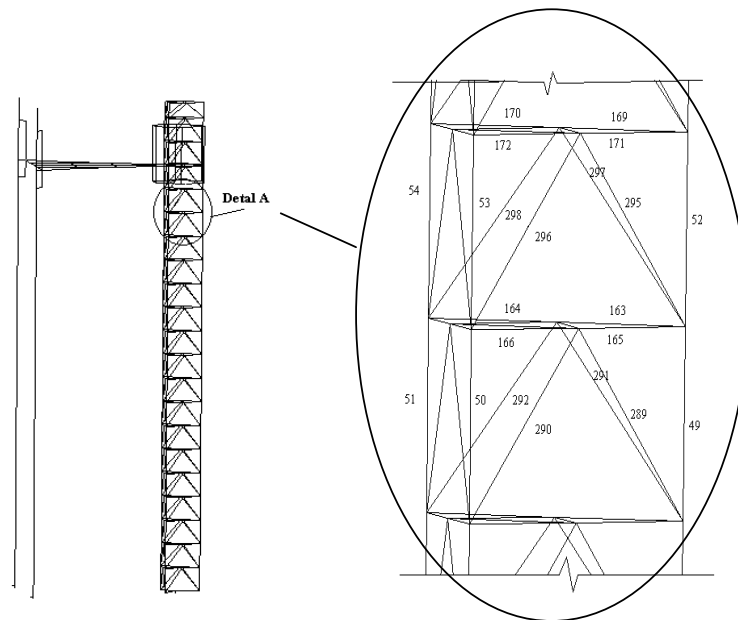


**Figure 5.2** Neka jack-up finite element model and detail of elements below the lower guide in the first leg

degrees) of each joint and the maximum one is selected as the critical one. The results of the reliability calculations for the 10 highest values are given in table 5.2 according to the 20-years design lifetime. The mean value of the fatigue life  $T_{mean}$  is also given in table 5.3. This mean time to fatigue failure is calculated based on the Taylor series expansion up to the first term of the random time to fatigue failure around mean values. For the general case, the Taylor series expansion is given by,

$$T_{fJ1} = f(\overbrace{a_{0J1}, a_{thJ1}, \delta_{Y_{J1}}, \delta_{f_{J1}}, C_{J1}, \delta_{F_{J1}}, \delta_{S_{J1}}, \delta_{SCF_{J1}}}^X) \quad (5.15)$$

$$T_{fJ1} = f(E[X]) + (X - E[X]) \left. \frac{df(x)}{dx} \right|_{x=E[X]} + \frac{1}{2} (X - E[X])^2 \left. \frac{d^2 f(x)}{dx^2} \right|_{x=E[X]} + \dots$$

If the higher terms of this series are ignored, the calculated random fatigue time will be as follows, which is an approximation to the exact value.

$$T_m = E[T_{fJ1}] \approx f(E[X]) \quad (5.16)$$

This type of approximation is called the tangent associate to  $f(X)$  by Ditlevsen (1981). However, a higher approximation, up to the second Taylor series expansion is recommended by Ditlevsen, which involves the variance of the random variables in the calculation of the mean fatigue time to failure.

**Table 5.1:** Characteristics of random variables in the fatigue limit state function

Parameter	variable	Distribution	Mean value $\mu$	Coefficient of variation COV
Initial crack size (mm)	$a_0$	Exponential	0.11	1.00
Member thickness (mm)	$a_{th}$	Normal	vary	0.04
Fatigue parameter in air Unit (Nmm <sup>-3/2</sup> , mm/cycle)	$\ln C_A$	Normal	-29.84	St.dev.=0.55
Fatigue parameter in water Unit (Nmm <sup>-3/2</sup> , mm/cycle)	$\ln C_A$	Normal	-31.01	St.dev.=0.77
Section failure model	$\delta_{tf}$	Normal	1.50	0.50
Geometry function model	$\delta_y$	Normal	1.00	0.10
Load model	$\delta_F$	Lognormal	1.00	0.10
Stress model	$\delta_S$	Lognormal	1.00	0.15
Stress concentration model	$\delta_{SCF}$	Lognormal	1.00	0.10
Fatigue parameter in air	$m$	Fixed	3.10	-----
Fatigue parameter in water	$m$	Fixed	3.50	-----

From table 5.2, it is clear that in most cases the highest failure probability occurs at the end of element (E) and at a hot spot point situated in the position of 270 degrees. However this will not always be valid for all of the components in a structure, as it will be observed in a branch tree later. This hot spot position has a combination of axial and in plane bending stresses. Moreover, due to the symmetry shape of the brace elements in the leg, the calculated failure

probability for each two elements in one bay have the same probability but this balance may not maintained after the first joint failure occurs.

**Table 5.2:** Failure probability around the intersection of joints, ( $P_f$ ), for 20 years lifetime.

Elements	0	45	90	135	180	225	270	315
296E, 298E	6.86E-5	6.63E-5	5.86E-3	5.80E-4	5.49E-5	4.78E-3	3.77E-2	5.17E-3
295E, 297E	6.58E-5	3.16E-4	3.11E-3	3.11E-4	6.64E-5	3.59E-3	2.79E-2	3.57E-3
290E, 292E	1.65E-5	1.59E-4	1.81E-3	1.52E-4	1.54E-5	2.21E-3	1.98E-2	2.25E-3
289E, 291E	3.31E-5	1.90E-4	2.07E-3	2.02E-4	3.84E-5	2.38E-3	1.97E-2	2.32E-3
284E, 286E	3.69E-6	3.73E-5	5.27E-4	3.81E-5	3.60E-6	7.08E-4	8.22E-3	7.03E-4

It is interesting to note that the calculated mean fatigue life for several hot spot points and elements is significantly higher than the design lifetime (20 years). Moreover, the variation of fatigue failure around the hot spot point shows good correspondence with the variation of the mean fatigue time i.e. the highest calculated failure probability coincides with the lowest mean fatigue life, see table 5.3. This observation can help to use the mean fatigue life as the bases for finding the critical hot spot and focus on it instead of using extensive time-consuming reliability calculations for each hot spot point to find the critical one.

Three random correction models  $\delta_F$ ,  $\delta_S$ ,  $\delta_{SCF}$  are applied in the fatigue limit state function to consider uncertainties in the load, in the stress and in the stress concentration factor model respectively. The uncertainties in the load and in the hot spot stress calculation are assumed to be independent in all states of the structure (intact or damage), but the uncertainty in the stress model is assumed to be dependent as the structure state changes from intact to damage.

**Table 5.3:** Mean fatigue life  $T_{\text{mean}}$  (in years) around the intersection of joints.

Elements	0	45	90	135	180	225	270	315
296E, 298E	589	337	178	349	619	190	89	185
295E, 297E	595	409	217	411	593	208	101	208
290E, 292E	805	483	255	489	817	241	115	239
289E, 291E	693	464	246	457	671	236	116	238
284E, 286E	1093	676	358	672	1098	331	159	332

Changes in the state of the structure due to failure of an element cause a change in the stress distribution of other elements and in the corresponding uncertainty. Therefore, the uncertainty in the stress calculations is represented by a random variable for each damage state. However, the uncertainty in the different states are assumed to be the same, e.g. in a

damaged state where joints  $J_1, J_2, \dots, J_{n-1}$  failed,  $\delta_{S_{Jn|J1,J2,\dots,J_{n-1}}}$  is still assumed lognormal with a mean value 1.0 and coefficient of variation 0.15.

The correlation between the random variables is an important parameter, which can affect the estimated failure probability, Vrouwenvelder (2004). No correlation between the random variables  $\delta_F$  and  $\delta_{SCF}$  is assumed either in each individual joint or between two joints in intact or damage state, but the stress model uncertainty ( $\delta_S$ ) is supposed to be correlated both at the different joints and in the different states of the structure. To specify this correlation, the time history of the stress process is used as an indication. Both for the intact and damaged state of the structure, the correlation coefficient is estimated with,

$$\rho_{\delta_{S_i}, \delta_{S_j}} = \frac{Cov[S_{J_i}, S_{J_j}]}{\sqrt{Var[S_{J_i}] \cdot Var[S_{J_j}]}} \quad (5.17)$$

where  $S_{J_i}$  and  $S_{J_j}$  are the hot spot stresses in the two joints  $J_i$  and  $J_j$  under investigation respectively. The same expression can be used to specify the correlation between joints when the structure is in a damaged state. The correlation between the stress model calculation in joint 296E270 (end of element 296 in hot spot 270) and joint 290E (correlation between  $\delta_{S_{J296}}$  and  $\delta_{S_{J290}}$ ) are calculated for several hot spots and sea states. The results are given in table 5.4, which show strong correlations between these model uncertainties.

Furthermore, it can be concluded from this table that the variation of the correlation coefficient around the intersection and the sea states is less significant. However, a small difference is observed for higher sea states (significant wave height 7.75 and 10.45) but since most fatigue damage arises from lower sea states (the lower sea states have a higher occurrence probability in scatter diagrams), it can be stated that the correlation does not vary so much with the significant wave height and therefore can sufficiently be represented only by a lower sea state.

**Table 5.4:** Correlation between stress uncertainty in joint 296E270 and several hot spot points in joint 290E for a number of sea states.

Position ( $\theta$ )	0	45	90	135	180	225	270	315
$H_S = 1.75$	0.992	0.995	0.995	0.995	0.992	0.988	0.988	0.988
$H_S = 3.25$	0.989	0.993	0.993	0.993	0.989	0.988	0.984	0.985
$H_S = 5.0$	0.984	0.989	0.990	0.989	0.984	0.988	0.978	0.978
$H_S = 7.75$	0.975	0.984	0.985	0.984	0.975	0.988	0.964	0.965
$H_S = 10.45$	0.968	0.982	0.983	0.982	0.968	0.988	0.951	0.952

This conclusion is furthermore validated by comparing the estimated correlation coefficient for other elements in the platform in which the same trend has been observed for its variation. Hence, it may generally be concluded that only one value would be appropriate to represent the correlation in the fatigue reliability analysis without considering any variation around the intersection or the sea state. However, for the reliability calculations in the following section, the variation of the correlation coefficient around the intersection has been taken into account due to the possibility of changing the sign of a correlation coefficient, see table 5.5. This table shows the correlation between hot spot stresses around the intersection of element 170, 298 and 52 when element 296 is in a damaged state. This table shows that the correlations between stress models before and after failure of element 296 is low.

By calculating the correlation between the stress uncertainties in two situations of intact and damaged state for other joints in the structure, it is possible to enter the estimated value in expression 5.10 to determine the failure probability of the second joint when the first joint has already failed.

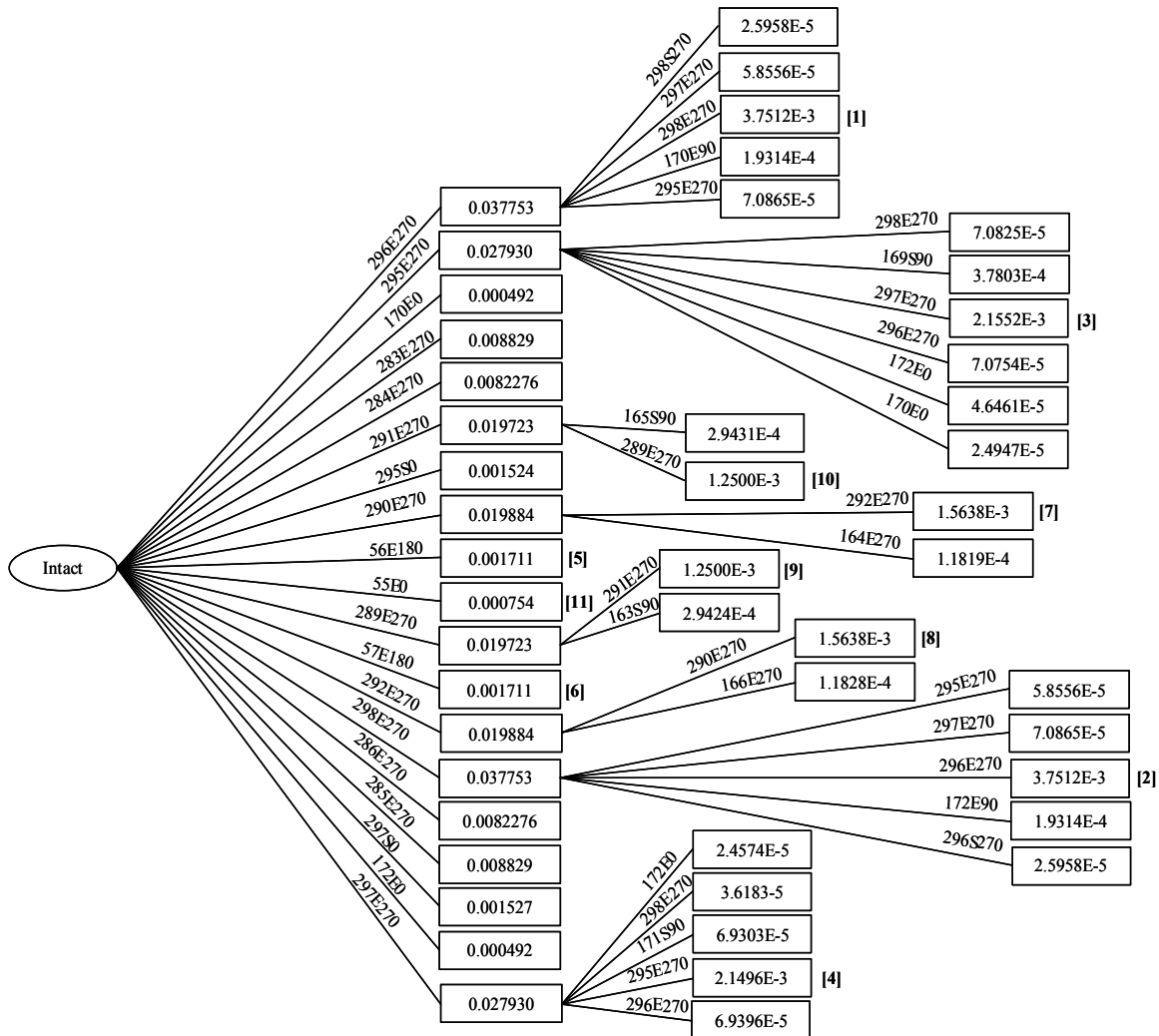


Figure 5.3 Branch tree obtained for fatigue failure sequences



**Table 5.5:** Correlation between stress uncertainties in several hot spot points around the intersection of the second joint failure when the first joint failure is 296E270.

Position ( $\theta$ )	0	45	90	135	180	225	270	315
<i>Ele170S</i>	-0.0384	0.0423	0.0422	0.0423	-0.0414	-0.0420	-0.0421	-0.0420
<i>Ele170E</i>	-0.0415	-0.0418	-0.0418	-0.0417	-0.0387	0.0422	0.0420	0.0420
<i>Ele298S</i>	0.0437	0.0438	0.0436	0.0433	0.0428	0.0427	0.0429	0.0432
<i>Ele298E</i>	0.0433	0.0447	0.0449	0.0448	0.0432	0.0419	0.0418	0.0421
<i>Ele52S</i>	0.0575	0.0587	0.0609	0.0627	0.0632	0.0622	0.0602	0.0581
<i>Ele52E</i>	0.0637	0.0615	0.0591	0.0580	0.0583	0.0597	0.0619	0.0638

Many sequences leading to the system collapse can be supposed for the jack-up, but the branch and bound technique can be applied to identify the important sequences leading to system collapse. Figure 5.3 shows the obtained branch tree for the jack-up platform in sequence of fatigue failure.

Due to the symmetric shape of the K bracing elements, two important joint failures are identified in the branch tree, 296E270 and 298E270, with a failure probability of 0.037753. It should be kept in mind that each element has two end joints, with letter S and E standing for the start and end of element respectively. Furthermore, the last three numbers indicate the critical position of the hot spot. The failure sequences with the failure probabilities smaller than  $2.0E-5$  are not shown in this figure.

Due to the symmetric shape of the structural element configuration, the most likely joint failure in the intact state is at the hot spot point 270 in the end of elements 296 and 298 respectively. The probability for this failure occurrence is 0.0377. The most likely collapse to occur is at the end joint of element 296 followed by failure of the end joint of element 298, for which its probability of occurrence is 0.0037. The second most likely failure sequence is the failure of the joint at the end of element 298 followed by the failure at the end of element 296. The eight highest failure sequences are ranked and shown in figure 5.3. It can generally be observed that there is an increase in the reliability from the first to the second fatigue failure and therefore there is a low probability of occurrence for the second fatigue failure, even after the first fatigue failure occurs.

To investigate the relative importance of the random variables in the limit state function, a sensitivity analysis should be carried out for all random variables. In the independent standard normal space, the relative importance of the corresponding random variable can be obtained from,

$$\alpha_i = -\frac{\nabla g_i}{\sqrt{[\nabla g][\nabla g]^T}} \text{ at the design point} \quad (5.18)$$

However, care should be given when the random variables are correlated. In this case, an importance ordering of the elements in the standard normal space does not imply the same importance ordering in the original space. Hence, a modification should be applied to transform dependent random variables into the independent space and later on calculate the

importance factor. The final importance factor resulted from this transformation is given by Der Kiureghian (2004) with the following expression,

$$\gamma_i = - \frac{\alpha_i J_{u,x} \hat{D}}{\|\alpha J_{u,x} \hat{D}\|} \quad (5.19)$$

where  $\hat{D} = \text{diag}[\sigma_i]$  is the diagonal matrix of the standard deviations and  $J_{u,x}$  is the triangular matrix obtained from the decomposition of the covariance matrix  $\hat{\Sigma} = J_{u,x}^{-1} (J_{u,x}^{-1})^T$ . These standard and covariance matrices are slightly different from the original standard and covariance of random variables and are calculated using the linear transformation of random variables, which are considered as equivalent normal of the variables at the design point, Der Kiureghian (2004). The result of the calculated importance factors for the variables in the most important sequence, failure of 296E270 followed by 298E270 is given in table 5.6.

**Table 5.6:** Relative importance of random variables for sequence 296E270 followed by 298E270

Random variable	Importance factor, $\gamma_i$ (%)	Random variable	Importance factor, $\gamma_i$ (%)
$a_0$ (J296E270)	0.021	$a_0$ (J298E270)	0.034
$a_{th}$ (J296E270)	0.0004	$a_{th}$ (J298E270)	0.0006
$\delta_y$ (J296E270)	2.621	$\delta_y$ (J298E270)	3.900
$\delta_{tf}$ (J296E270)	2.786	$\delta_{tf}$ (J298E270)	4.439
$C_A$ (J296E270)	6.988	$C_A$ (J298E270)	11.129
$\delta_F$ (J296E270)	2.528	$\delta_F$ (J298E270)	4.027
$\delta_S$ (J296E270)	5.654	$\delta_S$ (J298E270)	38.862
$\delta_{SCF}$ (J296E270)	2.528	$\delta_{SCF}$ (J298E270)	4.027
		$\delta_S$ (J298E270fJ296E270)	10.453

As is clear from this table, the highest contribution arises from uncertainty in the stress model in the second joint failure (J298E270). The fatigue characteristics ( $C_A$ ) of the first and second joint failure have an important influence. The initial and through thickness crack size have little effect on the total uncertainty and according to this sensitivity analysis these types of random variables can be assumed as the deterministic values in the reliability calculation. Other random variables have a moderate contribution with varying values between 2.5 to 5.7%. The sensitivity analysis shows that the total influence of the second joint is higher than the first one with 76.87% compared to 23.13%.

In the structural reliability, any sequences leading to the structural collapse are defined as the cut set, therefore the event of failure of the end joint of element 296 followed by the end joint 298 constitutes the first cut set,  $C_1 \equiv \{[T_{J298E270fJ296E270} \leq T_{life}] \cap [T_{J296E270} \leq T_{life}]\}$ . The most significant cut set event can be identified through the branch tree, shown in figure 5.3. The final system failure probability can therefore be calculated by combining the probability of all these cut set events. For very special cases, when all the cut sets are disjoint i.e. no two cut sets can simultaneously occur, the system failure probability is the summation of the

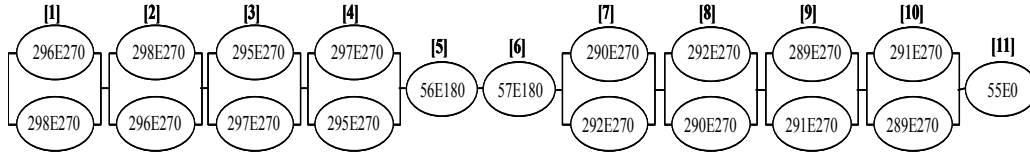


**Figure 5.4** System failure events as series and parallel system through eleven important fatigue failure sequences

probabilities of all cut set failure events. However, this is not the case for the system reliability calculation of the jack-up platform under investigation and a more advanced method is required.

In terms of series and parallel systems, the sequence leading to structural collapse (each cut set) constitutes the parallel system and the combination of all these sequences represents the series system. For the jack-up platform under investigation and based on eleven importance failure sequences leading to structural collapse, the series and parallel system model can be shown as the configuration presented in figure 5.4, where the first row shows the first joint failure and the second one the second failure sequences. According to this model, the system failure event can be represented with the following expression,

$$\Omega_{system} \equiv \bigcup_k \left[ \bigcap_{j \in C_k} \{g_j(x) \leq 0\} \right] \quad (5.20)$$

where  $C_k$  is the cut set number  $k$ . As has been discussed in section 3.4.4, in this expression due to simplification some intersections of surviving events of remaining members are not taken into account. The final system failure probability can be approximated with the following expression.

$$P_{f,system} = P(\Omega_{sys}) = P\left(\bigcup_k C_k\right) \quad (5.21)$$

When the structural failure event is modelled by such a series system of parallel subsystems, the final system failure probability can be evaluated according to the following steps. First, it is required to calculate the failure probability of each parallel system, then determine the correlation between the parallel systems and finally evaluate the probability of a series system. Furthermore, the intermediate step should be applied to model each parallel system as one equivalent safety margin. The equivalent linear safety margin can be derived for parallel systems (cut sets) using the method described in Gollwitzer and Rackwitz (1983). In this method, the equivalent safety margin of the equal element is defined in such a way that the corresponding reliability index of this element is equal to the final parallel system and it has the same sensitivity as the parallel system against changes in the basic variables.

When all the equivalent elements of parallel systems are estimated, the final system failure probability can be computed by calculating the multi-normal probability distribution as described in chapter 3 for series systems. However, the direct calculation of this multi-normal distribution with a sufficient accuracy and efficiency is difficult and impractical, especially when the dimension of the multi-normal exceeds five, Pandey (1998). Hence, several

approximation methods are recommended in literature to calculate this multi-normal distribution.

To calculate the multi-normal probability in a series system, two approaches are exercised here. At first, the first-order approximation method proposed by Hohenbichler and Rackwitz (1983) is applied. In this method, the dimension of the multi-normal probability is reduced in each step by one using the concept of conditional multiplication in such a way that the corresponding probability is equivalent to the multiplication of reduced conditional distributions and the probability content of a single dimension. The conditional distributions are then recast into unconditional distributions using the first order concepts (FORM). This approach is continued until all the multi-normal distributions are reduced into the multiplication of several uni-normal distributions, of which the number is equal to the dimension of the multi-normal distribution. Due to the linearization technique applied in this method, Tang and Melchers (1987) stated that the first order error might be quite significant in the case of a high correlation between random variables. Therefore, they recommend improving the first order multi-normal integral. They use the standard bivariate normal integral to calculate the conditional distribution, following the same algorithms explained earlier (see appendix E for more details about these methods). These approaches are called the Crude First Order Multi-Normal (Crude-FOMN) and Improved First Order Multi-Normal (Improved-FOMN) respectively. The system reliability index or the failure probability is calculated based on these two methods and given in table 5.7. The results show that the improved method gives a higher reliability index but generally the difference between these two methods is not so significant.

An alternative approach for system reliability calculation of a series system is to use the bound technique. The bound technique is originally derived from the general inclusion-exclusion rule of a probability calculation. The system failure probability of a series systems when the sequence of failures (cut sets) are correlated (dependent), can be estimated from the inclusion-exclusion rule (Boole, 1854), such as:

$$P(\Omega_{sys}) = P\left(\bigcup_i C_i\right) = \sum_i P(C_i) - \sum_{i < j} P(C_i \cap C_j) + \sum_{i < j < k} P(C_i \cap C_j \cap C_k) - \dots \quad (5.22)$$

The computation of the probability of the intersection event is difficult for a large number of components. Because of this difficulty, there has been a continued interest in developing bounds on the system probability that employ the marginal component probability (the first expression in the right hand side of equation 5.22) or the joint probability i.e. the bi-component probability or tri-component probability (the second and third term in the right hand side of equation 5.22 respectively), Song and Der Kiureghian (2003). For series systems, the probability bound using uni-component probability is given by Boole (1984) with an expression like 3.24. Since this bound is often too wide for a practical application, Ditlevsen (1979) proposed a better bound by involving the bi-component in addition to the uni-component probability in the probability calculation, as already given in expressions 3.25 and 3.26 for upper and lower bound respectively. The upper and lower bound are depending on the ordering of the cut sets and the order should be changed in such a way that the maximum of the lower bound and the minimum of the upper bound are derived. The results of the uni-component bounds and the Ditlevsen bounds for the series system shown in figure 5.4 are calculated and given in table 5.7. The uni-component bounds give wider ranges than the Ditlevsen bounds as already expected. Moreover, the Ditlevsen bounds are close to the

result of the crude-FOMN and improved-FOMN. The discrepancy between the results of the FOMN approaches and Ditlevsen bounds can apparently be related to the approximation applied in FOMN approach for the linearization of non-linear limit state and the correlation effect between each two linearized limit state functions. However, the differences are not so significant as can be observed from table 5.7.

**Table 5.7:** System reliability and failure probability of jack-up platform in sequences of fatigue failures

	Crude FOMN	Improved FOMN	Uni-component bounds		Ditlevsen bounds	
			Upper	Lower	Upper	Lower
$P_F$	0.019484	0.016548	0.021406	0.003751	0.019516	0.014704
$\beta$	2.0645	2.1309	2.0255	2.6737	2.0638	2.1779

If the system failure probability of a jack-up structure is considered as the result obtained from improved-FOMN, it can generally be concluded that the system failure probability of platforms is lower than the first component failure in fatigue and the system effect is more important.

The calculated lower failure probability for the system effect can be related to the redundancy of structures. After fatigue failure of the first element, the environmental loads are transmitted by the frame action of the remaining elements and significant increases in stress parameters of many surviving elements can be expected. However, because the first failure will typically occur in a diagonal or a horizontal brace, the increase in stress parameters is not too large and some extra time is required before an additional member fails. Thus, to have a sequence of two fatigue failures occurring subsequently, the first failure must occur early (earlier than the second one) and the second failure must occur in the interval time between the first failure and the lifetime of platform. This would be far less than just a single failure occurring and therefore the probability of occurrence of a sequence of failures is less than that of an individual first failure. For structures with a higher degree of redundancy, e.g. jack-up with X type of diagonal bracing elements, there will usually be a smaller change in the stress parameters and the system effects can be expected to be much larger than the platforms with the lower redundancy.

### 5.3 SYSTEM RELIABILITY IN COMBINATION OF FATIGUE FAILURE WITH EXTREME ENVIRONMENTAL LOADS

The platform, weakened due to a fatigue failure, may fail under extreme environmental loads that act on the structure subsequently. In this section, an attempt is made to determine the system failure probability when the first failure occurs in fatigue and is followed by extreme wave loads. The formulation for the initial failure is similar to the case of an entire sequence of failures in fatigue. The formulation for the subsequent failure under extreme loads is

presented in chapter 4. The failure modes utilized in this analysis are based on the formulations presented in the API RP 2A-LRFD (1993). For each element five limit state functions are considered here again. Two of these formulations are given to check the yield criteria (mode) and three other expressions to verify the buckling failure mode. The probability of occurrence of the sequence of fatigue failure followed by failure due to extreme environmental loads can be specified as,

$$P_{f,J1f m2} = P\left[\left(T_{fJ1} \leq T_{life}\right) \cap \left(U_{m2} > 1.0\right)\right] \quad (5.23)$$

where  $U_{m2}$  is the usage factor of the second failure element specified with one of the formulations of 4.11 to 4.15 according to its stress state while the first element has failed due to fatigue damage. The application of these formulations depends on the stress state of the elements. It means that if the element is under a combination of tension and bending stresses, the expressions 4.11 and 4.12 will be relevant and if the element is under the combination of compression and bending stresses, the formulation 4.13 to 4.15 should be applied.

To incorporate all these formulations in one model, the time history of the maximum usage factor described in section 4.5 is applied here as the bases for the ultimate failure calculation. Hence, the Weibull distribution is fitted on the maximum of the usage factor in accordance with the structural response due to extreme environmental loads (the hydrodynamic loads with a 50-year return period). Moreover, the Gumbell distribution is used to extend for the storm duration (3 hours).

In a similar way as applied for the sequences of pure fatigue failure leading to system collapse, all the random variables in the fatigue limit state function have been considered to be independent except the stress model uncertainty.

In fact, this correlation arises from the correlation between the hot spot stress and the axial and bending stresses respectively. It should be mentioned that this correlation is not high as is observed from table 5.8, which is calculated based on the hot spot stress history in the end joint of element 298 for the first failure in fatigue and the time history of the usage factor for the other elements as the second failure element in ultimate limit state.

**Table 5.8:** The correlation coefficient between the hot spot stress at the end of element 298 (point 270 degree) and the usage factor of other elements after failure of the first element in fatigue

Element	52	53	54	295	296	297	169	170	373	374
<i>Cor.</i>	0.052	0.026	0.034	0.070	0.067	0.072	0.068	0.069	0.069	0.064

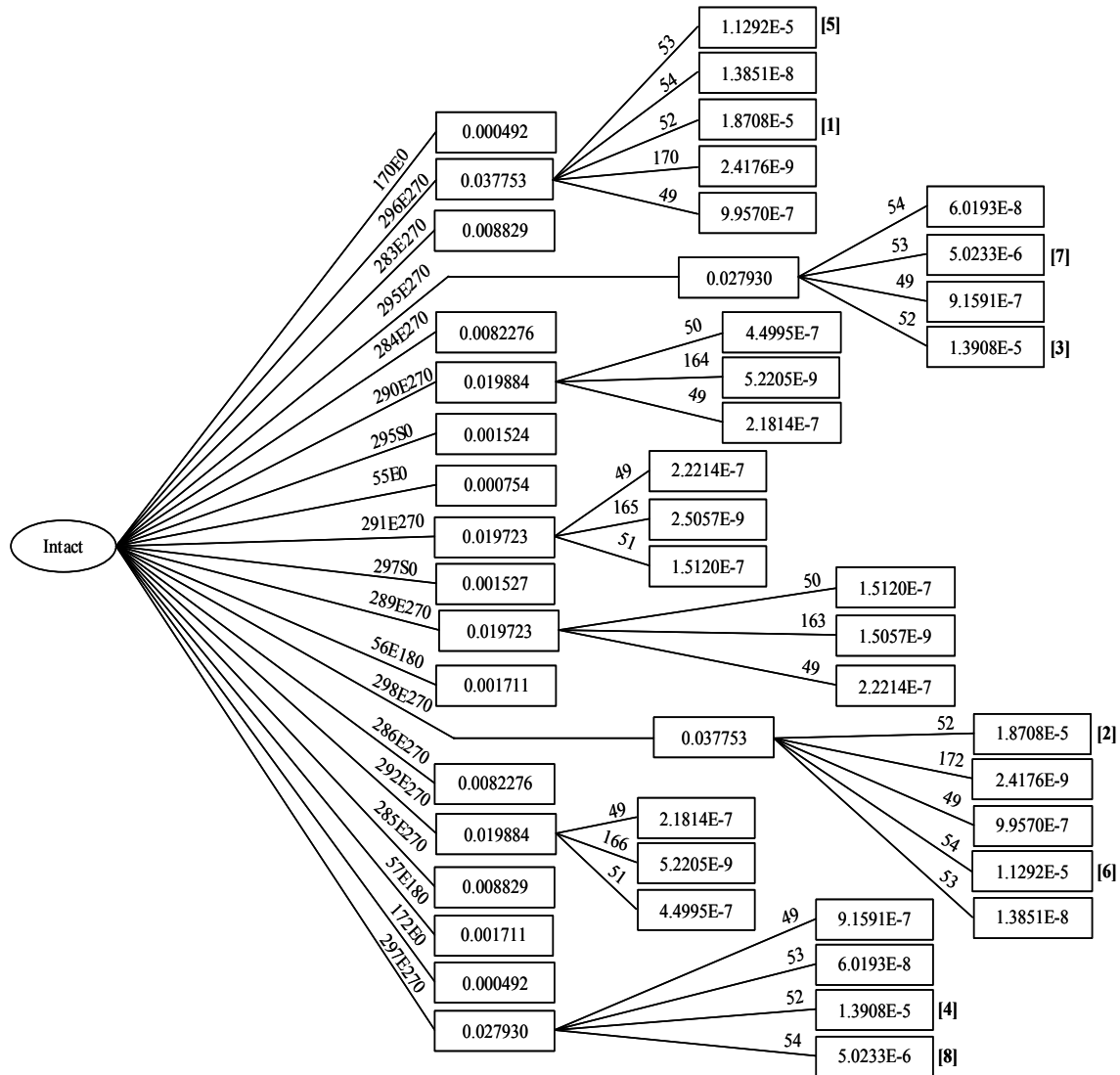


**Figure 5.5** Branch tree obtained for combination of fatigue failures and extreme environmental loads

Just as for the fatigue failures, several sequences can be supposed to cause a system collapse in the combination of the fatigue failure followed by the ultimate failure. The branch tree can be used to identify the important sequences leading to system collapse. The branch tree can be established by using the failure probability determined by expression 5.23 for several elements and the results are given in figure 5.5. The first important failure sequence is failure of chord element 52 in compression following the fatigue failure of the end of element 296 at the hot spot point 270. Due to the symmetrical configuration of the leg element, the same failure probability value is estimated for the second sequences, failure of chord element 52 in compression following the fatigue failure of the end of element 298 at the hot spot point 270. It generally shows that after the failure of the bracing elements in fatigue, the redistribution of

the stress in the remaining elements takes place in such a way that it increases the stress in the chord element and enhances the possibility of failure of this element.

Moreover, as can be observed from figure 5.5, the failure of chord element 52 contributes considerably in the four most significant sequences leading to structural collapse and a strong dependency is found for this element failure in a system reliability calculation. Comparing the failure probability calculated in the branch tree of the sequences in fatigue failures, figure 5.3, with the sequences in combination of fatigue and ultimate failure modes, it follows clearly that the fatigue failure probability sequences are much higher than the ultimate failure modes. Hence, the system failure probability in sequences of fatigue failure is more significant than the combination with extreme environmental loads.

For the eight important sequences shown in figure 5.5 the system failure probability can be calculated in terms of series and parallel systems. The sequences leading to structural collapse for the combination of fatigue failure and ultimate limit state constitute the parallel system and the union of these cut sets compose the series system. To calculate the system failure probability of the series system of a parallel subsystem, at first the equivalent limit state function is derived for each parallel system using the method described by Gollwitzer and Rackwitz (1983). The final system reliability is calculated by obtaining the failure probability of the whole series system using the multi-normal approximation or Ditlevsen bounds as explained in section 3.4. The correlation between each component in a series system is estimated through the combination of the correlation between the random variables as well as the limit state functions (fatigue and ultimate).

**Table 5.9:** System reliability index and the system failure probability of a jack-up platform calculated in a combination of sequences of fatigue failures and extreme environmental loads

	Crude FOMN	Improved FOMN	Uni-component bounds		Ditlevsen bounds	
			Upper	Lower	Upper	Lower
$P_f$	6.1618E-5	5.5294E-5	9.7858E-5	1.8708E-5	5.6839E-5	4.8896E-5
$\beta$	3.8396	3.8661	3.7245	4.1229	3.8594	3.8960

The system failure probability is computed according to the crude-FOMN and the improved-FOMN methods. Furthermore, the uni-component and Ditlevsen bounds are calculated and given in table 5.9 as well. The reliability indices obtained through the crude-FOMN and improved-FOMN methods are within the uni-component bounds, however, the crude-FOMN is outside of Ditlevsen bounds. Ditlevsen bounds give much closer values than the uni-component with the reliability index varying between 3.86 and 3.90. The improved-FOMN gives the value between Ditlevsen bounds and can here be supposed as the final system failure probability for combination of sequences in fatigue and extreme environmental loads.

Comparing this system failure probability with the results of table 5.7 for sequences of fatigue failures shows that the fatigue failure sequences are more critical than the combination with extreme environmental loads.



## 5.4 SYSTEM RELIABILITY FOR A COMBINATIONS OF FATIGUE AND FRACTURE FAILURE MODES

The results in chapter 4 and section 5.3 show that for the chosen jack up example combinations of a fatigue failure at the first joint and a fatigue failure in the second is more important than the combinations of fatigue and ultimate strength failure due to extreme environmental loads. In this section the combinations of fatigue failure at one and failure due to fracture at another joint will be considered. Four scenarios can be distinguished:

1. Fatigue failure of the first joint followed by a fracture failure of the second joint.
2. Fracture failure of the first joint followed by a fracture failure of the second joint.
3. Fracture failure of the first joint followed by a fatigue failure of the second joint.
4. Fatigue failure of the first joint followed by a fatigue failure of the second joint.

However, the last failure scenario, fatigue failure of the first joint followed by the fatigue failure of the second joint has already been investigated in section 5.2.

In the following sections a methodology for calculation of the system reliability for combined fatigue and fracture failure modes will be presented. Finally, all sequences will be combined to give the total system reliability. In the fracture formulation, the ratio between secondary to yield stresses ( $\sigma^S / \sigma_Y$ ) is assumed to be 1.0 as recommended by Shetty (1992). The same procedure can be applied for other ratios.

For the fracture limit state function in the following section, the crack size is assumed to occur due to fatigue degradation as indicated in chapter 4. Therefore, the fatigue-fracture interaction becomes a time-dependent problem and the time-variant reliability method should be applied. A time-variant method to deal with this problem has been presented by Marley (1991). In this method, the fatigue-fracture process is considered as a crossing problem, where the structural component fails when the strength, which deteriorates due to fatigue crack growth, is crossed by the load. The result of this method has been compared with a simple time-invariant approach, which assumes that the resistance is equal to the strength at the end of the service life. It is concluded that the approximated time-invariant method gives a higher failure probability but the difference is small and close to the more complex time-variant. In the following section, the simple method of the time-invariant has been applied for the fracture reliability calculation. Furthermore, this approach has been extended for the fracture failure of the second joint (system reliability).

### 5.4.1 Fatigue failure of the first joint followed by a fracture failure of the second joint

In this failure scenario, the first joint failure takes place through fatigue and is followed by the fracture failure of the second joint. Expression 5.7 will be used with some modifications to specify the fatigue crack size in the fracture limit state function. The crack size is therefore a random variable because it depends on several uncertain parameters such as fatigue characteristics, uncertainties in hydrodynamic models and calculations, etc. The statistics of a random fatigue crack size can be calculated using a Monte Carlo simulation technique and applying the fatigue crack growth formulation for the second joint (expression 5.7) without the correction term for the section failure ( $\delta_{fJ2}$ ) as,

$$\int_{a_{0J2}}^{a(t)} \frac{da}{\delta_{Y_{J2}}^m Y(a)^m (\sqrt{\pi a})^m} = v_{J2}^l \delta_{F_{J2}}^m \delta_{S_{J2}}^m \delta_{SCF_{J2}}^m C_{J2} A_{J2}^m \Gamma(1 + \frac{m}{B_{J2}}) T_{J1} \\ + v_{J2,fJ1}^l \delta_{F_{J2}}^m \delta_{S_{J201}}^m \delta_{SCF_{J2}}^m C_{J2} A_{J2,fJ1}^m \Gamma(1 + \frac{m}{B_{J2,fJ1}}) (T_{life} - T_{J1}) \quad (5.24)$$

The MCS has been carried out for several elements and eight hot spot points for each end of the member of the structure. The characteristics of the fitted lognormal distribution on crack size are determined using the first and second moment of the statistics resulting from the MSC technique for each hot spot. Since in the simulation of a fatigue crack size only the cases where  $T_{J1}$  is less than the lifetime of a platform is taken into account, this simulation would be the conditional simulation and the failure probability will be the conditional failure probability. The probability of failure for the combination of fatigue and fracture can therefore be estimated with the following expression.

$$P_{f,J1fJ2} = P \left[ (g_{fJ2} \leq 0) \mid (T_{J1} \leq T_{life}) \right] P \left[ T_{J1} \leq T_{life} \right] \quad (5.25)$$

The second expression in this formulation is the fatigue failure event of the first joint,  $[T_{J1} \leq$

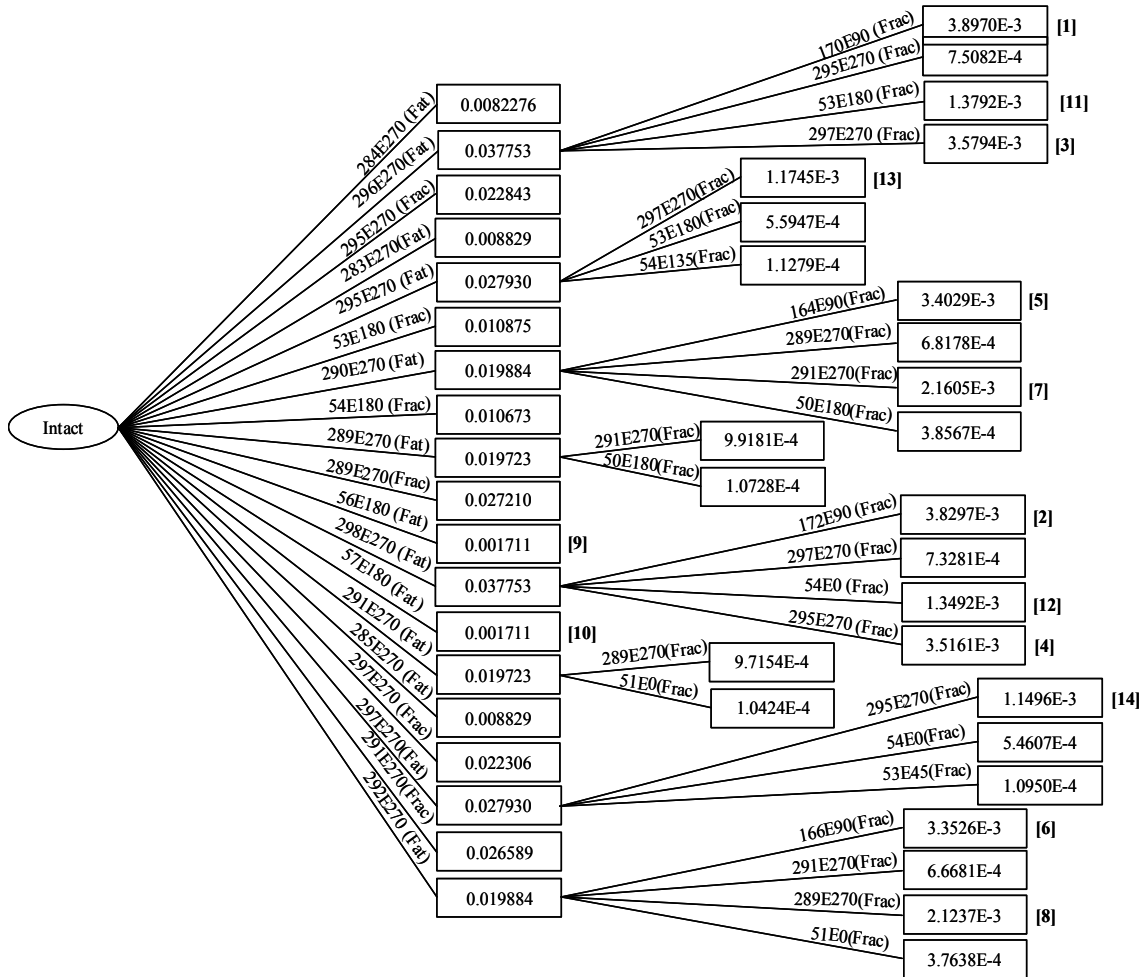


**Figure 5.6** Branch tree obtained for fatigue failure of the first joint and fracture failure of the second joint

$T_{life}$ ] and the conditional expression shows the subsequent fracture failure event  $[(g_{f2} \leq 0) | (T_{J1} \leq T_{life})]$ . To specify the time of the first element failure in fatigue, the formulation 5.4 is recalled. The fracture limit state function can be described by expression 4.16 or 4.17. In the following section the formulation 4.16 has been applied because it gives a more conservative failure probability than expression 4.17. However, as is shown in section 4.6, the maximum difference is less than 17% between these two methods (limit state 4.16 and 4.17).

The FORM approach is employed to estimate the failure probability of the first and second term in expression 5.25, but the crack size needed in the conditional expression is determined based on MCS. Details can be found in appendix I. Table 5.10 shows the characteristics of the random variables applied in the fracture limit state function.

Similar to fatigue failure, several hot spot points around the intersection of an element can be supposed to be susceptible for fracture failure. It is assumed the eight points regularly distributed around the intersection of an element and the failure probability is then calculated for each one separately and the highest one is selected as the critical one.

The results of the probability of failure for some elements (at both ends of the element) and their critical hot spot points are shown in table 5.11. These results are derived for the case that the first failure occurs at the end of element 296 due to fatigue damage and at the hot spot point 270. It can generally be observed that the failure probabilities of the both ends of element differ from each other and the highest one can be supposed to be the critical one.

Similar to fatigue failure sequences in section 4.2.4, all the random variables in the fracture limit state function are considered to be independent except the primary stress, which is the only random variable that is supposed to be correlated with the primary stress of other elements. The primary stress in the fracture limit state is calculated according to the extreme environmental wave loads that can be expected during the return period (here 50 years) but the stress history in fatigue is calculated through the long term combination of the several short term stress histories according to the scatter diagram.

**Table 5.10:** Statistic characteristics of random variables in fracture limit state function

Parameter	variable	Distribution	Mean value $\mu$	Coefficient of variation COV
Primary stress ( $kN/m^2$ )	$\sigma^p$	Gumbel	vary	vary
Fracture toughness ( $kN/m^2 \sqrt{mm}$ )	$K_{IC}$	Lognormal	6.5E6	0.25
Fatigue crack size ( $mm$ )	$a$	Lognormal	vary	vary
Geometry function	$\delta_y$	Normal	1.00	0.10
Load model	$\delta_F$	Lognormal	1.00	0.10
Yield stress ( $kN/m^2$ )	$\sigma_Y$	Lognormal	6.89E5	0.08
Stress concentration factor	$\delta_{SCF}$	Lognormal	1.00	0.10

**Table 5.11:** The failure probability of the second element failure in fracture when the first failure is in fatigue at the hot spot point of  $270^\circ$  in the end of element 296. The term S stands for start and E for the end of the element.

Element	169	170	172	295	297	53
H. S. Point	90	270	315	90	270	270
$P_f(S)$	2.1624E-6	9.8906E-7	1.6628E-9	3.6049E-6	5.8564E-5	3.5074E-4
H.S. Point	270	90	0	270	270	180
$P_f(E)$	1.1016E-7	3.8970E-3	7.5210E-5	7.5082E-4	3.5794E-3	1.3792E-3

The important sequences of this failure scenario are found by using the branch tree method. The branch tree is established through the failure probability determined by expression 5.25 for the combination of fatigue and fracture failure mode and the failure probability results higher than  $1.0E-4$  are shown in figure 5.6.

The most important failure sequence is fatigue failure of the joint at the end of element 296 (hot spot 270) followed by the fracture failure of the end of element 170 (hot spot point 90). The highest fourteen failure sequences identified through this branch tree are ranked in figure 5.6 and the system reliability calculation is carried out according to these sequences. The procedure to calculate the system reliability is similar as before.

The results of the system failure probabilities and the reliability indices according to the crude-FOMN and improved-FOMN are shown in table 5.12. The results of the uni-bounds and Ditlevsen bounds are calculated and shown in table 5.12 as well. As is clear, the results of the FOMN are within the uni-component bounds but crude-FOMN is outside of the Ditlevsen bounds. The Ditlevsen bounds give close results for the upper and lower bound. Since the improved-FOMN is within the Ditlevsen bounds, this failure probability can be assumed as the system failure probability of the jack-up platform for the combination of fatigue and fracture failure modes with a value of 0.0317.

**Table 5.12:** System failure probability calculated for the combination of sequences of fatigue failure of the first joint followed by fracture failure of the second joint

	Crude FOMN	Improved FOMN	Uni-component bounds		Ditlevsen bounds	
			Upper	Lower	Upper	Lower
$P_f$	0.03306	0.03178	3.3802E-2	3.8970E-3	0.03258	0.03161
$\beta$	1.8376	1.8553	1.8276	2.6609	1.8442	1.8577

### 5.4.2 Fracture failure of the first joint followed by a fracture failure of the second joint

In this failure scenario, the first joint failure occurs in fracture and followed by fracture failure of the second joint. For the first joint failure, the method described in section 4.6 is applied here. The required crack size in the fracture limit state function is obtained by using the fatigue expression 4.19 when the time is set equal to the lifetime of structure.

After failure of the first joint in fracture, the crack size for the second joint failure is computed in accordance with the fracture limit state function of the first joint and the fatigue formulation of the second joint. It means that at first the characteristic of the random crack size is determined using MCS and fracture expression 4.16. Then, the simulated crack size from fracture limit state is substituted in the fatigue formulation to specify  $T_{JI}$  (expression 5.3 without the section failure model uncertainty,  $\delta_{tf}$ ). However, only the values of random crack size, which makes  $T_{JI}$  less than the lifetime ( $T_{life}$ ), are collected from the MCS. Now by substituting the simulated  $T_{JI}$  in expression 5.24, the random crack size for the second joint failure is determined. By repeating this simulation several times, the statistics of the random crack size for the second joint failure are found. Now, the statistical characteristics of the random crack are substituted in the fracture limit state to calculate the sequences of the second joint failure in fracture. Since in this approach, only the simulated values of the crack when fracture failure occurs are selected from the MCS, the calculated failure probability is the conditional failure probability. The failure of this sequence can be estimated from,

$$P_{f,J1fJ2} = P\left[(g_{fJ2} \leq 0) | (g_{fJ1} \leq 0)\right] P[g_{fJ1} \leq 0] \quad (5.26)$$

where the second expression is the probability of a fracture failure event of the first joint,  $[g_{fJ1} \leq 0]$  and the conditional expression shows the subsequent fracture failure event,  $[(g_{fJ2} \leq 0) | (g_{fJ1} \leq 0)]$ . The FORM approach has been applied to estimate the failure probability for the first and second term of this expression. The MCS has only been used to simulate the random crack size needed in fracture limit state. For the first failure, the fatigue formulation is utilized but for the second joint failure, the combination of fracture and fatigue expressions have been applied to simulate the crack size. Details can be found in appendix I.

**Table 5.13:** System reliability index and system failure probability calculated for the combination of sequences of the fracture failure of the first and second joint

	Crude FOMN	Improved FOMN	Uni-component bounds		Ditlevsen bounds	
			Upper	Lower	Upper	Lower
$P_f$	0.02208	0.02207	0.0221	0.01087	0.02208	0.02207
$\beta$	2.0126	2.0127	2.0125	2.2947	2.0126	2.0127

The primary stress is the only random variable that is supposed to be correlated with the primary stress of other joints. The primary stress in the fracture limit state is calculated according to the extreme environmental wave loads that can be expected during the return period (here 50 years, see section 4.6).

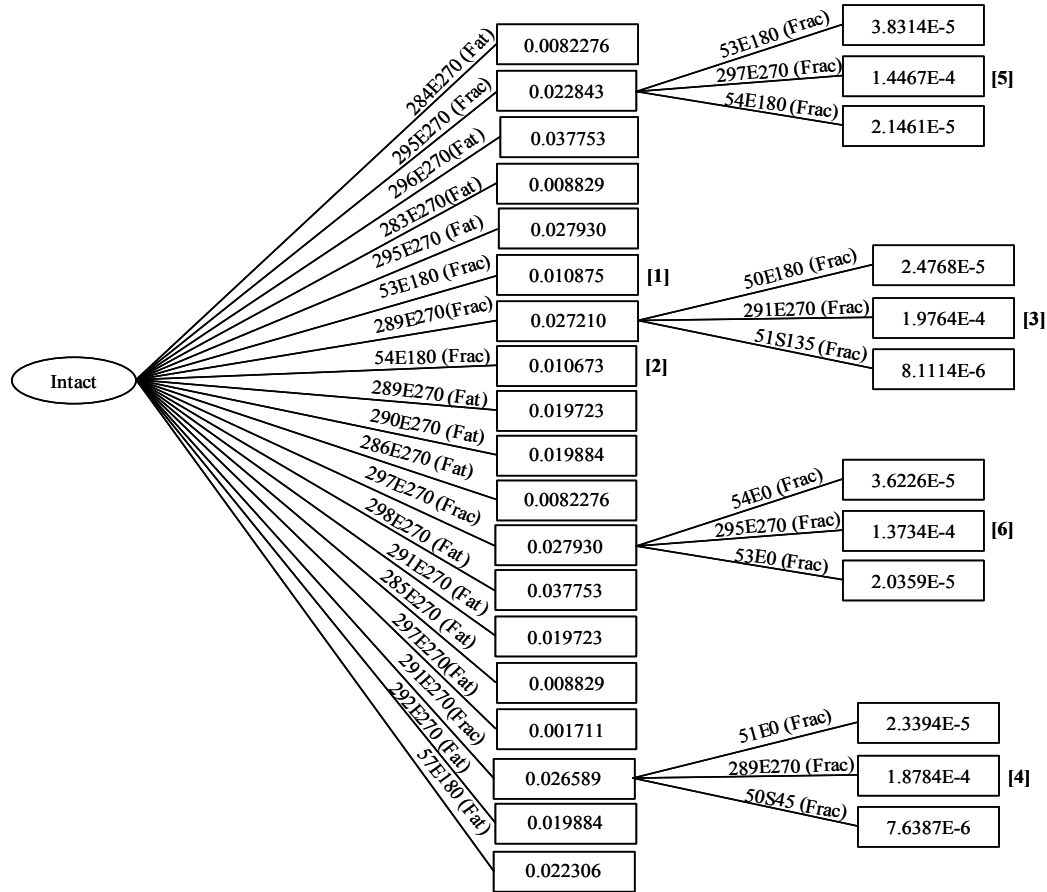


**Figure 5.7** Branch tree obtained for combination of the first joint failure in fracture and the second joint failure in fracture

The calculated failure probabilities for this failure scenario are presented in figure 5.7 for several important sequences leading to structural collapse. Failure probabilities less than  $1.0\text{E-}6$  are not shown in this figure.

The first and second important failure sequences are the fracture failure of the chord element 53 and 54 with the failure probabilities 0.0108 and 0.0106 respectively. The highest six failure sequences identified through this branch tree are ranked in figure 5.7 and the system reliability calculation is computed in accordance with these sequences and is given in table 5.13. It is clear from result that the reliability index for this failure scenario is higher than the previous one.

#### 5.4.3 Fracture failure of the first joint followed by a fatigue failure of the second joint

In this failure scenario, the first joint failure occurs in fracture and is followed by fatigue failure of the second joint. The same approach for the first joint failure in fracture is used as it is carried out in the previous section. The only difference is the second failure, which is assumed to occur in fatigue instead of fracture.

For the second joint failure, the same expression for fatigue failure (5.7) is used here again but the random time to the first joint failure is estimated in accordance with the fracture limit state function and fatigue crack growth. It means that the MCS is used to simulate the crack size of the first joint by using the fracture formulation. Then, the simulated fracture crack size is substituted in the crack growth expression for the first joint to obtain  $T_{J1}$  (expression 5.3 without section failure model uncertainty,  $\delta_{tf}$ ). Since in this calculation, only the simulated values of the crack size when  $T_{J1}$  is less than  $T_{life}$  (fracture failure occurs) are selected from MCS, the calculated failure probability is therefore the conditional failure probability. The failure probability for this sequence can be obtained from the following expression.

$$P_{f,J1J2} = P \left[ (T_{J2J1} < T_{life}) | (g_{J1} < 0) \right] P [g_{J1} < 0] \quad (5.27)$$

The second expression is the fracture failure event in the first joint,  $[g_{J1} \leq 0]$  and the

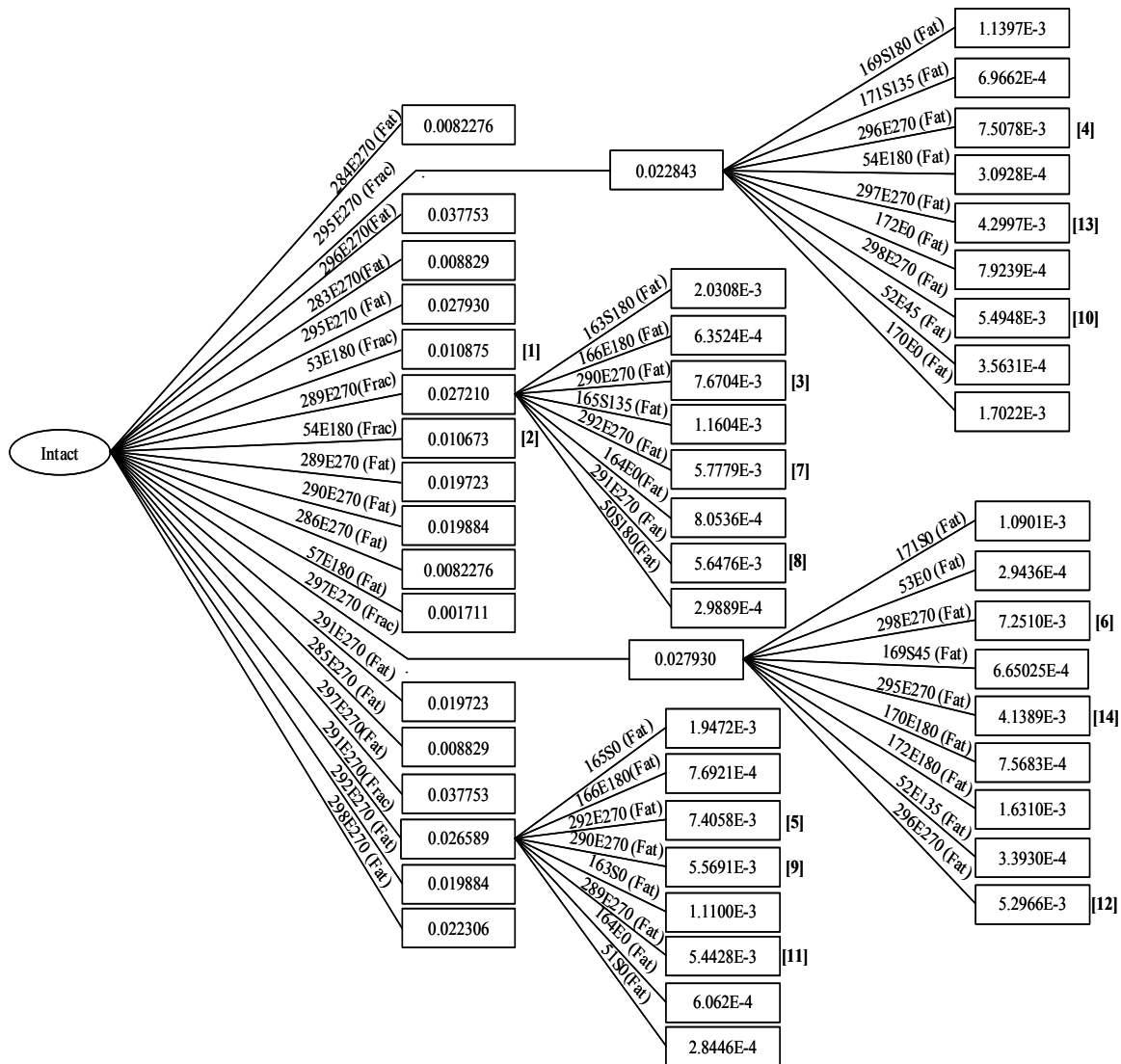


**Figure 5.8** Branch tree obtained for the combination of the first joint failure in fracture followed by the second joint failure in fatigue

conditional expression shows the subsequent fatigue failure event,  $[(T_{J2fJ1} \leq T_{life}) | (g_{fJ1} \leq 0)]$ . In this failure scenario, the primary stress is supposed to be the only correlated random variable with the primary stress of other joints for the system calculation. Furthermore, the stress uncertainty model in the fatigue limit state is also correlated with the primary stress in the fracture limit state. Details can be found in appendix I.

The branch tree has been established and the result is shown in figure 5.8 for the failure probability higher than  $1.0E-4$ . The highest fourteen failure sequences identified through this branch tree are ranked in this figure as well. The system reliability calculation is carried out in accordance with these sequences are given in table 5.14. As is clear from figure 5.8, one of the important failure sequences is fracture failure of bracing element 289 followed by fatigue failure of element 290.

Comparing the calculated system failure probabilities in table 5.14 shows that the Ditlevsen bounds give closer results than the uni-component bounds with the values varying between 0.0724 and 0.0820. The result of crude-FOMN is out of the Ditlevsen bounds but the improved-FOMN is within these bounds and can be supposed as the final system failure probability for this failure scenario. If we compare this failure probability with the values calculated for other failure scenarios, it can be concluded that this failure scenario gives the highest failure probability and care should be given to this failure state. However, it should be kept in mind that the result is probably a conservative approximation and conservative because of using the simplified time-invariant reliability approach, and applying the design storm with return period 50 years.

**Table 5.14:** System reliability index and system failure probability calculated for the combination of sequences of fracture failure of the first joint followed by fatigue failure of the second joint

	Crude FOMN	Improved FOMN	Uni-component bounds		Ditlevsen bounds	
			Upper	Lower	Upper	Lower
$P_f$	0.0825	0.0760	0.08916	0.01087	0.08208	0.07242
$\beta$	1.3885	1.4320	1.3459	2.2947	1.3912	1.4580

The comparison of the calculated system failure probability for sequences of fracture failure of the first joint followed by fatigue failure of the second joint failure with the results of table 5.13 (fracture failure of the first and second joint) and table 5.12 (fatigue failure of the first joint followed by the fracture failure of the second joint) shows that this failure scenario gives higher failure probability than the other combinations. Moreover, it shows that the fracture failure is an important failure mechanism.



#### 5.4.4 System failure probability calculation for combinations of fracture and fatigue failures

In this section we combine all failure sequences identified in the previous sections to calculate the final system failure probability of the Neka jack-up platform for the combination of fatigue and fracture. The forty-one important sequences identified in the previous sections are shown in figure 5.9. The final system failure probability is based on the failure probability calculated for each of the failure sequence and its correlation, which is estimated between the random variables and the limit state functions (see appendix F).

The results are given in table 5.15 in accordance with the FOMN approaches and Ditlevsen bounds. The crude-FOMN and improved-FOMN results are within the Ditlevsen bounds. The Ditlevsen bounds give narrower results than the uni-component bounds. The final system failure probability for the jack-up structure can be supposed as the result of improved-FOMN with the value 0.1143. It is clear that this value is higher than the first joint failure in fatigue

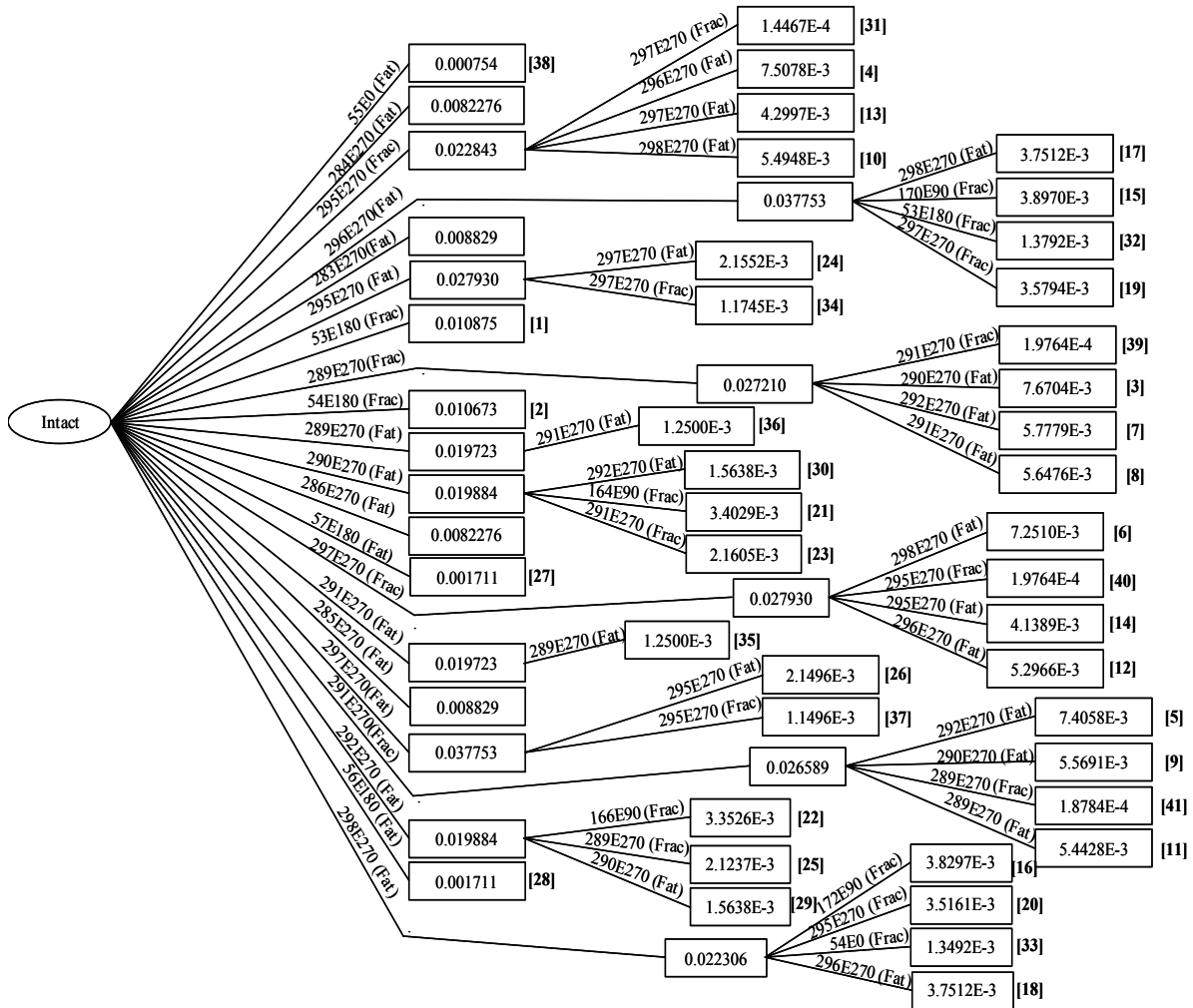


**Figure 5.9** Branch tree obtained for the combination of the important sequences in fatigue and fracture failure of the first and the second joint

or fracture and care should be given to this type of failure in the structural analysis of jack-up platforms, when ageing is being investigated.

**Table 5.15:** System reliability index and system failure probability calculated for all combinations of fracture and fatigue in the first and the second joint failures

	Crude FOMN	Improved FOMN	Uni-component bounds		Ditlevsen bounds	
			Upper	Lower	Upper	Lower
$P_f$	0.12719	0.11443	0.13641	0.0108	0.13037	0.10406
$\beta$	1.1398	1.2033	1.0966	2.2947	1.1246	1.2588

## 5.5 CONCLUDING REMARKS

In redundant structures such as jack-up platforms, failure of one element in fatigue or fracture may not lead to the structural collapse. Therefore, the system effect is considered in a reliability calculation.

In this chapter, several system reliability calculations have been investigated under different failure sequences. The approaches to examine the factors leading to structural collapse are related to fatigue failure, fracture failure and ultimate failure due to extreme environmental loads. From chapter 4, it is observed that the result of the first joint failure in the ultimate failure mode is not the dominant one. Hence, the combination of the failures in fatigue and fracture are investigated.

There are four possibilities for combination of sequences in fatigue and fracture. The first combination is the first and second joint failures in fatigue. The other three possibilities, i.e. combination of fatigue and fracture, fracture and fracture, fracture and fatigue of the first and the second joint respectively have been investigated for the system reliability calculation.

A methodology for fatigue failure sequences of the first and second joint is presented to take into account fatigue degradation up to the time of fatigue failure. The result of the sequences of fatigue failure, calculated for eleven important sequences leading to structural collapse as given in table 5.7, shows that the system failure probability is lower than the first element failure probability and the system effect would be essential to be evaluated.

For other three combinations of fracture and fatigue failure, the Monte Carlo simulation technique has been utilized to simulate the crack size due to fatigue or fracture failure. If the joint fails in fracture, the fracture formulation has been applied to simulate the crack size and if the joint fails in fatigue, the fatigue formulation is employed. Eight points around the intersection have been selected as the possible points for fatigue or fracture failure and the critical one, which gives the highest failure probability, is shown in each failure sequence. The failure probability of the structural system in combination of fatigue and fracture failure modes has been calculated through the combination of forty-one significant failure sequences

identified in the branch tree. As shown in table 5.15, the calculated system failure probability for the combination of fatigue and fracture is higher than the pure failure sequences in fatigue or the sequences in combination of fatigue and extreme environmental loads. Moreover, this failure probability is higher than the first joint failure in fatigue or fracture individually and the conclusion may be drawn that this type of structural failure deserves significant attention during the ageing of jack-up platforms. However, it should be kept in mind that in practical situation the platform will be inspected regularly (annual, intermediate and full inspection). Hence, the information acquired from inspection not only can be used to update the component failure probability (as shown in section 4.4) but also the system failure probability. Therefore, the actual failure probability of platform will change depending on inspection results. This system updating has not been investigated in this research work.

For fracture reliability analysis, a simple but time-invariant approach has been applied with the extreme stresses estimated from a design storm (50 years). This assumption may lead to the conservative result due to the use of the time-invariant approach from one side. From the other side, the maximum stress calculated in the design storm is based on 3 hours storm duration with the return period of 50 years, which under realistic conditions the storm duration may be longer or more (larger or smaller) sea state may encounter during the critical period of the lifetime of platform. This can lead to deviations from the calculated fracture failure probability, which need not to be conservative. Therefore, this should be subject of further investigation for the combination of time-invariant and design storm method.

The referenced time applied for the fracture and fatigue reliability calculation is the lifetime of the structure (20 years). However, the provided method for system reliability calculation can be carried out for other service time periods e.g. one or four years. In this case, the information acquired from the inspection can explicitly be incorporated in the system reliability and it could be suggested that the system failure probability estimated with or without inspection will be lower than the results for the lifetime period. For the calculation of the crack size for the second joint failure in fracture and fatigue, the time of the first joint failure ( $T_{J1}$ ) being less than the lifetime ( $T_{life}$ ), is always selected from a MCS to make sure that the first joint failure occurs before the second one.

The question of how the deteriorated structure in the first fatigue failure may fail in the other failure modes has been considered as well. In the new failure scenario, the sequences leading to structural failure are assumed to occur in the combination of fatigue and extreme environmental loads. The failure probability under extreme environmental loads is calculated through the time history of the usage factor and the failure event is combined with the fatigue failure event to specify the sequence failure in fatigue and ultimate failure modes. The final system failure probability is then estimated in accordance with the combination of eight important failure sequences leading to structural collapse. The result shows that the system failure probability in this case is smaller than the whole sequences in the fatigue failures, as shown in table 5.9 with the failure probability of  $5.53 \times 10^{-5}$ .



## 6 CONCLUSIONS

---

### 6.1 General

The main problems for this research work as formulated in Chapter 1 are related to:

- The limited investigations on the fatigue damage of jack-up platforms.
- The occurrence of fatigue damage, for jack-up platforms as production facilities.
- The uncertainty in the characteristics of fatigue, both environmental loads and material properties.
- The specific structural stress states of jack-up platforms, which differ from jackets or tension leg platforms.
- The possibility of a combination of fatigue failure with the other failures such as ultimate failure or fracture failure modes.
- The failure of one element may not lead to the structural collapse and therefore to failure of the system.

The goal was to develop a reliability approach, which may be used to monitor the safety of jack-up platforms. Moreover, to specify a degradation model arising from fatigue damage in order to make it possible to investigate fatigue damage in combination with other failure modes resulting from extreme environmental loads i.e. ultimate or fracture failure modes. Furthermore, to explore the system effects on the reliability of a structure and investigate which factors may affect the estimated failure probability.

Firstly will be discussed to which extent the key questions, related to jack-up structures on component and system level have been answered.

Secondly the way that the problem finally has been dealt with will be explained, compared to the intended approach, as well as the new elements, which have been introduced, and how the results of this approach are compared to earlier research. Then conclusions will be drawn from these results, indicating where improvements have been achieved and finally suggestions for the further research on the research on the ageing of jack-up platforms will be given.

Although the methods used in this thesis are commonly known reliability-based methods, the particular circumstances for offshore jack-up platforms are the basis for an approach during the ageing and consequently the stress state of jack-up platforms. The approach aims at reflecting realistic situations occurring during the lifetime of a jack-up structure.

The research on the effect of ageing on jack-up platforms started the last decade with the aim to evaluate the possibility of extending the lifetime. Results of research on the ageing of jack-up platforms are rarely reported in the literature and more work is required to investigate the effect of ageing on this type of structures. The cause of this rare amount of investigation has not been explored but the availability of design rules and requirements of classification societies may play a role. Not only the move to operations in deeper water, other applications and changes in environmental conditions, but also the increasing average age of the platforms combined with the fact that the fatigue failure has been observed to be a major source of degradation for fixed platforms, induced the interest to search for methods enabling a reliable prediction of the lifetime.

To specify a formulation for fatigue degradation, the mechanics of fatigue has been presented showing that the fatigue crack growth model can be used to specify the fatigue crack propagation through the structural thickness. A semi-elliptic shape has been applied to model the crack propagation in depth and circumference. The geometry function is an important factor in the fatigue formulation because it takes into account the nature of stress and the crack size in the fatigue crack propagation. The geometry function should be specified in accordance with the configuration of the jack up platform and its stress states. Several formulations have been presented to specify the geometry function of tubular elements for which most are based on the expression of Raju and Newman. The presented formulations for the geometry functions of tubular elements are generally derived for the specific stress states of jacket platforms, which are not appropriate to use directly for jack-up platforms. Therefore, some modifications have been proposed to consider the actual stress state of jack-up platforms.

Several methodologies for fatigue reliability calculations, ultimate limit states calculations and finally fracture failures of jack-up platforms have been proposed and the results of these methods have been compared to the traditional methods. In the following sections, these results are discussed and presented.

## **6.2 Reliability computation approaches**

Generally, three reliability approaches are recognized: analytical approximation, simulation and numerical integration. The numerical integration method is only suitable in case of a limited number of random variables and a simple limit state function, making this approach not suitable in case of a fatigue or fracture failure modes in offshore structures not only because many random variables are involved but also as the limit state functions are complex. The analytical approximations such as First and Second Order Reliability method (FORM and SORM) or simulation methods such as Monte Carlo and Importance Sampling (MCS and IS) will be more appropriate. However, the simulation method is more time consuming and sometimes in the case of MCS this may not lead to accurate results when the required number of simulations is too large.

In the analytical approximation methods, the original limit state function is approximated by the Taylor series expansion up to the first or second order in accordance with the non-linearity of the failure surface at hand. The first order (FORM) is used when the first term is appropriate and in case of non-linearity, the second order (SORM) may be applied. However, in this case, first the result of the first order approximation should be estimated and then the curvature of the second order is incorporated in the calculations.

To investigate the efficiency of the reliability computation methods, several computer programs for the three limit state functions of fatigue, fracture and ultimate limit state functions have been provided to calculate the failure probabilities in accordance with the two analytical approximations (FORM and SORM) and the simulation methods (MCS and IS). The results obtained for the case of the fatigue limit state show that, although the calculation time needed for FORM is less than the other methods, this technique gives a good approximation compared to the SORM and IS methods with a maximum difference of 2 % for the reliability index.

To check the accuracy of the developed computer program, the same fatigue limit state function has been entered into the STRUREL program. The results show good agreement between the FORM and SORM approaches of the developed program and the solution of FORM and SORM derived in STRUREL respectively. The maximum difference in the calculated reliability index is less than 0.35 % for SORM.

The results of the reliability calculation for the ultimate limit state function lead to the following conclusions:

- The FORM approach gives a close approximation compared to other methods with a 3% higher reliability index. In this case the FORM result is on the unconservative side, compared to other methods but this difference is generally not significant.
- The same values have been calculated for the FORM of the provided program and the STRUREL results. A somewhat higher value is observed for the SORM results of the provided program compared to STRUREL with 0.2% difference in the reliability index. The discrepancy between these two algorithms can be attributed to the analytical derivation method used in the provided program and the numerical method used by STRUREL.

The results of the reliability calculations for the fracture limit state function yield to the following conclusions:

- The SORM approach gives higher reliability indices than FORM but these are close to each other with a maximum difference of 0.4%. Furthermore, FORM results are maximum 0.3% lower than the IS solution and there is a close agreement between the provided program and the STRUREL solutions.

The following conclusions may be drawn from estimated reliability indices for the three limit state functions for the fatigue, fracture and ultimate limit state functions:

- The provided program gives a good approximation for FORM and SORM results in comparison with the STRUREL program.

- The FORM approach can be applied as a base for reliability calculations; however, in the case of the ultimate limit state a little higher reliability index can be expected for the FORM approach.

### 6.3 Fatigue reliability calculation

In fatigue reliability calculations, the hot spot stress ranges have to be determined. The hot spot stress range has been estimated by using the influence factor, where the effect of planar and non-planar elements has been taken into account. The peak counting method is then applied to determine the distribution of the stress range. The test of goodness of fit shows that the Weibull distribution gives the best fit among different distribution functions for the short-term stress range, and this distribution function is therefore applied in the fatigue reliability calculations.

The geometry function plays an important role because it takes into account several corrections arising from the effects of loading and crack geometries. Since the structural characteristics of a jack-up platform differ significantly from a fixed jacket platform, the behaviour of the structure is different and the traditional expressions for the geometry function used in tubular elements of jacket platforms have been modified for jack-up platforms.

The first modification is related to the bending to membrane stress ratio ( $\alpha$ ). As it is shown in figure 4.7, the bending to membrane stress ratio ( $\alpha$ ) changes the fatigue reliability considerably and if no proper ratio is selected, the estimated reliability may vary significantly. The calculated  $\alpha$  ratio for jack-up platforms shows that it varies between zero and one for several hot spot points around the intersection of a brace/chord joint as shown in table 4.4, and differs significantly from the values 4 and 5 recommended for jacket platforms. Hence, attention should be given in the selection of  $\alpha$  ratio in the geometry function.

The second modification is associated with the correction of the geometry function for the weld toe profile. A new geometry function for jack-up platforms is established, based on the combination of the Raju and Newman expressions with a correction term for the weld toe discontinuity and an exact  $\alpha$  ratio determined from the stress time history. The results of this method have been compared with the geometry functions given by Moan, Kirkemo, and Aghakouchak in table 4.5. It is observed that:

- The proposed method gives a higher reliability index than the Kirkemo and Moan approach with a maximum difference of 14% and 20% respectively for each method, however lower than Raju-Newman without the correction of Smith and Hurworth.
- The Aghakouchak results are higher than the proposed method with a maximum difference of 10%.

The comparison of the proposed method with other ones indicate that if the exact  $\alpha$  ratio is not selected in the fatigue reliability calculation, the result may lead to an incorrect estimation of the reliability index of jack-up platforms.



The P-M and JONSWAP wave spectra have been widely applied in offshore engineering to model the wave energy spectra. The first spectrum is used for the fully developed sea states and the second one for the fetch limit condition. The proper selection of spectra may be in question. To investigate the effect of the choice of a spectrum on the fatigue reliability, the fatigue reliability calculation has been carried out for these two spectral models and the estimated reliability indices are compared with each other as shown in figure 4.9 for several service times. The results show that the JONSWAP spectrum generally gives a higher reliability index than P-M but are not significant. The highest differences for the first five years are limited to 2% and increasing to 3% at the end of the service time.

The estimated and reported overall damping of jack-up platforms in the references vary significantly from 0.02 to 0.10 and hence there is some uncertainty about the proper selection of this value. The effect of the variation of the structural damping on fatigue reliability has also been investigated. The results indicate that the fatigue reliability indices grow with an increasing damping ratio as can be seen from figure 4.10. However, this growth is not so significant for damping ratios between 0.05 and 0.07 when the highest differences are 2% but the distinction becomes more considerable with a maximum of 13% for damping ratios between 0.02 and 0.05 and 24% between 0.02 and 0.10 at the end of service time.

The stress process in a jack-up structure is non-linear and broad-banded. The stress range of the nonlinear and broad-banded process can be determined using the rain flow counting method. Since this method is complex and time consuming, less complex and easier analytical formulations are recommended. In this research work, a stress range based on the Weibull distribution of peak counting is proposed. This method is compared to other models presented by Wirsching and Light (W&L), Zhao and Baker (Z&B), as well as a nonlinear Hermite model presented by Winterstein. The fatigue reliability results calculated with these methods are compared with the rain flow counting method as well. The following conclusions are drawn:

- The rain flow counting method gives the lowest fatigue reliability indices compared to the other methods for different sea states. This method is time consuming but generally believed to be the best model.
- The correction model of W&L gives the highest reliability indices and would be unconservative if used in a reliability analysis.
- The narrow-banded and Z&B correction model gives also higher reliability indices than the rain flow counting method but they are close to each other and lower than W&L.
- The non-linear Hermite model shows some discrepancy for the higher sea states.
- The proposed Weibull model gives a better approximation for the higher sea states and almost the same results as other methods for the lower sea states compared to the rain flow counting method.

The inspection of a platform during operation provides valuable information to update the fatigue reliability. The application of this information in the reliability updating of a jack-up platform is shown for two cases of information. The fatigue reliability increases with the introduction of the inspection information for a no-crack detection or detecting a crack and finally repairing.

#### 6.4 Extreme sea states

The maximum stresses in the structural elements occur when the platform is confronted with extreme sea states that may occur in a specific reference period. The inverse FORM method presented by Winterstein has been applied to specify the extreme sea state or design storm for a 50-year return period. A proposed approach based on method described by Videiro and Moan is applied to determine the reliability of structural elements under extreme environmental loads using the time history of the usage factor. The results of the traditional methods are for two cases, with and without correlation between axial and bending stresses, compared with the proposed method and the conclusion is that:

- The proposed method gives a good approximation for the reliability of an element comparing to the traditional method when the correlation between axial and bending stresses is accounted for.
- The benefit of the proposed method is that the axial stress state variations from tension to compression or vice versa can directly be taken into account in the reliability calculations.

The estimated failure probability based on the design sea state (storm) is a conditional probability. The extreme wave that the structure may experience during its lifetime (20 years) can be larger than the design storm with the return period of 50 years. In this situation, the long-term (unconditional) failure probability should be applied. An approximate approach is presented in appendix H to calculate the long-term failure probability. The results show a moderate difference between design storm (50 years) and long-term approach for the chord elements (52 and 53) but the discrepancy increase for the diagonal bracing elements (295 and 296)

#### 6.5 Fracture reliability methods

The fatigue degradation emerges its effect in the structural joint as a flaw. The combination of this flaw with extreme environmental loads may cause fracture failure. This type of failure mode has also been investigated in this research work and the results of the fracture assessment diagram recommended by the British Standard Institute are compared with the Dijkstra method. The crack size is an important factor in the fracture limit state function. In this research work, this crack is assumed to occur through the fatigue degradation and is therefore specified with the fatigue crack growth expression. Since some of the parameters in the fatigue formulation are random variables, the MCS technique has been applied to simulate the variables. The statistic characteristics of the random crack size for several service times of the platform have been estimated. The results show that the lognormal distribution gives the best-fitted results according to the test of the goodness of fit using Chi-square on the random fatigue crack size.

By using the characteristics of the lognormal distribution of the random fatigue size calculated by MCS in both fracture limit state functions based on the Dijkstra method and the fracture assessment diagram, the reliability indices have been estimated for several secondary to yield stress ratio and service times. The comparisons of the results show that the reliability indices of the Dijkstra method give higher values than the fracture assessment for several secondary to yield stress ratios and service times.

The general comparison of fatigue, ultimate and fracture reliability calculations for one element in the jack-up platform (the intersection of bracing element 295 with the chord) shows that the fatigue failure mode gives the lowest reliability or the highest failure probability with a reliability index 2.96 compared to other failure modes. The fracture failure gives the reliability index value of 3.41 when the secondary stress is close to the yield stress and has a lower reliability index than the extreme environmental loads with the value of 8.76 but is not significantly far from values for fatigue. The reason for this high reliability index for ultimate limit state can be attributed to this fact that the original structural design of the jack-up platform has been carried out on the basis of the ultimate limit state check, and therefore a proper safety can be expected with this calculation. Moreover, other reasons can be related to the design sea storm method used to specify the extreme wave loads. As shown in appendix H, the approximated long-term reliability index for this element is less than the one for the design sea storm (50 years return period) with the value 6.84 but it is higher than the failure probability in fatigue and fracture.

## 6.6 System reliability calculations

The system reliability of the jack-up platform under several failure sequences leading to structural collapse has been investigated. At first, a methodology for fatigue sequences leading to structural collapse has been presented to take into account fatigue degradation up to the time of fatigue failure. Sensitivity analysis is carried out to identify the importance of random variables. The comparisons of the sensitivity results show that:

- The highest contribution to the total uncertainty arises from the stress model in the second joint failure with 39%. However, the fatigue characteristic ( $C_A$ ) shows also more influence than others with 11% for the second joint and 7% for the first joint. The initial and through thickness crack size have little effect on the total uncertainty and can be assumed as the deterministic variables in the reliability calculation.

The correlation between the limit states is specified according to the correlation between the random variables of the stress uncertainty. By using the time history of the stress process in each hot spot point, this correlation has been specified.

Each failure sequence event leading to a structural failure in the branch tree is modelled as a parallel subsystem and the structural failure event is formed as the series system, which combines all the parallel subsystems.

The equivalent safety margin of a parallel system has been established in such a way that the relevant reliability index of the equivalent element is identical to the final parallel system and the random variables have the same sensitivity as the parallel system against changes in the basic variables. The First Order Multi Normal (FOMN) and bound techniques have been employed to compute the final failure probability of a series system.

The result of the sequences of fatigue failure calculated for eleven important sequences leading to structural collapse shows that:

- A system reliability index resulting from Ditlevsen bounds techniques is varying between 2.06 and 2.18.

- The system reliability index calculated through the FOMN approaches gives a good approximation with the Ditlevsen results with maximum differences less than 6 percent.
- The system failure probability of a structure in this failure mode can be supposed, as the value calculated by the improved-FOMN being 0.0165, which is lower than the first element failure probability.

The structure, which is weakened in the first fatigue failure, may fail in the other scenario that has already been described. In the new scenario, the sequences leading to a structural failure are assumed to occur in the combination of fatigue and extreme environmental failure modes, respectively. The extreme environmental failure probability is calculated through the time history of the usage factor and is combined with the fatigue failure to determine the failure probability of the sequence failure in fatigue and ultimate failure modes. The correlation between these two limit states is calculated using the time history of the usage factor and hot spot stresses in the individual hot spot points. The final system failure probability is calculated according to the combination of eight important failure sequences leading to structural collapse. The FOMN and bound techniques have been applied to compute the system failure probability. The results show that:

- A close value has been observed for the upper and lower Ditlevsen's bound with the reliability index varying between 3.86 and 3.60 respectively.
- The improved-FOMN method gives reliability index between the Ditlevsen bounds.
- The system failure probability in this case has a great influence on the final failure probability and decreases significantly, however the overall system failure probability for this failure sequence is less than the pure failure sequences in fatigue.

There are four possibilities for the combination of fatigue and fracture. The first combination, which is the first and second joint failures in fatigue, has already been investigated. The other three possibilities, i.e. the combination of fatigue and fracture, fracture and fracture, fracture and fatigue of the first and second joint respectively have been suggested for a system reliability calculation. For each failure scenario, the Monte Carlo simulation technique has been utilized to simulate the crack size due to fatigue or fracture failure. If a joint fails in fracture, the fracture formulation has been applied and if the joint fails in fatigue, the fatigue formulation has been used to simulate the crack size. The failure probabilities of these three failure scenarios have been estimated for important sequences leading to structural collapse and are shown in tables, 5.12, 5.13 and 5.14 for the combination of fatigue and fracture, fracture and fracture, fracture and fatigue for the first and second joint failures respectively. The results show that:

- The combination of fracture failure of the first joint with the fatigue failure of the second joint gives a higher failure probability than the others with a value 0.076. This failure scenario is also high in comparison with the pure failure sequences in fatigue. The system failure probability in this case is higher than the first joint failure in fatigue or fracture. Therefore, care should be given to this failure scenario.
- The minimum system failure probability occurs from a combination of a fracture failure of the first and second joints respectively with a value of 0.022.

The failure probability of the structural system in the whole combination of fatigue and fracture failure modes has been calculated through the forty-one significant failure sequences identified in the branch tree leading to structural collapse in the previous sections. The final failure probability is calculated using FOMN and Ditlevsen bounds. The results show:

- The Ditlevsen bounds give the closest failure probability index for the upper and lower bound with values varying between 0.13 and 0.10 respectively.
- The improved-FOMN result is within the Ditlevsen bounds and can be supposed as the final system failure probability for the whole combination of fatigue and fracture with a value of 0.11.
- The calculated system failure probability is higher than the first failure element in fatigue and more than the sequences in combination of fatigue and extreme environmental loads. Moreover, for this case the system failure probability is also higher than the sequences in pure fatigue failures.

Higher failure probabilities in a combination of fatigue and fracture show significant structural effects in a combination of fatigue and fracture and this failure scenario needs attention. Moreover, this high failure probability could obviously clarify why the classification societies enforce regular inspection programs to be undertaken during the service time of platform.

## 6.7 Main findings

The general conclusions that may be drawn are related to the results of the reliability calculations, the method used for the reliability calculations and the applicability for this type of calculations.

### The results:

- Several failure scenarios leading to the structural collapse are examined and some methodologies for the system failure probability calculations have been presented. The results show that the sequences in combination of fatigue and fracture failures give the highest failure probability and care should be given to this type of failure modes in jack-up platforms.
- The failure probabilities of fatigue and fracture failure modes are higher than the extreme environmental loads. This high probability can be attributed to this fact that the original design of jack-up platform is carried out on the basis of the extreme environmental loads and little attention has been given to the fatigue or fracture failure modes.

### The method:

- The proposed method for the reliability calculations for extreme environmental loads is corresponding to the traditional method when the correlation between axial and bending stresses in the traditional method is accounted for.

- The model for the fatigue crack presented for the fracture reliability calculation includes the interaction of fatigue and fracture. The information derived from the inspection of the structure should be used to update not only the fatigue but also the fracture reliability.
- The advantage of the proposed method for the system reliability calculation is the possibility of incorporating damage due to fatigue or fracture up to the time of calculation for the first, second and higher joint failures.
- Due to the uncertainty in fatigue, fracture and ultimate environmental loads, the reliability approach applied in this research work would be an interesting method to take these uncertainties into account. The specification of the characteristic models of random variables are a challenging aspect and can change the estimated reliability.

#### **The applicability:**

- The method developed for fatigue reliability calculation in the present research is a basis for a tool to monitor the structural safety of a jack-up platform using an improved model of fatigue crack growth based on the actual stress history of jack-up platforms. However, a jack-up platform may be working on many different locations in varying water-depths and environmental conditions, an assessment of the reliability over the life time is more complex.
- The ageing of a jack-up platform is related to the fatigue damage and the safety of a platform can be monitored during the service time by calculating the fatigue reliability. Hence, the inspection of a platform could be scheduled in such a way that the safety is kept higher than the target value (target reliability).

### **6.8 Future developments in the reliability analysis of jack-up platforms**

Following the main conclusions the topics that deserve further investigation concerning the applicability and the method are briefly discussed below.

- The geometry function specified for a jack-up platform is originally established on the Raju and Newman formulation and a correction for the weld discontinuity due to the welding. This model needs more investigation and should be validated with the experimental results derived from the structural elements of jack-up platforms.
- In this research the time history of the structural response is used to determine the probability distribution of the stress range. The frequency response method would be an alternative procedure to calculate the stress distribution but may lead into incorrect results for jack-up platforms due to the non-linearity in the structural response. The new frequency Volterra method, which takes this non-linearity into account, would be an option to be used for stress calculation of jack-up platform.
- Due to the restricted information about the statistical data of the random variables needed for fatigue and fracture reliability analysis of jack-up platforms, the statistical

data of some random variables, e.g. the load calculation and the stress concentration factors, are selected for the example application based on the existing information for jacket platforms. Consideration should be given to the different operational conditions for jack-up platforms related to water-depth, environmental conditions. More investigation is required to validate this type of information for jack-up platforms and statistical information should be attributed to the random variables.

- The calculated failure probability is based on a single directional wave, which is conservative. A better estimation can be obtained by taking the failure probability estimated for other possible direction into account. This case needs more study and further investigation.
- The calculated failure probability in this research work is based on limited number of sea states and hydrodynamic wave load simulations, which involves a statistical uncertainty in the calculations. Incorporating the statistical uncertainty in reliability calculation may lead to more realistic estimation of the failure probabilities. This subject would be interesting for further research work.
- Due to memory restriction a one leg detailed model of the jack-up platform has been used. The fully detailed model of three legs may have some effect on the final results. The investigation of a fully detailed model of three legs model could provide insight in the model uncertainties related to the simplified platform.
- The calculated system failure probability is based on the design storm method (50 years return period). The actual storm encounter during the lifetime of platform may be higher than this return period. More investigation should be carried out to improve the proposed method for the long-term approach.
- The system failure probability is calculated for the fracture and fatigue interaction based on the time-invariant method. The actual problem is time-variant method. The result can be improved by using a more advanced time-variant approach. Further research work on this issue is recommended.

## Nomenclature

### Roman letters:

$a$	Crack depth
$a_0$	Initial crack depth
$a_D$	Detectable crack size
$a(t)$	Crack depth at time $t$
$a_{th}$	Crack depth through the thickness
$c$	Half crack length
$c_0$	Half initial crack length
$da/dN$	Crack growth rate
$f_{by}$	Bending stresses in $y$ direction
$f_{bz}$	Bending stresses in $z$ direction
$f_C$	Axial compression stress
$f_S$	Probability density function of stress range
$g()$	limit state function
$m$	Fatigue crack growth exponent
$t$	Thickness of plate, time
$t_{cr}$	The critical propagation time of a crack
$t_f$	Time to develop a section failure
$t_I$	Time of inspection
$h_x(x)$	Importance sampling density function
$A$	Scale factor of the Weibull distribution
$A_c$	Cracked area
$A_j$	Sectional constants (e.g. area or sectional modulus)
$B$	Shape factor of the Weibull distribution
$C_A$	Fatigue material characteristic in depth
$C_C$	Fatigue material characteristic in length
$E[ ]$	Expectation operator
$E_I$	Event of inspection
$F$	Boundary-correction factor for tension stress
$F_{bn}$	Capacity of the element in the bending stress
$F_{cn}$	Capacity of the element in the axial compression stress
$F_{H_S}(h_S)$	Distribution function of the significant wave height
$F_{T_Z H_S}(t h)$	Distribution function of conditional zero crossing period
$F_{nom,j}$	Nominal sectional forces and moments
$F_{AR}$	Correction of capacity for cracked element
$F_{xc}$	Capacity of the element in the buckling
$H$	Ratio between boundary-correction factors of bending and tension stresses
$H_A$	Ratio between boundary-correction factors of bending and tension stresses for deepest point of a crack (crack depth)
$H_C$	Ratio between boundary-correction factors of bending and tension stresses for end surface point of a crack (crack length)
$H_{ij}$	The component of the second order partial derivation of the limit state function at the design point
$H_S$	Significant wave height



---

$K$	Stress intensity factor
$K_I$	Linear elastic stress intensity factor
$K_{IC}$	Material toughness
$K_{max}$	Maximum stress intensity factor
$K_{min}$	Minimum stress intensity factor
$K_r$	Fracture parameter
$K_{rf}$	Non-dimensional fracture parameter
$L_r$	Plastic collapse parameter
$L_0$	Choleski decomposition of correlation matrix in Normal space
$M_k$	Correction of geometry function for weld toe profile
$N(t)$	Number of stress cycle at time $t$
$P_D$	Probability of crack detection
$P_{D,n}$	Probability of crack detection after $n$ independent inspection
$P_f$	Failure probability
$P_{f,SORM}$	Failure probability calculated with SORM method
$P_i$	The relative occurrence frequency of $i^{\text{th}}$ sea-state
$Q$	Shape factor in Raju and Newman expression
$R$	Correlation matrix in original space
$R_0$	Correlation matrix in Normal space
$R_{act}$	Acting fracture radius
$R_f$	Radius of the fracture failure
$S$	Stress range
$T_{J1}$	Random time of fatigue crack propagation for the first joint
$T_{J2J1}$	Random time of fatigue crack propagation for the second joint after failure of the first joint
$T_{life}$	Design lifetime of platform
$T_r$	Return period
$T_{SS}$	Sea state duration
$T_Z$	Zero-crossing period
$X_{mpme}$	Expected value of the extreme response
$Y$	Geometry function
$Y_A$	Geometry function for deepest point of a crack (crack depth)
$Y_C$	Geometry function for end surface point of a crack (crack length)
$Y_{unwelded}$	geometry function of a semi-elliptical crack using Raju and Newman equation

#### Greek letters:

$\alpha$	Ratio between bending and membrane stresses
$\alpha_i$	Component of unit normal to the failure surface (direction cosine)
$\alpha^*$	Unit normal vector at the design point
$\beta$	Reliability index (based on FORM)
$\beta_{f,SORM}$	Reliability index calculated with SORM approach
$\delta_F$	Model uncertainty in load
$\delta_S$	Model uncertainty in stress
$\delta_{SCF}$	Model uncertainty in stress concentration factor
$\delta_{tf}$	Random correction factor for section failure
$\phi$	Angle that defines the position of point

---

$\phi()$	Standard Normal density function
$\kappa_i$	Main curvature of the limit state at the design point
$\lambda$	Wirsching correction factor
$\lambda_D$	Mean detectable crack size
$\mu_i$	Mean value of random variable $X_i$
$\nu_0$	Expected frequency of zero-crossings of the stress process
$\nu^l$	The long-term average peak-frequency of the stress range
$\nu_p$	Expected frequency of the peaks of the stress process
$\rho_c$	Correction factor to account for the plasticity interaction
$\rho_{0,ij}$	Component of correlation matrix in Normal space
$\rho_{ij}$	Component of correlation matrix in original space
$\sigma_a$	Applied axial stress
$\sigma_{ab,i}$	Applied in-plane bending stress
$\sigma_{ab,o}$	Applied out-of-plane bending stress
$\sigma_{ac}$	Plastic collapse strength in the cracked condition for the axial capacity
$\sigma_b$	Bending stress
$\sigma_{bc,i}$	Plastic collapse strength in the cracked condition for the in-plane bending capacity
$\sigma_{bc,o}$	Plastic collapse strength in the cracked condition for the out-of-plane bending capacity
$\sigma_f$	Flow strength
$\sigma_{hs,i}$	Hot spot stress
$\sigma_i$	Standard deviation of random variable $X_i$
$\sigma_{n,i}$	Nominal stress
$\sigma^P$	Primary stress
$\sigma_{ref}$	Reference stress for plastic collapse consideration
$\sigma^S$	Secondary stress
$\sigma_t$	Tension stress
$\sigma_U$	Ultimate tensile strength
$\sigma_Y$	Yield strength
$\tau$ Service time	Service time of the structure
$\omega_i$	Weighting function of $i^{th}$ sea state
$\psi_L(t)$	Fatigue loading function at time $t$
$\psi_{L,nb}(t)$	Fatigue loading function at time $t$ for narrow-banded stress process
$\psi_R(t)$	Fatigue strength function at time $t$
$\Delta K$	Stress range intensity factor
$\Delta K_A$	Stress range intensity factor for deepest point of a crack (crack depth)
$\Delta K_C$	Stress range intensity factor for end surface point of a crack (crack length)
$\Delta\sigma_{total}$	Total bending and tension stress range
$\Phi()$	Standard Normal distribution
$\Phi_n()$	Standard multi-Normal distribution of degree $n$
$\Gamma()$	Gamma function
$\nabla g(u^*)$	Gradient vector of the limit state at the design point

---

Abbreviation

A-D	Anderson-Darling test
API	American Petroleum Institute
COV	Coefficient Of Variation
DSA	Deterministic Spectrum Amplitude
FEM	Finite Element Method
FOMN	First Order Multi-Normal
FORM	First Order Reliability Method
IF	Influence factor
IPB	In-Plane Bending
IS	Important Sampling
JONSWAP	Joint North Sea Wave Project
K-S	Kolmogorove-Smirnov test
MCS	Monte Carlo Simulation
ML	Maximum Likelihood
NDT	Non-Destructive Test
NDSA	Non-Deterministic Spectrum Amplitude
NOSDA	Nonlinear Offshore Structure Dynamic Analysis program
OPB	Out-of-Plane Bending
P-M	Pearson-Moskowitz
POD	Probability Of Detection
SCF	Stress Concentration Factor
SORM	Second Order Reliability Method
W&L	Wirsching and Light
Z&B	Zhao and Baker

## References

- Aghakouchak A. and Stierner S.F., (2001), "Fatigue reliability assessment of tubular joints of existing offshore structures", *Canadian Journal of Civil Engineering*, Vol. 28, pp.691-698.
- Ambartzumian R., Der Kiureghian, A., Ohanian, V. and Sukiasiana H., (1998), "Multinormal probability by sequential conditioned importance sampling: theory and application", *Probabilistic Engineering Mechanics*, Vol. 13, Issue 4, p.p. 299-308.
- Ament P.C.H., (1998), "Corrosion Fatigue of Structural Steel in Sea Water", *Ph.D. thesis*, Delft University of Technology, ISBN 90-407-1693-5/CIP.
- API RP 2A-LRFD, (1993), "Recommended Practice for Planning, Designing and Constructing Fixed Offshore Platforms – Load and Resistance Factor Design", *First Edition*, American Petroleum Institute, Washington DC, USA.
- Au S.K. and Beck J.L., (1999), "A new adaptive importance sampling scheme for reliability calculation", *Structural Safety*, Vol. 21, p.p. 135-158.
- Baker, M.J., Kountouris I.S. and Ohmart R.D., (1988), "Weld Defects in an Offshore Structure – A Detailed Study", *Proceeding of the 5th International conference on BOSS*, Trondheim, Norway.
- Batistia R.C., Roitman N., and Magluta C. (1986), "Damping factors estimates for a jack-up platform obtained from a hydroelastic reduced model", *Fifth International Symposium on Offshore Engineering*, Brazil, pp.769-784..
- Bennett, W.T., (1994), "Site Specific Assessment of Mobile Jack-up Units", Technical and Research Bulletin 5-5A, *Society of Naval Architects and Marine Engineers*, Jersey City, NJ.
- Bokalrud T. and Karlsen A., (1982), "Control of Fatigue Failure in Ship Hulls by Ultrasonic Inspection", *Norwegian Maritime Research*, Vol. 10, No. 1, p.p. 9-15.
- Boole, G., (1854), "Laws of thought", American Reprint of 1854 ed., *Dover*, New York.
- Breitung, K., (1984), "Asymptotic Approximations for Multinormal Integrals", *Journal of Engineering Mechanics*, ASCE, Vol. 110, No. 3, p.p. 357-366.
- BS7910, (1999), "Guidance on Methods for Assessing the Acceptability of Flaws in fusion Welded Structures", *British Standard Institute*, BSI, Draft.
- Bucher C.G. and Bourgund U., (1990), "A Fast and Efficient Response Surface Approach for Structural Reliability Problems", *Structural Safety*, Vol. 7, p.p. 57-66.
- Bury K.V., (1975), "Statistical Models in Applied Science", *John Wiley*, ISBN 0-471-12590-3, New York.
- Cassidy, M.J., (1999), "Non-linear Analysis of Jack-up Structures Subjected to Random Waves", *Ph.D. thesis*, ASCE, Vol.93, p.p. 171-200.
- Chakrabarti. S. K., (1987), "Hydrodynamics of Offshore Structures", *Computational Mechanics Publications*, Springer-Verlag, ISBN 0-905451-66-X.

- Collins, J.A., (1993), “ Failure of Materials in Mechanical Design: Analysis, Prediction, Prevention”, *Johan Wiley & Sons*, ISBN 0-471-55891-5, New York.
- Cornell, C.A., (1967), “ Bound on the reliability of structural system”, *Journal of Structural Div.*, ASCE, Vol.93, p.p. 171-200.
- Cortie M.B and Garrett G.G., (1988), “ On the Correlation Between the C and m in the Paris Equation for Fatigue Crack Propagation”, *Engineering Fracture Mechanics*, Vol.30, No.1, pp.49-58.
- Daghigh M. and Shabakhty N., (2003), “ A Modified Moment Method for Structural Reliability”, *Proceeding of 14th European Conference on Safety and Reliability*, ESREL2003, Vol.1, p. p. 465-470.
- Daghigh, M., Hengst, S., Vrouwenvelder, A. and Boonstra H., (1997), “System reliability analysis of jack-up structures under extreme environmental conditions”, *Proceeding of the Behaviour of Offshore Structure*, BOSS97, p.p. 127-143.
- Daghigh, M., (1997), “Structural System Reliability Analysis of Jack-up Platforms under Extreme Environmental Conditions”, *Ph.D. thesis*, Delft University of Technology, ISBN 90-370-015-6.
- Dalane J.I. (1993), “System Reliability in Design and Maintenance of Fixed Offshore Structures”, *Ph.D. Thesis*, Department of Marine Structures, The Norwegian Institute of Technology, Trondheim, Norway
- Das P.K. and Zheng Y., (2000), “Cumulative formation of response surface and its use in reliability analysis”, *Probabilistic Engineering Mechanics*, Vol. 15, p.p. 309-315.
- Der Kiureghian A., (2004), “First- and Second-Order Reliability Methods”, To be published as a chapter in *Engineering Reliability Handbooks*, E. Nikolaidis and D. Ghiocel, Editors, CRC Press.
- Der Kiureghian A., Lin H.Z. and Hwang S.J., (1987), “Second-Order Reliability approximations”, *Journal of Structural Mechanics*, Vol.113, No.8, pp.1208-1225.
- Der Kiureghian A. and Liu P.L, (1986), “Structural Reliability under Incomplete Probability Information”, ASCE, *Journal of Engineering Mechanics*, Vol. 112, No. 1, pp.85-104.
- Det Norske Vertias, (2002), “Fatigue Strength Analysis of Offshore Steel Structures”, *Recommended Practice RP-C203*, October, Hovik, Norway.
- Det Norske Vertias, (2000), “Environmental Conditions and Environmental Loads”, *Classification Notes No. 30.5*, March, Hovik, Norway.
- Det Norske Vertias, (1992), “Strength Analysis of Main Structures of Self-Elevating Units”, *Classification Notes No. 31.5*, February, Hovik, Norway.
- Det Norske Vertias, (1992), “Structural Reliability Analysis of Marine Structures”, *Classification Notes No. 30.6*, July, Hovik, Norway.
- Det Norske Vertias, (1984), “Fatigue Strength Analysis for Mobile Offshore Units”, *Classification Notes No. 30.2*, August, Hovik, Norway.
- Dijkstra O.D., Van Manen S.E. and Gijsbers F.B.J., (1994), “Probabilistic maintenance planning for the tubular joints in the steel gates in the Eastern Scheldt storm surge barrier”, *International Journal*

of TNO Building and Construction Research and the School for Advanced Studies in Construction in The Netherlands (HERON), Vol. 39, No.2, p.p. 35-63.

Ditlevsen O. and Madsen H.O., (1996), “ Structural Reliability Methods”, *John Wiley and Sons Ltd.*, ISBN 0471960861, England.

Ditlevsen O. and Madsen H.O., (1981), “ Uncertainty Modeling with Application to Multidimensional Civil Engineering System”, *MacGraw-Hill Inc.*, ISBN 0-07-017046-0.

Ditlevsen O., (1979), “ Narrow reliability bounds for structural systems”, *Journal of Structural Mechanics*, Vol.7, No.4, p.p. 453-472.

Downing S.D. and Socie D.F. (1982), “Simple Rainflow Counting Algorithm”, *International Journal of Fatigue*, Vol.4, pp. 31-40.

Efthymiou M., (1988), “Development of SCF formula and generalized influence functions for use in fatigue analysis”, *Offshore Tubular Joint Conference (OTJ 88)*, Surrey, UK

Engelund S. and Rackwitz, R. (1993), “ A benchmark Study on Importance Sampling Techniques in Structural Reliability”, *Structural Safety*, Vol. 12, No.4, p.p.255-276.

Etube L.S., (2001), “ Fatigue and Fracture Mechanics of Offshore Structures”, *St. Edmundsbury Press Limited*, Suffolk, UK, ISBN 1-86058-312-1.

Faber M.H., Sorensen, J.D., Rackwitz, R., Thoft-Christensen P. and Bryla P. (1992), “ Reliability Analysis of An Offshore Structures: A Case Study”, *Proceedings of the 11th International Conference on Offshore Mechanics and Arctic Engineering (OMAE)*, Calgary, Canada, June.

Farnes, K. A. and Moan T., (1994), “Extreme dynamic, nonlinear response of fixed platforms using a complete long-term approach”, *Applied Ocean Research*, No. 15, pp. 317-326.

Farnes, K.A. (1990), “ Long-term Statistics of Response in Non-linear Marine Structures”, *Proceedings of the 11th International Conference on OMAE*, Calgary, Canada, June.

Guan X.L. and Melchers R.E., (2001), “ Effect of response surface parameter variation on structural reliability estimates”, *Structural Safety*, Vol. 23, No.2, p.p.429-444.

Gollwitzer S. and Rackwitz R., (1983), “Equivalent Components in First-Order System Reliability”, *Reliability Engineering*, Vol. 5, p.p. 99-115.

Grigoriu M., (1993), “On the spectral representation method in simulation”, *Probabilistic Engineering Mechanics*, Vol. 8, NO.2, p.p. 75-90.

Grundlehner G.J., (1995), “ Systematic Model Tests on a Harsh Environment Jack-up in Elevated Condition”, *Proceeding of 5th International Jack-up Conference*, London, UK.

Guenard, Y.F., (1984), “ Application of System Reliability Analysis to Offshore structures”, Report No. RMS-1, Department of Civil Engineering, Stanford University.

Gumbel E.J., (1958), “Statistics of Extremes”, *Columbia University Press*, New York, USA.

- Hambly E.C, Imm G.R. and Stahl B., (1990), "Jack-up Performance and Foundation Fixity under Developing Storm Conditions", *Proceeding of Offshore Technology conference, (OTC 6466)*, May 7-10, Houston, Texas, USA.
- Hanna, S.Y. and Karsan, D.I., (1989), "Fatigue modeling for reliability based inspection and repair of welded tubular offshore structure", *8th International Conference on Offshore Mechanics and Arctic Engineering*, The Hague, Netherlands, p.p. 657-666.
- Harland L.A., Vugts J.H., Jonathan P. and Taylor P.H., (1996), "Extreme Responses of Non-Linear Dynamic System Using Constrained Simulations", *Proceeding of 15th Offshore Mechanics and Arctic Engineering Conference*, Florence, Italy.
- Hasofer A.M. and Lind N.C., (1974), "Exact and Invariant Second-Moment code format", *Journal of Engineering Mechanics*, Vol. 100, Issue 1, p.p.111-121.
- Hasselmann K., Barnett T.P., Bouws E., Carlson H., Cartwright D.E., Enke K., Ewing J.A., Gienapp H., Hasselmann D.E., Kruseman P., Meerburgh A., Muller P., Olbers D.J., Richter K., Sell W. and Walden H., (1973), "Measurements of wind-wave growth and swell decay during the Joint North Sea Wave Project (JONSWAP)", *Deutsches Hydrographisches Zeitschrift Reihe*, Suppl. A12, p.p. 1-95.
- Hasofer A.M. and Lind N., (1974), "An Exact and Invariant First-Order Reliability Format", *Journal of Engineering Mechanics Division*, ASCE, Vol. 100, EM1, p.p. 111-121.
- Hohenbichler, M. and Rackwitz, R., (1988), "Improvement of Second-order Reliability Estimates by Importance Sampling", *Journal of Engineering Mechanics*, ASCE, Vol.114, No.12, pp. 2195-2199.
- Hohenbichler M. and Rackwitz R., (1983), "First-Order concepts in System Reliability", *Structural Safety*, Vol. 1, Issue 3, p.p.177-188.
- Hohenbichler M. and Rackwitz R., (1981), "Non-normal dependent vectors in structural safety", *Journal of Engineering Mechanics Division*, ASCE, Vol. 107, EM6, p.p. 1227-1238.
- Hovde, G.O., (1995), "Fatigue and overload reliability of offshore structural systems, considering the effect of inspection and repair", *Ph.D. thesis*, Department of Marine Structures, The Norwegian institute of Technology, Trondheim, Norway, May.
- Hunter, D., (1976), "An upper bound for the probability of a union, with applications", *Journal of Appl. Probab.*, Vol. 13, p.p. 597-603.
- Ibrahim, Y., (1991), "Observations on Application of Importance Sampling in Structural Reliability Analysis", *Structural Safety*, Vol. 9, No.4, p.p.269-281.
- Jensen J.J., (1990), "Fatigue Damage due to Non-Gaussian Response", *Journal of Engineering Mechanics*, Vol.116, No.1, pp. 240-245.
- Jensen J.J., Mansour A.E. and Pedersen T., (1991), "Reliability of Jack-up Platforms against Overturning", *Marine Structures*, Vol. 4, p.p. 203-229.
- JCSS, (2004), "JCSS Probabilistic Model Code Part 3: Resistance Models, Draft", *The Joint Committee on Structural Safety (JCSS)*, April.

- Karadeniz, H., Van Manen S. and Vrouwenvelder A., (1983), "Probabilistic Reliability Analysis for the Fatigue Limit State Analysis of Gravity and Jacket Type Structures", *Journal of Structural Engineering*, Vol. 118, No.3, p.p. 684-700.
- Karamchandani, A.K., Dalane J.I., and Bjerager P., (1992), "A System Reliability Approach to Fatigue of Structures", *Journal of Structural Engineering*, Vol. 118, No.3, p.p. 684-700.
- Karamchandani, A., (1987), "Structural System Reliability Analysis Methods", *Report No.83*, John Blume Earthquake Engineering Center, Stanford University, California, U.S.A.
- Karlsen A., (1986), "Stress intensity factors for tubular joint fatigue life prediction", *DnV report* 86-1981 and 86-1211.
- Karunakaran, D., (1993), "Nonlinear dynamic response and reliability analysis of drag-dominated offshore platforms", *Ph.D. thesis*, Department of Marine Structures, The Norwegian institute of Technology, Trondheim, Norway, November.
- Karunakaran, D. and Spidsoe N., (1995), "Verification of Methods for Simulation of Nonlinear Dynamic Response of Jack-up Platforms", *Proceeding of 5th International Jack-up Conference*, London, UK.
- Kim S.H. and Na S.W., (1997), "Response surface method using vector projected sampling points", *Structural Safety*, Vol. 19, No.1, p.p. 3-19.
- Kirkemo, F. (1988), "Application of probabilistic fracture mechanics to offshore structures", *Applied Mechanic Review*, ASME Vol. 41, No.2, pp. 61-84.
- Kjeoy H., Boe N.G. and Hysing T., (1989), "Extreme-response of jack-up platforms", *Journal of Marine Structures*, Vol.2, p.p. 305-334.
- Kountoris I.S. and Baker M.J., (1989), "Defect Assessment – Analysis of defects detected by MPI in an offshore structure", *CESLIC Report No. OR6*, Dept. of Civil Engineering, Imperial college, London, UK.
- Koyluoglu HU and Nielsen S.R.K., (1994), "New approximation for SORM integrals", *Structural Safety*, Vol.13, No. 4, p.p. 235-246.
- Kuang J.G., Potvin A.B. and Leick R.D., (1975), "Stress concentration in tubular joints", *OTC 2205*, Houston, Texas, USA.
- Lee J.S., Karkovski .B. and Yakubovich A.N., (1993), "Investigation of Response Surface for Reliability Analysis of Structural System", *Offshore Mechanics and Arctic Engineering*, Volume II, p.p. 323-325.
- Liu P.L. and Der Kiureghian A., (1991), "Optimization Algorithms for Structural Reliability", *Structural Safety*, Vol. 9, p.p. 161-177.
- Liu P., and Massie. W.W., (1988), "NOSDA – Nonlinear Dynamic Analysis Program for Offshore Structures", *Research Report*, Faculty of Civil Engineering, Workgroup Offshore Technology, Delft University of Technology, December.
- Loseth R. and Bjerager P., (1989), "Reliability of Offshore Structures with Uncertain Properties under Multiple Load Process", *Proceedings of the 21st Annual OTC*, Paper No.5969, Houston, USA



- Madsen H.O., (1997), "Stochastic Modeling of Fatigue Crack Growth and Inspection", *Probabilistic methods for structural design*, Edited by C. Guedes Soares, Kluwer Academic Publishers, ISBN 0-7923-4670-X.
- Madsen, H.O., (1989), " Stochastic modeling of fatigue crack growth ", *In lecture notes for ISPRA Course: Structural Reliability, ISPRA course*, November 13-17, Lisboa.
- Madsen H.O., Krenk S. and Lind N.C. (1986), "Method of Structural Safety", *Prentice-Hall*, Inc. Englewood Cliffs, New Jersey, ISBN 0-13-579475-7.
- Mahadevan S. and Raghothamachar P., (2000), " Adaptive simulation for system reliability analysis of large structures", *Computer and Structures*, Vol.77, Issue 6, p.p. 725-734.
- Marex (Marine Exploration Limited), (1979), " Hutton Area, main study report and addendum", *Marex House*, UK.
- Marley M.J., (1991), "Time Variant Reliability under Fatigue Degradation", *Ph.D. Thesis*, Department of Marine Structures, The Norwegian Institute of Technology, Trondheim, Norway
- Mebarki A. and Sellier A., (1995), "Importance zone and importance sampling in reliability analysis of civil structures", *International journal of Pressure vessels and Piping*, Vol.61, p.p.513-526.
- Melchers R. M., (1999), "Structural Reliability Analysis and Prediction ", *John Wiley and Sons Ltd.*, ISBN 0471983241, England.
- Melchers, R.E., (1991), "Simulation in time-invariant and time-variant reliability problems", *Proc. 4th IFIP Conference on Reliability and Optimization of Structural System*, Rackwitz, R. and Thoft-Christensen P. (Eds), Springer, Berlin, p.p.39-82.
- Melchers, R.E., (1990), " Search-base Importance Sampling ", *Structural Safety*, Vol. 9, No.2, p.p.117-128.
- Melchers, R.E., (1989), " Importance Sampling for Structural Reliability", *Structural Safety*, Vol. 6, No.1, p.p.3-10.
- Moan T., Wei Z. and Vardal O.T., (2001), "Initial Crack Depth and POD Data based on Underwater Inspection of Fixed Steel Platforms", *8th International Conference on Structural Safety and Reliability (ICOSSAR2001)*, Newport Beach, California, USA.
- Moan T., Wei Z. and Vardal O.T., (2001), "Initial Crack Depth and POD Data based on Underwater Inspection of Fixed Steel Platforms", *8th International Conference on Structural Safety and Reliability (ICOSSAR2001)*, Newport Beach, California, USA.
- Moan T., and Song R. (1997), "Implication of Inspection Updating on System Fatigue Reliability of Offshore Structures", *Journal of Offshore Mechanics and Arctic Engineering (OMAE)*, August, Vol.122, pp. 173-180.
- Moan T., Hovde G.O. and Blanker A.M. (1993), " Reliability-Based Fatigue Design Criteria for Offshore Structures Considering the Effect of Inspection and Repair", *Proceedings of the 25th Annual Offshore Technology Conference (OTC)*, Paper no. 7189, Houston, USA, May 3-6.

- Morooka C. K. and Yokoo I.H., (1997), "Numerical simulation and spectral analysis of irregular sea waves ", *International Journal of Offshore Mechanics and Arctic Engineering*, Vol.7, No.3, p.p. 189-196.
- Moses, F., (1982), "System reliability developments in structural engineering", *Structural Safety*, Vol.1, Issue 1, p.p.3-13.
- Muhammed A., Pisarski H.G. and Stacey A., (2000), "Using Wide Plate Test Results to Improve Predictions from Probabilistic Fracture Mechanics", *Proceeding of 13th European Conference on Fracture*, ECF 13, 6-9 September 2000, San Sebastian, Spain.
- Naess A., (1985), "Fatigue Handbook for Offshore Steel Structures", *Tapir Publishers*, Trondheim, Norway.
- Nie J. and Ellingwood B.R., (2000), "Directional methods for structural reliability analysis", *Structural Safety*, Vol.22, p.p.233-249.
- NORSOK (1998), "Design of Steel Structures", *Norwegian Technology Standards Institution*, Rev.1, N-004, December, Oslo, Norway.
- Nowak A. and Collins K.R., (2000), "Reliability of Structures ", *McGraw-Hill Inc.*, ISBN 0070481636, U.S.A.
- Oakely A., Brown M., Warren P.A. and Barltrop N.D.P., (1994), " Optimized Inspection Scheduling for Offshore Structures, A Probabilistic Approach", *The seventh International Conference on the Behavior of Offshore Structures (BOSS 94)*, Vol.3, Structures, pp.101-127.
- O'Dowd, (2001), "Advanced Fracture Mechanics", *Lectures on Fundamentals of Elastic, Elastic-Plastic and Creep Fracture*, Imperial College of Science, Technology and Medicine, Department of Mechanical Engineering.
- Olsson A., Sandberg G., and Dahlblom O., (2003), "On Latin hypercube sampling for structural reliability analysis", *Structural Safety*, Vol. 25,p.p.47-68.
- Onoufriou T., (1999), "Reliability based inspection planning of offshore structures", *Marine Structures*, Vol.12, p.p. 521-539.
- Onoufriou T. and Dixon A., (1996), "Review of jack-up inspection and repair practice", *International Conference on Offshore Mechanics and Arctic Engineering (OMAE 1996)*.
- Pandey, M. D. and Sarkar, A., (2002), "Comparison of a simple approximation for multinormal integration with an importance sampling-based simulation method", *Probabilistic Engineering Mechanics*, Vol. 17, No. 2, p.p. 215-218.
- Pandey M.D., (1998), "An Effective Approximation to Evaluate Multinormal Integrals", *Structural Safety*, Vol. 20, Issue 1, p.p. 51-67.
- Paris P.C., Erdogan, F., (1963), " A Critical analysis of crack propagation laws", *Journal of Basic Engineering*, ASME, Vol.85, pp. 528-534.
- Pierson W.J. and Moskowitz L., (1964), " A proposed spectral form for fully developed wind seas based on the similarity theory of S.A. Kitaigorodskii", *J. Geophys. Res.*, Vol.69, No.24, pp. 5181-90.

- Raju I.S. and Newman J.C., (1986), "Stress Intensity Factor for Circumferential Surface Crack in pipes and rods under bending and tension loads", *Fracture Mechanics*, ASTM, Vol.17, pp.789-805.
- Raju I.S., and Newman J.C., (1981), "An Empirical stress Intensity Factor Equation for the Surface Crack", *Engineering Fracture Mechanics*, Vol.15, pp.185-192.
- Rook D.P., and Cartwright D.J., (1976), "Compendium of stress intensity factors", HMSO. London, U.K.
- Sarkani, S., Michaelov G., Kihl D.P. and Beach J.E., (1996), "Fatigue of welded steel joints under wideband loadings", *Probabilistic Engineering Mechanics*, Vol.11, pp. 221-227.
- Shabakhty, N., Van Gelder, P. and Boonstra, H., (2003), "System Reliability of Jack-up structures based on fatigue degradation", *Proceeding of 14th European Conference on Safety and Reliability, ESREL2003*, Vol.2, p. p. 1437-1446.
- Shabakhty N. and Daghigh M. (2003), "Effect of Soil-Structure Models on Stochastic Response of Jack-up Platforms", *Proceeding of 14th European Conference on Safety and Reliability, ESREL2003*, Vol.2, p. p. 1433-1436.
- Shabakhty N., Van Gelder, P. and Boonstra, H., (2002), "Reliability analysis of Jack-up platform based on fatigue degradation", *Proceeding of the 21st International conference on Offshore Mechanics and Arctic Engineering*, OMAE 2002-28360, June 23-28, Oslo, Norway.
- Shabakhty N., (2001), "Reliability Analysis of Offshore Structure, Deterioration process, Reassessment and Fatigue in Offshore Structure ", *Second progress report on fatigue reliability of jack-up platform*, Faculty of Mechanical Engineering and Marine Technology, Workgroup SOCP, Delft University of Technology, The Netherlands, Dec.
- Shabakhty N., Boonstra H., and Hengst, S., (2001), "Remaining Fatigue Capacity of Jack-up Platforms based on Fatigue reliability analysis", *Proceeding of International Conference on Hydraulic Structure*, Vol. 3, p.p. 3-13, May 2-3, Kerman, Iran.
- Shabakhty N., (2000), "Reliability analysis of offshore structure, Uncertainty, Random variable and Reliability ", *First progress report on fatigue reliability of jack-up platform*, Faculty of Mechanical Engineering and Marine Technology, Workgroup SOCP, Delft University of Technology, The Netherlands, Sep.
- Shang-Xian W., (1985), "Shape change of surface crack during fatigue growth", *Engineering Fracture Mechanics*, Vol. 22, No.5, pp.897-913.
- Sharp J.V., (1992), "Ageing offshore structures: a review of recent UK research", *Offshore Mechanics and Arctic Engineering*, OMAE 1992, V. III-B, Material Engineering, p.p. 391-398
- Shetty, N. and Baker M.J., (1990), "Fatigue Reliability of Tubular Joints in Offshore Structures: Reliability Analysis", *Proceeding of the 9th International Conference on OMAE*, Houston, USA, February.
- Shetty, N., (1992), "System reliability of fixed offshore structures under fatigue deterioration", *Ph.D. thesis*, Department of Civil Engineering, Imperial College of Science, Technology and Medicine, London, April.
- Siddiqui, N.A. and Ahmad S., (2001), "Fatigue and fracture reliability of TLP tethers under random loading", *Marine structures*, No. 14, p.p. 331-352.

- Sih G.C. (1973), "Handbook of stress-intensity factors for researchers and engineers", *Lehigh University*, Institute of Fracture and Solid Mechanics, Bethlehem.
- Smith, I.J. and Hurworth, S.J., (1984), "The effect of geometry changes upon the predicted fatigue strength of welded joints", *Res. Report No. 244*, Welding Inst, Cambridge, England.
- Snijder H.H., Gijbbers, F.B., Dijkstra, O.D. and ter Avest, F.J., (1987), "Probabilistic Fracture Mechanics Approach of Fatigue and Brittle Fracture in Tubular Joints", *Proceeding of Steel in Marine Structures*, No. TS56, Delft, The Netherlands, June.
- Sobczyk K., and Spencer, Jr. B.F., (1992), "Random Fatigue: From Data to Theory", *Academic press Inc.*, ISBN 0-12-654225-2
- Solin, J., (1990), "Analysis of spectrum fatigue tests in sea water", *Proceeding of the 10th International Conference on Offshore Mechanics and Arctic Engineering (OMAE)*, Vol.2
- Sobczyk K. and Spencer B.F.J. (1992) "Random Fatigue, From Data to Theory", *Academic press*, ISBN 0-12-654225-2.
- Song J. and Der Kiureghian A., (2003), "Bounds on System Reliability by Linear Programming", *Journal of Engineering Mechanics*, Vol.129, No.6, p.p.627-636.
- STRUREL, (1997), "A Structural Reliability Analysis Program", Munchen, Germany.
- Tada H., Paris P.C. and Irwin G.R., (2000), "The stress analysis of cracks handbook", New York. ASME, ISBN 0-86058-304-0
- Tada R. et al, (1973), "The stress analysis of cracks handbook", *Dell Research Corporation*, Hellertown, Pennsylvania.
- Tanaka S., Ichikawa M. and Akita S., (1981), "Variability of  $m$  and  $C$  in the Crack Propagation Law  $da/dN=C(\Delta K)^m$ ", *International Journal of Fracture*, Vol. 17, pages 121-124.
- Tang L.K. and Melchers R.E., (1987), "Improved Approximation for Multinormal Integral", *Structural Safety*, Vol.4, Issue 4, p.p.81-93.
- Taylor P.H., Jonathan P. and Harland L.A., (1997), "Time Domain Simulation of Jack-up Dynamics with the Extreme of a Gaussian Process", *Journal of Vibration and Acoustics*, Vol. 119, p.p.624-628.
- Thoft-Christensen, P. and Murotsu Y., (1986), "Application of structural system reliability theory", ISBN 3-540-16362-X, Spring-Verlag, Berlin.
- Thoft-Christensen and Baker M.J., (1982), "Structural Reliability Theory and its applications", *Springer-Verlag, Berlin*, Heidelberg, ISBN 3-540-11731-8.
- Tichy M., (1994), "First-order third moment reliability method", *Structural Safety*, Vol. 16, p.p.189-200.
- Torhaug R., (1996), "Extreme Response of Nonlinear Ocean Structures: Identification of Minima Stochastic Wave Input for Time-domain Simulation", *Ph.D. thesis*, Stanford University, USA.
- Tromans P.S., Hagemeyer P. and Wassink H.R. (1992), "The statistics of the extreme response of offshore structures", *Ocean Engineering*, Vol.19, No.2, pp.161-181.

- Tromans P.S., Anaturk A., and Hagemeyer P., (1991), "A New Model for the Kinematics of Large Ocean Waves-Application as a Design Wave", *Proc. 1st Offshore and Polar Engineering (ISOPE) Conference*, Edinburgh, Vol.3, pp. 64-71.
- Tvedt, L., (1983), "Two Second-Order Approximations to the Failure Probability", *Veritas Report RDIV/20-004-83*, Det Norske Veritas, Oslo, Norway.
- Van de Graaf J.W., Tromans P.S., Vanderschuren L. and Jukui B.H., (1993), "Failure Probability of Jack-up under Environmental Loading in the central North Sea", *4th International conference on The Jack-up Platform, Design, Construction and Operation*, Edited by Boswell L.F. and D'Mello C., The City University London, 21-22 September.
- Videiro P.M., and Moan T. (1999), "Reliability Based Design of Marine Structures", *Proceeding of OMAE*, 11-16 July, St.John's, Newfoundland, Canada.
- Virkler D.A., Hillberry B.M. and Goel P.K., (1979), "The statistical nature of fatigue crack propagation", *Journal of Engineering Materials and Technology*, Trans. ASME, Vol. 101 No.2.
- Vrouwenvelder, A., (2004), "Spatial correlation aspects in deterioration models", *The second International Conference on Lifetime Oriented Design Concepts*, March 1-3, Bochum, Germany.
- Vrouwenvelder, A., Edwards G., Kerstens J. and Heidweiller A., (1985), "Ultimate Limit State Reliability Analysis for Offshore Structures", *Report Institute TNO for Building Materials and Building Structures*, No. B-84-563/62.6.0402, Delft, The Netherlands.
- Waarts, P.H. and Vrouwenvelder, A., (1998), "The use of directional sampling in structural reliability", *The Eighth IFIP WG 7.5 Conference on reliability and optimization of structural systems*, Krakow, Poland.
- Wheeler J.D., (1970), "Methods for Calculating Forces Produced on Piles in Irregular Waves", *Journal of Petroleum Technology*, March.
- Wirsching P.A., Paez T. L., and Ortiz K. (1995), "Random Vibration, Theory and Practice", ISBN 0-471-58579-3, John Wiley & sons, New York, NY.
- Wirsching P.H. and Light, M.C., (1980), "Fatigue under wide-band random stresses", *Journal of the structural Div.*, ASCE, Vol. 106, p.p.1593-1607.
- Winterstein S.R., Ude T.C., Cornell C.A., Bjerager P. and Haver S., (1993), "Environmental Parameters for Extreme Response: Inverse FORM with Omission Factors", *Proceeding of ICOSSAR 93*, August, Innsbruck, Austria.
- Winterstein S.R., (1988), "Nonlinear Vibration Models For Extremes and Fatigue", *Journal of Engineering Mechanics*, Vol.114, No.10, pp.1772-1790.
- Wordsworth A.C. and Smedley G.P., (1978), "Stress concentrations at unstiffened tubular joints", *European Offshore Steels Research Seminar*, November.
- Zhao Y.G. and Ono T., (2001), "Moment methods for structural reliability", *Structural Safety*, Vol. 16, p.p.189-200.
- Zhao W. and Baker J., (1990), "A new stress-range distribution for fatigue analysis under wave loading", *Environmental Forces on Offshore Structures and their Predictions*, Vol.26, pp.271-291.

## Appendix A Geometry function

### A.1 Raju and Newman geometry function

In fatigue and fracture limit states, the geometry function has to be specified. This function plays an important role in fatigue and fracture because it takes into account the crack geometry and the mode of loading. Raju and Newman (1981) derived an expression for the geometry function  $Y_\phi$  for a surface crack in a finite plate exposed to a remote tension and bending loads. Later, they demonstrated that the difference in the geometry function between semi-elliptical cracks in a plate and a pipe with a low thickness to diameter ratio is small (Raju and Newman, 1986). In the investigation of Karlsen (1986) a good agreement is observed between the numerical results of a finite element calculation K and T joints and the Raju-Newman's expression with correction factors to assume the local stress concentration introduced at the weld toe.

The geometry function of the Raju and Newman method has been fitted on the finite element results for two types of remote tension and bending loads applied to a surface crack. The inferred geometry function from this research is given by

$$Y_\phi = (1/Q)^{1/2} \frac{1 + H\sigma_b/\sigma_t}{1 + \sigma_b/\sigma_t} F\left(\frac{a}{t}, \frac{a}{c}, \frac{c}{b}, \phi\right) \quad (\text{A.1})$$

where  $\sigma_t$  and  $\sigma_b$  are the remote uniform tension and bending stresses respectively.  $\sigma_b/\sigma_t$  shows the ratio between bending and tension stresses.  $a$  is the crack depth,  $c$  is the half the crack length,  $t$  is the thickness of the plate,  $b$  is the half width of the panel and  $\phi$  is the angle that defines the position of the point considered in the crack front, see figure 2.3.  $Q$  is the shape factor;  $F$  and  $H$  define the boundary-correction factor. According to this method, the shape factor  $Q$  for an ellipse is given by the square of the complete elliptic integral of the second kind and is approximated by the following expression.

$$Q = 1.0 + 1.464 \left(\frac{a}{c}\right)^{1.65} ; \frac{a}{c} \leq 1 \quad (\text{A.2})$$

The boundary-correction factor for tension  $F$  is given by the following expression,

$$F = \left[ M_1 + M_2 \left(\frac{a}{t}\right)^2 + M_3 \left(\frac{a}{t}\right)^4 \right] f(\phi) g(\phi) f_w \quad (\text{A.3})$$

where

$$M_1 = 1.13 - 0.09 \left(\frac{a}{c}\right), M_2 = -0.54 + \frac{0.89}{0.2 + (a/c)}, M_3 = 0.50 + 14.0 \left(1 - \frac{a}{c}\right)^{24} - \frac{1}{0.65 + (a/c)}$$

$$f(\phi) = \left[ \left(\frac{a}{c}\right)^2 \cos^2(\phi) + \sin^2(\phi) \right]^{0.25} \quad g(\phi) = 1 = \left[ 0.1 + 0.35 \left(\frac{a}{t}\right)^2 \right] (1 - \sin \phi)^2 \quad (\text{A.4})$$

$f_w$  is the finite-width correction factor which is calculated from the following expression,

$$f_w = \left[ \sec \left( \frac{\pi c}{2b} \sqrt{a/t} \right) \right]^{1/2} \quad c/b \leq 0.5 \quad (\text{A.5})$$

The boundary-correction factor for bending is given by multiplying the  $F$  function with the new term  $H$ , which is specified according to the following expression,

$$H = H_1 + (H_2 - H_1) \sin^p(\phi) \quad (\text{A.6})$$

where

$$p = 0.2 + \left( \frac{a}{c} \right) + 0.6 \left( \frac{a}{t} \right)$$

$$H_1 = 1 - 0.34 \left( \frac{a}{t} \right) - 0.11 \left( \frac{a}{c} \right) \left( \frac{a}{t} \right), \quad H_2 = 1 + G_1 \left( \frac{a}{t} \right) + G_2 \left( \frac{a}{t} \right)^2$$

$$G_1 = -1.22 - 0.12 \left( \frac{a}{c} \right), \quad G_2 = 0.55 - 1.05 \left( \frac{a}{c} \right)^{0.75} + 0.47 \left( \frac{a}{c} \right)^{1.5}$$

In a welded joint a correction term for the local stress intensity magnification factor should be applied. This correction appears from nonlinearity in stress arising from local stress concentrations at the weld toe. Smith and Hurworth (1984) recommended the following expression to take this nonlinearity into account,

$$M_k(a) = 1 + M_{red}(\rho, \theta) \left[ 1.24 \exp \left( \frac{-22.1a}{t} \right) - 3.17 \exp \left( \frac{-357a}{t} \right) \right] \quad (\text{A.7})$$

where  $M_{red}$  is introduced in order to include effects of local weld toe smoothing by for example grinding. Furthermore,  $\rho$  and  $\theta$  are the weld toe radius and angle respectively. By multiplying this correction into the Raju and Newman geometry function, the final geometry function for tubular elements can be specified.

## A.2 Geometry function according to method of Moan et al. (1993)

Due to coalescence of cracks, Moan et al. (1993) recommend to use two different stages one stage before and the other one during and after coalescence. They also explain that the two-dimensional crack growth model proposed by Raju and Newman may give a wrong aspect ratio evolution due to the coalescence of the crack. The crack aspect ratio ( $a/c$ ) before coalescence is given with the following expression,

$$\frac{a}{c} = \exp(-ka) \quad ; \quad \text{for } \frac{a}{t} \leq \left( \frac{a}{t} \right)_{\text{coalescence}} \quad (\text{A.8})$$

where  $k$  has a minimum value of 0.2, which corresponds to the low stress level where only a few crack initiation points are present with a great intermediate distance. The  $k$  can be calculated with the following formulation.

$$k = K_{ref} \left( \frac{S_b}{S_{ref}} \right) \sqrt{\frac{t}{t_{ref}}} \geq 0.2 \quad (\text{A.9})$$

The reference values are given as  $K_{ref} = 0.2 \text{ mm}^{-1}$ ,  $S_{ref} = 116.0 \text{ N/mm}^2$  and  $t_{ref} = 26.0 \text{ mm}$ . The crack aspect ratio during and after coalescence is given with the following relationship,

$$\frac{a}{c} = \frac{1}{\eta_1 \left( \frac{a}{t} - \left( \frac{a}{t} \right)_{\text{coal}} \right) + 1} + \frac{\alpha - 1}{\alpha + 1} \left( \frac{a}{t} - 1 \right) \eta_2 + \left( \frac{a}{c} \right)_{\text{failure}} ; \text{ for } \frac{a}{t} > \left( \frac{a}{t} \right)_{\text{coalescence}} \quad (\text{A.10})$$

where  $\eta_1$  and  $\eta_2$  are parameters that specify the crack aspect ratio during and after coalescence, and are assumed to be 150 and 0.15 respectively as specified in Moan et al.(1993). Furthermore,  $(a/t)_{\text{coal}}$  and  $(a/c)_{\text{failure}}$  are the crack shape and crack aspect ratio at the coalescence and through-thickness of an element, which are considered to be 0.05 and 0.1 respectively as given in Moan et al.(1993). By substituting this aspect ratio in the Raju and Newman formulations, the geometry function can be derived for tubular elements.

### A.3 Geometry function according to the proposed method in this research

In this research a two-dimensional crack growth formulation of Raju and Newman is applied to specify the geometry function for tubular elements with the modification of the bending to membrane stress ratio for each hot spot and the correction of the weld toe profile recommended by Smith and Hurworth (1984).

If formulation 2.6 is rewritten in accordance with the multiplication of the geometry function and the stress range, the following expression, which is independent of the load history and only depends on the crack shape, can be derived,

$$\frac{dc}{da} = \frac{C_C}{C_A} \left( \frac{\Delta K_C}{\Delta K_A} \right)^m = \frac{1}{1.1^m} \left( \frac{Y_C \sqrt{c}}{Y_A \sqrt{a}} \right) = \frac{1}{1.1^m} \left( \frac{1 + H_C \alpha}{1 + H_A \alpha} \right) \frac{F\left(\frac{a}{t}, \frac{a}{c}, 0, 0\right)}{F\left(\frac{a}{t}, \frac{a}{c}, 0, 90\right)} = g\left(\frac{a}{t}, \frac{a}{c}, \alpha\right) \quad (\text{A.11})$$

Where  $Y_A$  and  $Y_C$  are the geometry function for the deepest point  $A$  ( $\phi = \pi/2$ ) and the end surface point  $C$  ( $\phi = 0$ ) respectively as shown in figure 2.3. It should be kept in mind that only the bending to membrane stress ratio ( $\alpha = \sigma_b / \sigma_t$ ) from the stress history remains in this expression; therefore, by using this formulation a relation between the crack propagation in depth and in circumference direction for a specific  $\alpha$  can numerically be generated. Starting from the initial small crack size  $(a/t)_0$  with the initial crack aspect ratio  $(a/c)_i = 0.1$  the new crack length is calculated according to the formulation A.11 and the finite difference approach. Therefore the crack length in each iteration  $(c_n/t)$  can be estimated from the last iteration  $(c_{n-1}/t)$  in accordance with the following expression,

$$\frac{dc}{da} \approx \frac{\Delta c}{\Delta a} = \frac{c_n - c_{n-1}}{a_n - a_{n-1}} , \quad \frac{c_n}{t} = \frac{c_{n-1}}{t} + \left( \frac{a_n}{t} - \frac{a_{n-1}}{t} \right) g\left(\frac{a_{n-1}}{t}, \frac{a_{n-1}}{c_{n-1}}, \alpha\right) \quad (\text{A.12})$$

By substituting the calculated crack shape for the specific  $\alpha$  ratio in each iteration in the expressions A.1 for two cases of  $\phi = \pi/2$  and  $\phi = 0$ , the geometry function  $Y_A$  and  $Y_C$  can be numerically specified for the whole fatigue crack propagation model. However, it should not be forgotten to apply the correction of the weld toe profile recommended by Smith and Hurhworth (1984) for tubular elements. In the fatigue and fracture reliability calculations, the proposed method for the geometry function is carried out in the attached subroutine to the original reliability calculation program for each iteration process.



## Appendix B Description of jack-up platform

### B.1 Structural description

The platform under investigation is the three legged type with the derrick cantilevered over the side. Figure B.1 shows an overview of the platform in the site. The original technical specification of the Neka jack-up platform has been ordered by *Rauma-Repola* offshore company (Finland) and the platform is constructed in cooperation with the Iran Marine Industry Co. (SADRA). Friede and Goldman is the designer of this type of platform and the characteristics of the platform are specified in accordance with the second model of the class L-780 to operate in water depths of 95 meter in harsh environments. The weight of hull is 80820 kN. The platform dimensions, length and width are 54.86 and 53.34 m respectively. The hull depth is 7.62 m and the hull draft (structural load line) is 4.57 m. The height of the double bottom is 1.524 m. The lattice legs have been designed from the frame structure with three tubular chords in each corner.



**Figure B.1:** An overview of Neka (Iran Khazar) jack-up platform in the site

The height of the double bottom is 1.524 m. The lattice legs have been designed from the frame structure with three tubular chords in each corner.

**Table B.1:** Characteristics of Neka jack-up platform

Characteristic	Dimensions
Leg design length	125 m
Distance between leg guides	14.3 m
Centre to centre of forward and aft legs	31.177 m
Centre to centre of aft legs	36.0 m
Bay height (legs)	6.0 m
Side length of the triangular truss leg	9.9 m

The chords provided with two gear racks on each side and are interconnected by horizontal and diagonal tubular bracings. The main leg characteristics are given in table B.1 and B2. Each bay of leg has 3 chord elements, 6 horizontal braces, 6 diagonal braces and 3 internal span breakers, i.e. in total 18 elements. Table B.2 gives the structural details of each bay.

**Table B.2:** Structural details of lattice leg

Element type No.	Specification	Diameter $\times$ thickness (mm $\times$ mm)	Length (m)
1	Chord element	800 $\times$ 50	6.0
2	Horizontal braces	400 $\times$ 28	4.95
3	Diagonal braces	360 $\times$ 28	7.78
4	Internal span breakers	200 $\times$ 12	4.95

The leg-hull interface of the jack-up model is provided with a fixation system consisting of a clamping mechanism and in this case the linear spring model is considered to represent the leg-hull connection. Figure B.2 shows the leg-deck configuration applied for the jacking system of Neka jack-up platform for two cases of floating and clamping system when the fixation systems are engaged. More detail about the characteristic of the linear clamping system is given by Daghigh (1997).

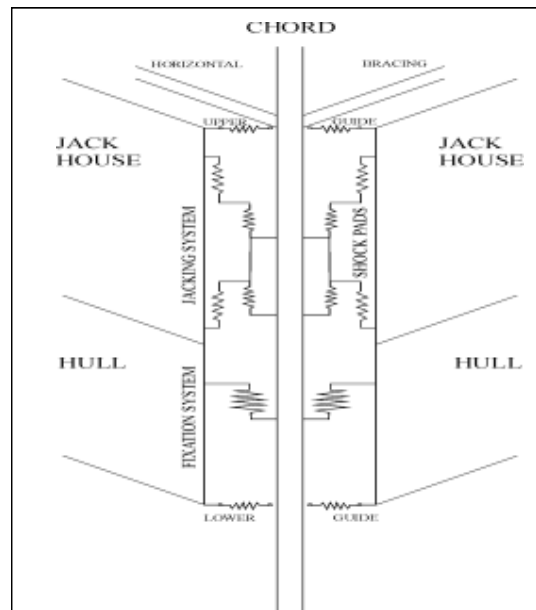


**Figure B.2** Three-dimensional jacking structure for the fixed and floating jacking system, after Daghigh (1997)

## B.2 Environmental description

Daghigh (1997) recommended to use the North Sea conditions for the load calculation. This assumption is in line with the specification of the environmental conditions given by Friede

and Goldman for the design of the platform. Therefore, the information of the *Hutton* area of the North Sea from *Marex* report (Marex, 1979) is used to specify the environmental conditions. The key environmental parameters applied in the ultimate limit state analyses are given as follows, Marex (1979),

- Water depth (including tide and storm surge) 95 m
- Significant wave height  $H_S=16.1$  m
- Wave period  $T_Z=13.6$  s
- One minute sustained wind speed 36.5 m/s  
(at reference level 10 m above mean sea level)
- Extreme surface current velocity 1.2 m/s

These environmental parameters are specified in accordance with a 50-year return period as recommended in the *Site Specific Assessment of Mobile Jack-up Units*, Bulletin 5-5A (Bennett, 1994) for extreme environmental conditions. The wind force is calculated for the whole part of the platform above the water level and the power formulation recommended in Bulletin 5-5A is applied to specify the variation of the wind velocity above the sea level. Moreover, the hydrodynamic loads arising from currents are calculated by simply adding the current velocity given by a current profile to the simulated random water particle velocity. For the fatigue analysis, the current loads may normally be neglected as recommended in the Bulletin 5-5A (Bennett, 1994). In the ultimate reliability analysis, only the tidal current velocity is taken into account with the power exponent type model recommended by DNV (2000) to model the variation of current velocity with the water depth.

### B.3 Soil-structure interaction and Natural period

At the bottom of each leg is a spud can to reduce the penetration of leg into the soil and transfer the load from structure to seabed. In the finite element analysis of the jack-up, six linear springs models (three transitional and three rotational springs) are used to model the soil-structure interaction with the following characteristics,

$$\begin{aligned}
 \text{Transitional} \quad k_x, k_y &= 1.269 \times 10^7 \text{ kN/m} \\
 \text{Vertical} \quad k_z &= 1.338 \times 10^7 \text{ kN/m} \\
 \text{Rotational} \quad k_{xx}, k_{yy} &= 3.259 \times 10^8 \text{ kNm/rad} \\
 \text{Transitional} \quad k_{zz} &= 5.215 \times 10^8 \text{ kNm/rad}
 \end{aligned}$$

The three calculated natural periods of the structure based on this foundation characteristic are 6.79, 4.10 and 1.547 seconds for surge, sway and torsional modes respectively.

### B.4 Hydrodynamic coefficients

The hydrodynamic coefficients used in this analysis are  $C_D=0.65$  and  $C_M=2.0$  as recommended in of the *Site Specific Assessment of Mobile Jack-up Units*, Bulletin 5-5A

(Bennett, 1994). The hydrodynamic loads have been determined with the NOSDA program. The hydrodynamic coefficients for the equivalent legs are calculated in accordance with Bulletin 5-5A (Bennett, 1994). In this specification, the equivalent hydrodynamic coefficients are given based on the equivalent volume and the flow direction. Two cases, with and without marine growth have been considered for the elements below and above the MWL+2 respectively. Moreover, the minimum marine growth thickness 12.50 mm is added to the elements below the MWL+2. Furthermore, below the water level, the increase of roughness leads to the increase of drag coefficient, which is recommended  $C_D=0.7$  for the parametric study by Daghigh (1997). Table B.3 shows the hydrodynamic coefficients of jack-up legs for the heading direction. Moreover,  $D_{EQ}$  shown in this table is the equivalent diameter for the hydrodynamic calculation, which is estimated in accordance with the total volume of one bay.

**Table B.3:** Equivalent hydrodynamic coefficients and diameter

Parameter	Without marine growth ( $t_m=0$ mm)	With marine growth ( $t_m=12.5$ mm)
$C_D$	2.669	2.777
$C_M$	1.830	1.824
$D_{EQ}$	1.954	2.053

## B.5 Equivalent structural leg model

In the finite element analysis of jack-up platform, only one leg is modelled in detail due to computer restrictions. For the other legs, equivalent stiffness characteristics are applied in the FEM analyses. The stiffness of the equivalent jack-up leg is characterized by the beam

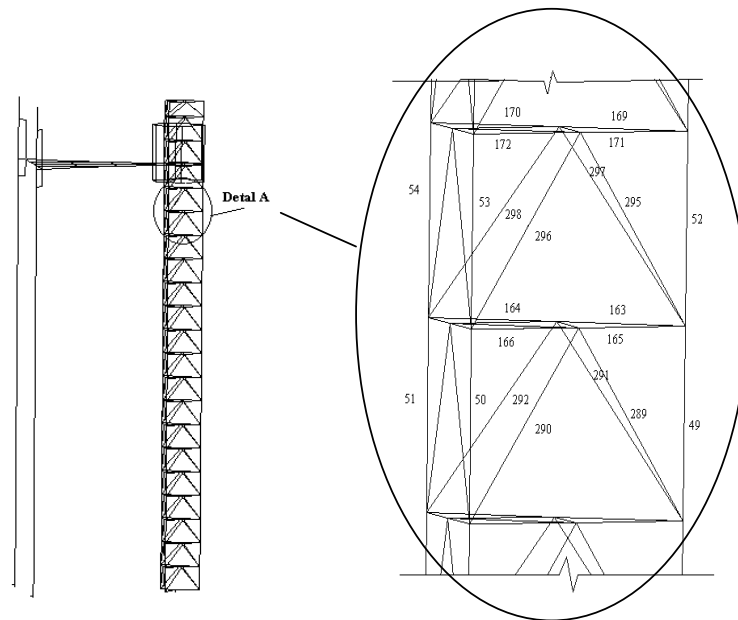


**Figure B.2** Neka jack-up finite element model and detail of elements below the lower guide in the first leg

property given in Bulletin 5-5A (Bennett, 1994) and DNV (1984). The equivalent shear area of leg is specified in term of the “equivalent shear area“ of a two-dimensional lattice configuration. The stiffness properties are assumed to be the same for all direction unless the chords have different areas. This model is restricted for the symmetrical configuration of leg components. The equivalent stiffness parameters of a beam for a leg with three chords are given in table B.4. The finite element model of jack-up model is also shown in figure B.2.

**Table B.4:** Equivalent stiffness characteristics

Characteristic	Description	Quantity
A	Area	$4374.3 \times 10^{-4} \text{ (m}^2\text{)}$
$A_{QY} = A_{QZ}$	Shear area	$5746.5 \times 10^{-5} \text{ (m}^2\text{)}$
$I_Y = I_Z$	Moment of Inertia	$7144.93 \times 10^{-3} \text{ (m}^4\text{)}$
$I_T$	Torsional inertia moment	$9386.90 \times 10^{-4} \text{ (m}^4\text{)}$

## Appendix C Sea scatter diagram

For the calculation of the hydrodynamic load, the significant wave height and its attributed zero-crossing period has to be specified. As explained in section 3.4.6, the significant wave height is a slow time-dependent random variable and its variation is given as the sea scatter diagram. In this research work, the scatter data of the Hutton area at the Stevenson station (Marex, 1979) is used to specify the sea state. The scatter diagram of this station is shown in the figure C.1. These data have been acquired from three years recorded information of sea states in the Stevenson station by Marex (1979). The number in each contour shows the number of observations of sea state per total number of one thousand observations in a year.

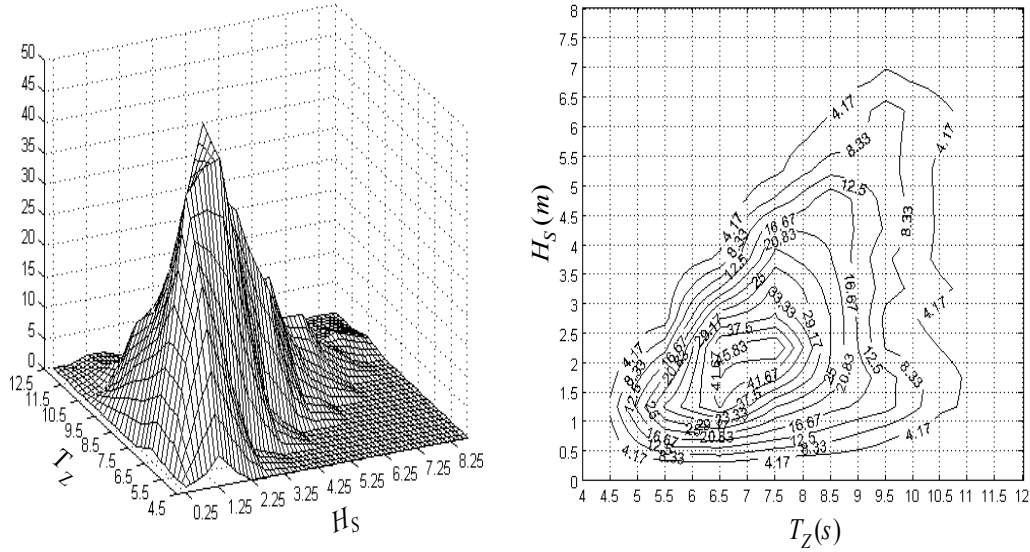


**Figure C.1:** Wave scatter diagram of Stevenson Station

To specify the extreme environmental loads for the jack-up platform, the design storm method has been used. Therefore, it is required to establish a probabilistic approach to predict the extreme environmental load for a specific return period, assumed to be 50 years here. The inverse FORM method recommended by Winterstein et al. (1993) is applied because with this method it is possible to take into account the joint distribution of environmental parameters. The joint distribution of environmental parameters is specified in accordance with the DNV specification notes (no. 30.5, 2000) in which the combined Weibull and lognormal distributions are recommended to specify the significant wave height ( $H_s$ ) and the conditional zero crossing period ( $T_z | H_s$ ). The Weibull distribution is specified with the following expressions,

$$f_{H_s}(H_s) = \frac{\omega}{H_1} \left( \frac{H_s - H_0}{H_1} \right)^{\omega} \exp \left( - \left( \frac{H_s - H_0}{H_1} \right)^{\omega} \right) \quad (C.1)$$

The parameters of this distribution is calculated based on characteristics of the sea scatter diagram given by the *Marex* report (Marex, 1979) for the Stevenson station, see figure C.1. The Weibull distribution parameters are estimated in accordance with this scatter diagram as  $H_0=0.86$ ,  $H_1=2.555$ ,  $\omega=1.391$ . The conditional zero crossing period ( $T_Z | H_S$ ) is specified with the following density function,

$$f_{T_Z}(T_Z | H_S) = \frac{1}{\sqrt{2\pi\sigma T_Z}} \exp\left(-\frac{1}{2}\left(\frac{\ln(T_Z) - \mu}{\sigma}\right)^2\right) \quad (C.2)$$

where the characteristics of this distribution are calculated in accordance with the following expression, DNV (notes no. 30.5, 2000),

$$\begin{aligned} \mu &= E[\ln T_Z] = a_0 + a_1 H_s^{a_2} \\ \sigma &= \sqrt{E[(\ln T_Z - \mu)^2]} = b_0 + b_1 \exp(b_2 H_s) \end{aligned} \quad (C.3)$$

The parameters of the mean values of the log-normal distributions are obtained for the Stevenson station  $a_0$ ,  $a_1$  and  $a_2$  respectively as 0.7, 1.2154 and 0.1264 and for the standard deviation of the log-normal distribution  $b_0$ ,  $b_1$  and  $b_2$  as 0.005, 0.2266, -0.161 respectively.

In the inverse FORM approach, the contour of the environmental parameters such as the significant wave height and zero crossing period is related to a specific return period,  $T_r$ , according to the following expression,

$$\sqrt{U_1^2 + U_2^2} = \Phi^{-1}\left(1 - \frac{T_{SS}}{T_r}\right) \quad (C.4)$$

where  $T_{SS}$  is the sea state duration and is taken here as 3 hours. Two auxiliary normal random variables  $U_1$  and  $U_2$ , which can be specified through the distribution function of the significant wave height,  $F_{H_S}(h_s)$  and the conditional zero crossing period,  $F_{T_Z|H_S}(t|h)$  respectively are specified with the following formulations,

$$\begin{aligned} U_1 &= \Phi^{-1}(F_{H_S}(h_s)) \\ U_2 &= \Phi^{-1}(F_{T_Z|H_S}(t|h)) \end{aligned} \quad (C.5)$$

By using this expression and formulation C.4, the  $H_S$ - $T_Z$  contour for 10, 20, and 50 years return periods can be drawn for the Stevenson station as shown in figure 4.13 of chapter 4.

Since the application of the whole of a scatter diagram for load calculations is time consuming, the computation is restricted to 5 blocks of the scatter diagram. Hence, the five sea-states shown in table C.1 are assumed as being representative for the whole scatter and the long-term calculations are carried out based on the combination of these sea states.

The associated mean zero crossing period  $T_Z$  for a specific significant wave height ( $H_S$ ) is obtained in accordance with the following formulation, which is recommended by the Marex (1979) report.

$$T_z = \sqrt{10.17 H_s + 30.24} \quad (C.6)$$

**Table C.1:** The sea states used for the long-term stress analysis in fatigue reliability

Sea State	$H_S$ (m)	$T_Z$ (s)
1	1.75	6.93
2	3.25	7.96
3	5.00	9.00
4	7.75	10.44
5	10.45	11.68

## Appendix D Influence Factors (Stress Concentration Factors)

In the fatigue reliability calculations, the hot spot stress range has to be obtained. At first, the hot-spot stress process is calculated by multiplying the nominal stress derived in the finite element analysis with the Stress Concentration Factor (SCF). Several SCF's have been presented in the literature but since the formulations of Efthymiou (1988) cover most the geometry of the joints in the jack-up model and also consider different types of loading conditions from planar and non-planar bracing elements, this formulation has therefore been used in this work.

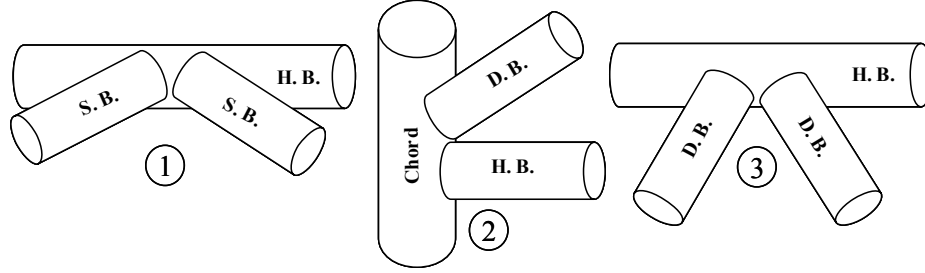


**Figure D.1:** Three types of intersections identified in the jack-up platforms for chord, horizontal brace (H.B.), diagonal brace (D.B.) and span-breaker (S.B.) intersections

The hot spot stress process is calculated for eight points around the intersection in such a way that its angular distribution covers the whole section for each 45 degrees. The hot-spot stresses are calculated through the method presented by Efthymiou (1988) using the Influence Factor ( $IF$ ), which considers the effect of the SCF arising in planar and non-planar braces, with the following expression,

$$\sigma_{hs,i}(t) = \sum_{j=1}^n IF_{ij} \frac{F_{nom,j}(t)}{A_j} = \sum_{j=1}^n IF_{ij} \sigma_{n,j} \quad (D.1)$$

where  $F_{nom,j}$  are the nominal sectional forces and moments determined from the finite

**Table D.1:** Stress concentration factor ( $SCF_{one}$ ) for the intersection of element when one element is only loaded

Joint		Axial load		In-plane Bending	Out-of-plane Bending
Type of intersection	Element	Saddle	Crown	Crown	Saddle
Chord & H.B & D.B (type 2)	D.B	2.407	2.949	2.480	1.405
	H.B	4.832	2.937	2.116	3.072
H. Brace & D. Brace (type 3)	D.B	2.781	4.640	2.593	2.245
H. Brace & S.B. (type 1)	S.B	3.571	3.170	2.106	2.152



element analysis,  $A_j$  are the corresponding sectional constants (e.g. area or sectional modulus), and  $n$  is the total number of degrees of freedom in all bracing member ends and in the two chord ends. In general, there are six load cases for each free end but a common approach for the fatigue analysis of offshore platforms is to neglect the effect of the torsional moments and shear forces in the fatigue damage calculation.

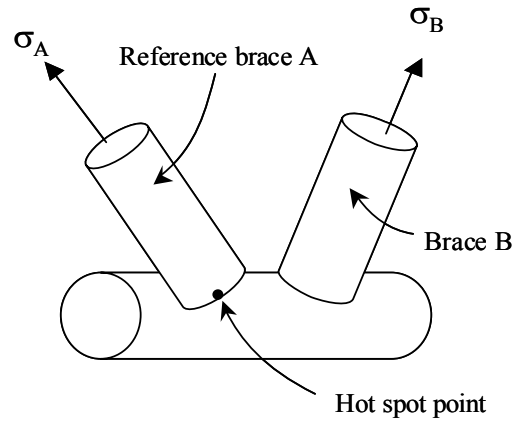


**Figure D.2:** Definition of Influence function

The influence factors are calculated for three types of joint configurations in accordance with the geometry characteristics of the chords, braces and span-breakers. These joints are illustrated in figure D.1 and the calculated influence factors are given in accordance with combination of SCF from table D.1 for the case that only one member is loaded and table D.2 when the element is loaded in the balance load. For example, the hot spot stress for axial load only can be calculated with the following expression, when the influence of other element is taken into account, see figure D.2,

$$\sigma_{hs} = \sigma_A SCF_{un} + \sigma_B \underbrace{\frac{A_B \sin \theta_B}{A_A \sin \theta_A} [SCF_{one} - SCF_{balanced}]}_{IF} \quad (D.2)$$

where  $\sigma_A$  and  $\sigma_B$  are the stress in the brace  $A$  and  $B$  respectively.  $\theta_A$  and  $\theta_B$  are the smallest angle of brace  $A$  and  $B$  with the horizontal element and,  $A_A$  and  $A_B$  are the cross section area of brace  $A$  and  $B$  respectively.  $SCF_{one}$  is the stress concentration factor when one element is only loaded and can be specified with table D.1. Moreover,  $SCF_{balanced}$  is the stress concentration factor when the element is loaded in the balance load and is given by table D.2. In this equation only the effect of axial load has been considered but in the practical situation the effect of in-plane bending and out-of-plane bending stresses should be added. More details about this method and the effect of out-of-plane elements have been given in Efthymiou (1988).

**Table D.2:** Stress concentration factor ( $SCF_{balanced}$ ) for the intersection of element when the element is loaded in the balance load

Joint		Axial load		In-plane Bending	Out-of-plane Bending
Type of intersection	Element	Saddle	Crown	Crown	Saddle
Chord & H.B & D.B (type 2)	D.B	2.174	2.174	2.480	2.6250
	H.B	3.316	3.3156	2.116	3.611
H. Brace & D. Brace (type 3)	D.B	2.276	2.276	2.593	3.402
H. Brace & S.B. (type 1)	S.B	2.365	2.365	2.106	2.955

## Appendix E The computer programs

In this research work, several computer programs have been modified and written to carry out the reliability calculation, to calculate the hydrodynamic loads and to estimate the stress ranges. In the following sections the procedures of calculation methods are presented in detail.

### E.1 RELIABILITY CALCULATION ALGORITHMS

As discussed in chapter 3, the calculation of the reliability index or the failure probability requires a searching algorithm to find the closest distance from the limit state function to the origin in the normal standard space. In this research work, two algorithms of gradient projection method described in Nowak and Collins (2000) and the modified version of Hasofer and Lind (1974) presented by Liu and Der Kiureghian (1991) have been applied for the reliability calculations of fatigue, fracture and ultimate limit state functions and some computer programs have been written to carry out these calculations. These two methods are presented in the following sections and the advantage or disadvantage of each method is described.

#### E.1.1. Reliability calculation based on the Nowak algorithm

The algorithm of Nowak and Collins (2000) is originally known as the gradient projection method, which solves the original problem by generating a sequence of the points to converge to the optimal solution. Hence, the bases of this method is an iteration procedure to satisfy the condition that the design point is situated on the limit state function and has the shortest distance ( $\beta$ ) to the origin in the normal standard space. To satisfy this condition, for  $n$  random variables with the limit state function e.g.  $g(X_1, X_2, \dots, X_n) \leq 0.0$ , an iterative procedure is required to solve a set of  $(2n+1)$  simultaneous equations with  $(2n+1)$  unknowns:  $\beta, \alpha_1, \alpha_2, \dots, \alpha_n, z_1^*, z_2^*, \dots, z_n^*$ , where  $\alpha_i$  is the direction cosine (sensitive factor), which is estimated from the following expression,

$$\alpha_i = -\frac{\partial g}{\partial Z_i} \bigg|_{(z_1^*, \dots, z_n^*)} / \sqrt{\sum_{j=1}^n \left( -\frac{\partial g}{\partial Z_j} \bigg|_{(z_1^*, \dots, z_n^*)} \right)^2} \quad (E.1)$$

To calculate the derivation of the limit state function in the normal space, the following chain rule is applied,

$$\frac{\partial g}{\partial Z_i} = \frac{\partial g}{\partial X_i} \frac{\partial X_i}{\partial Z_i} = \frac{\partial g}{\partial X_i} \sigma_{X_i}^{eq} \quad (E.2)$$

Moreover, the following condition confirms that  $\alpha_i$  is the direction cosine,

$$\sum_{i=1}^n (\alpha_i^2) = 1 \quad (E.3)$$

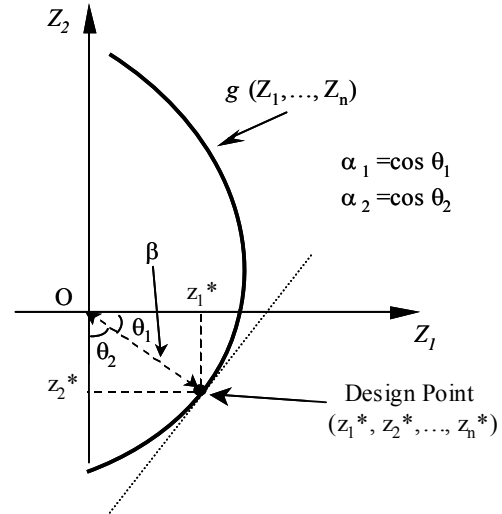


**Figure E.1:** Design point and reliability index for a nonlinear limit state in normal standard space

where the relation between the design point and the direction cosine is specified with the following formulation,

$$z_i^* = \beta \alpha_i \quad (\text{E.4})$$

Now, the design point should satisfy the expression  $g(x_1^*, x_2^*, \dots, x_n^*) = 0.0$  to confirm that this point is situated on the limit state function. In accordance with these conditions, the following steps should be followed to determine the reliability index:

1. Formulate the limit state function and appropriate parameters for all random variables involved,  $x_i$  ( $i=1, \dots, n$ ).
2. Specify an initial design point  $\{x_i^*\}$  by assuming values for  $n-1$  of the random variables (the mean value is often a reasonable choice). Solve the limit state function  $g(x_1^*, x_2^*, \dots, x_n^*) = 0.0$  for the  $n^{\text{th}}$  variable. This ensures that the design point is on the failure boundary.
3. For each of the design point values  $x_i^*$  corresponding to a non-normal distribution, calculate the equivalent normal mean ( $\mu_i^{\text{eq}}$ ) and standard deviation ( $\sigma_i^{\text{eq}}$ ) by the following expressions,

$$\mu_{X_i}^{\text{eq}} = x_i^* - \sigma_{X_i}^{\text{eq}} \left[ \Phi^{-1} \left( F_{x_i}(x_i^*) \right) \right] \quad (\text{E.5})$$

$$\sigma_{X_i}^{\text{eq}} = \phi \left( \frac{x_i^* - \mu_{X_i}^{\text{eq}}}{\sigma_{X_i}^{\text{eq}}} \right) / f_{x_i}(x_i^*) = \phi \left( \Phi^{-1} \left( F_{x_i}(x_i^*) \right) \right) / f_{x_i}(x_i^*) \quad (\text{E.6})$$

where  $F_{x_i}(x_i^*)$  and  $f_{x_i}(x_i^*)$  are cumulative and density probability distribution of non-normal distribution. If one or more  $x_i^*$  values corresponds to a normal distribution, then the equivalent normal parameters are simply the actual parameters.

4. Estimate the reduced variables  $\{z_i^*\}$  corresponding to the design point  $\{x_i^*\}$  using

$$z_i^* = (x_i^* - \mu_{X_i}^{\text{eq}}) / \sigma_{X_i}^{\text{eq}} \quad (\text{E.7})$$

5. Determine the partial derivatives of the limit state function with respect to the reduced variable using equation E.2. Define a column vector  $\{G\}$  as the vector whose elements are the partial derivatives,

$$\{G\}^T = \{\nabla g_1, \nabla g_2, \dots, \nabla g_n\}^T \text{ where } \nabla g_i = - \frac{\partial g}{\partial z_i} \Big|_{\text{evaluated at design point}} \quad (\text{E.8})$$

6. Determine an estimation of the reliability index ( $\beta$ ) by the following expression,

$$\beta = \{G\}^T \{z^*\} / \sqrt{\{G\}^T \{G\}} \quad (\text{E.9})$$

7. Calculate the column contains cosine vectors,

$$\alpha = \{G\} / \sqrt{\{G\}^T \{G\}} \quad (\text{E.10})$$

8. Determine the new design point in the reduced variable space for  $n-1$  of the variables using expression E.4.

9. Calculate the corresponding design point values in the original space for the  $n-1$  variables in the step 7, using the inversed formula presented in step 4,  $x_i^* = \mu_{X_i}^{eq} + z_i^* \sigma_{X_i}^{eq}$
10. Determine the value of the remaining random variables (i.e. the one that is not found in steps 8 and 9) by solving the limit state function  $g(x_1^*, x_2^*, \dots, x_n^*) = 0.0$ . This calculation is the same as the second step.
11. Repeat steps 3 up to 10 until  $\beta$  and the design point  $\{x_i^*\}$  converge.

The benefit of this procedure is that it starts from an initial point which is situated on the limit state function and repeated in each iteration to ensure that the point is on the failure boundary. The disadvantage of this algorithm is that for some non-normal random variables the iteration of calculation of the design point may lead into the values in which the equivalent normal distribution cannot be estimated from the expressions E.5 and D6. Furthermore, if there is a correlation between random variable, it is not clear how the correlation is incorporated. However, Nowak and Collins (2000) recommends to apply the modified expressions of the sensitivity factor (formula E.10) and the expression for the calculation of the reliability index (formula E.9) by multiplying them with the correlation coefficient matrix  $[\rho]$  such as,

$$\begin{aligned}\alpha &= [\rho] \{G\} / \sqrt{\{G\}^T [\rho] \{G\}} \\ \beta &= \{G\}^T \{z^*\} / \sqrt{\{G\}^T [\rho] \{G\}}\end{aligned}\tag{E.11}$$

But incorporating this correction it makes that the direction cosine ( $\alpha$ ) is violating the essential assumption of expression E.3 i.e. the summation of  $\alpha_i^2$  does not become one. Furthermore, in some situations the iteration of this algorithm does not converge to a specific value due to the noisy condition of the fatigue and fracture limit state functions in the numerical procedure to calculate the geometry function and the integral of fatigue strength function. These problems lead to the application of another algorithm for the reliability calculation, which makes it possible to solve these problems and control the convergence criteria to increase the efficiency of the method. In the following section this method is described in detail.

### E.1.2. Reliability calculation based on Liu and Der Kiureghian Algorithm

This method is a modified version of procedure presented by Hasofer and Lind (1974) to improve the convergence criteria by adding a line search scheme. The search direction for this algorithm is an extension of the gradient projection search direction described in the previous section. In the gradient projection algorithm, the starting trial point is located on the limit state and will be on the limit state for other iteration to the end. But the improved algorithm, starts outside of limit state and will converge to the point that is located on the limit state at the end. The ordinary Hasofer and Lind approach uses the following iteration formula to find the design point

$$z_{i+1} = z_i + \lambda_i d_i \tag{E.12}$$

where step size  $\lambda_i$  is set into one and the step direction vector  $d_i$  is estimated from:

$$d_i = \frac{[\nabla g(z_i)z_i - g(z_i)]}{|\nabla g(z_i)|^2} [\nabla g(z_i)] - z_i \quad (E.13)$$

In the improved version recommended from Liu and Der Kiureghian (1991), a new trial point is chosen in accordance with a step size obtained by using a merit function. The merit function is a function that its global minimum is located at the design point and the solution of this function in each iteration step converge to the design point. The step size is therefore specified in such a way that it minimizes the merit function,

$$\lambda_i = \arg \min \{m(z_i + \lambda d_i) - m(z_i)\} \quad (E.14)$$

Where the merit function  $m(z)$  should be defined in terms of  $z$ . In practice it is a feasible way to find a value  $\lambda_i$  so that the merit function is sufficiently reduced. The so-called Armijo rule provides such an approach whereby the step size is taken as  $b^k$ ,  $k=1,2,\dots$  and

$$\lambda_i = \max_{k \in \mathbb{N}} \left\{ m(z_i + \lambda d_i) - m(z_i) \leq ab^k (\nabla m(z_i) d) \right\} \quad (E.15)$$

$a$  is the positive user defined constant associated with Armijo-type line search schemes. It influences on how the user wants the merit function to decrease at each step. A typical value is 0.5. The following merit function is suggested to be appropriate for the reliability calculation,

$$m(z) = \frac{1}{2} \left| z - \frac{[\nabla g(z)z]}{|\nabla g(z)|^2} [\nabla g(z)] \right|^2 + \frac{1}{2} c |g(z)| \quad (E.16)$$

where  $c$  is a positive constant. The step directional vector in this formulation has been given in such a way that it minimizes the merit function.

According to this modification, the procedure for the reliability calculation is as follows:

- a. Transform the user-defined starting vector  $\mathbf{x}$  in the original space (e.g., the mean values of random variables) into the vector  $\mathbf{u}$  in the standard normal space in accordance with the following expression,

$$T: \quad \mathbf{u} = L_0^{-1} \begin{Bmatrix} \Phi^{-1}(F(x_1)) \\ \vdots \\ \Phi^{-1}(F(x_n)) \end{Bmatrix} \quad (E.17)$$

where  $L_0$  is the Choleski decomposition of the correlation matrix  $R_0$ , which is calculated with  $R_0 = L_0 L_0^T$ . The  $R_0 = [\rho_{0,ij}]$  is the correlation matrix between random the variables in the Normal space and can be related to the correlation of the random variables in the original space,  $R = [\rho_{ij}]$ , with the following expression, (Der Kiureghian and Liu, 1986).

$$\rho_{ij} = \int_{-\infty}^{\infty} \int_{-\infty}^{\infty} \left( \frac{x_i - \mu_i}{\sigma_i} \right) \left( \frac{x_j - \mu_j}{\sigma_j} \right) \varphi_2(z_i, z_j, \rho_{0,ij}) dz_i dz_j \quad (E.18)$$

The close form approximate expression to relate  $\rho_{ij}$  into  $\rho_{0,ij}$  is provided in Der Kiureghian and Liu (1986) for several probability distributions. This expression is

used in this section to obtain the equivalent correlation between each two random variables

- b. Transform vector  $\mathbf{u}$  from standard normal space into  $\mathbf{x}$  in the original space.
- c. Compute the gradient vector of the limit state function in the standard normal space,

$$\nabla_{\mathbf{u}} g = \frac{\partial g}{\partial \mathbf{u}} = \frac{\partial g}{\partial \mathbf{x}} \frac{\partial \mathbf{x}}{\partial \mathbf{u}} = \frac{\partial g}{\partial \mathbf{x}} (\mathbf{J}_{\mathbf{x}, \mathbf{u}}) = \frac{\partial g}{\partial \mathbf{x}} (\mathbf{J}_{\mathbf{u}, \mathbf{x}})^{-1} \quad (\text{E.19})$$

- d. Estimate the step size  $\lambda_i$  in accordance with the maximum expression (E.15) and the merit function expression (E.16).
- e. Obtain the new iteration point by using the step size that is calculated with expression (E.15) in formulation (E.11).
- f. The calculation is continuing until convergence is achieved or the user-defined maximum of iteration is reached:

## E.2 MODIFIED PROGRAM FOR HYDRODYNAMIC LOAD CALCULATIONS

To obtain the hydrodynamic loads on a jack-up platform, an improved version of the NOSDA program has been developed. The original NOSDA program (Liu and Massie, 1988) uses the Deterministic Spectrum Amplitude (DSA) for the simulation of the wave surface. In this method, the wave surface in each time step is computed by using the Airy wave theory with the uniformly distributed random phase, as,

$$\eta(x, t) = \sum_{i=1}^N A_i \cos(\omega_i t - k_i [x \cos \theta + y \sin \theta] - \varepsilon_i) \quad (\text{E.20})$$

where  $\omega_i$  is a set of equally-spaced discrete wave frequency and  $k_i$  is its associate wave number.  $\varepsilon_i$  is the random phase angle distributed uniformly in the range  $0 \leq \varepsilon_i \leq 2\pi$ . Moreover,  $x$  and  $y$  are the coordinates of a point in the horizontal Cartesian system and  $\theta$  is the wave direction measured from  $x$ -axis.  $A_i$  is determined with the following expression,

$$A_i = \sqrt{2G_{\eta}(\omega_i)\Delta\omega} \quad (\text{E.21})$$

where  $G_{\eta}(\omega_i)$  is the wave frequency spectrum, which is specified based on P-M or JONSWAP spectra. This method is called the Deterministic Spectrum Amplitude (DSA). But, as Grigoriu (1993), Morooka and Yokoo (1997) demonstrated, this approach does not lead to the Gaussian nature of the wave surface except for a high number of random phase combinations. Hence, for a limited number of phase combinations, they recommend to apply the random Rayleigh amplitude in addition to the random phase to represent better the Gaussian nature of the wave surface.

**Table E.1:** Statistic characteristics of wave surfaces simulated in accordance with DSA and NDSA methods

Significant wave height ( $H_s$ )		Stand. Dev.	Skewness	Kurtosis
1.75	DSA	0.4837	0.0222	2.5333
	NDSA	0.4350	-0.0021	3.0902
3.25	DSA	0.9066	0.0212	2.5439
	NDSA	0.8096	0.0007	3.0742
5.00	DSA	1.3914	0.0089	2.5453
	NDSA	1.2400	0.0007	3.0240
7.75	DSA	2.1372	0.0113	2.5393
	NDSA	1.944	-0.0018	3.0642
10.45	DSA	2.8704	0.0298	2.5100
	NDSA	2.6203	0.0137	3.0809
16.10	DSA	4.2882	0.0459	2.5376
	NDSA	3.9841	0.0094	3.0824

Therefore, the amplitude in this model is estimated with,

$$A_i = \sqrt{2G_\eta(\omega_i)\Delta\omega} \sqrt{\frac{z_{1i}^2 + z_{2i}^2}{2}} \quad (\text{E.22})$$

where  $z_{1i}$  and  $z_{2i}$  are two independent standard normal random variables. This model is known as the Non-Deterministic Spectrum Amplitude (NDSA) and is applied in the modified version of the NOSDA program.

Table E1 shows the results of the statistical characteristics of the wave surfaces simulated in accordance with the DSA and the NDSA for combinations of 90 discrete wave frequencies (N) and totally 22 minutes simulation of time history. The time step of simulation has been set into 0.25 second. A comparison of the statistic results for these two models indicates that the DSA is more non-Gaussian than the NDSA. Moreover, the NDSA satisfies the condition of wave simulation recommended by DNV (note 30.5, 2000) and would be an appropriate method for the hydrodynamic load calculation. By using this irregular wave surface simulation and Airy wave theory, the water particle velocity and acceleration induced by the waves can be estimated for a specific point. The hydrodynamic loads are therefore calculated for the jack-up platform using the Morison equation.

### E.3 SYSTEM RELIABILITY, CRUDE AND MODIFIED FIRST ORDER MULTI NORMAL (FOMN)

In chapter 3 it is shown that the reliability of series and parallel systems can be calculated in accordance with the probability content of a standard multi-normal distribution. The First Order Multi Normal (FOMN) concept can be applied to estimate the failure probability. This method, which was firstly proposed by Hohenbichler and Rackwitz (1983) and later modified by Tang and Melchers (1987), is essentially based on reducing the original multi-normal space by one through a multiplication of the conditional distributions and using the FORM approach to linearize the nonlinear term and estimate these conditional probabilities. According to this method, the probability content of a standard correlated normal vector  $X$  with  $n$  components can generally be estimated with,

$$\Phi_n(-\beta; R_X) = P\left(\bigcap_{i=1}^n X_i \leq -\beta_i\right) \quad (\text{E.23})$$

where  $\beta_i$  is the reliability index of  $i^{\text{th}}$  component of  $\beta=[\beta_i]$  and  $R_X$  is a positive definite correlation matrix of the vector  $X$ . The first step in FOMN is to transform the correlated standard normal vector  $X$  with the correlation matrix  $R_X=[\rho_{ij}]$  into the uncorrelated standard vector  $U$  by the so-called Rosenblatt transformation. This linear transformation may be described by,

$$X = \alpha U \quad (\text{E.24})$$

where  $\alpha$  is the lower triangular matrix, of which its component is related to the component of the correlation matrix with the following expressions,

$$\alpha_{11} = 1, \quad \alpha_{21} = \rho_{21}, \quad \alpha_{22} = \sqrt{1 - \alpha_{21}^2} \quad (\text{E.25})$$

$$\alpha_{i1} = \rho_{i1} \quad i=3,4,\dots,n \quad (\text{E.26})$$

$$\begin{cases} \alpha_{ij} = \left( \rho_{ij} - \sum_{k=1}^{j-1} \alpha_{ik} \alpha_{jk} \right) / \alpha_{jj} \\ \alpha_{ii} = \left( 1 - \sum_{j=1}^{i-1} \alpha_{ij}^2 \right)^{1/2} \end{cases} \quad j=2,3,\dots,i-1 \quad i=3,4,\dots,n \quad (\text{E.27})$$

By substituting the equations E.25-E27 into the expression E.23, the probability content can be calculated with the following expression.

$$\Phi_n(-\beta; R_X) = P\left(\bigcap_{i=1}^n X_i \leq -\beta_i\right) = P\left(\bigcap_{i=1}^n \left\{ \sum_{j=1}^i \alpha_{ij} U_j + \beta_i \right\} \leq 0\right) \quad (\text{E.28})$$

The dimension of the multi normal probability can be reduced by one through the conditioning on  $U_1 \leq -\beta_1$  as,

$$\Phi_n(-\beta; R_X) = P\left(\bigcap_{i=2}^n \left\{ \sum_{j=1}^i \alpha_{ij} U_j + \beta_i \leq 0 \right\} \middle| U_1 \leq -\beta_1\right) \underbrace{P(U_1 \leq -\beta_1)}_{\Phi(-\beta_1)} \quad (\text{E.29})$$

It is noted that the probability content of the first term in the right hand side of this expression has one dimension less than original one and only depends  $U_1$ . Furthermore, this conditioning does not affect  $U_2, U_3$ , etc, since all other variables are independent of each other. The conditional probability of equation E.29 can be estimated by using the following unconditional expression on  $U_1$ ,

$$P\left(\bigcap_{i=2}^n \left\{ \sum_{j=1}^i \alpha_{ij} U_j + \beta_i \leq 0 \right\} \middle| U_1 \leq -\beta_1\right) = P\left(\bigcap_{i=2}^n \left\{ \alpha_{i1} \hat{U}_1 + \sum_{j=2}^i \alpha_{ij} U_j + \beta_i \leq 0 \right\}\right) \quad (\text{E.30})$$

where  $\hat{U}_1$  is required to be constrained for  $\hat{U}_1 \leq -\beta_1$ . The conditional distribution function of  $U_1$  given that  $U_1 \leq -\beta_1$  can be obtained with,

$$F(u) = P(U_1 \leq u | U_1 \leq -\beta_1) = \begin{cases} \Phi(u) / \Phi(-\beta_1), & u \leq -\beta_1 \\ 1, & u > -\beta_1 \end{cases} \quad (\text{E.31})$$

Hence,  $\hat{U}_1$  can be determined with the following expression.

$$\hat{U}_1 = \Phi^{-1}\left[\Phi(-\beta_1)F(\hat{U}_1)\right], \quad \hat{U}_1 \leq -\beta_1 \quad (\text{E.32})$$

Since in this expression any continuous distribution can be used to specify  $F(\hat{U}_1)$ , and in the FORM approach the normal probability distribution is of a more interest, the normal distribution is used to specify the  $F$  function, i.e.

$$\hat{U}_1 = \Phi^{-1}\left[\Phi(-\beta_1)\Phi(\hat{U}_1)\right] \quad (\text{E.33})$$

The expression E.29 can now be rewritten by using E.30 and E.33 as,

$$\Phi_n(-\beta; R_X) = P\left(\bigcap_{i=2}^n \left\{ \alpha_{i1} \Phi^{-1}(\Phi(-\beta_1)\Phi(U_1)) + \sum_{j=2}^i \alpha_{ij} U_j + \beta_i \leq 0 \right\}\right) \Phi(-\beta_1) \quad (\text{E.34})$$



The first term in the right hand side of this equation is a non-linear function with one-dimensional space less than the original one. The next task is to linearize each of the non-linear terms (limit state function) at the “design point” in the  $U$  space by using a FORM approach. Typically this approximation for the  $i^{\text{th}}$  term of equation E.34 gives

$$P\left(\left\{\alpha_{i1}\Phi^{-1}(\Phi(-\beta_1)\Phi(U_1)) + \sum_{j=2}^i \alpha_{ij}U_j + \beta_i \leq 0\right\}\right) \approx P\left(\sum_{j=1}^i \gamma_{ij}U_j + \beta_i^{(2)} \leq 0\right) \quad i=2,3,\dots,n \quad (\text{E.35})$$

where  $\gamma_{ij}$  are the direction cosines and  $\beta_i^* = \beta_i^{(2)}$  is the distance of origin to the limit state function at the design point determined by the FORM approach. The above intersection of the  $(n-1)$  hyperplane in the  $U$  space can be recast in the original correlated  $X$  space using the second moment algebra, so that it becomes,

$$\begin{aligned} \Phi_n(-\beta; R_X) &= P\left(\bigcap_{i=2}^n \left\{\sum_{j=1}^i \gamma_{ij}U_j + \beta_i^{(2)} \leq 0\right\}\right) \Phi(-\beta_1) \\ &= P\left(\bigcap_{i=2}^n X_i^{(2)} \leq -\beta_i^{(2)}\right) \Phi(-\beta_1) \\ &= \Phi_{n-1}(-\beta^{(2)}; R_X^{(2)}) \Phi(-\beta_1) \end{aligned} \quad (\text{E.36})$$

where  $R_X^{(2)}$  contains the correlation between any two linear hyperplane. Repetition of the whole process for the first term of the right hand side of the expression E.36 for  $(n-1)$  times eventually produces the multiplication of  $(n)$  normal distributions, as

$$\Phi_n(-\beta; R_X) \approx \Phi(-\beta_1) \Phi(-\beta_2^{(2)}) \dots \Phi(-\beta_n^{(n)}) \quad (\text{E.37})$$

which shows that the multinormal probability content can be approximated into multiplication of  $(n)$  times normal probabilities. The procedure explained in this section shows the general concepts of FOMN approach.

In the provided computer program for crude-FOMN, the FORM method has been applied to estimate the values  $(\beta_2^{(2)}, \beta_3^{(3)}, \dots, \beta_n^{(n)})$  and the linear limit state functions in expression E.35. Fortunately the first term in this expression is the only non-linear and hence it is possible to recast this in a two dimensional  $(U_1, V)$  space. Thus, if the linear space  $(U_2, U_3, \dots, U_n)$  is condensed into a  $V$  space, an equivalent limit state function in  $(U_1, V)$  may be given with,

$$g(U_1, V_i) = \rho h(U_1) + \alpha_2 V_i + \beta_i = 0 \quad i=2,3,\dots,n \quad (\text{E.38})$$

where

$$\rho = \alpha_{i1} ; \alpha_2 = (1 - \alpha_{i1}^2)^{1/2} ; h(U_1) = \Phi^{-1}(\Phi(-\beta_1)\Phi(U_1)) ; V_i = \left[ \sum_{j=2}^i \alpha_{ij}U_j \right] / \alpha_2 \quad (\text{E.39})$$

The purpose is now to determine the linear limit state and the minimum distance of the origin to the limit state function  $(\beta_i^* = \beta_i^{(2)})$  at the design point. The search for the minimum distance  $\beta_i^*$  in the equation E.38 can be reformulate into the following form,

$$\min (\beta_i^*)^2 = U_1^2 + V_i^2 \quad i=2,3,\dots,n \quad (\text{E.40})$$

subject to

$$g(U_1, V_i) = 0 \quad (E.41)$$

After substituting  $V_i$  from E.39 into E.40, the minimization form becomes,

$$\min (\beta_i^*)^2 = U_1^2 + (\beta_i + \rho h(U_1))^2 / \alpha_2^2 \quad (E.42)$$

The minimization is equal to the finding of the root of the following equation,

$$G(U_1) = d(\beta_i^*)^2 / d(U_1) = 0 \quad \text{or} \quad G(U_1) = \alpha_2^2 U_1 + (\beta_i + \rho h(U_1)) h'(U_1) = 0 \quad (E.43)$$

where  $h'(U_1)$  is the derivation of  $h(U_1)$ . The shape of  $G(U_1)$  is almost flat and the root can be obtained easily with one of the typical approaches. In our computer program, the Newton-Raphson method has been applied to determine this root. In accordance with this method, the iteration procedure becomes finding the  $U_1$  with the following expression,

$$U_1^{k+1} = U_1^k - G(U_1^k) / G'(U_1^k) \quad (E.44)$$

where  $G'(U_1)$  is the derivation of  $G(U_1)$ . This algorithm is fast and stable and in many cases a limited number of iterations are necessary to converge to  $U_1^*$ . After obtaining  $U_1^*$  and substitution in the expressions E.41, and E.43,  $V_i^*$  and  $\beta_i^*$  can be calculated. It should be kept in mind that the new correlation matrix  $R_X^{(2)}$  should be determined in the  $U$  space and not in  $(U_1, V)$  space, since the dimensions of the linear space vary. By using the expression E.39, the coefficients of the linear limit state function in expression E.35 can be calculated. This procedure can be continued to find the whole of the values  $\beta$  required in the expression E.37.

The error may sometimes be quite significant in the case of a high correlation in  $X$  or high dimensions due to the linearization of the non-linear limit state function in expression E.35. Therefore, this requires a better approximation for the probability calculation, which is termed as an improved-FOMN. This method is essentially based on improving the calculation method for the conditional distribution of expression E.29. Instead of using expression E.31 for the conditional distribution, the exact probability is estimated through the bivariate normal integral. Recalling the conditional probability in expression E.29 and carrying out a reverse Rosenblatt transformation, the following expression for conditional distribution can be derived.

$$\begin{aligned} P_{i, \text{imp}} &= P\left(\sum_{j=1}^i \alpha_{ij} U_j + \beta_i \leq 0 \mid U_1 \leq -\beta_1\right) = P(X_i \leq -\beta_i \mid X_1 \leq -\beta_1) \\ P_{i, \text{imp}} &= P((X_i \leq -\beta_i) \cap (X_1 \leq -\beta_1)) / P(X_1 \leq -\beta_1) \\ P_{i, \text{imp}} &= \Phi_2(-\beta_1, -\beta_i; \rho_{i1}) / \Phi(-\beta_1) \end{aligned} \quad (E.45)$$

where  $\Phi_2(\cdot)$  is the bi-variate normal probability distribution. By using this formulation, the improved-FOMN probability can be estimated with the following expression,

$$\Phi_n(-\beta; R_X) = P\left(\bigcap_{i=2}^n \left\{ \sum_{j=1}^i \gamma_{ij} U_j + \beta_{i, \text{imp}}^{(2)} \leq 0 \right\}\right) \Phi(-\beta_1) \quad (E.46)$$

where  $\beta_{i, \text{imp}}^{(2)} = -\Phi^{-1}(P_{i, \text{imp}})$  and the rest of the procedure is identical with the crude-FOMN approach.

#### E.4 CYCLE COUNTING: PEAK AND RAINFLOW COUNTING METHODS

In fatigue reliability calculation, the stress range needs to be specified. In this research work two peak and rainflow counting methods are applied. For this purpose, two computer programs have been extended based on the peak counting method described in Madsen et al. (1986) and the rainflow counting method given by Downing and Socie (1982). At first the time history of the hot spot stress process is calculated based on the multiplication of the nominal stresses calculated by a FEM and the Influence Factors given in appendix D.

For the peak counting method, a local maximum of the stresses is then calculated and paired with a local minimum of the same size and the equivalent stress history is obtained. Furthermore, the local maxima and minima are paired to form the stress range independent of their relative location in the stress history. Finally, a specific distribution function (Weibull) is fitted on the estimated stress ranges.

In the rainflow counting method, the hot spot stress history is firstly converted into series of peaks and troughs. The interest of this method is the stress range, which specified as the difference in stress between a peak and the next trough. An overall range is therefore specified as the measure between a peak and a trough that is not in the next one but is in the one that occurs later, or between a trough and a later peak. This procedure is presented by Downing and Socie (1982) in detail. The base is on the one-dimensional vector array to keep track of those peaks and troughs, which have not formed a closed loop. In other words, once a closed loop has been determined, the peak and trough associated with it can be eliminated from the vector. The following steps show the procedure of the rainflow counting calculation when  $X$  is the range under consideration and  $Y$  is the previous range adjacent to  $X$ . At first the peaks and troughs should be rearranged to begin and end with the maximum peak or minimum trough and put them into a vector.

1. Read the (next) peak or trough in a vector, if it reaches the end of data stop the calculation.
2. Form ranges  $X$  and  $Y$  by reading the data from the first step.
3. Compare ranges  $X$  and  $Y$ :
  - a. If  $X < Y$ , go to step 1
  - b. If  $X \geq Y$ , go to step 4
4. Count the range  $Y$ , discard the peak and trough of  $Y$  and finally go to step 2.

According to this procedure a computer program has been developed to calculate the stress range in the specific hot spot points of the bracing/chord intersections. The Weibull distribution is fitted on the stress range and the characteristics of the distribution have been utilized in the fatigue reliability calculations to estimate the reliability index.

## Appendix F Calculation procedure of Correlation between limit state functions

In the system reliability calculations, the correlation between series and parallel systems should be included. This correlation has been established in accordance with the correlation between the random variables individually and the contributions of the random variables in the limit state functions. In a real situation, most of the random variables such as fatigue characteristics ( $m$ ), initial crack size ( $a_0$ ), fracture parameter ( $K_{IQ}$ ) of one element may have a spatial correlation with another element but in this investigation this spatial correlation has not been considered. Only the stress model correction ( $\delta_S$ ) is assumed to have a spatial correlation, which is determined with the available time history of the hot spot stress process. In the following sections, the method applied to specify the correlation between parallel and series systems are presented.

### I.1 Correlation of a parallel system

To calculate the failure probability of the sequence of fatigue failures in the end joints of member 296 followed with 298 at the hot spot points 270, see figure 5.3, the correlation between the elements of parallel systems have to be determined, as well as the equivalent failure probability. The general expression of the fatigue failure of the first joint in the term of the fatigue limit state function is given as follows,

$$g_{f1}(a_{0,J1}, a_{th,J1}, \delta_{Y_{J1}}, \delta_{f_{J1}}, C_{J1}, \delta_{F_{J1}}, \delta_{S_{J1}}, \delta_{SCF_{J1}}) = \frac{\delta_{f_{J1}}}{\sqrt{J1} \delta_{F_{J1}}^m \delta_{S_{J1}}^m \delta_{SCF_{J1}}^m C_{J1} A_{J1}^m \Gamma(1 + \frac{m}{B_{J1}})} \int_{a_{0,J1}}^{a_{th,J1}} \frac{da}{\delta_{Y_{J1}}^m Y(a)^m (\sqrt{\pi a})^m} - T_{lifetime} \quad (F.1)$$

If the FORM approach is used to calculate the failure probability, the tangent hyperplane approximation on the limit state function of the first joint failure in fatigue (296E270) can be given in accordance with the following expression,

$$g_{f1} = -\sum_{i=1}^8 \alpha_i U_i + \beta_1 \quad (F.2)$$

In the expression of the second joint failure (equation 5.7), some of the random variables of the first joint failure are also included. Therefore, the first eight random variables will be the same as for the first joint failure and the other nine random variables belong to the second joint failure. However, the last random variable belongs to the stress uncertainty of the second joint failure following the first joint failure and is correlated to the stress uncertainty in the first joint failure and second joint failure. The general expression for the second joint failure is as follows,

$$g_{J2,fJ1}(a_{0,J1}, a_{th,J1}, \delta_{Y_{J1}}, \delta_{f_{J1}}, C_{J1}, \delta_{F_{J1}}, \delta_{S_{J1}}, \delta_{SCF_{J1}}, a_{0,J2}, a_{th,J2}, \delta_{Y_{J2}}, \delta_{f_{J2}}, C_{J2}, \delta_{F_{J2}}, \delta_{S_{J2}}, \delta_{SCF_{J2}}, \delta_{S_{J2}}) = \frac{\delta_{f_{J2}} \int_{a_{0,J2}}^{a_{th,J2}} \frac{da}{\delta_{Y_{J2}}^m Y(a)^m (\sqrt{\pi a})^m} - \sqrt{J2} \delta_{F_{J2}}^m \delta_{S_{J2}}^m \delta_{SCF_{J2}}^m C_{J2} A_{J2}^m \Gamma(1 + \frac{m}{B_{J2}}) T_{J1}}{\sqrt{J2} \delta_{F_{J1}}^m \delta_{S_{J2,fJ1}}^m \delta_{SCF_{J2}}^m C_{J2} A_{J2,fJ1}^m \Gamma(1 + \frac{m}{B_{J2,fJ1}})} + T_{J1} - T_{lifetime} \quad (F.3)$$

This expression can be written in the standard normal space in accordance with the FORM approach as,

$$g_{J2,fJ1} = -\sum_{i=1}^8 \gamma_i U_i - \sum_{i=9}^{16} \gamma_i U_i - \gamma_{17} U_{17i} + \beta_2 \quad (F.4)$$

Now, the correlation between these two linear limit state functions can be estimated as,

$$\rho[g_{fJ1}, g_{J2,fJ1}] = \frac{Cov[g_{fJ1}, g_{J2,fJ1}]}{D[g_{fJ1}] D[g_{J2,fJ1}]} \quad (F.5)$$

Where  $D[ ]$  shows the standard deviation of the limit state function. Since the standard deviation is equal to one for the limit state function, it is only required to calculate the covariance between two limit state functions. The covariance between these two limit state functions can be estimated with the following expression,

$$Cov[g_{fJ1}, g_{J2,fJ1}] = \sum_{i=1}^8 \alpha_i \gamma_i + \alpha_7 \gamma_{15} Cov[U_7, U_{15}] + \alpha_7 \gamma_{17} Cov[U_7, U_{17}] \quad (F.6)$$

In this expression  $U_7$ ,  $U_{15}$  are related to the stress uncertainty in the first and second joint ( $\delta s_{J1}$ ,  $\delta s_{J2}$ ) respectively, and  $U_{17}$  corresponds to the stress uncertainty of the second joint when the first joint has failed ( $\delta s_{J2fJ1}$ ). The correlation between these uncertainties can be estimated based on the stress time history of the hot spot stress processes. These correlations are in the standard space, therefore the method described by Der Kiureghian and Liu (1986) is applied to change the correlation from the non-normal (here lognormal) space into the normal space.

## 1.2 Correlation of series system

When the failure probabilities of the parallel systems have been calculated, the final system reliability can be obtained in accordance with the combination of the series system. At first, the equivalent linear safety margin has been derived for parallel systems, using the method described in Gollwitzer and Rackwitz (1983). In this method, the equivalent safety margin of the equal element is obtained in such a way that the corresponding reliability index of this element is equal to the final parallel system and has the same sensitivity as the parallel system against changes in the basic variables. There are 17 random variables for each equivalent safety margin. The final system reliability is obtained by combining these limit state functions and the correlation between the random variables. For instance, the correlation between the first and third cut set shown in figure 5.4 can be estimated in accordance with the linear limit state function, see figure F.1. The linear equivalent limit states are defined with the following expressions.

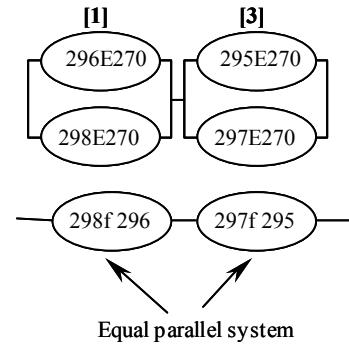


**Figure F.1:** Correlation between the first and the third cut set

$$g_{C1} = -\sum_{i=1}^{17} \xi_i U_i + \beta_{C1} \quad , \quad g_{C3} = -\sum_{i=1}^{17} \eta_i U'_i + \beta_{C3} \quad (F.7)$$

The correlation between them can be estimated with the following expression.

$$\begin{aligned} Cov[g_{C1}, g_{C3}] &= \sum_{i=1}^{17} \sum_{j=1}^{17} \xi_i \eta_j Cov[U_i, U'_j] = \xi_7 \eta_7 Cov[U_7, U'_7] + \xi_7 \eta_{15} Cov[U_7, U'_{15}] \\ &+ \xi_7 \eta_{17} Cov[U_7, U'_{17}] + \xi_{15} \eta_7 Cov[U_{15}, U'_7] + \xi_{15} \eta_{15} Cov[U_{15}, U'_{15}] + \xi_{15} \eta_{17} Cov[U_{15}, U'_{17}] \\ &+ \xi_{17} \eta_7 Cov[U_{17}, U'_7] + \xi_{17} \eta_{15} Cov[U_{17}, U'_{15}] + \xi_{17} \eta_{17} Cov[U_{17}, U'_{17}] \end{aligned} \quad (F.8)$$

where  $\xi$  and  $\eta$  are the equivalent cosine direction of the random variables estimated for the equivalent first and second cut set respectively in accordance with the method presented by Gollwitzer and Rackwitz (1983). In this expression, the stress uncertainties have been assumed to be the only variables that have a correlation with each other in the intact and damage states and the other terms are independent. The covariances between the variables are obtained using the time history of the stress processes. When in the failure sequences some elements of other failure sequences are included, for instance the first and second cut sets in the figure 5.4, the covariance between equivalent limit states have to be modified and calculated in such a way that this correlation can be taken into account. For this case, the covariance between two cut sets can be calculated with the following expression, see figure F.2,

$$\begin{aligned} Cov[g_{C1}, g_{C2}] &= \sum_{i=1}^{17} \sum_{j=1}^{17} \xi_i \eta_j Cov[U_i, U'_j] = \sum_{i=1}^8 \xi_i \eta_{i+8} + \sum_{i=1}^8 \xi_{i+8} \eta_i + \xi_7 \eta_7 Cov[U_7, U'_7] + \\ &\xi_{15} \eta_{15} Cov[U_{15}, U'_{15}] + \xi_{17} \eta_{17} Cov[U_{17}, U'_{17}] + \xi_7 \eta_{17} Cov[U_7, U'_{17}] + \xi_{17} \eta_7 Cov[U_{17}, U'_7] \\ &+ \xi_{15} \eta_{17} Cov[U_{15}, U'_{17}] + \xi_{17} \eta_{15} Cov[U_{17}, U'_{15}] \end{aligned} \quad (F.9)$$

The same procedure has been applied for the sequences of failures in a combination of fatigue and other failure modes i.e. fracture and ultimate limit states with regard to their common and correlated random variables. In the ultimate limit state only the usage factor and in the fracture limit state only the primary stress has been considered as a correlated variable with the stress uncertainty in the fatigue limit state function.

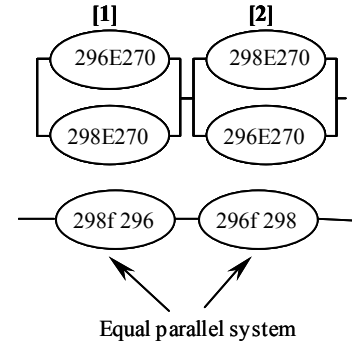


**Figure F.2:** Correlation between the first and the second cut set

## Appendix G Modelling of random variables

There are several sources of uncertainty in jack-up platform. Some of them are random in nature (physic) and others are due to restricted information (measurement and statistical uncertainty) or modelling of actual phenomena (load and structural modelling). The wave and hydrodynamic loading characteristics (significant wave height, drag and inertia coefficient), the structural material properties (yield and ultimate stresses, Young modulus), structural dimensions (thickness, diameter, length), fatigue parameters ( $C$  and  $m$ ) and fracture parameter ( $K_{IC}$ ) are examples of physic uncertainty. This type of uncertainty is measured by collecting information from tests or environmental data. Due to restricted information or the method applied to measure the quantity, statistical and measurement uncertainties are used in the calculation. For instance, the approximation of a structural model in a finite element analysis, the wave load modelling and the calculation of stress concentration factors are considered in the model uncertainty. The uncertainty is represented with a random variable. There is limited information about the model uncertainty for jack-up platforms. Therefore, some of the model uncertainties have been taken from other offshore platforms (jacket platforms). However, these models should be modified to reflect the real situation of jack-up platforms. This concerns the load model, stress concentration and stress calculation.

The uncertainty in the long-term environmental data can be described with the joint distribution of the significant wave height and zero crossing period in the form of a scatter diagram based on recorded data at a particular location. This can also be represented in terms of a marginal distribution for significant wave height and a distribution for zero-crossing periods conditional on the significant wave heights, as given in appendix C. For a stress range in fatigue reliability calculations, this uncertainty is described by the Weibull distribution with a scale parameter  $A$  and a shape parameter  $B$ , see section 2.3.4.

Uncertainty in the load calculation ( $\delta_F$ ) is composed of contributions from wave load calculations, which partially arise from the inertia ( $C_M$ ) and drag terms ( $C_D$ ) in the Morison equation, the use of a simplified wave theory (Airy), and finally from the external loads (live and dead). Since there is little information about these variables, the lognormal distribution with a mean 1.0 and the COV=0.1 are used in this research work, as recommended by Dalane (1993) for jacket platform.

According to the DNV specification, (notes 30.2, 1984) it is recommended to use a normal distribution for  $\ln C$  in which its mean being  $-29.84$  for an element in air or in the case of cathodic protection, and a standard deviation of  $0.55$ . Moreover,  $m$  is supposed to be deterministic parameter with the value  $3.1$ . For an element in seawater without cathodic protection, the mean and standard deviation of  $\ln C$  in accordance with this specification are  $-31.01$  and  $0.77$  respectively, and  $m$  is set to  $3.5$ . Due to restricted information about the fatigue characteristics of the high tensile steel material used in the jack-up platform, the values recommended by the DNV specification are applied.

Data on probabilistic types of initial weld defects in jack-up platforms are rarely reported in the literature. More detail about this random variable is given in section 2.4.1. The initial crack depth is taken as the exponential distribution with a mean value of  $0.11 \text{ mm}$ , Bokalrud and Karlsen (1982).

Usually a random geometry correction factor  $\delta_Y$  is used in the reliability analysis to consider uncertainties arising from simplifications, crack coalescences and weld geometry effects. The statistics of  $\delta_Y$  is assumed invariant to crack size, which implies that the geometry function  $Y_A(a)$  can be randomized by simply multiplying by  $\delta_Y$ . In the literature, this random variable is usually modelled as a normal variable with a coefficient of variation in the range 0.05-0.20 (Dalane, 1993, Hovde, 1995, Shetty 1992). In the present study, the geometry function is modelled in accordance with the Newman and Raju (1981) method and by adding the empirical correction term given by Smith and Hurhworth (1984).  $\delta_Y$  is therefore modelled as the normal distribution with the coefficient of variation 0.1.

The uncertainty in the stress concentration factor ( $\delta_{SCF}$ ) arises from the discrepancy between the parametric formula and the measured SCF. The lognormal distribution is usually applied to specify with the mean value equal 1.0 but there is a scatter in the coefficient of variation reported in the literature ranging from 0.05 to 0.25, (Aghakouchak and Stierner, 2000; Dalane, 1993; Shetty 1992). Since there is not sophisticated information about this variable for jack-up platform, the value recommended by Dalane is used, COV=0.1.

The stress model ( $\delta_s$ ) is presented in the fatigue analysis to take into account the uncertainty in the stress calculations due to the simplification of the actual model in FEM, the soil-structure interaction, and any other uncertainty in the structural aspects. In the literature the uncertainty in this variable is sometimes combined with the load model, (Shetty, 1992, Aghakouchak and Stierner, 2001). As the load model, usually the lognormal distribution is used to describe the probability distribution of this random variable with the mean value 1.0. Dalane (1993) recommended to use the coefficient of variation of 0.1 to specify this random variable. Because reliable data about this random variable for the jack-up platform are lacking a value of 0.15 is taken for this variable because of the simplification of the leg elements in applied FEM model. Only this variable is assumed for the spatial correlation in the stress model of the jack-up platform and its correlation is estimated in accordance with the time history of stress process.

The fracture toughness ( $K_{IC}$ ) is usually obtained from tests on simple specimens and a considerable scatter is generally observed in the test results. Furthermore, the fracture toughness may be affected by the plate thickness, the stress state, the temperature and the place where the sample is taken (weld metal, heat affected zone or parent metal). Usually, the lognormal distribution is recommended in the literature (Shetty, 1992, Marley, 1991, Hovde, 1995) to specify the uncertainty in the fracture toughness. The coefficient of variation between 8 to 25% is reported based on the literature review performed by Marley (1991). However, the range between 20 and 30% is also reported by Shetty (1992). Herein the coefficient of variation 0.25 is assumed for the fracture toughness.

The mean values reported for the linear-elastic fracture toughness ranges from 2800 to 7000 MPa $\sqrt{mm}$  (Shetty, 1992, Hovde, 1995). Due to limited available information for the fracture toughness of high strength steel material used in the jack-up platform, the relationship  $K_{IC} = \sqrt{E\sigma_Y\delta_{IC}}$  is applied to specify the mean value of the fracture toughness with the crack tip opening displacement  $\delta=0.3$  and the mean value of the yield stress  $\sigma_Y=689$  MPa. Therefore, for this study the mean value  $K_{IC}$  is assumed to be 6500 MPa $\sqrt{mm}$ . This fracture toughness



---

As the other material parameters, the uncertainty in yield stress ( $\sigma_Y$ ) arises from many sources such as manufacturer, the thickness of plate and fabrication procedure. The total uncertainty is therefore a function of the variability within each batch and variability between batches. Usually the lognormal distribution is used to model this uncertainty (Shetty, 1992). The coefficient of variation ranges from about 0.05 to 0.12 depending on the plate thickness and nominal yield stress. To be consistent with the data used by Daghigh (1997) for the Neka jack-up platform the yield stress is assumed lognormal with mean 689 MPa and coefficient of variation 0.08.

## Appendix H Long-term failure probability

In chapter 4, the failure probability is calculated for the extreme (wave) environmental loads using the design storm approach. This method incorporates some uncertainty in the reliability calculation due to the random nature of the extreme wave that may occur during the lifetime of platform. In the following section an approximation is made to estimate the long-term failure probability.

The stress distribution for a member within one sea state is given by the Weibull distribution according to section 4.5.2. The structure is loaded by a sequence of sea states during the lifetime. The failure occurs due to the maximum peak stress in one of the heavy sea states. If we follow the Turkstra's rule, it is possible to assume that the failure occurs in the sea state with the highest significant wave height in the lifetime, and not in other sea states. A small error may be made by this assumption. But, the Turkstra rule is convenient, as we only need to consider  $H_S$  as an ordinary random variable with a distribution corresponding to the maximum in the lifetime (20 years).

At first, the significant wave height and its corresponding zero crossing period for the 1000-years return period is calculated based on method given by Winterstein et al. (1993). The estimated significant wave height and its corresponding zero crossing period are 18.668 (m) and 12.162 (s) respectively. For this condition the hydrodynamic loads are calculated with the NOSDA program and the structural analysis is carried out by ANSYS program (FEM analysis) to estimate the axial and bending stresses. In table H.1, the calculated reliability index in accordance with this wave height and corresponding ultimate limit state are given.

Now, the conditional reliability indices  $\beta_1$  and  $\beta_2$  for two sea states with given fixed values of the significant wave height are available. For example consider the chord element 53, where  $\beta_1=2.189$  in case the significant wave height is 18.7 m ( $H_{SI}$ ) with a corresponding return period of 1000 years. The encounter probability in the 20 years lifetime of platform for this significant wave height can be calculated with the following formulation, Chakrabarti (1987),

$$P_E = 1 - \left(1 - \frac{1}{T_R}\right)^l \quad (\text{H.1})$$

where  $T_R$  is the return period (here 1000 years) and  $l$  is the given duration (here 20 years).

The encounter probability according to this formulation is  $P_{E1}=0.0198$ . For other sea state with  $\beta_2=3.861$  the significant wave height is 16.1 m ( $H_{SI}$ ) and the corresponding return period 50 years. The encounter probability for this significant wave height is  $P_{E2}=0.332$ . So,  $\beta$  can be written as a function of  $H_S$  or  $P_E$ . The best way is to write  $\beta$  as a function of the standard normal random variable  $u$

**Table H1:** The conditional and unconditional (long-term) reliability indices

Element	Design storm		Unconditional (Long-term)
	Hs=16.1 (50 years)	Hs=18.67 (1000 years)	
296	6.689	5.325	5.401
295	8.762	7.323	6.846
52	3.948	2.547	3.273
53	3.861	2.189	3.001

corresponding to  $P_E = \Phi(u)$ . From  $P_{E1} = \Phi(u_1)$  follows  $u_1 = -2.058$  and from  $P_{E2} = \Phi(u_2)$  follows  $u_2 = -0.433$ . Now, the limit state function to find the long-term reliability index can be formulated with,

$$Z = v - \beta \quad (\text{H.2})$$

where  $v$  is a standard Gaussian random variable and  $\beta$  is given by the following expression.

$$\beta = \beta_1 - (\beta_2 - \beta_1) \frac{u - u_1}{u_2 - u_1} \quad (\text{H.3})$$

In this formulation  $u$  is the random variable, which is directly related to the encounter probability. In this model, it is supposed that the sea state that is encountered during the lifetime of the platform has a random nature and this model incorporates implicitly this randomness. Furthermore, the actual variation of the reliability index with the encounter probability is of a non-linear manner, however, this linear model will impose some approximation to the exact value but it may be suggested as the first approximation. The following standard rules can be applied to estimate the mean and the variance of  $Z$ .

$$\begin{aligned} \mu(Z) &= \beta_1 - (\beta_2 - \beta_1) \frac{u_1}{u_2 - u_1} \\ \sigma^2(Z) &= \left( \frac{\beta_2 - \beta_1}{u_2 - u_1} \right)^2 + 1 \end{aligned} \quad (\text{H.4})$$

This mean and variance leads in the end to the following unconditional reliability index.

$$\beta_{long} = \frac{\mu(Z)}{\sigma(Z)} = \frac{\beta_1 u_2 - \beta_2 u_1}{\sqrt{(\beta_2 - \beta_1)^2 + (u_2 - u_1)^2}} \quad (\text{H.5})$$

The calculated long-term reliability index for several elements (and approaches) is given in table H1, which shows that the long-term reliability index is less than the 50 years return period.

## Appendix I Failure probability for combined fatigue and fracture failure modes

In section 5.4, several combinations of fatigue and fracture have been assumed for system failure probability calculation. In this appendix, the methods for calculation of the failure probability for these sequences are presented in detail.

### I.1 Fatigue failure of the first joint followed by a fracture failure of the second joint

The first joint failure takes place through the fatigue degradation and is followed by the fracture failure of the second joint. For the first joint failure, the failure probability is calculated with the fatigue limit state function when the critical crack size is the thickness of element. This method is presented in section 4.3.2 in detail, where the bending to membrane stress ratio is estimated from the time history of the hot spot stress process. The limit state function for the first joint failure in fatigue is,

$$Z_1 = \frac{\delta_{f_{J1}}}{v_{J1}^l \delta_{F_{J1}}^m \delta_{S_{J1}}^m \delta_{SCF_{J1}}^m C_{J1} A_{J1}^m \Gamma(1 + \frac{m}{B_{J1}})} \int_{a_{0,J1}}^{a_{th,J1}} \frac{da}{\delta_{Y_{J1}}^m [Y(a)(\sqrt{\pi a})]^m} - T_{life} \quad (I.1)$$

The failure probability  $P [Z_1 \leq 0]$  is determined by FORM. For the second joint failure the limit state function is given by (4.16),

$$Z_2 = [1 - 0.14 L_{r,J2}^2][0.3 + 0.7 \exp(-0.65 L_{r,J2}^6)] - \frac{\delta_{Y,J2} Y(a) \sqrt{\pi a} (\delta_{F,J2} \delta_{SCF,J2} \sigma_{J2}^P + \sigma_{J2}^S)}{K_{IC,J2}} - \rho_c \quad (I.2)$$

Also, the failure probability  $P [Z_2 \leq 0]$  is determined by FORM. In this expression, it is assumed that a crack occur due to fatigue degradation and its dimension  $a(t)$  can be determined from the crack growth formulation (5.24) for the second joint as,

$$\int_{a_{0,J2}}^{a(t)} \frac{da}{\delta_{Y_{J2}}^m Y(a)^m (\sqrt{\pi a})^m} = v_{J2}^l \delta_{F_{J2}}^m \delta_{S_{J2}}^m \delta_{SCF_{J2}}^m C_{J2} A_{J2}^m \Gamma(1 + \frac{m}{B_{J2}}) T_{J1} \\ + v_{J2,J1}^l \delta_{F_{J2}}^m \delta_{S_{J201}}^m \delta_{SCF_{J2}}^m C_{J2} A_{J2,J1}^m \Gamma(1 + \frac{m}{B_{J2,J1}}) (T_{life} - T_{J1}) \quad (I.3)$$

In this expression,  $T_{J1}$  should be specified. Since, it is supposed that the first joint failure occurs in fatigue,  $T_{J1}$  can be obtained from fatigue crack growth formulation (5.3), where the critical crack size ( $a_{cr,J1}$ ) is equal to the thickness of element.

$$T_{J1} = \frac{\delta_{f_{J1}}}{v_{J1}^l \delta_{F_{J1}}^m \delta_{S_{J1}}^m \delta_{SCF_{J1}}^m C_{J1} A_{J1}^m \Gamma(1 + \frac{m}{B_{J1}})} \int_{a_{0,J1}}^{a_{cr,J1}} \frac{da}{\delta_{Y_{J1}}^m [Y(a)(\sqrt{\pi a})]^m} \quad (I.4)$$

Now, we use MCS to simulate  $T_{J1}$ . However, only the values less than  $T_{life}$  should be selected to confirm that the failure of the first joint occurs before the second one (conditional expression in equation 5.25). The design point estimated in the FORM approach for the failure probability calculation of the first joint can also be applied to improve the simulation. Finally, the lognormal distribution is used to specify the probability distribution of the crack size, in which its mean and standard deviation are obtained from simulation. By substituting

the statistical characteristics of a random crack into the fracture limit state function (I.2), the failure probability can be determined using the FORM approach. The failure probability of the failure sequences is therefore a multiplication of the conditional probability (I.2) for the second joint failure in fracture and the probability of the first joint failure in fatigue,

$$P_{f\text{seq}} = P[Z_1 \leq 0] \times P[Z_2 \leq 0].$$

### I.2 Fracture failure of the first joint followed by a fracture failure of the second joint

This failure scenario is more complex than the first one, however, the method is almost the same. The first joint failure takes place through fracture failure and is followed by a fracture failure of the second joint. To calculate the first joint failure in fracture, the method described in section 4.6 is employed here. The limit state function for the first joint failure in fracture is,

$$Z_3 = [1 - 0.14L_{r,J1}^2][0.3 + 0.7 \exp(-0.65L_{r,J1}^6)] - \frac{\delta_{Y,J1} Y(a) \sqrt{\pi a} (\delta_{F,J1} \delta_{SCF,J1} \sigma_{J1}^P + \sigma_{J1}^S)}{K_{IC,J1}} - \rho_c \quad (\text{I.5})$$

where the crack size ( $a$ ) is specified in accordance with the fatigue crack growth expression as explained in section 4.6. The failure probability  $P[Z_3 \leq 0]$  is determined by FORM. Almost the same approach described in section I.1 is used for the second joint failure in fracture. The difference is in the critical crack size in expression I.4. Since the first joint has failed due to the combination of a crack and extreme environmental loads, the crack size should be reached to a critical size in the fracture expression (4.16), i.e.

$$Y(a) \sqrt{\pi a} = \frac{K_{IC,J1}}{\delta_{Y,J1} (\delta_{F,J1} \delta_{SCF,J1} \sigma_{J1}^P + \sigma_{J1}^S)} \left( [1 - 0.14L_{r,J1}^2][0.3 + 0.7 \exp(-0.65L_{r,J1}^6)] - \rho_c \right) \quad (\text{I.6})$$

Hence, the expression I.6 is used to simulate the critical crack size for the first joint failure. Now, the MCS is used to simulate the crack size in expression I.6 and apply it in expression I.4 to calculate  $T_{J1}$ . Only the values less than  $T_{life}$  is selected in simulation to confirm that the failure of the first joint occur before the second one. By repeating several times this procedure and substituting in the expression I.3, the statistical characteristics (mean and standard deviation) of a crack size for the second joint can be obtained. The failure probability of the second joint failure in fracture can now be calculated with the FORM approach and using the limit state function I.2, where the statistics of crack size are estimated from the fracture formulation (I.6). The failure probability of the failure sequence can finally be computed by multiplying the first and second probability determined in the FORM approach, i.e.  $P_{f\text{seq}} = P[Z_3 \leq 0] \times P[Z_2 \leq 0]$ .

### I.3 Fracture failure of the first joint followed by a fatigue failure of the second joint

The calculation procedure for this failure scenario is similar to the method described in section I.2. The difference is on the second joint failure. The first joint failure probability is similar to the method described in section I.2. For the second joint failure in fatigue, the expression 5.8 is utilized again to specify the limit state function, but some modification should be applied into  $T_{J1}$  to account the fact that the failure of the first joint occur in fracture. Rewrite the fatigue limit state of the second joint failure as,

$$Z_4 = \frac{\delta_{J2} \int_{a_{0,J2}}^{a_{h,J2}} \frac{da}{\delta_{Y_{J2}}^m \left[ Y(a)(\sqrt{\pi a}) \right]^m} - v_{J2}^l \delta_{F_{J2}}^m \delta_{S_{J2}}^m \delta_{SCF_{J2}}^m C_{J2} A_{J2}^m \Gamma(1 + \frac{m}{B_{J2}}) T_{J1}}{v_{J2,fJ1}^l \delta_{F_{J2}}^m \delta_{S_{J2,fJ1}}^m \delta_{SCF_{J2}}^m C_{J2} A_{J2,fJ1}^m \Gamma(1 + \frac{m}{B_{J2,fJ1}})} + T_{J1} - T_{life} \quad (I.7)$$

since the first joint has failed in fracture, the critical crack size in expression I.4 should be reached to a critical size of the fracture expression. Therefore, the expression I.6 is used to simulate the critical crack size in accordance with the method described in section I.3. By substituting the estimated statistical characteristics of the critical crack size in the expression I.4 and combining with formulation I.7, the second joint failure probability in fatigue can be obtained. However, it should be kept in mind that the values of the crack size, which makes  $T_{J1}$  less than  $T_{life}$ , are selected in the simulation to confirm that the first joint failure occurs in fracture. The failure probability for the second joint failure  $P[Z_4 \leq 0]$  can finally be obtained by using FORM approach. In the end, the probability of the sequence for this failure scenario can be computed by multiplying the probability of the first joint failure in fracture,  $P[Z_3 \leq 0]$  and the second joint failure in fatigue  $P[Z_4 \leq 0]$ , i.e.  $P_{fseq} = P[Z_3 \leq 0] \times P[Z_4 \leq 0]$ .

## **Samenvatting**

### ***Lange duur betrouwbaarheid van jack-up platforms, het effect van vermoeiing, breuk en extreme belastingen op de constructieve betrouwbaarheid***

Zelfheffende platforms werken op zee onder wisselende omstandigheden. Een voorbeeld is het verschil in locaties waar de platforms worden ingezet, waardoor niet alleen de waterdiepte varieert maar ook de weersomstandigheden en de bodem condities kunnen veranderen. Een verandering in de boordiepte leidt eveneens tot andere beladingscondities. Om een betrouwbare voorspelling van de levensduur van de zelfheffende platforms te kunnen maken is inzicht nodig in de factoren die daar invloed op uit kunnen oefenen. Een zelfheffend platform is meestal samengesteld uit drie poten die een horizontale doos constructie (het platform) ondersteunen. In en op het platform zijn onder meer de verblijven, installaties voor energieopwekking, machines, installaties en uitrustingen voor het boorbedrijf of de productiefaciliteiten, de opslag voor boorpijpen en casing en voorraden ondergebracht. Het zelfheffende platform verschilt qua constructie fundamenteel van vaste of drijvende offshore installaties op zee. De vraag naar meer flexibiliteit, onder meer bij de ontwikkeling van de zogenaamde marginale velden, maakt de inzet van zelfheffende platformen attractief voor toepassingen als productie-eenheid in dieper waters.

Het onderwerp van dit onderzoek is de betrouwbaarheid van zelfheffende platforms met het doel de mogelijkheden voor de verlenging van de levensduur te onderzoeken. Dit deel van het onderzoek concentreert zich op de constructie waarbij vermoeiing, breuk en het falen als gevolg van extreme belastingen een rol spelen. Daarbij speelt de onzekerheid, bijvoorbeeld als gevolg van de belastingen, maar ook materiaal eigenschappen en het modelleren van de constructie een rol. Deze onzekerheden worden onderzocht omdat een deterministische benadering, die bij het ontwerp onontbeerlijk is, hierbij geen oplossing kan bieden.

Voor het berekenen van de betrouwbaarheid wordt een methode voorgesteld die gebaseerd is op een verfijnde methode voor het bepalen van de spanningen in een constructie. Het bezwijken van een constructie kan bijvoorbeeld het gevolg zijn van een breuk in een onderdeel ten gevolge van extreme belastingen in combinatie met een reeds bestaande imperfectie in een onderdeel als gevolg van het fabricage proces of vermoeiing.

Om statistische gegevens over de scheur te verkrijgen wordt de zogenaamde Monte Carlo Simulatie techniek gebruikt, waarmee de groei van de scheur als gevolg van vermoeiing kan worden bepaald.

Voor het bezwijken van de constructie onder extreme belastingen worden de axiale en buig spanningen in een onderdeel van de constructie gecombineerd om de ‘time history of the usage factor’ te bepalen.

Het effect van de redundantie van de constructie is onderzocht door kans op bezwijken voor de combinaties van verschillende vormen van bezwijken te onderzoeken door de vergelijking van de waarschijnlijkheid daarvan voor elkaar opvolgende verschillende vormen van breuk, onder meer als gevolg van bij extreme belastingen. Daarbij is gebruik gemaakt van verschillende technieken die bij de bepaling van de betrouwbaarheid van constructies worden gebruikt en die geschikt zijn gemaakt voor de condities die voor zelfheffende platformen van toepassing zijn.

## **Curriculum vitae**

Naser Shabakhty was born on 10<sup>th</sup> October 1967 in Karbala, Iraq. He obtained a B.Sc. in Civil Engineering from Ahwaz University (Jundishapour) in 1990. From 1991 to 1992 he was serving his military service. After successfully passing the national examination in 1992, he joined Isfahan University of Technology to continue his higher education in Structural Engineering. During his post graduation, he was involved in several research projects, such as investigating the effect of penetration of CL, SO<sub>4</sub> and CO<sub>2</sub> ions using different epoxy layers on a surface of concrete samples to increase the durability of a concrete pole; he also investigated the possibility of strengthening an adobe structure against earthquakes in the rural zone of Iran. His latest project has been established in cooperation with UNDP and Iranian Housing Foundation (Boniad Maskan), to investigate the possibility of strengthening an adobe structure and preparing a guideline for planning and construction of such buildings to mitigate the earthquake damage. Finally, he obtained his M.Sc. in Structural Engineering from Isfahan University of Technology in 1995.

After his study, he was appointed chief of the inspection team for structural construction in one of the sections of the Karkheh Dam and continued to work there until 1998. Then, he joined the International Imam Khomini Airport as a supervisor in the construction of the infrastructure of the airport until the end of 1999.

After passing a national exam, Naser Shabakhty obtained a scholarship from the Ministry of Science, Research and Technology (MSRT) of Iran to pursue his PhD in offshore engineering. He started his PhD research in the faculty of Mechanical Engineering and Marine Technology of the Delft University of Technology in December 1999 under the supervision of Prof. ir. S. Hengst, Ir. H. Boonstra, Dr. P. Van Gelder and Prof. ir. A.C.W.M Vrouwenvelder. During his research work, he followed several courses in marine engineering, the hydrodynamics of ships and offshore structures, organized by the International Hydraulic Education (UNESCO-IHE) and Research School for Fluid Mechanics (JM Burgerscentrum) in Delft. He wrote several progress reports and presented papers in the International Conferences on Hydraulic Structures (ICHS 2001) in Kerman-Iran, Offshore Mechanics and Arctic Engineering (OMAE 2002) in Oslo-Norway and European conference on Safety and Reliability (ESREL 2003) in Maastricht-The Netherlands.